Influence of the CRISPR/Cas mediated Knockout of 5-Lipoxygenase on Tumour Cells

Dissertation

zur Erlangung des Doktorgrades

der Naturwissenschaften

vorgelegt beim Fachbereich Biochemie, Chemie, Pharmazie (14)

der Johann Wolfgang Goethe-Universität

in Frankfurt am Main

von

Hannah Weißer

aus Oberursel/Ts., Deutschland

Frankfurt am Main

22. August 2022

(D30)

Vom Fachbereich 14, Biochemie, Chemie und Pharmazie der
Johann Wolfgang Goethe-Universität als Dissertation angenommen.

Dekan: Prof. Dr. Clemens Glaubitz

Gutachter: Prof. Dr. Dieter Steinhilber
PD Dr. Tobias Schmid

Datum der Disputation: 20.12.2022

It's gonna take a lot to drag me away from you
There's nothing that a hundred men or more could ever do
I bless the rains down in Africa
Gonna take some time to do the things we never had – ooh oh

Toto

Contents

List of Figures

List of Tables

Abbreviations

5-FU	5-Fluorouracil
ActD	Actinomycin D
ALOX	Arachidonate LO gene
AA	Arachidonic acid
ALL	Acute lymphoblastic leukaemia
ANOVA	Analysis of variance
AP-2	Activating protein 2
APS	Ammonium peroxydisulphate
ATCC	American Type Culture Collection
ATP	Adenosine triphosphate
BCA	Bicinchoninic acid assay
BLT	Leukotriene B_4 receptor
BSA	Bovine serum albumin
CAM	Cell adhesion molecule
Cas9	CRISPR-associated protein 9
CBA	Cytometric bead array
CD	Cluster of differentiation
ChIP	Chromatin immunoprecipitation
CK20	Cytokeratin 20
$cPLA_2$	Cytosolic phospholipase A2
CRISPR	Clustered regularly interspaced short palindromic repeats
crRNA	crispr RNA
CysLT	Cysteinyl leukotriene receptor
DEA	Differential expression analysis
DMEM	Dulbecco's modified eagle medium
DMSO	Dimethyl sulfoxide
DNA	Deoxyribonucleic acid
DHA	Docosahexaenoic acid
DSMZ	Deutsche Sammlung von Mikroorganismen und Zellkulturen
ECM	Extracellular matrix
EDTA	Ethylenediaminetetraacetic acid
ELISA	Enzyme-linked immunosorbent assay

eLO3	Epidermis-type lipoxygenase 3
EGR-1	Early growth response protein 1
EMT	Epithelial-mesenchymal-transition
EPA	Eicosapentaenoic acid
EpCAM	Epithelial cell adhesion molecule
ERK	Extracellular signal-regulated kinases
ETE	Eicosatetraenoic acid
Eto	Etoposide
EtOH	Ethanol
FACS	Fluorescence-activated cell sorting
FBS	Fetal bovine serum
FLAP	5-Lipoxygenase-activating protein
fMLP	*N*-Formylmethionyl-leucyl-phenylalanine
g	Gravitational acceleration
GM-CSF	Granulocyte-macrophage colony-stimulating factor
GPCR	G protein-coupled receptor
GPx	Glutathione peroxidase
gRNA	guide RNA
h	Hours
HDR	Homology-directed repair
HETE	Hydroxyeicosatetraenoic acid
HIF-1α	Hypoxia-inducible factor 1α
HIV	Human immunodeficiency virus
HpETE	Hydroperoxyeicosatetraenoic acid
HpODE	Hydroperoxyoctadecadienoic acid
HUVEC	Human umbilical vein endothelial cells
Ig	Immunoglobulin
IL	Interleukin
KD	Knockdown
KO	Knockout
KI	Knock-In
LC-MS/MS	Liquid chromatography coupled tandem mass spectrometry
LLOQ	Lower limit of quantification
LO	Lipoxygenase

LT	Leukotriene
LTA_4	Leukotriene A4
LTA_4H	Leukotriene A4-hydrolase
LTB_4	Leukotriene B4
LTC_4	Leukotriene C4
LTC_4S	Leukotriene C4-synthase
LTD_4	Leukotriene D4
LTE_4	Leukotriene E4
MAPK	Mitogen-activated protein kinase
MCP-1	Monocyte chemoattractant protein 1 also known as CCL2
MEK	Mitogen-activated protein kinase kinase
MeOH	Methanol
MET	Mesenchymal-epithelial-transition
MHC	Major histocompatibility complex
miRNA	microRNA
MM6	Mono Mac 6 cell line
mRNA	Messenger RNA
MS	Mass spectrometry
$NADPH/NADP^+$	Nicotinamide adenine dinucleotide phosphate
NHEJ	Non-homologous end joining
NF-κB	Necrosis factor κB
OAG	1-Oleoyl-2-acetyl-sn-glycerol
PAF	Platelet-activating factor
PAGE	Polyacrylamide gel electrophoresis
PAM	Protospacer-adjacent motif
PBS	Phosphate buffered saline
PCR	Polymerase chain reaction
PD-1	Programmed cell death protein 1
PDGF	Platelet-derived growth factor
PD-L1	Programmed cell death 1 ligand 1
PGC	PBS/glucose
PI	Propidium iodide
PKA	Protein kinase A
PMA	Phorbol-12-myristate-13-acetate
PMNL	Polymorph nuclear leukocyte

PPAR	Peroxisome proliferation activated receptor
pRB	Retinoblastoma protein
PUFA	Polyunsaturated fatty acid
RNA	Ribonucleic acid
ROS	Reactive oxygen species
ROR	Retinoid-related orphan receptor
RT	Reverse transcriptase
RT-qPCR	Real-time quantitative polymerase chain reaction
RXR	Retinoid X receptor
S1P	Sphingosine-1-phosphate
SD	Standard deviation
SDS	Sodium dodecyl sulfate
SEM	Standard error of the mean
SP1	Specificity protein 1
SPM	Specialized pro-resolving mediator
TBS	Tris-buffered saline
TE	Trypsin-EDTA
TEMED	N,N,N’,N’-Tetramethylethylenediamine
TGF	Transforming growth factor
TGFBR	TGF-β receptor
TNF	Tumour necrosis factor
tracrRNA	trans-activating RNA
Tris	Tris-(hydroxymethyl)-aminomethane
VEGF	Vascular endothelial growth factor
VEGFR	Vascular endothelial growth factor receptor

1 Abstract

This work investigated the influence of the CRISPR/Cas9 mediated knockout of 5-lipoxygenase (5-LO) on different adherent tumour cell lines derived from solid tumours. For this, the 5-LO expressing tumour cell lines HCT-116, HT-29, and U-2 OS were transiently transfected using a plasmid carrying the CRISPR/Cas9 complex sequence to the *ALOX5* gene. Subsequently, cells were selected using Puromycin and analysed via Western blotting and DNA Sanger sequencing. Cells that were transfected with a control plasmid missing the guide RNA sequence, were used as a control for all experiments.

Differential gene expression analysis, performed after next-generation RNA sequencing, revealed that the expression of various genes was altered after the knockout of 5-LO. In HCT-116 cells, 28 genes were expressed differentially in all 5-LO knockout single-cell clones, while in HT-29 cells the expression of 18 genes and in U-2 OS cells of 234 genes was influenced by the knockout of 5-LO. These findings were validated by real-time qPCR. A lot of the genes that were influenced by the 5-LO knockout are known to be connected to epithelial-mesenchymal-transition (EMT), a process necessary for tumour metastasis. The results from RNA sequencing were the starting point for further investigations.

In the following, different aspects of the tumour cell lines were examined. In HT-29, as well as in U-2 OS cells, it was shown that knockout of the 5-LO resulted in impaired cell proliferation. Also, the formation of three-dimensional tumour spheroids was altered. In HT-29 cells, the knockout of 5-LO increased the number of cells in spheroids. In contrast, in U-2 OS cells, the number of cells per spheroid was decreased, even though the diameter of the spheroids was increased, due to more loosely packed spheroids. The difference between 5-LO positive and negative U-2 OS cells became even more obvious after embedding the spheroids in an artificial extracellular matrix. In that scenario, cells lacking the 5-LO formed smaller spheroids that did not have the same ability to grow into the extracellular matrix as 5-LO positive cells did. Also, directed cell migration was strongly influenced by the knockout of 5-LO. In both, HCT-116 and U-2 OS cells, directed cell migration towards a serum gradient was increased in 5-LO knockout single-cell clones.

Pharmacological inhibition of the enzyme was used to investigate, whether canonical or non-canonical functions were responsible for the previously mentioned effects. Therefore, vector control cells were treated with the 5-LO inhibitors Zileuton and CJ-13610 in different concentrations. Interestingly, only some of the effects mediated by the complete knockout of 5-LO could be reproduced by inhibiting the enzyme, leading to the suggestion, that canonical, as well as non-canonical functions of 5-LO, play a role in these tumour cells.

To conclude, it was shown in this study, that 5-LO affects various cellular functions when expressed in adherent tumour cell lines. These cell line-dependent effects result in altered gene expression, enhanced proliferation, and spheroid formation, as well as impaired cell motility, and can be mediated by enzymatic activity as well as other non-canonical functions.

2 Introduction

2.1 Lipoxygenases

Lipoxygenases (LOs) are non-haem iron-carrying enzymes that stereo-selectively introduce molecular oxygen to polyenoic fatty acids possessing a 1-cis,4-cis-pentadiene system (1). Six different lipoxygenase genes are known in humans, originally named after their site of reaction with arachidonic acid: *ALOX5, ALOX12, ALOX12B, ALOX15, ALOX15B, and ALOXE3*. The *ALOX5* gene is located on chromosome 10 and will be surveyed in more detail later in this chapter. All other *ALOX* genes can be found clustered on chromosome 17 (2).

Besides arachidonic acid other polyunsaturated fatty acids (PUFAs) like linoleic acid, eicosapentaenoic acid (EPA), and docosahexaenoic acid (DHA) can serve as a substrate for lipoxygenases (3). Free fatty acids are preferred over esterified and cause the need for liberation from e.g., membrane phospholipids by enzymes like cytosolic phospholipase A2 ($cPLA_2$) (4) and other phospholipases.

All LOs have a close homologue structure consisting of one polypeptide that is organized in two different domains. The N-terminal domain is responsible for the enzymatic activity as well as binding of membranes and by this the cellular localization while the C-terminal domain is the catalytic domain in which the non-heme iron ion is located (5).

ALOX12 encodes for 12-LO, the first lipoxygenase discovered in humans in 1974 (6), which is predominantly found in platelets and is therefore referred to as platelet-type 12-LO (7). Besides its distinction in platelets, it can also be found in the skin (8) just like *ALOX12B* and *ALOXE3*. *ALOX12B* encodes for the 12*R*-LO which contrary to all other LOs produces the respective *R* product instead of *S* enantiomers (9). This enzyme is co-expressed in the skin with the epidermis-type lipoxygenase 3 (eLO3) encoded by the *ALOXE3* gene and both enzymes are involved in epidermal development and water homeostasis (10) (11). 12/15-LO, encoded by the *ALOX15* gene, can be found in macrophages, eosinophils, and epithelial cells of the respiratory tract (12) (13) (14) while 15-LO2, encoded by the *ALOX15B* gene, is found in M2 macrophages as well as lung, prostate, skin, and cornea (15) (16).

2.2 5-Lipoxygenase

5-Lipoxygenase (5-LO) is the key enzyme in the formation of pro-inflammatory leukotrienes (LTs) (17) and other bioactive lipid mediators like 5-oxo-ETE (18) or - in cooperation with other lipoxygenases - specialized pro-resolving mediators (SPMs) like lipoxins and resolvins (19). It is predominantly expressed in different immune cells like

mast cells, macrophages, and granulocytes and is located in the soluble compartment of either the nucleus or the cytosol. Two different phosphorylation sites are determining for cellular localization. Protein kinase A-mediated phosphorylation at Ser523 leads to cytosolic localization and by this inhibits 5-LO activity (20) while the phosphorylation of Ser271 inhibits the nuclear exports and results in contrary effects (21). Upon activation by different stimuli, 5-LO translocates to the nuclear envelope where it forms a complex with Ca^{2+}-activated $cPLA_2$ and the 5-LO activating protein (FLAP). This complex releases arachidonic acid from phospholipids in the nuclear membrane and subsequently catalyses a two-step reaction. In the first step, oxygen is introduced to the fatty acid in a dioxygenation reaction to yield the intermediate product 5(*S*)-hydroperoxy-6,8,11,14-eicosatetraenoic acid (5-HpETE). In the second step, this intermediate gets dehydrated to form the highly unstable epoxide leukotriene A_4 (LTA_4). Subsequently, LTA_4 can in the following either be hydrolysed by LTA_4-hydrolase (LTA_4H) receiving LTB_4 or, to receive the so-called cysteine-containing leukotrienes LTC_4, LTD_4 and LTE_4, gets conjugated to glutathione by LTC_4-synthase (LTC_4S) (22).

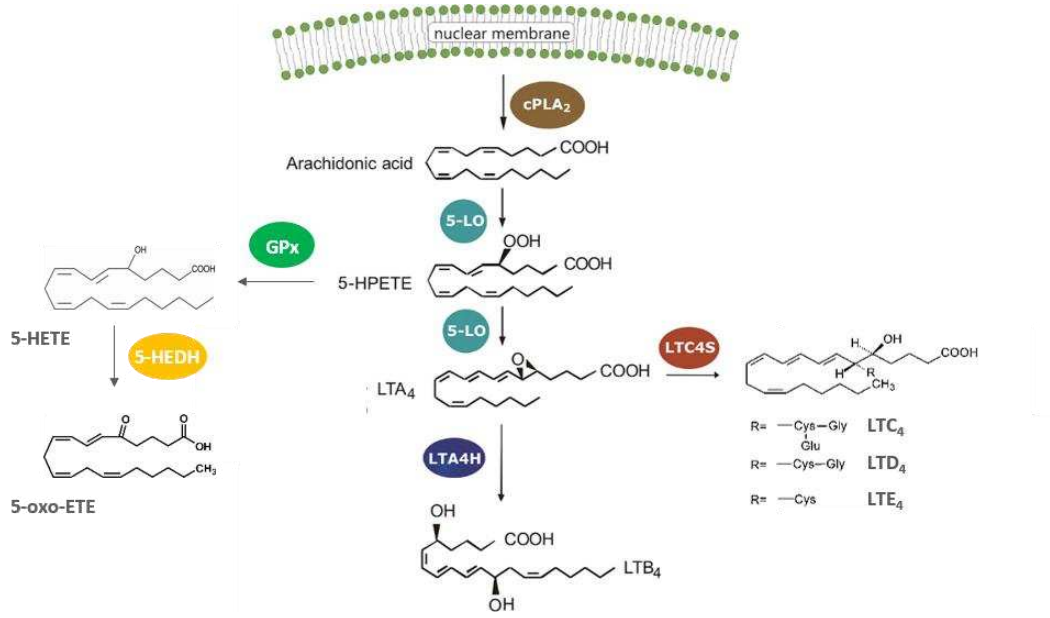

Figure 2.1 Leukotriene biosynthesis mediated by 5-lipoxygenase*. Figure taken and modified from (3). GPx: Glutathione peroxidase, 5-HEDH: 5-hydroxyeicosanoid dehydrogenase*

2.2.1 Expression of 5-LO

ALOX5, the gene encoding for human 5-LO, can be found on chromosome 10, covers a range of 71.9 kbp, and is organized in 14 exons separated by 13 introns. The mature 5-LO protein has a molecular weight of 78 kDa and consists of 673 amino acids. Alternative splicing can result in different isoforms of the enzyme and until now at least seven isoforms could be characterized although some of the physiological functions remain to be identified (23) (24). By containing eight GC boxes, the promoter that regulates *ALOX5* gene expression is a GC-rich promoter and therefore transcription factors like SP1 can regulate its activity (25). It was shown that in myeloid cells not expressing 5-LO, DNA-

methylation is responsible for silencing the gene (26). Mutations can occur in the promoter region of 5-LO that either delete parts of the GC-rich elements or integrate another GC-box and lead to alterations in pathophysiological processes like asthma (27) or atherosclerosis (28). Vitamin D was found to be another regulator of 5-LO expression as multiple vitamin-D-response elements have been identified in different loci, one of them located in intron 4 (29). Additionally, it has been shown that $1,25(OH)_2D_3$ – the biologically active form of vitamin D – in combination with TGF-β increases 5-LO enzyme expression up to 100-fold in the monocytic cell line Mono Mac 6 (30). Other known enhancers of enzyme expression besides p53, which will be discussed later, are Smad3 and Smad4 which are downstream effectors of TGF-β signalling (31). This regulation takes place in the distal part of the gene in exons 10-14. Phorbol-12-myristate-13-acetate (PMA), dimethyl sulfoxide (DMSO), interleukin-3 (IL-3) and granulocyte-macrophage colony-stimulating factor (GM-CSF) as well as AP-2, c-myc, EGR-1 and -2, NF-κB, and the nuclear receptors RXRα and RORα have been described to regulate 5-LO expression (32) (25) (33) (34) (35).

2.2.2 5-LO structure

The first crystal structure of mammalian LOs was solved in 1997 from rabbit 15-LO (36). For a long time only homology models were available for human 5-LO (37), but in 2011 the structure of a mutant form of 5-LO - the so-called stable 5-LO - could be crystallised. In this mutant form, several amino acids are deleted or substituted to stabilise the structure (38). Due to the different alterations, it is questionable whether native 5-LO crystals would look the same but nevertheless, it is the best approximation to the actual crystal structure of human 5-LO known so far.

Like all known lipoxygenases the 5-LO protein consists of an N-terminal C2-like domain (amino acids 1-114) built-up of eight β-sheet structures and a bigger C-terminal domain, structured in α-helices and containing the catalytic domain with a non-heme iron ion in its centre (39) (40).

The C2-like domain is responsible for Ca^{2+}-mediated membrane binding and therefore covers the membrane-binding region as well as the Ca^{2+}-binding site. The three tryptophan residues W13, W75 and W102 were shown to be responsible for the membrane interaction (41) (42). Residues N43, D44 and E46 mediate the Ca^{2+}-binding via ion interactions (39).

The catalytic domain contains three histidine residues (H367, H372 and H550) and the carboxylate residue of the terminal isoleucine (I673) that lock the central iron in its distinct position (38) (43). Two ATP binding sites can be found in the enzyme, one situated in the C2-like domain and one near the catalytic domain (amino acids 73-83 and 193-209) (44). Two aspects are interesting about the ATP binding of 5-LO. Although two different binding sites were identified in the enzyme, 5-LO only binds ATP in an equimolar ratio and after the binding of ATP, no hydrolysis delivering energy to the enzyme is required to raise enzymatic activity.

2.2.3 Regulation and stimulation of 5-LO activity

Various factors are described to regulate 5-LO enzyme activity. One of those is its cellular localisation. 5-LO can be found in the cytosol as well as in the nuclear compartment depending on the cell type and status of activation. In resting peritoneal macrophages, monocytes and peripheral eosinophilic and neutrophilic granulocytes, 5-LO is primarily localised in the cytoplasm (45) (46) while in mast cells and alveolar macrophages it is evenly distributed between the nucleus and the cytoplasmic compartment (47) (48) (49). Nevertheless, this distribution underlies rapid changes due to different biological processes. Nuclear localisation of 5-LO was shown to lead to a stronger enzymatic activity and by this higher amounts of leukotrienes (50) (51) (52). Only in eosinophil granulocytes, nuclear import of 5-LO leads to a decrease in LTC_4 synthesis (46). Given the fact that LTC_4-synthase is almost exclusively found on the cytosolic side of the nuclear envelope, this seems to be plausible (53). Different stimuli can lead to nuclear import of 5-LO, among these are activation of neutrophils as well as differentiation of mast cells and macrophages. Nuclear import sequences can be found at R112, K158 and R518 (54) (55). Those sequences can be activated individually but yield the greatest effect if activated simultaneously (56). Besides nuclear import - and thereby activating - sequences, several export sequences are known as well. Phosphorylation at Ser271, initiated by p38 MAPK signalling, leads to nuclear export resulting in cytosolic localisation and thereby inhibits 5-LO activity in most cells (57) (58) while phosphorylation at serine 523 mediated by PKA inhibits the nuclear import of 5-LO resulting in impaired activity as well (59). Another phosphorylation site at Ser663 has been described but could not be validated by MS analysis so far (60). Besides, the presence of substrates or small molecules like Ca^{2+} and ATP as well as the redox tonus of the cell strongly influences the product formation of 5-LO.

Mechanisms that stimulate 5-LO enzyme activity besides its cellular localisation are known as well. Upon activation with different stimuli, the 5-LO translocates to the nuclear membrane where a complex with FLAP and $cPLA_2$ is formed and the enzymatic cascade gets started. Among those stimuli are *N*-formylmethionyl-leucyl-phenylalanine (fMLP), a chemotactic peptide known to activate polymorph nuclear leukocytes (PMNL) and macrophages, platelet-activating factor (PAF) and ionophore A23187. All those effectors lead to Ca^{2+}-influx which in the following mediates the translocalisation of 5-LO (61). In homogenates of human PMNL, it was shown that 1-Oleoyl-2-acetyl-sn-glycerol (OAG) *in vitro* can strongly increase 5-LO product formation. These effects could be completely reversed in the presence of Ca^{2+} and membrane phospholipids (62). 5-LO inhibition can be mediated by sphingosine-1-phosphate (S1P) which administers anti-inflammatory regulation in this way (63).

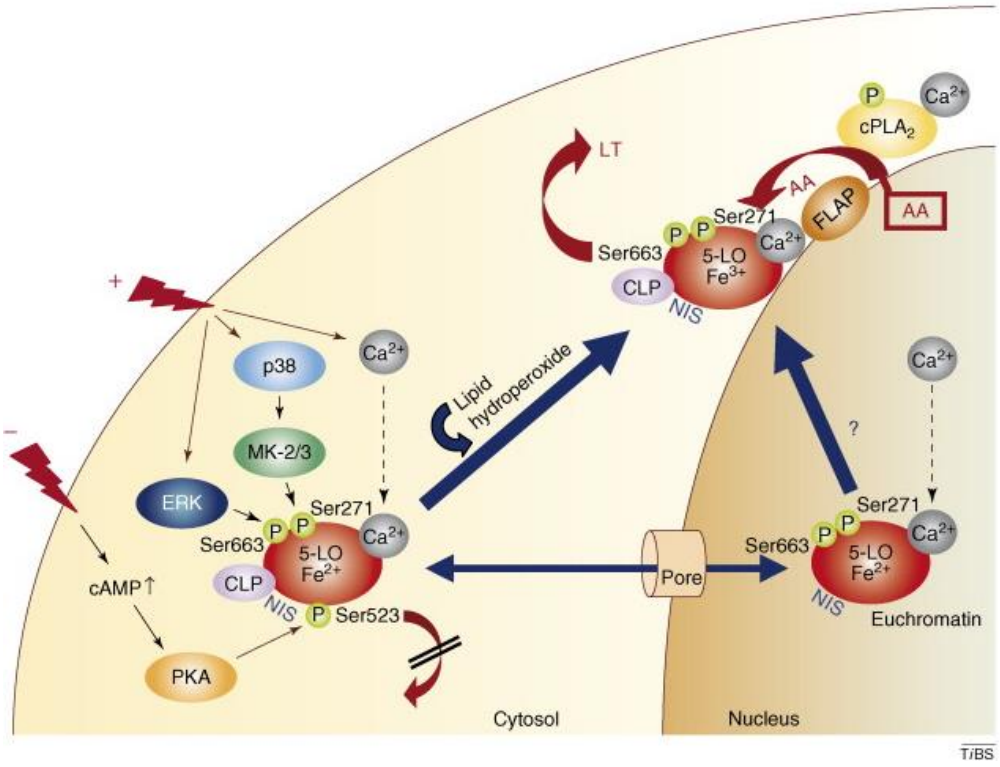

Figure 2.2 Localization and activation of 5-LO. *Figure taken and modified from (22).*

2.3 Leukotrienes and other lipid mediators

Leukotrienes (LTs) are potent lipid mediators active in the immune system that execute their effects by binding to G-protein-coupled receptors (BLT1/2 and CysLT1/2) located in the cellular membrane of their target cells (64). Through this, LTs initiate and advance inflammation and are important players in host defence reactions. On the other hand, they also participate in the genesis and progression of pathophysiological incidents like allergic conditions or chronic inflammatory diseases. Multiple factors can influence the tightly regulated biosynthesis of those mediators. Enzymatic activity of all proteins involved in the synthesis of the different leukotrienes - 5-LO, $cPLA_2$, FLAP, LTA_4H and LTC_4S - can be controlled via phosphorylation leading to an increase or a decrease in the product formation respectively, depending on the site of phosphorylation (65) (66) (67). On the other hand, malnutrition and the immune deficiency caused by HIV infection were shown to lead to decreased leukotriene formation and resulted in impaired immune reactions to host infections (68) (69) (70) (71) (72).

Leukotrienes were shown to influence different pathological processes and diseases located in the respiratory tract like asthma (73) (74) (75) (76), pulmonary hypertension (77) and fibrosis (78), or systemic inflammatory conditions like arthritis (79), chronic inflammatory bowel diseases (80), osteoporosis (81), and psoriasis (82). Additionally, plaque formation of foam cells can be driven by LTs resulting in atherosclerosis (28) (83) (84). Besides, there is evidence that 5-LO activity and its products are connected to

carcinogenic events originating from different tissues like the bladder (85), colon (86), lung (87), pancreas (88) (89), and prostate (90). Also, it was shown that 5-LO influences leukemic stem cell maintenance in BCR-ABL-induced chronic and acute myeloid leukaemia (91) (92).

2.3.1 Leukotriene B4

Leukotriene B_4 is an effective chemotactic agent and plays a significant role in the activation and recruitment of monocytes, eosinophils and neutrophils (93) (94) (95). This leukocyte recruitment is necessary for the extravasation of immune cells into the inflamed tissue in the innate immune response. LTB_4 recruits neutrophil granulocytes and in later stages of inflammation also eosinophil granulocytes (96). Also, the liberation of superoxide and lysosomal enzymes such as lysozyme and β-glucuronidase from PMNL, helping to fight intruders, is triggered (97) (98). In B-lymphocytes, LTB_4 mediates the liberation of IgM, IgG and IgE and by this, also contributes to the adaptive immune response (99) (100) (101). In addition, peroxisome proliferator-activated receptor α (PPARα) can be activated in different immune cells by LTB_4 (102).

LTB_4 mediates its effects via BLT1 and BLT2, two G-protein coupled receptors (GPCR; G_q or G_i) (103) (104). Its affinity to BLT1 is 20-fold higher than to BLT2. BLT1 is predominantly found on the cell surface of leukocytes and to a lesser extent in the spleen, thymus, and bone marrow (105). Upon activation, BLT1 mediates chemotaxis and was shown to be connected to pathophysiological processes like anaphylaxis, bronchial asthma, atherosclerosis, and ischemic reperfusion injury (106). Complete genomic knockout of BLT1 in mice reversed all LTB_4-mediated effects in neutrophil granulocytes proving its involvement in those pathological processes (107) (108).

On the contrary, BLT2 is expressed ubiquitously and can be found on the surface of a variety of cells. Here, it can also mediate its effects upon activation with 12-(S)-HpETE, 12- and 15-(S)-HETE (109). Besides LTB_4 and the other lipids of the leukotriene cascade, the BLT2 receptor is mainly activated by 12-hydroxyheptadecatrienoic acid (12-HHT) that is produced by activated platelets and macrophages (110).

2.3.2 Cysteinyl leukotrienes

Cysteine-containing leukotrienes execute their effects mostly in the respiratory system. They are among the strongest known bronchoconstrictors (111) (112) (113) and increase the mucus secretion (114) (115) (116) as well as capillary permeability of blood vessels (94). Also, cysteinyl leukotrienes are known to control ongoing fibrosis and increasing vascularisation of the tracheae, which is connected to the disease progression of asthma (117).

All cysteinyl leukotrienes can bind to the two receptors CysLT1 and CysLT2 which also belong to the GPCR family ($G_q/G_{i/0}$, depending on the cell type) (118) (119). CysLT1 is expressed on the surface of eosinophil granulocytes, monocytes, macrophages, and in the smooth muscles of the respiratory system (120) (121) (122) (123). CysLT2 expression is widely spread in the body and can be found on eosinophil granulocytes, peripheral monocytes, macrophages, and endothelial cells (124) (125) (126) as well as in the heart, the adrenal gland and the brain (119) (127) (128). Activation of both receptors leads to recruitment of macrophages and proliferation of smooth muscle cells as well as fibrosis, while only CysLT1 activation mediates bronchoconstriction, maturation of dendritic cells and blood vessel impairment (124) (125) (129).

2.3.3 5-oxo-ETE

5-oxo-ETE is formed in platelets and leukocytes by 5-hydroxyeicosanoid dehydrogenase (5-HEDH) through oxidation of 5-(S)-HETE. Intracellular $NADP^+$ levels regulate 5-oxo-ETE synthesis. Oxidative stress and superoxide anions mediate the degradation of NADPH to $NADP^+$ which increases levels of 5-oxo-ETE (130) (131). 5-oxo-ETE is a chemoattractant for neutrophil and eosinophil granulocytes and mediates Ca^{2+}-mobilisation, integrin expression and actin polymerisation by activation of the OXE-receptor (132) (133). This receptor also belongs to the family of GPCR and is predominantly expressed on monocytes as well as neutrophil and eosinophil granulocytes (134) (135).

2.4 Pharmacological targeting of 5-LO: 5-LO inhibitors and CysLT1-antagonists

As it was shown that 5-LO and the 5-LO products participate in different diseases, inhibiting the enzyme itself, or FLAP and other components of the 5-LO machinery, as well as antagonising the respective receptors was thought to be an interesting therapeutic option. 5-LO inhibitors can be divided into three classes: iron ligand, redox-active and non-redox inhibitors. Iron ligand inhibitors mediate their function by forming a chelate complex with the central iron of the enzyme. BW A4C inhibits 5-LO in granulocytes with an IC50 value of 40 nM (136) while its successor Zileuton mediates the same effects in a concentration of 0.6 µM (137). Redox-active inhibitors like AA-861 also use the central iron ion as a target by reducing it from Fe^{3+} to Fe^{2+}. This mechanism results in high promiscuity as they have an impact on all redox-sensitive structures. Also, they can induce the formation of reactive oxygen species (ROS) and by this, influence the redox tonus of the cells (138). Non-redox active inhibitors directly interact with the enzyme by displacing arachidonic acid from its active site. ZD2138 and ZM230487 inhibit the enzyme with IC50 values of 20 or 50 mM, respectively (139). As the presence of hydroperoxides like 13(S)-Hydroperoxy-(9Z,11E)-octadecadienoic acid (13(S)-HpODE) strongly impairs the activity of said structures, no approval was achieved for the inhibitory drugs. Until today, the 5-LO inhibitory drug Zileuton is the only FDA-approved drug for the pharmacological treatment

of asthma, and therefore its usage is limited to the US. In Europe, no 5-LO inhibitor has been approved by now. All drugs tested so far failed due to severe side reactions or weak efficacy (140) (141) (142).

Antagonising the CysLT1 receptor showed more promising results. By now, three different drugs have been approved for the treatment of asthma; montelukast (143), zafirlukast (144) (145) and pranlukast (146) (147).

In isolated leukocytes, the FLAP inhibitors MK-886, MK-0591 and BAY X1005 all showed promising results but failed *in vivo* (148) (149) (150).

2.5 Cancer

The terminus 'cancer' covers all types of abnormal, neoplastic malignancies from different types of tissues. Nearly all types of tissues can develop such malignancies and some tissues even multiple different types. While most cancers are denominated by their sites of origin like colorectal cancer or pancreatic cancer, different types of cancer can also be determined by the cells or tissue they arose from (151) (152). Carcinomas sprouting from epithelial cells are by far the most frequent type of cancer and can be subdivided into adenocarcinomas (origin from mucus- or fluid-producing cells), basal cell carcinomas, squamous cell carcinomas and transitional cell carcinomas usually descend from the urogenital tract. Sarcomas are malignancies of bones and other connective tissues like muscles, tendons, fat or blood vessels. Uncontrolled cell growth of B- or T-lymphocytes are called lymphoma, while leukaemia, the most common cancer in children, originates from blood cell forming bone marrow and is characterized by large numbers of non-functional leukocytes. Leukaemia can be separated into acute and chronic forms and depending on the cells of origin in myeloid and lymphoblastic leukaemias with acute lymphoblastic leukaemia (ALL) being the most frequent one (153). Multiple myelomas are neoplasia of plasma cells while melanomas originate from melanocytes.

Today, cancer-related deaths are the second most common course of death in Germany with almost 240,000 cases per year and only diseases of the coronary system outperform this. In 2018, more than half a million people got diagnosed with cancer (154). Globally, this number even exceeds 9 million new cases per year (155). The cumulative incidence worldwide to evolve cancer during a lifespan of 74 years is for both sexes combined about 20% and in highly developed industrial countries in Eastern Europe even about 25%, meaning that every 4^{th} person in Germany is likely to develop cancer throughout their lifetime. In males, lung and prostate cancers are the most common types of cancer, while females predominantly suffer from breast cancer, followed by colorectal and lung cancer. These numbers show strong evidence of the need for new therapeutic opportunities and fundamental research in the field of malignant neoplasia.

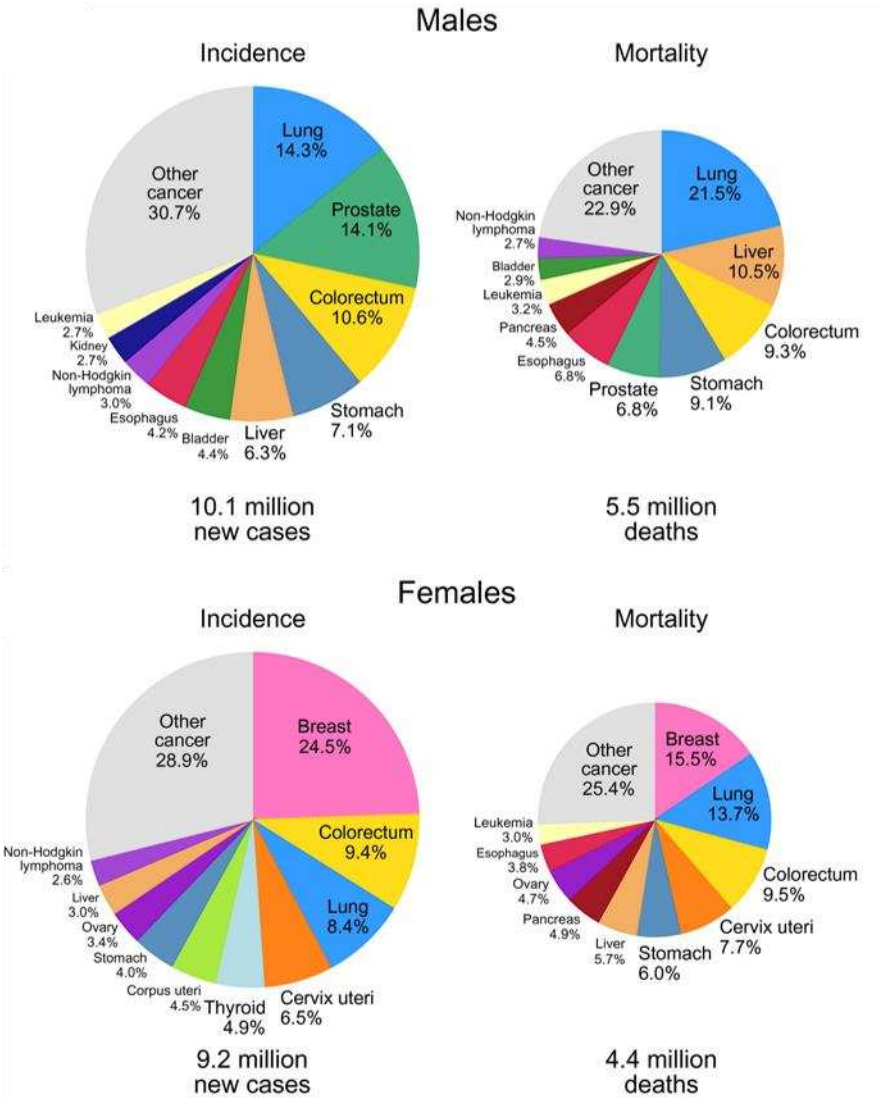

Figure 2.3 Incidence and mortality of cancer in 2020. *Figure taken and modified from (155).*

In 2000, Hanahan et al. postulated in 'Cell', that even though more than 100 types of cancers and many different subtypes are known so far, cancer always maintains an alteration of cell proliferation and homeostasis and can be determined by six distinct hallmarks; self-sufficiency in growth signals, insensitivity to growth-inhibitory (antigrowth) signals, evasion of programmed cell death (apoptosis), limitless replicative potential, sustained angiogenesis, as well as tissue invasion and metastasis (**Figure 2.3**) (156). In general, these properties can be gained by mutations either in tumour suppressor genes and/or in proto-oncogenes. Usually, numerous of those mutations occur in one cell and cumulatively lead to tumourigenesis (157). As the integrity of DNA is one of the best-protected features within each cell, a first mutation at some point of the DNA surveillance and repair machinery - known as 'genomic instability' - is of need, if tumourigenesis is to take place (158).

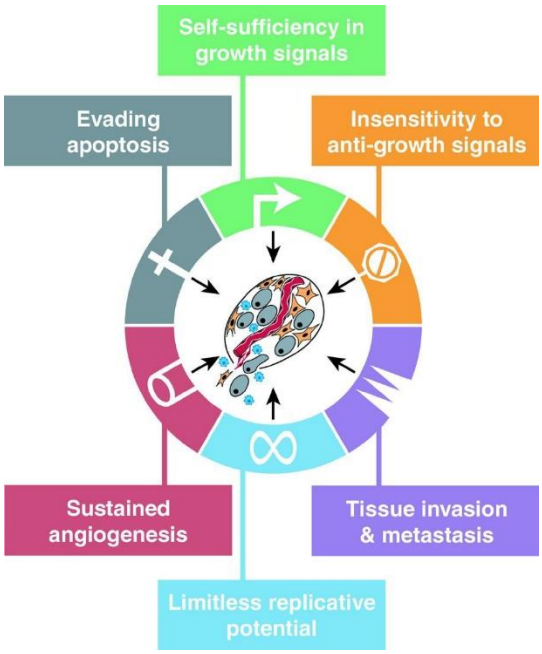

Figure 2.4 The hallmarks of cancer. *Figure taken from (156).*

2.5.1 Self-sufficiency in growth signals

In healthy tissues, cell proliferation is a tightly regulated process. Different ligands mediating growth signals bind extracellularly to transmembrane receptors and initiate intracellular signalling cascades. These ligands comprise signalling molecules like growth factors, components of the extracellular matrix (ECM) and cell-cell-adhesion as well as -interaction molecules. In some tumours, growth factor receptors fulfil the initiation of intracellular signalling independent of these physiological ligands. Three different mechanisms are known that result in growth signal autonomy. Some types of cancer cells can create a positive feedback loop by synthesising and secreting their own growth signals for autocrine stimulation to take place (159). An example are sarcomas which are known to produce platelet-derived growth factors (PDGFs) for such purpose (160) as well as TGF-α producing gliomas (161). The second point of action is the receptor itself. Often, growth factor receptors are tyrosine kinases and mediate their action after ligand binding and dimerization of the receptor by auto-phosphorylation of a tyrosine residue and subsequent phosphorylation and activation of different proteins of the signalling cascade. In cancer, those receptors can either be over-expressed resulting in hypersensitivity to physiological growth signals or structurally modified resulting in ligand-independent activation. Alterations in growth factor receptors that have been found in many types of tumours can be mediated by different stimuli like the human papillomavirus and are connected to a poor prognosis for the patients (162) (163) (164) (165). Also, the type of receptors expressed on the cell surface can be altered. Integrins are receptors that link cells to extracellular matrix structures and by this receive and cascade information from the cells' environment to the inside. Subtypes preferring growth-stimulating signals are over-expressed in multiple types of cancers (166) (167) (168). As integrins are a broad

family of cellular molecules, they can pass a variety of information and participate not only in cell proliferation but also in resistance to apoptosis, metastasis and angiogenesis (169) (170) (171) (172). The third main player in the self-sufficiency of growth signals is the intracellular signalling cascade. Most prominent is the Ras/Raf/MEK/ERK-pathway that is altered in more than every 3rd tumour resulting in uncontrolled transition of growth signals (173) (174) (175) (176).

2.5.2 Insensitivity to anti-growth signals

Quiescence is a reversible cellular condition that a lot of cells exhibit due to different environmental influences or distinct cellular functions. In this state, cells exit the proliferative phase but remain ready to re-enter if needed. Usually, quiescence is associated with a G0-arrest mediated by different stimuli (177) (178). Those signals can be the privation of mitogenic factors, lacking cell adhesion as well as high cell density (contact inhibition). All these factors can be present in tumours, so cancer cells need to develop mechanisms to evade these signals. For receiving anti-proliferative signals, the retinoblastoma protein (pRB) and its family members p107 and p130 play a crucial role. Their main duty is to regulate the activity of the transcription factor E2F and by this control the cell cycle progression (179). pRB was the first discovered tumour suppressor and its loss of function accounts for 30% of all non-small cell lung cancers, 50% of multiple myeloma and almost all cases of small cell lung cancer and retinoblastoma in children (180). A potent regulator of this machinery is transforming growth factor β (TGF-β). This cytokine controls a multitude of cellular processes. Its anti-proliferative action is proceeded by mediating the dephosphorylation of pRB and p130 via p15 and p21 upregulation and by this, reinforcing the complexation of dephosphorylated pRB with E2F (181) (182). In tumours, this regulatory mechanism can be dysregulated in different ways. TGF-β receptors (TGFBR) can be either downregulated or mutated to prevent binding and anti-proliferative signalling (183) (184) (185) (186). Additionally, mutations of Smad4, a downstream transducer of TGF-β signalling, p15 and pRB itself occur which result in uncontrolled proliferation and contribute to tumourigenesis (187) (188) (189) (190). Another process inhibiting cell proliferation is the terminal differentiation of cells that can be regarded as the respective opponent mechanism. Here, cells enter a post-mitotic state and lose their proliferative properties (191). One well-known regulator of quiescence is c-myc, a proto-oncogene regulating the activity of Mad/Max complexes (192) (193). These complexes induce final differentiation but over-expression of c-myc inhibits this machinery and withholds the cells in the proliferative state and by this, contributes to cancer initiation and progression (194) (195) (196) (197).

2.5.3 Evading apoptosis

Apoptosis, known as programmed cell death, is one of the most crucial physiological processes needed for a multitude of purposes such as embryogenesis, homeostasis,

proper function of the immune system, and certainly, prevention of tumourigenesis (198). Evading this process for the most part results in cancer. If any type of apoptosis-inducing signal appears, a complex machinery launches and - in a multi-step process - a cell with all its compartments completely disappears within less than a day. This elaborate process is regulated by sensor molecules and mediated by effectors with both classes providing a potential point of attack for tumour cells. Via the extrinsic pathway, apoptosis-inducing signals can be mediated by different cell surface receptors binding specific extracellular ligands. The tumour necrosis factor (TNF) superfamily provides different receptors that recognise ligands inducing apoptosis such as FasL, TNFα, Apo2L and Apo3L (199) (200) (201) (202). Upon binding of the specific ligands, intracellular proteins like FADD or TRADD, possessing a death domain, bind to the respective receptor and form a death-inducing complex that activates procaspase-8 and initiates the subsequent cascade (203). Alterations in all of the previously mentioned players destabilise this tightly regulated process and, in most cases, contribute to malignant processes (204) (205). In contrast to this, apoptosis can also be mediated via the intrinsic pathway. Different stimuli act receptor-independently as initiators of the programmed cell death in either a positive or a negative fashion. Positive signals are stress sensors that recognize and circulate harmful processes like radiation, redox tonus, different toxins or hypoxia (206) (207) (208) (209). Negative signals cover the absence of certain signal molecules, cytokines or growth factors (210). If activated, the intrinsic apoptotic pathway acts on the mitochondria that subsequently release cytochrome c which activates the caspase machinery and just like the extrinsic pathway launches the execution pathway leading to exhaustive cell disaggregation. The most prominent regulator of this process is tumour suppressor p53 also regarded as the 'guardian of the genome' (211). In each one of two examined tumours, p53 is mutated showing its relevance in apoptosis and tumourigenesis (212). The most recently elucidated perforin/granzyme pathway is another starting point for the induction of apoptosis. This pathway is initiated by cytotoxic T-cells via secretion of the membrane-disaggregating protein perforin and granzymes, a group of serine-protease enzymes able to cleave cell components (213). A crucial role of this pathway is to eliminate infected cells as well as an immune response to degenerated cells (214). Reduced expression of the components is connected to tumourous malignancies like lung cancer (215).

2.5.4 Limitless replicative potential

In 1961, gerontologist Leonard Hayflick together with cytogeneticist Paul Moorhead published a science revolutionising work on the cultivation of human cells. They were the first to discover that in contrast to cancer cells, healthy human fibroblasts stopped proliferating after a precise number of replications – today known as the Hayflick limit (216). They divided culturing of cells into three phases with phase III being characterised by senescence of the cells. If this state is reached once, no further proliferation could be induced. This heavily contradicts the unlimited capability of (cultured) cancer cells to divide which determines their immortality. Hayflick could also show, that this limited

capacity to replicate is not determined by extracellular factors but by the cell itself and that this feature cannot be manipulated e.g., by freezing the cell. Additionally, it was clear that this limitation is not time-dependent but is hooked on the number of DNA replications. Later it was found that the so-called telomeres communicate this effect, known as the end-replication problem. During DNA replication, duplication of the very end of the antisense strand is not thoroughly fulfilled (217). By this, with every DNA replication, chromosomes decrease in size (around 100 bp) which limits the number of possible replications as, if all of the telomeres were lost and chromosomal ends were unprotected, they undergo end-to-end chromosomal fusions and thus provoke cell death. Immortal tumour cells found a way to evade this process. An enzyme possessing reverse transcriptase ability called the telomerase is responsible for extending the telomeres, consisting in humans of plenty repeats of GGTTAG, to the chromosomes. In healthy organisms, this protein can only be found in germline and other stem cells providing them with immortality while all other cells repress its transcription by the chromatin environment. Though, in the great plurality of human cancers examined, telomerase activity could be confirmed giving the solution for the limitless replicative potential of tumour cells (218) (219) (220).

2.5.5 Sustained angiogenesis

Growing tumours face one major problem during their evolution. If the sheer mass of the tumour increases, fewer nutrients and oxygen are available, and distribution of these rare nutritive substances is hard to perform within the tumour body. In healthy tissue, no cell is further than 100 µm distant from a blood vessel supplying it with sufficient nutrients (221). In sound growing tissues this condition is ensured by tightly regulated angiogenesis, a multifactorial program that controls the development of new blood vessels. This process is initiated by cytokines like vascular endothelial growth factor (VEGF) that bind to the respective receptors (VEGFRs), possessing tyrosine kinase activity, on the cell surface of endothelial cells. Upon activation, intracellular transphosphorylation launches different subsequent signal cascades that result in different effects like increased vascular permeability and survival as well as migration and enhanced proliferation of endothelial cells (222). Thrombospondin-1, an ECM protein, and the main opponent of VEGF, prevents neovascularization by binding to CD36 receptors on the surface of endothelial cells (223) (224). Apart from that, other mechanisms and molecules are known that regulate angiogenesis in humans (225). This narrow interaction of pro- and anti-angiogenic stimuli ensures proper vascularisation in healthy organisms. By a multitude of tumours, this regulation is manipulated to ensure sufficient nutritional maintenance. Like for other neoplastic processes described earlier either positive regulators can be over-expressed or negative players downregulated. And in fact, in pancreatic, breast and hepatic cancer as well as other neoplasia, over-expression of VEGF could be detected and is usually connected to poor prognosis for the patients (226) (227) (228) (229). This elevated VEGF secretion of tumour cells can often be mediated after the stimulus of hypoxia and is carried out via the HIF-1α pathway (230). Additionally, elevated levels of VEGFRs, as well

as suppression of thrombospondin-1, could be elucidated as mechanisms for enhanced angiogenesis during tumourigenesis (231) (232) (233) (234) (235).

2.5.6 Tissue invasion and metastasis

Neoplasia in general can be divided into two groups: benign and malignant growth. What differentiates them the most, is the capability to invade other tissues and spread all over the body (236). While benign tumours are characterised by only one location and distinct borders that separate them from the surrounding tissues, malignant tumours on the contrary are able to leave their site of action either into the surroundings or even to other parts of the body worsening the prognosis drastically. In fact, about 67% of all cancer deaths can be correlated to metastasis that evolved from the original tumour (237). Drivers for this course are deficiency of oxygen and nutrients in the primary tumour mass that encourage tumour cells to undergo epithelial-to-mesenchymal transition (EMT) and spread over the body to find a new location with a sufficient supply of aforesaid matters (238). This process of unhitching from the tumour mass and invading new areas is an extremely complex process regulated by numerous factors. Changes in the expression of extra- and intracellular molecules are needed to perform such tasks. On the cell surface, cell-to-cell adhesion is mostly mediated by specialised cell adhesion molecules (CAMs) while adhesion to the ECM is performed by integrins (239). Besides, both types of surface proteins also circulate information from the cells' environment and need to be altered for the cell to loosen and become independent. E-cadherin is one of the most prominent CAMs of epithelial cells and a well-known marker for EMT. During this multifactorial process, expression of E-cadherin is strongly decreased, and this loss of expression is present in most metastatic tumours (240). In contrast, another CAM named N-cadherin is upregulated during EMT which describes the 'cadherin switch' characteristically during EMT. Its function is to enhance tumour cell migration and proliferation at the new site of action (241). Additionally, integrin classes switch to enable cell adhesion at a different site with changed ECM molecules (167). Another substantial process for invading the surrounding tissue is the degradation of the environmental ECM that allows cells to move from their distinct location to another (242). By expressing different types of proteases and other enzymes, migrating tumour cells can overcome almost every obstacle (243). This expression can either be performed by the cancer cell itself or - triggered by the cancer cell - by cells in the tumour environment (244) (245).

In 2011, Hanahan and Weinberg published an update on emerging hallmarks of cancer now also containing deregulation of cellular energetics, as well as avoiding immune destruction, and the two enabling characteristics of tumours: tumour-promoting inflammation and the before-mentioned genomic instability (246).

2.5.7 Reprogramming energy metabolism

Enforced cell proliferation and tumour growth rapidly consume all nutrients available in the tumour surroundings. Besides the before-mentioned evading mechanisms of increased angiogenesis and tumour metastasis, another mechanism was clarified to solve this problem. In cancer cells, a change in the energy metabolism of glucose has been reported (247). The so-called 'aerobic glycolysis' produces less ATP than the physiological glucose metabolism but at the same time scrapes oxygen which is a valuable good. In addition, the decreased yield of ATP is compensated by an upregulation of GLUT1 transporters and thereby enforced glucose uptake (248). Additionally, intermediates of the glycolysis have been shown to be imported into anabolic pathways supplying the cells with amino acids and nucleotides (249). Besides, heterogenic tumours were identified that consisted of different subtypes of cells: cells performing aerobic glycolysis and thereby secreting lactate as a waste product and a second type of cell with altered energy metabolism that consumes the lactate in order to generate energy (250). This symbiosis is an exemplification of the rather recently elucidated model of complex tumours consisting of a variety of different cells (251). Another mechanism of altered cell metabolism can be found in cells expressing mutant isocitrate dehydrogenase manipulating the citrate cycle (252).

2.5.8 Evading immune destruction

In recent years, numerous articles were published, which discuss the connection between tumourigenesis and the innate and adaptive immune system. As it is known that every 4th tumour is associated with chronic inflammation mediated by the immune system, this connection seems reasonable (253). Nevertheless, the immune system seems to play a controversial role in cancer progression. While chronic inflammation establishes an improved matrix for tumourigenesis, simultaneously the immune system tries to fight malignancies (254). As all cells in the body are constantly monitored by the body-own defence mechanisms, under normal circumstances malignant cells are easily identified by the expression of unphysiological e.g., mutated proteins. Once intracellularly digested and presented in MHCI molecules on the cell surface, abnormal proteins are identified by cytotoxic T-cells and an adaptive immune response leads to the disposal of the affected cell (255). Tumour cells must somehow find a way, to escape this surveillance system and different of these ways are known by now. Mutations in the antigen-presenting MHC molecules and over-expression of PD-L1 (programmed cell death 1 ligand 1), a transmembrane protein, that binds to PD-1 (programmed cell death protein 1) receptors on T- and B-cells and suppresses the immune response of those cells, are ways to reduce the immune response (256) (257). Also, enhanced secretion of immune modulators like IL-10 and TGF-β have been identified as immune escape mechanisms (258) (259). Additionally, the tumour microenvironment can strongly influence the immune response to tumour cells and the presence of immunosuppressive leukocytes has been shown in multiple tumours (260).

Besides, multiple other features are known by now, that enable, support, or even reinforce tumourigenesis, making it one of the most complex and multifactorial biological processes of all.

2.6 5-LO and cancer

Besides all previously mentioned illnesses like asthma, atherosclerosis, fibrosis or systemic inflammatory diseases, there is evidence that 5-LO is also involved in carcinogenic events (261). Given its primary expression in leukocytes, it is no surprise that 5-LO and its products participate in different types of leukaemia where they have an impact on cancer stem cells and resistance to certain therapeutic treatments (91) (262) (263).

More surprisingly, it is well known that various solid tumours of different origins such as prostate, breast, pancreas, and colon frequently express 5-LO even though these tissues do not express the enzyme under physiological conditions. In the last years, more and more malignant tissues were identified, that express 5-LO. Here it can be found in different stages of the tumours from primary tumour cells to existent tumour cell lines (264). Additionally, 5-LO expressing tumours are distinguished by increased tumour size, vascularization and metastasis, a potentially poor prognosis regarding the survival expectancy of the patient as well as bad responsiveness to the treatment with cytostatic drugs (265) (266) (267) (268) (269).

Besides the 5-LO enzyme itself, other proteins of the leukotriene cascade are elevated in different solid tumours. FLAP was found to be over-expressed in a multitude of epithelial cancer cell lines and its presence in breast cancer tissues worsened the patients' prognosis just like 5-LO does (270). Expression of the BLT2 receptor in human pancreatic cancers (89), as well as the CysLT2 receptor in colorectal adenocarcinomas (271), was shown to be associated with the same challenges as the presence of LTA_4-hydrolase in oral carcinogenesis of hamsters (272), while $cPLA_2$ and LTC_4-synthase contribute to malignancies of the hematopoietic system (273) (274). In neuroblastoma, the most common paediatric cancer type, the whole cascade of the leukotriene biosynthesis can be found and favours tumour progression (275).

Ancillary, lipid mediators of the 5-LO cascade were shown to stimulate tumour cell viability. Treatment of pancreas carcinoma cells with 5-HETE and LTB_4 leads to pro-proliferative and anti-apoptotic effects via MAPK/Akt signalling (276) (277). The same effects could be observed carried out by LTD_4. After treatment with this lipid mediator, in healthy and malignant intestinal epithelial cells enhanced proliferation and cell survival were shown (278) (279). Tumourigenic effects of 5-LO products could also be affirmed in other approaches using colon carcinoma cells (280) (281). In malignant mesothelioma, LTA_4 and its progenitor 5-HETE acted as transcriptional regulators for VEGF and thereby contributed to increased angiogenesis (269). On its part, LTB_4 carried out mitogenic and pro-metastatic effects by activation of BLT2 receptors (282).

Supporting these findings, in various studies, cell-cycle arrest and induction of apoptosis could be achieved by treating 5-LO expressing cancer cells with different 5-LO inhibitors (283) (88) (284) (285) (286). AA-861, a selective 5-LO inhibitor, was shown to suppress proliferation in leukeaemic, as well as prostate, oesophageal and breast cancer cells (287) (288) (289), while MK-886, a FLAP inhibitor, induces apoptosis in prostate and gastric cancer (290) (291) (292). Comparable results could be shown for the dual 5-LO inhibitor and CysLT receptor antagonist Rev-5901 which induced apoptosis in different human as well as rodent cell lines, and *in vivo* attenuated tumour growth in a mouse model (88) (293) (294) (275). Besides induction of apoptosis, LTB_4 receptor antagonist LY293111 was also shown to mediate cell cycle arrest in pancreatic tumour cells (295) (296). However, as comparably high concentrations of the inhibitors were applied and they are known to mediate pleiotropic effects, it is of question if these effects are achieved only by inhibition of the enzymatic function of 5-LO (297) (298) (299) (300) (301) (302) (303).

Also, 5-LO protein expression in the presented tumour cells is rather low compared to physiological amounts in leukocytes which is also true for the enzymatic activity. Nevertheless, previous studies could show, that by knocking down the 5-LO in solid tumour cells proliferation and viability of the cells could be altered (269) (304) (305) (306) (307). Since it is known that 5-LO executes various non-canonical functions independent of the enzymatic activity, it is conceivable that one or more of those functions or even one yet completely unknown new function of the 5-LO protein is accountable for these findings.

2.7 Non-canonical functions of 5-LO: Interaction with p53, β-catenin and DICER and transcriptional regulation

2.7.1 p53

In 2004, Catalano et al. were the first to propose a connection between 5-LO and p53 since they could show that upregulation of 5-LO resulted in the inhibition of apoptosis (308). This effect could also be achieved by adding 5-LO products but not with an enzymatically inactive mutant form of 5-LO suggesting that this regulation depends on the enzymatic activity of 5-LO. Vice versa, it was shown that p53 in return also regulates 5-LO gene expression (309) (310). By binding to a transcriptional enhancer region in intron G of the *ALOX5* gene, p53 can induce 5-LO expression. This was confirmed by using mutant p53 lacking the ability to bind DNA that did not enlarge 5-LO protein formation. Also, a co-localisation of the two proteins could be detected upon the treatment with cytostatic drugs and 5-LO was shown to alter the expression of p53 target genes giving rise to the assumption that the reciprocal regulation is far more complex than yet known (311).

2.7.2 β-catenin

The Wnt/β-catenin signalling pathway plays an important role in various physiological and pathophysiological processes like proliferation, differentiation, homeostasis, apoptosis, and tumour initiation (312) (313). In different types of leukaemia, a dysregulation of the Wnt/β-catenin pathway could be observed, and this often went hand-in-hand with altered 5-LO expression (314). In fact, it was shown that there is a direct chaperone-like interaction of 5-LO and β-catenin and that this interaction hinders the proper function of β-catenin (262). In addition, there is evidence that in myeloid leukemic stem cells, knockout of 5-LO decreased β-catenin expression and prohibits chronic myeloid leukaemia (91).

2.7.3 DICER

In 1999, various interaction partners of the 5-LO could be identified, using the yeast two-hybrid system (315). Several were further studied in the following years and one of those was the microRNA (miRNA) processing protein DICER (316). miRNAs are a big family of small non-coding RNAs executing various functions of which most are probably still unknown. By binding to mRNAs, they convey translational repression or degradation of their targets. As miRNAs perform such a heterogeneous pool of functions, it is obvious that a protein processing those oligonucleotides can have a great impact on cellular processes. In fact, it was shown, that miRNAs participate in the regulation of the immune system and that alterations in this machinery can result in intensified inflammation and neoplasia (317) (318). Given the fact that 5-LO binds and interacts with DICER and that DICER activity can be modified by 5-LO, 5-LO may intervene in this system as well (319). But since those findings are only confirmed *in vitro* by now, it remains of question, whether this interaction is relevant for physiological and pathophysiological processes.

2.7.4 Transcriptional regulation

Marius Kreiß, a member of our group, recently published his work in which he was able to show how 5-LO can act as a transcriptional regulator in monocytic cells (320). In his study, CRISPR/Cas was used to knockout 5-LO from Mono Mac 6 cells, a monocytic cell line, and RNAseq revealed numerous regulated genes. Among them, *PTGS2*, encoding for cyclooxygenase-2 and *KYNU*, encoding for kynureninase, were affected the most by the 5-LO knockout. Other genes were found to be regulated that could cause alterations in cellular processes like immune reactions and cell adhesion, as well as proliferation and differentiation of the cells. As it was shown in a ChIP assay, that 5-LO interacts directly with the euchromatin, it was assumed, that the regulation of transcription is mediated either by binding to transcription factors or acetylated histones.

2.8 Short excursion: Genome editing by CRISPR/Cas technology

In 2012, Emmanuelle Charpentier and Jennifer Doudna discovered a novel technique for genome editing (321) (322). The CRISPR/Cas technology often referred to as a 'genomic scissor', was rewarded with the Nobel Prize for chemistry in 2020. CRISPR is an acronym for 'clustered regularly interspaced short palindromic repeats' and originally this system is used by different bacteria and Achaea species as an immune response to viral infections. Charpentier and Doudna managed to modify this system so that nowadays it can be used to easily modify the DNA of all kinds of species.

In bacteria, former overcome virus infections lead to the incorporation of viral DNA into the host bacterial DNA. These viral sequences are clustered in a so-called CRISPR array and separated by palindromic sequences (323) (324). Once translated to RNA, a complex of an endonuclease and RNase III leads to the segmentation of this RNA molecule into small sections (325). Each section now contains one specialized RNA sequence able to recognize virus DNA called crispr RNA (crRNA) in a complex with the tracrRNA (trans-activating RNA), a second RNA molecule able to bind an endonuclease, and said endonuclease Cas9 (for **C**RISPR-**as**sociated protein 9). These complexes can specifically recognize and cut DNA from already known viruses (326) (327).

Gene technology uses this system in a modified manner. crRNA and tracrRNA are fused to one chimeric RNA molecule - the so-called guide RNA (gRNA) - that can bind a specific DNA locus as well as the needed Cas9 enzyme (328). The Cas enzyme is a two-domain endonuclease and by this, leads to double-strand breaks of the DNA (329). For recognition, the gene locus must possess a PAM (protospacer-adjacent motif) sequence consisting of an NGG sequence at its 3'-site to activate the Cas9 enzyme. The induced double-strand break is recognized by repair machineries and either homology-directed repair (HDR) or non-homologous end joining (NHEJ) is the result (330). NHEJ can result in small mistakes like the insertion, deletion, or substitution of one or more bases and, in the case of a frameshift mutation, can lead to the production of nonsense-mRNA or -proteins and their subsequent degradation (331). On the other hand, HDR can be used for the insertion of a desired sequence into the DNA by providing a template sequence (332).

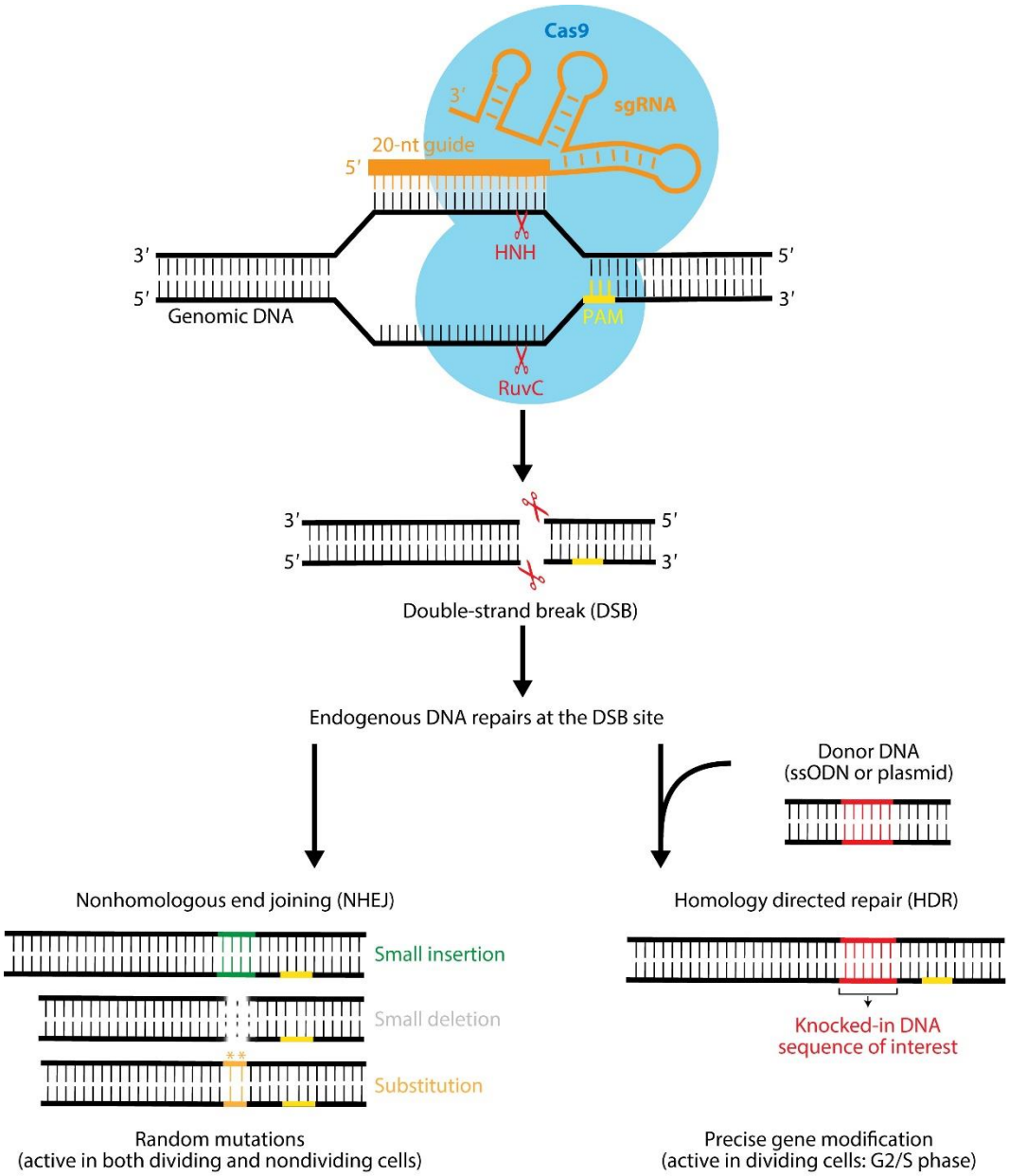

Figure 2.5 CRISPR/Cas9 mechanism. *Figure taken from (333). HNH and RuvC are distinct nuclease domains.*

In this work, CRISPR/Cas technique was used to knock out one specific gene - the 5-lipoxygenase - to investigate the function of the said gene but this technique can have a variety of different applications. CRISPR/Cas technology simplifies the modulation of cellular models as well as transgenic animal models for research purposes and by this, is a major intensifier for fundamental research in genetic diseases (334). In biological approaches, it can be used to enhance, accelerate and facilitate yields of food production or extraction of biological materials for all kinds of purposes addressing some of the biggest current challenges of mankind (335) (336). While drug development is already one of the multiple fields of application, a promising perspective orientation is an application as a therapeutic treatment for genetic disorders (337).

3 Previous work and aim of the study

3.1 5-LO activity in HCT-116, HT-29, and U-2 OS cells is impaired even though the complete LT biosynthesis machinery is expressed

Previous work of our group evaluated the expression of 5-LO in solid tumour cell lines from different origins. Here, the two colorectal cancer cell lines HCT-116 and HT-29, as well as the osteosarcoma cell line U-2 OS and the pancreatic cell line Capan-2 all showed expression of 5-LO even though healthy tissue samples of the same origin do not express any 5-LO enzyme (338).

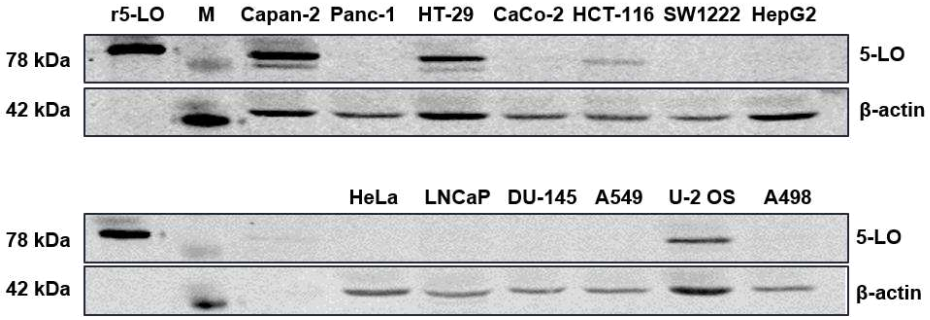

Figure 3.1 5-LO expression in tumour cell lines derived from solid malignancies. *Capan-2 and Panc-1: pancreatic carcinoma, HT-29, CaCo-2, HCT-116, and SW1222: colon carcinoma, HepG2: hepatocellular carcinoma, HeLa: cervix carcinoma, LNCaP, and DU-145: prostate carcinoma, A549: alveolar carcinoma, U-2 OS: osteosarcoma, A498: kidney carcinoma. One representative blot from three individual experiments is shown.*

During her bachelor's and following master's thesis, Tamara Göbel adopted this topic and investigated the expression of the whole leukotriene synthesis machinery. Besides 5-LO, all other enzymes and proteins needed for the biosynthesis of leukotrienes were expressed which was confirmed either at mRNA or at protein level.

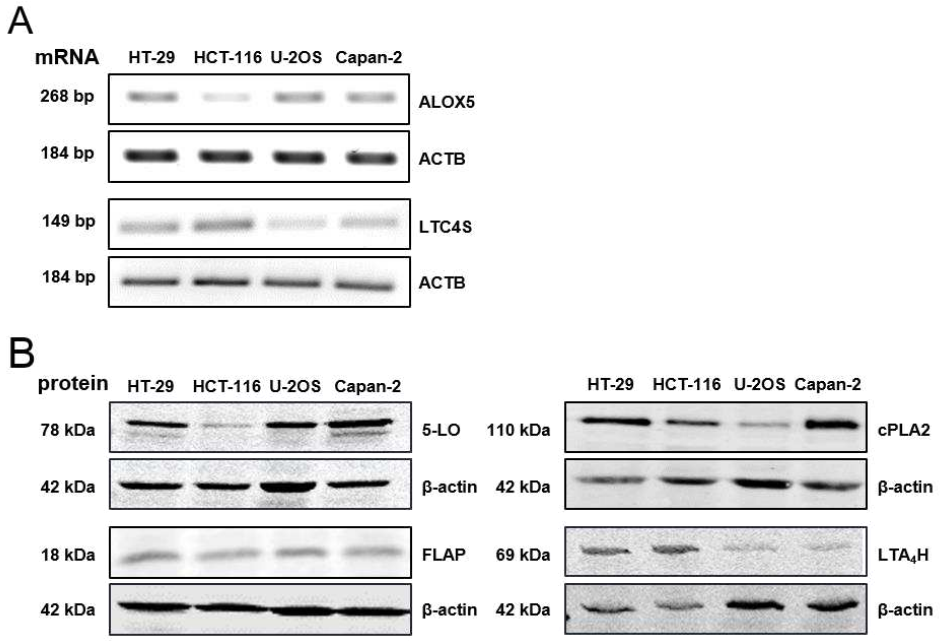

Figure 3.2 Analysis of the leukotriene machinery. *(A) mRNA expression of ALOX5 and LTC_4-synthase (LTC4S) in HCT-116, HT-29, U-2 OS, and Capan-2 cells. (B) Protein expression of 5-LO, FLAP, cPLA2, and LTA_4-hydrolase in the four cell lines. One representative gel, respectively blot, from three individual experiments is shown.*

Since the presence of all enzymes necessary for LT formation was assured, the actual activity of the LT cascade was measured. Intact cells, cell homogenates, and 100,000 x g supernatants were used and 5-HETE and LTB_4 were quantified. For all four cell lines, lipid mediator production was the lowest in stimulated intact cells, while cell homogenates and moreover using the 100,000 x g supernatants led to higher amounts of formed lipid mediators. Except for Capan-2 cells, LTB_4 could hardly be measured in any cellular state. 5-HETE production was rather low in intact cells but could be increased by disrupting cell integrity. As a reference, polymorph nuclear leukocytes (PMNL) were used as they are known to possess a strong 5-LO activity. In those, disruption of the cells led to no increase in the enzymatic activity.

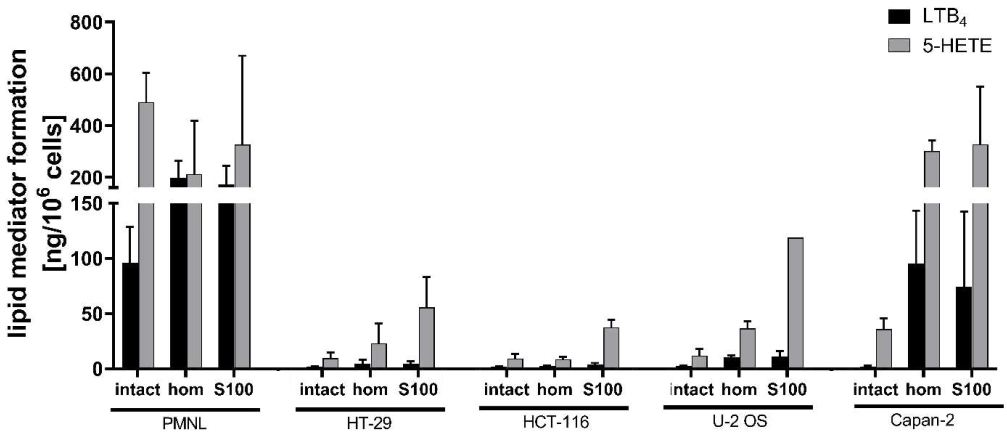

Figure 3.3 Lipid mediator formation in solid tumour cell lines. *Comparison of LTB_4 and 5-HETE formation in intact cells, cell homogenates, and 100,000 x g supernatants (S100) of human PMNL, HT-29, HCT-116, U-2 OS, and Capan-2 cells. The cells were incubated in PGC buffer supplemented with 20 µM AA and 1 mM Ca^{2+}. For the formation of 5-LO products, the intact cells were stimulated with Ca^{2+} ionophore (A23187, 2.5 µM). The broken cell preparations received 1 mM ATP instead. The samples were then incubated for 10 minutes at 37 °C and lipid mediator formation was analysed by LC/MS-MS. The values represent the mean + SD of 3-11 independent experiments. Intact: intact cells, hom: cell homogenates, S100: 100,000 x g supernatants.*

As it is known that cellular localization is a potent regulator of the 5-LO activity, immunostainings of 5-LO were prepared and examined via confocal microscopy. In the two colorectal cancer cell lines HT-29 and HCT-116, 5-LO was almost exclusively located in the cytosolic compartment while U-2 OS and Capan-2 cells showed a completely even distribution of 5-LO between cytosolic and nuclear compartments.

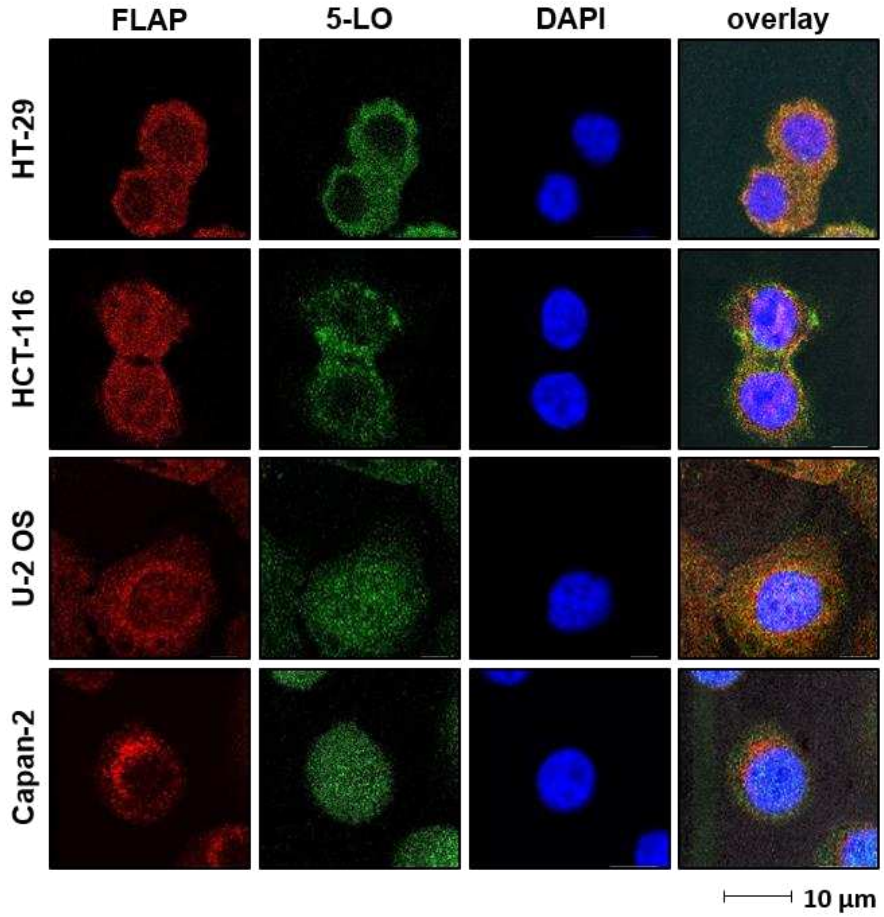

***Figure 3.4 Cellular localisation of 5-LO in 5-LO expressing tumour cells**. Immunostaining and confocal microscopy analysis of cellular localization of 5-LO and FLAP in HT-29, HCT-116, U-2 OS, and Capan-2 cells. DAPI was used for nuclear staining. Images were acquired by a Leica TCS-SP5 confocal microscope (Leica, Wetzlar, Germany) and elaborated using LAS X software (Leica, Wetzlar, Germany). One representative picture from three individual experiments is shown.*

3.2 Aim of this study

All in all, it was shown that all chosen solid tumour cell lines express the complete leukotriene cascade but produce only small amounts of lipid mediators.

Since decent levels of 5-LO protein are expressed in all investigated tumour cell lines, these findings lead to the assumption, that 5-LO expression provides some benefit for those tumour cells. As only small amounts of the lipid mediators are measured, this beneficial function is most probably independent or at least partly independent from the formation of such lipids. Until now, little is known about the functional consequences of 5-LO expression in solid tumour cells. All conducted studies so far used different knockdown techniques to investigate functions of 5-LO in tumour cells, but all commonly used knockdown technologies share the disadvantage of a small leftover enzyme expression that could be enough for at least non-canonical functions of 5-LO.

Therefore, this study aimed to:

- Generate different 5-LO expressing cell lines carrying a complete genomic knockout of 5-LO
- Verify the knockout on DNA and protein level
- Investigate differential gene expression induced by the knockout of 5-LO
- Examine functional consequences in the cell lines caused by altered gene expression or other mechanisms mediated by the 5-LO knockout

4 Materials and methods

The following chemicals were used for this work.

Table 4.1 *Chemicals*

Chemicals	Supplier
1,4-Diazabicyclo[2.2.2]octan (DABCO)	Carl Roth, Karlsruhe, Germany
2-Propanol	VWR International, Radnor, USA
5-Fluorouracil (5-FU)	Sigma-Aldrich, St. Louis, USA
Acetic acid	PanReac AppliChem ITW Reagents, Darmstadt, Germany
Acrylamide 4K solution, (30%) Mix 37.5:1	PanReac AppliChem ITW Reagents, Darmstadt, Germany
Actinomycin D (ActD)	Sigma-Aldrich, St. Louis, USA
APS (Ammonium peroxydisulfate)	Carl Roth®, Karlsruhe, Germany
Bromophenol blue	Merck KGaA®, Darmstadt, Deutschland
BSA (Bovine Serum Albumin)	Sigma-Aldrich, St. Louis, USA
Chloroform	PanReac AppliChem ITW Reagents, Darmstadt, Germany
Crystal violet	Merck KGaA®, Darmstadt, Deutschland
4',6-Diamidino-2-phenylindol (DAPI)	Sigma-Aldrich, St. Louis, USA
Dimethylsulfoxide (DMSO)	PanReac AppliChem ITW Reagents, Darmstadt, Germany
Ethanol (EtOH) ROTIPURAN®	Carl Roth®, Karlsruhe, Germany
Ethylenediaminetetraacetic acid (EDTA)	Merck KGaA®, Darmstadt, Deutschland
Etoposide (Eto)	Sigma-Aldrich, St. Louis, USA
Glycerol	PanReac AppliChem ITW Reagents, Darmstadt, Germany
Glycine	PanReac AppliChem ITW Reagents, Darmstadt, Germany
HCl (Hydrochloric acid)	VWR International, Radnor, USA
Methanol (MeOH)	VWR International, Radnor, USA
Mowiol® 4-88	Carl Roth, Karlsruhe, Germany
N,N,N',N'-Tetramethylethylenediamine (TEMED)	PanReac AppliChem ITW Reagents, Darmstadt, Germany
NaOH (Sodium hydroxide) pellets	VWR International, Radnor, USA
NP-40 (IPEGAL CA-630)	PanReac AppliChem ITW Reagents, Darmstadt, Germany
Paraformaldehyde (PFA)	Sigma-Aldrich, St. Louis, USA
Ponceau S	Merck KGaA®, Darmstadt, Deutschland
Propidium iodide (PI)	Sigma-Aldrich, St. Louis, USA
Puromycin	Enzo Life Sciences GmbH, Lörrach, Germany
Sodium acetate (NaAc)	Carl Roth®, Karlsruhe, Germany
Sodium chloride (NaCl)	PanReac AppliChem ITW Reagents, Darmstadt, Germany

Sodium dodecyl sulfate (SDS)	PanReac AppliChem ITW Reagents, Darmstadt, Germany
Tris-HCl	PanReac AppliChem ITW Reagents, Darmstadt, Germany
Triton® X-100	PanReac AppliChem ITW Reagents, Darmstadt, Germany
Trypan blue	gibco©by life technologies™, Thermo Fisher Scientific Waltham, USA
Tween® 20	PanReac AppliChem ITW Reagents, Darmstadt, Germany
UltraPure™ Agarose	Thermo Scientific™, Waltham, USA
UltraPure™ Distilled Water	Thermo Scientific™, Waltham, USA
β-Mercaptoethanol	Sigma-Aldrich, St. Louis, USA

The following devices, equipment, and instruments were used for this work.

Table 4.2 *Devices, equipment, and instruments*

Device	**Manufacturer**
Bürker counting chamber	Paul Marienfeld GmbH & Co.KG, Lauda-Königshofen, Germany
Centrifuge 5424 R	Eppendorf AG, Hamburg, Germany
CO_2 Incubators, CB 210 E3	BINDER GmbH, Tuttlingen, Germany
FACSDiva™ flow cytometer	BD™ Biosciences, Franklin Lakes, USA
FACSVerse™ flow cytometer	BD™ Biosciences, Franklin Lakes, USA
FCAP Array™ Software (version 3.0)	BD™ Biosciences, Franklin Lakes, USA
FlowJo software (version 10)	BD™ Biosciences, Franklin Lakes, USA
GraphPad Prism (version 8.00)	GraphPad Software, San Diego, USA
HERAEUS LaminAir® HB 2448	Thermo Scientific, Waltham, USA
Heraeus Multifuge X3 FR	Thermo Scientific, Waltham, USA
HERAsafe™ HS 18	Thermo Scientific, Waltham, USA
i-control™ software for Tecan readers	Tecan Trading AG, Männedorf, Switzerland
Illumina NextSeq 2000 Sequencing System	Illumina Inc., San Diego, USA
LAS X software	Leica, Wetzlar, Germany
Leica TCS-SP5 confocal microscope	Leica, Wetzlar, Germany
MicroAmp fast 96-well reaction plates	Applied Biosystems™, Forster City, USA
MIDI 1 Electrophoresis Unit	Carl Roth GmbH & Co. KG, Karlsruhe, Germany
Mini Trans-Blot® Electrophoretic Transfer Cell	BIO-RAD, Hercules, USA
Mini-PROTEAN Tetra Cell	BIO-RAD, Hercules, USA
NanoDrop™ 2000 spectrophotometer	Thermo Scientific, Waltham, USA
Odyssey® 9120 Infrared Imaging System	LI-COR Biosciences, Bad Homburg, Germany
Odyssey® nitrocellulose membranes	LI-COR Biosciences, Bad Homburg, Germany
PeqSTAR 96 Universal Gradient	Peqlab Biotechnologie GmbH, Erlangen, Germany

Power PAC 300	BIO-RAD, Hercules, USA
PowerPac Basic Power Supply	BIO-RAD, Hercules, USA
QuantSeq Bluebee data platform	Lexogen GmbH, Vienna, Austria
Qubit 4 Fluorometer	Thermo Scientific, Waltham, USA
Sanger sequencing	Microsynth AG Balgach, Switzerland
Sigma 3K30	Sigma Laborzentrifugen GmbH, Osterode, Germany
Sonoplus HD 200, sonotrode MS72	BANDELIN electronic GmbH & Co. KG, Berlin, Germany
StepOnePlus™ Real-Time PCR System	Applied Biosystems, Foster City, USA
Tecan infinite® M200 plate reader	Tecan Trading AG, Männedorf, Switzerland
Trans-Blot® Turbo™ Transfer System #1704150	BIO-RAD, Hercules, USA
Varifuge 3.0RS	Heraeus Holding GmbH, Hanau, Germany
Vortex-Genie® 2	Scientific Industries Inc., Bohemia, USA
Zeiss Axio Vert.A1 microscope	Carl Zeiss AG, Oberkochen, Germany
Zeiss LSM 780	Carl Zeiss AG, Oberkochen, Germany
Zen black software (version 2.0)	Carl Zeiss AG, Oberkochen, Germany
Zen blue software (version 2.6)	Carl Zeiss AG, Oberkochen, Germany

The following kits and reagents were used for this work.

Table 4.3 *Kits and reagents*

Kit/Reagent	Manufacturer
10x Annexin V binding buffer	BD™ Biosciences, Franklin Lakes, USA
Agilent High Sensitivity DNA Kit	Agilent Technologies Inc., Santa Clara, USA
Agilent RNA 6000 Nano Kit	Agilent Technologies Inc., Santa Clara, USA
Annexin V – (FITC/APC)	BD™ Biosciences, Franklin Lakes, USA
BD FACSFlow™	BD™ Biosciences, Franklin Lakes, USA
CBA Human Fractalkine Flex Set	BD™ Biosciences, Franklin Lakes, USA
CBA Human MCP-1 Flex Set	BD™ Biosciences, Franklin Lakes, USA
Calcein-AM	Merck KGaA®, Darmstadt, Deutschland
Cell proliferation reagent WST-1	Sigma-Aldrich, St. Louis Missouri, USA
CellTiter-Glo® 3D Cell Viability Assay	Promega Corporation, Madison, USA
cOmplete™ Mini, EDTA-free Protease Inhibitor Cocktail	Roche Diagnostik GmbH, Mannheim, Germany
DNase I, RNase-free	Thermo Scientific™, Waltham Massachusetts, USA
DuoSet ELISA Ancillary Reagent Kit 2	R&D Systems Inc., Minneapolis, USA
EveryBlot blocking buffer	BIO-RAD, Hercules, USA
Fc blocking reagent	Miltenyi Biotec B.V. & Co. KG, Bergisch Gladbach, Germany
Gel Loading Dye, Purple (6X)	New England BioLabsRInc., Ipswich Massachusetts, USA
GeneRuler 100 bp DNA Ladder	Thermo Scientific™, Waltham Massachusetts, USA
High-capacity RNA-to-cDNA™ Kit	Thermo Scientific™, Waltham Massachusetts, USA
Human PDGF-AA DuoSet ELISA	R&D Systems Inc., Minneapolis, USA

Human Soluble Protein Master Buffer Kit	BD™ Biosciences, Franklin Lakes, USA
Lipofectamine LTX with Plus Reagent	Thermo Scientific™, Waltham Massachusetts, USA
Matrigel®	Corning Incorporated, New York, USA
PageRuler™ Prestained Protein Ladder	Thermo Scientific™, Waltham Massachusetts, USA
PhosSTOP™, Phosphatase Inhibitor Cocktail	Roche Diagnostik GmbH, Mannheim, Germany
Phusion® High-Fidelity DNA polymerase	New England Biolabs, Ipswich, USA
Pierce™ BCA Protein Assay Kit	Thermo Scientific™, Waltham Massachusetts, USA
PowerUP SYBR Green mix	Thermo Scientific™, Waltham Massachusetts, USA
QuantSeq 3'mRNA-Seq Library Prep Kit FWD for Illumina	Lexogen GmbH, Vienna, Austria
RiboRuler High Range RNA Ladder	Thermo Scientific™, Waltham Massachusetts, USA
RNase A, DNase and protease-free (10 mg/mL)	Thermo Scientific™, Waltham Massachusetts, USA
RNeasy Plus Kit	Qiagen Inc., Germantown, USA
RSB buffer	Illumina Inc., San Diego, USA
TGF beta-2 Human ELISA Kit	Thermo Scientific™, Waltham Massachusetts, USA
Trans-Blot Turbo RTA Mini 0.2 µm Nitrocellulose Transfer Kit, for 40 blots #1704270	BIO-RAD, Hercules, USA
TRIzol™ Reagent	Invitrogen™, Carlsbad, USA

4.1 Cell culture

4.1.1 Cell culture material

The following media and reagents were used for cell culture work.

Table 4.4 *Cell culture media and chemicals*

Media and Reagents	Supplier
DMEM, no phenol red	gibco© by life technologies™, Thermo Fisher Scientific, Waltham, USA
DMEM, powder, high glucose, pyruvate	
Dulbecco's Phosphate-Buffered Saline (PBS)	
Dulbecco's Modified Eagle Medium (DMEM)	
Fetal bovine serum (FBS)	
Fetal bovine serum (FBS)	Capricorn Scientific GmbH, Ebsdorfergrund, Germany
McCoy's 5A (Modified) Medium	gibco© by life technologies™, Thermo Fisher Scientific, Waltham, USA
Opti-MEM™ Reduced Serum Medium	
Penicillin-Streptomycin (10,000 U/mL)	
Sodium Pyruvate (100 mM)	
StemPro™ Accutase™ Cell Dissociation Reagent	
Trypsin/EDTA Solution (TE), 0.5% (10x)	

The following material was used for cell culture work.

Table 4.5 *Cell culture material*

Cell culture material	Supplier
8-well Nunc™ Lab-Tek™ II CC2™ Chamber Slide System	Thermo Scientific™, Waltham Massachusetts, USA
96-Well black bottom plate	Thermo Scientific™, Waltham Massachusetts, USA
Bio-One ThinCert™ Tissue Culture	Greiner Bio-One International GmbH, Kremsmünster, Austria
CELLSTAR® Cell culture flasks 250 mL, 75 cm^2	
CELLSTAR® Cell culture flasks 50 mL, 25 cm^2	
CELLSTAR® Cell culture flasks 650 mL, 175 cm^2	
CELLSTAR® Multiwell plates 12-well	
CELLSTAR® Multiwell plates 24-well	
CELLSTAR® Multiwell plates 6-well	
CELLSTAR® Multiwell plates 96-well	
CELLSTAR® Reaction tubes 15 mL blue	
CELLSTAR® Reaction tubes 50 mL blue	
Cell strainer EASYSTRAINER KLEIN, 20 µm	

Corning 96-well Spheroid Microplates	Corning Incorporated, New York, USA
Costar® Stripette® 10 mL	
Costar® Stripette® 25 mL	
Costar® Stripette® 5 mL	
Costar® Stripette® 50 mL	
Coverslips	Thermo Scientific™, Waltham Massachusetts, USA
Culture-insert 2-well system for 24-well plates	ibidi GmbH, Gräfelfing; Germany
FACS tubes	ratiolab GmbH, Dreieich, Germany
Microcentrifuge tube 1,5 mL	nerbe plus GmbH & Co. KG, Winsen/Luhe, Germany
Reaction tubes 2 mL	Greiner Bio-One International GmbH, Kremsmünster, Austria
Universal Fit Pipet Tips 10, 100, 1000 µL	Corning Incorporated, New York, USA

4.1.2 Cell lines

All cell lines used were human adherent cell lines derived from different solid tumours and obtained from DSMZ (Deutsche Sammlung von Mikroorganismen und Zellkulturen) or ATCC (American Type Culture Collection; U-2 OS). They were cultured at 37°C in a humidified 5% CO_2 atmosphere and split twice a week. Splitting and seeding were performed under a laminar flow hood.

Table 4.6 *Cell lines*

Cell line	Tissue	Tumour type	Cell culture medium
HT-29	Colon	Adenocarcinoma	McCoy's 5A (Modified) Medium supplemented with 10% (v/v) fetal bovine serum, 100 µg/mL penicillin-streptomycin, and 1 mM sodium pyruvate
HCT-116	Colon	Carcinoma	Dulbecco's Modified Eagle Medium (DMEM) supplemented with 10% (v/v) fetal bovine serum, 100 µg/mL penicillin-streptomycin, and 1 mM sodium pyruvate
U-2 OS	Bone	Osteosarcoma	Dulbecco's Modified Eagle Medium (DMEM) supplemented with 10% (v/v) fetal bovine serum, 100 µg/mL penicillin-streptomycin, and 1 mM sodium pyruvate
Capan-2	Pancreas	Adenocarcinoma	McCoy's 5A (Modified) Medium supplemented with 10% (v/v) fetal bovine serum, 100 µg/mL penicillin-streptomycin, and 1 mM sodium pyruvate
HeLa	Cervix	Adenocarcinoma	Dulbecco's Modified Eagle Medium (DMEM) supplemented with 10% (v/v) fetal bovine serum, 100 µg/mL penicillin-streptomycin, and 1 mM sodium pyruvate

4.2 Generation of 5-LO knockout cells

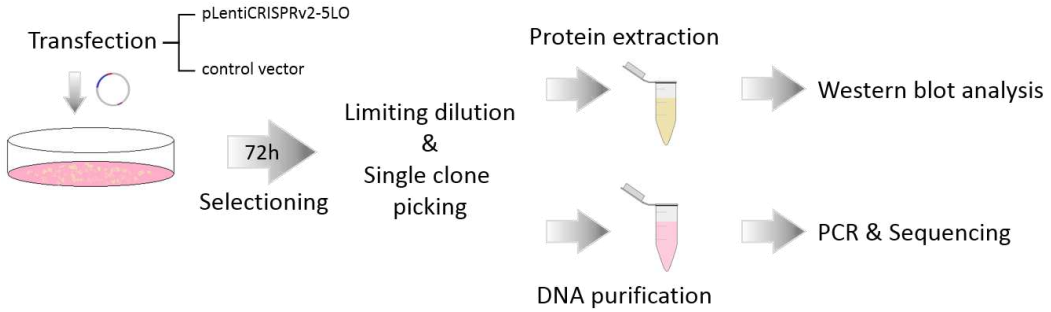

Figure 4.1 Schematic display of the generation and validation of the 5-LO knockout cells.

4.2.1 Transfection

To perform the 5-LO knockout, cells were transiently transfected using Lipofectamine LTX with Plus Reagent with two different CRISPR/Cas-plasmids (pLentiCRISPRv2-5LO-1 and -2, Addgene plasmid #52961, **Figure 4.2**) carrying a gRNA sequence directed to exon 2 (sequence on target: TGGATCACCGGCGATGTCGAGG) or exon 6 (sequence on target: GTGTTGATCCGGCGCTGCAC) of the *ALOX5* gene and a Puromycin resistance provided by Dr. Duran Sürün (Technical University Dresden). An empty vector control plasmid missing the gRNA sequence (pLentiCRISPRv2-NTC1) was used to generate control cells for all experiments.

All three cell lines were seeded in 6-well plates (HCT-116: $6.25*10^5$ cells/well, HT-29: $7.5*10^5$ cells/well, $6.7*10^5$ cells/well). After 24 hours of adhesion, 3.75 µg/well plasmid DNA was added to the plus reagent in Opti-MEM™ Reduced Serum Medium, mixed with equal amounts of LTX reagent in Opti-MEM™, and left for 30 minutes. Cells were washed twice with the medium and incubated with the DNA/LTX-mix suspended in Opti-MEM™ for 6 hours at 37°C, 5% CO_2 in a humidified atmosphere. The DNA/LTX mix was discarded and complete growth medium without antibiotics was added. After 24 hours medium was renewed again and cells were kept for another 48 hours at 37°C, 5% CO_2 in a humidified atmosphere.

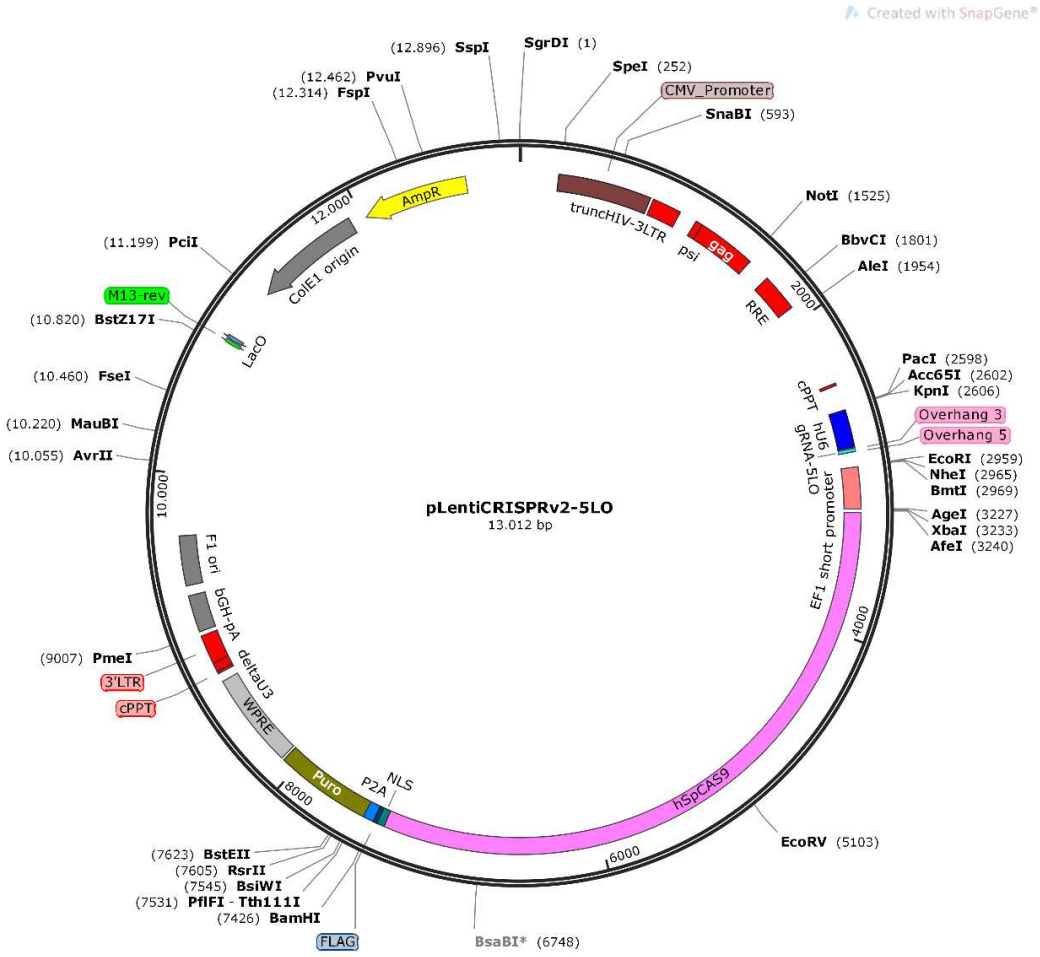

Figure 4.2 Plasmid map of pLentiCRISPRv2-5LO-1.

4.2.2 Puromycin selection and limiting dilution

72 hours after transfection, Puromycin (HT-29: 2 µg/mL, HCT-116, U-2 OS: 10 µg/mL) was added to eliminate all cells not carrying the plasmids. As a control untransfected cells were seeded and treated with Puromycin in the same manner. After 72 hours of incubation at 37°C, 5% CO_2 in a humidified atmosphere supernatants were discarded, cells were washed twice with PBS, detached using TE, and counted. Subsequently, cells were diluted in complete growth medium to receive a suspension containing 1200 cells/mL. In a second dilution step, 200 µL of the cell suspension were further diluted in 12 mL medium, resulting in statistically 2 cells in each 100 µL of the suspension. Cells were seeded in a 96-well plate (100 µL/well) and left for 3 weeks at 37°C, 5% CO_2 in a humidified atmosphere. Cells carrying the control vector were used as mixed clones and no further dilution and selection were performed.

4.2.3 Single clone picking

Plates were examined and all wells only containing one colony were chosen for further procedure. The medium was discarded, cells were washed twice with PBS and 100 µL StemPro™ Accutase™ was added to detach the single clones. Single-cell clones were transferred to one well of a 24-well plate and incubated at 37°C, 5% CO_2 in a humidified atmosphere. Cultures were further expanded until cells were ready for analysis.

4.2.4 Characterisation of 5-LO knockout on protein level

4.2.4.1 Preparation of cell lysates

Cells were detached using TE, centrifuged (2,000 x g, 5 min, 4°C), and washed twice using ice-cold PBS. After each washing step the cell suspensions were centrifuged (2,000 x g, 5 min, 4°C) and the supernatants were discarded. Finally, the cell pellets were resuspended in lysis buffer (composition see Table 4.7) containing protease and phosphatase inhibitors (cOmplete™ Mini, EDTA-free Protease Inhibitor Cocktail, PhosSTOP™, Phosphatase Inhibitor Cocktail) and incubated for 15 minutes on ice. Next, the lysates were frozen at -20°C, quickly thawed, and homogenized using ultrasonication (10% pulse, 3 times for 10 sec). Homogenates were centrifuged (10,000 x g, 10 min, 4°C) to remove the debris, supernatants were transferred to new tubes and protein concentrations were determined.

Table 4.7 *Composition of cell lysis buffer*

Lysis Buffer	
Tris-HCl (pH 7.4)	20 mM
NaCl	150 mM
EDTA	2 mM
Triton-X 100	1%
NP-40	0.5%
Water	ad 100 mL

4.2.4.2 Determination of protein concentrations

Protein concentrations were determined using the bicinchoninic acid (BCA) method employing the Pierce BCA Assay Kit. For this purpose, cell lysates were diluted at 1:10, the assay was conducted according to the manufacturer's protocol and absorbance was measured at 562 nm using a Tecan M200 plate reader.

4.2.4.3 SDS-PAGE and Western blotting

For SDS-PAGE, 10% polyacrylamide gels were used (composition see **Table 4.8**). Protein lysates were diluted with water to a final concentration of 1-3 µg/µL, mixed with 5x loading buffer (table 4.9, plus 10% β-mercaptoethanol), and incubated for 5 minutes at 96°C.

22 µL of the samples were loaded in the gel pockets and proteins were separated by electrophoresis in SDS running buffer (composition see **Table 4.9**, 10 min, 80 V followed by 80-95 min, 130 V). For size determination 1 µl of PageRuler™ Prestained Protein ladder was used, and recombinant 5-LO served as a positive control. Afterwards, the separated proteins were blotted onto nitrocellulose membranes in transfer buffer (**Table 4.10**; 225 mA, 80 min).

To prevent unspecific antibody binding membranes were incubated in blocking buffer for 1 hour at room temperature and afterwards incubated with the respective antibodies (**Table 4.11**). Antibodies were diluted in blocking buffer and membranes were incubated overnight at 4°C or 3 hours at room temperature. Following that, membranes were washed three times with TBS/Tween (0.1%) and one time using pure TBS (**Table 4.12**). Secondary antibodies were diluted in blocking buffer and membranes were incubated for one hour at room temperature under light protection. After incubation membranes were washed three times with TBS/Tween (0.1%) and once with TBS. Scanning was performed with an Odyssey Infrared Imaging System.

Table 4.8 *Composition of 10% SDS-gel*

10% SDS-gel			
Running gel (10%)		**Stacking gel (4%)**	
30% AA/Bis-AA (37.5:1)	333.36 µL	30% AA/Bis-AA (37.5:1)	133.39 µL
Tris-HCl (pH 8.8)	253.29 µL	Tris-HCl (pH 6.8)	252.03 µL
SDS 10% (v/v)	10 µL	SDS 10% (v/v)	10 µL
TEMED	1.14 µL	TEMED	1.5 µL
APS	10.29 µL	APS	6 µL
Water	ad 1000 µL	Water	ad 1000 µL

Table 4.9 *Composition of loading buffer and SDS running buffer*

5x loading buffer	
Tris-HCl (pH 6.8)	250 mM
EDTA	5 mM
Glycerol	50% (v/v)
SDS	10% (w/v)
Bromophenol blue	0.05% (w/v)
Water	ad 100 mL

SDS running buffer	
Tris-HCl	25 mM
Glycine	192 mM
SDS	3.5 mM
Water	ad 1000 mL

Table 4.10 *Composition of transfer buffer*

Transfer buffer	
Tris-HCl	24.8 mM
Glycine	192 mM
Methanol	20% (v/v)
Water	ad 1000 mL

Table 4.11 *List of antibodies*

Antigen	Company	Clonality	Species	Dilution
5-Lipoxygenase (66326-1-Ig)	Proteintech, Manchester, United Kingdom	monoclonal	mouse	1:2000
5-Lipoxygenase (ab169755)	Abcam, Cambridge, United Kingdom	monoclonal	rabbit	1:1000
5-Lipoxygenase (160402)	Cayman Chemical, Ann Arbor, USA	polyclonal	rabbit	1:1000
5-Lipoxygenase (610695)	Becton Dickinson BD Biosciences, Franklin Lakes, USA	monoclonal	mouse	1:1000
β-actin (I-19, sc-1616)	Santa Cruz Biotechnology, Dallas, USA	polyclonal	goat	1:5000
β-actin (C-2, sc-8432)	Santa Cruz Biotechnology, Dallas, USA	monoclonal	mouse	1:2000
IRDye 800CW anti-rabbit	LI-COR Biosciences, Lincoln, USA		donkey	1:15000
IRDye 800CW anti-mouse	LI-COR Biosciences, Lincoln, USA		donkey	1:15000
IRDye 680 LT anti-mouse	LI-COR Biosciences, Lincoln, USA		donkey	1:15000
IRDye 680 LT anti-goat	LI-COR Biosciences, Lincoln, USA		donkey	1:15000

Table 4.12 *Composition of TBS buffer*

TBS buffer	
Tris-HCl (pH 7.4)	50 mM
NaCl	100 mM
Water	ad 1000 mL

4.2.5 Characterisation of 5-LO knockout on DNA level

4.2.5.1 DNA isolation and sequencing

Complete knockout of the *ALOX5* gene on all two, respectively three, alleles was assured by sequencing of genomic DNA. Therefore, cells were detached using TE, counted, and 10^7 cells were centrifuged, the supernatant was discarded, and cells were resuspended in

1 mL of TRIzol reagent. Subsequently, DNA was isolated according to the manufacturer's protocol, and parts of exon 2 or exon 6 of the *ALOX5* gene (depending on the CRISPR/Cas guide RNA used) were amplified using polymerase chain reaction (PCR) technique (primers see **Table 4.13**, composition and program see **Table 4.14**). The resulting PCR products were purified, and DNA sequences were analysed by Sanger sequencing using the respective forward primers.

Table 4.13 *Primers for validation of genomic knockout of 5-LO*

		Binding site	sequence	Tm[°C]	manufacturer
HW_001	fwd	exon 6	GGCCAGCTCAGGTATGATGA	59.4	Eurofins Genomics GmbH, Ebersberg, Germany
HW_002	rev	exon 6	CTGCAGTTAGCGTCTTGGTG	59.4	
HW_3	fwd	exon 2	ACAAAGGCTCAGGAGACCAC	59.4	
HW_4	rev	exon 2	GAACTTTCGGTTCTTGGGAAGC	60.3	
HW_5	fwd	exon 2	CATTGTGGGGATCCACTGTCA	59.8	
HW_6	rev	exon 2	AGGAGAACAGGCAATCAGGC	59.4	
HW_7	fwd	exon 2	GGTCGTAGCACTGAGCCTTG	61.4	
HW_8	rev	exon 2	TACAGTGCTTTGAGGACAGGAA	58.4	

Table 4.14 *Composition of PCR mix and PCR program for validation of genomic knockout of 5-LO*

PCR Mix	
dNTP mix (10 mM)	1 µL
Template gDNA	0.25 µg
Forward primer	2.5 µL
Reverse primer	2.5 µL
5x Phusion buffer	10 µL
Phusion polymerase	0.5 µL
Water	ad 50 µL

PCR program		
98°C	30 sec	
35 cycles:	98°C	10 sec
	69°C	15 sec
	72°C	30 sec
72°C	5 min	

4.3 RNA sequencing

RNA sequencing was performed with the kind help of Marius Kreiß (our group) and Silvia Rösser from the group of Dr. Tobias Schmid at the department of Patho Biochemistry, University Hospital Frankfurt.

4.3.1 RNA isolation

As RNA with excellent quality is required for RNA sequencing, total RNA from $5*10^6$ cells per cell line was isolated with the RNeasy Plus Kit from Qiagen according to the manufacturer's manual. This kit also supplies additional columns for gDNA separation, so it is not required to enzymatically deplete DNA. Concentration of RNA samples was determined using a NANODROP2000 spectrophotometer. RNA was stored at -20°C until further use.

4.3.2 RNA quality control

RNA samples were diluted to a concentration of 200 ng/µL and quality control was performed on the Agilent 2100 bioanalyzer using the Agilent RNA 6000 Nano Kit according to the manufacturer's protocol.

4.3.3 Library preparation and amplification

To generate an Illumina compatible library of sequences close to the 3'-end of polyadenylated RNA, RNA samples were diluted to a concentration of 100 ng/µL and library preparation was performed with the QuantSeq 3'mRNA-Seq Library Prep Kit FWD for Illumina by Lexogen according to the manufacturer's protocol.

The optimal number of PCR cycles for the end-point PCR during the library amplification was determined by RT-qPCR. Therefore, a real-time qPCR master mix was added to all RNA samples, and 35 cycles of PCR with the subsequent program were executed (**Table 4.15**, primers see **Table 4.16**). To calculate the optimal number of cycles, the number of cycles to receive 50% of the maximum signal was determined and $\sqrt{3}$ cycles were subtracted as the 10-fold amount of RNA would be used for the end-point PCR. Library amplification was now performed as prescribed in the QuantSeq user's manual.

Table 4.15 *Composition of real-time qPCR mix and qPCR program for determination of optimal cycle number*

Real-time qPCR mix	
PowerUP SYBR Green	10 µL
Fwd primer	0.06 µL
Rev primer	0.06 µL
Water	8.75 µL
cDNA	1.13 µL

Real-time qPCR program		
98°C	30 sec	
35 cycles:	98°C	10 sec
	65°C	20 sec
	72°C	30 sec
72°C	1 min	

Table 4.16 *Primers for Qantseq library generation*

	sequence	**manufacturer**
MK_LexLib_qPCR_fwd	ACACGACGCTCTTCCGATCT	Eurofins Genomics GmbH,
MK_LexLib_qPCR_rev	AGACGTGTGCTCTTCCGATCT	Ebersberg, Germany

4.3.4 Library quality control

Quality control of DNA library samples was performed again on the Agilent 2100 bioanalyzer using the Agilent High Sensitivity DNA Kit according to the manufacturer's protocol.

4.3.5 RNA sequencing

As an equimolar mixture of all DNA libraries was needed for RNA sequencing, in a first step DNA concentrations were measured with the Qubit fluorometer according to the 'Qubit 4 Fluorometer User Guide'. All libraries were mixed according to the average library size and concentration and diluted with RSB buffer (Illumina) to a final concentration of 750 pM. 20 µL of this library mix sample were loaded to the Illumina NextSeq 2000 Sequencing System. 10 cycles for each index sequence and 50 cycles for the actual RNA sequencing were passed.

Analysis was performed with the help of the QuantSeq Bluebee data platform as well as the RSem platform. All genes yielding a log2-fold change higher than 1 and an adjusted p-value smaller than 0.05 were regarded as differentially expressed. Raw data are available under NCBI Sequence Read Archive (accession numbers GSE197947, link https://www.ncbi.nlm.nih.gov/geo/query/acc.cgi?acc=GSE197947).

4.4 RNA isolation and real-time qPCR

On behalf of generating samples for real-time PCR, 10^6 cells were lysed in 1 mL TRIzol reagent, and RNA was isolated according to the manufacturer's protocol. In the last step, RNA was resuspended in 50 µL of ultrapure water and RNA concentration was determined using a NANODROP2000 spectrophotometer.

4.4.1 RNA integrity

To ensure RNA integrity has been maintained, 1 µg of RNA was transferred to a reaction tube and RNase-free water was added to receive a total volume of 2 µL. Next, 2 µL of RiboRuler loading dye were added and the samples were incubated for 10 minutes at 70°C. Samples then were loaded on a 1% agarose gel containing ethidium bromide and separated for 45 minutes at 100 V. RNA integrity was assured by the presence of two distinct bands for the 18S and 28S ribosomal subunit.

4.4.2 DNA depletion

To remove all remaining genomic DNA, 2 µg of the RNA samples were transferred to a reaction tube and 1 µL 10x reaction buffer with $MgCl_2$ for DNAseI as well as 2 µL DNAseI were added, and the mixture was filled with water to receive a total volume of 10 µL. All samples were vortexed and incubated at 37°C for 30 minutes followed by the addition of 1 µL EDTA (50 mM) and another incubation for 10 minutes at 65°C. To precipitate the residing RNA, 1.1 µL 3 M NaAc and 55 µL 100% EtOH were added to the DNAseI digestion and stored overnight at -20°C. The precipitate was purified by centrifugation (12,000 x g, 30 min, 4°C), a washing step with 500 µL ice-cold ethanol (70%), and another centrifugation (12,000 x g, 15 min, 4°C). Finally, the RNA pellet was resuspended in 50 µL ultrapure water and RNA concentration was measured with a NanoDrop 2000 spectrophotometer.

4.4.3 cDNA synthesis

In a final step, mRNA was reverse transcribed to cDNA with the 'high capacity RNA-to-cDNA-Kit'. 2 µg purified RNA were mixed with 10 µL 2x RT buffer, 1 µL reverse transcriptase enzyme, and filled with water to a final volume of 20 µL. This mix was incubated at 37°C for 60 minutes followed by heat inactivation of the enzyme for 5 minutes at 95°C.

4.4.4 Real-time qPCR

For further analysis, cDNA was diluted at 1:10 to yield a final concentration of 10 ng/µL. Real-time qPCR was performed in MicroAmp fast 96-well reaction plates on a StepOnePlus™ Real-Time PCR System with PowerUp SYBR green fluorescent dye, using specific primers for the different targets (composition and program see **Table 4.17**, primers see **Table 4.18**). Data were normalized to *ACTB* and the respective controls using the $2^{-\Delta\Delta CT}$ method. All samples were measured in technical triplicates per run.

Table 4.17 *Composition of real-time qPCR mix and RT-qPCR program*

Real-time qPCR mix	
PowerUP SYBR Green	5 µL
Fwd primer	0.05 µL
Rev primer	0.05 µL
Water	3.9 µL
cDNA (10 ng/µL)	1 µL

Real-time qPCR program		
95°C	10 min	
40 cycles:	95°C	15 sec
	60°C	1 min

Table 4.18 *Primers used for real-time qPCR*

Gene	GeneID (NCBI)	Primer Sequence (5' → 3') fwd	Primer Sequence (5' → 3') rev
ABCC2	1244	CCCTGCTGTTCGATATACCAATC	TCGAGAGAATCCAGAATAGGGAC
ACKR3	57007	CTATGACACGCACTGCTACATC	CTGCACGAGACTGACCACC
ACTB	60	AGAGCTACGAGCTGCCTGAC	AGCACTGTGTTGGCGTACAG
ADGRG1	9289	GAGCCCTCAGAACATCAGCC	AGAGGTCAGTTTCGACTCCAG
ADGRL3	23284	TGAGTCCGACCACCAATCTG	TCATACACTACAAATCCTGTGCC
ADGRL4	64123	CTCAGTCCTGTGGCGAAAATG	GGTTACTGCTGGATCTGAAGC
ADIRF	10974	CAGGAAACCATCGACAAGACTG	TCATTTCAGGAGGCCGAATTTTT
AKAP12	9590	GAGATGGCTACTAAGTCAGCGG	CAGTGGGTTGTGTTAGCTCTTC
ALDH1L1	10840	AGATTGCAGTGATTGGACAGAG	CCAAAGCCTGGTATTTTGCCA
APOBEC3C	27350	CTTGGTTCTGCGACGACATAC	TCCTGGTAACATGGATACTGGAA
APOBEC3F	200316	TTTCTCGTCGGAATACCGTCT	CAAAGGGGCTACTGAGCACTT
APOBEC3G	60489	GCATCGTGACCAGGAGTATGA	GTCAGGGTAACCTTCGGGT
ANK3	288	GAAGATGCAATGACCGGGGA	CTAAAGCCCATGTAACCCTCTG
ARHGEF4	50649	ACCATCTTCGGGAACATCGAG	CTGGAAGTCGGCTTGATGCT
ARPC3	10094	GTGCAATTCCAAAAGCCAAGG	GGCTCTCATCACTTCATCTTCC
ASXL3	80816	AACACCCCAACTCACCAATGA	CATTCAGACAGGCTAATGGAGAG
ATP11C	286410	TGGAGAAGAGAAACGAGTTGGC	GGGCTAGTTGGTGTGTCTACT
BCL2A1	597	TACAGGCTGGCTCAGGACTAT	CGCAACATTTTGTAGCACTCTG
BHLHE41	79365	TTAACCGCCTTAACCGAGCAA	AGTGGAACGCATCCAAGTCG
BMPR1B	658	CTTTTGCGAAGTGCAGGAAAAT	TGTTGACTGAGTCTTCTGGACAA
BST2	684	CACACTGTGATGGCCCTAATG	GTCCGCGATTCTCACGCTT
C1orf198	84886	GTTCAGTATCTCCGCCCTATCC	GGGTCAGCGACTGGAACTC
CCL2	6347	CAGCCAGATGCAATCAATGCC	TGGAATCCTGAACCCACTTCT
CDH6	1004	AGAACTTACCGCTACTTCTTGC	TGCCCACATACTGATAATCGGA
CFI	3426	GGTGAGGTGGACTGCATTACA	CCTCCCACAATTCGTTTCCTTC
CHN1	1123	CCAACTTTATGTGGGGTCTCATT	TTGACATGCTTCAAGTCTGGC
CNN1	1264	CTGTCAGCCGAGGTTAAGAAC	GAGGCCGTCCATGAAGTTGTT
COL8A1	1295	GGGAGTGCTGCTTACCATTTC	AGCGGCTTGATCCCATAGTAG
COL20A1	57642	TGGTGATTCTGGTGACGGAC	CACCCACAGCGAAGACGTT
CPA4	51200	AGGTGGATACTGTTCATTGGGG	TTGCTGATCTCGTCTCCATTTC
CRAT	1384	GTACCACAGTGACGGGACAC	CCGGTTCACCTTGTCTTTGAT
CSAG1	158511	GAGACCAGGTGGACTGGAGTA	TCTTGGGAACCTCTTTGGTGT
CX3CL1	6376	ACCACGGTGTGACGAAATG	TGTTGATAGTGGATGAGCAAAGC
DDIT4	54541	TGAGGATGAACACTTGTGTGC	CCAACTGGCTAGGCATCAGC
DMKN	93099	CAGAGCGGAGAGGAAAGCAC	GCCTCACTGACTTTAGAGCCAG
DOCK4	9732	ATGTGGATACCTACGGAGCAC	CCAATTTCCAATGACAGGCCATA
DRAXIN	374946	CATTGCCCTACCCCGAGAAG	CCCTGCGTCTCTTGTGCTC
DSC2	1824	CCAATTCCTTGTTCGATGCTAGA	GGCCGTGTCAGATTGAACC
EDN2	1907	CGTCCTCATCTCATGCCCAAG	AGGCCGTAAGGAGCTGTCT
ETV1	2115	CTGAACCCTGTAACTCCTTTCC	AGACATCTGGCGTTGGTACATA
EVI2A	2123	GAAGCAATGGCGATTTTCTGG	TTGCATCACTAGGTTGGGTCC
FAP	2191	ATGAGCTTCCTCGTCCAATTCA	AGACCACCAGAGAGCATATTTTG
FAM78A	286336	AGCTCAGCATCGAGGTGAAC	GTTGGCATTGGGCTTGACC
FGD4	121512	TCTCATCAGTCGCTTTGAAGGA	GGGTTCTAGGAGCATTTAGGTTC
FMNL2	114793	CAGGGAGCATGGATTCGCAG	TCAGGAGGTAGGTTCATAGCATT
FOXA2	3170	GGAGCAGCTACTATGCAGAGC	CGTGTTCATGCCGTTCATCC

GALM	130589	CCAGTTCTCGCGCATCAGT	GCCATCCAGGGTGTATGTCA
GPR132	29933	AAAACGGTTACAATGGAAACGC	GAAGGACACGTTGTTGCAGG
HAS2	3037	CTCTTTTGGACTGTATGGTGCC	AGGGTAGGTTAGCCTTTTCACA
HES7	84667	CGGGATCGAGCTGAGAATAGG	GCGAACTCCAATATCTCCGCTT
HIST1H2AC	8334	CTCGCGCCAAAGCGAAATC	CTGCGTAGTTGCCTTTACGGA
HSPA1A	3303	ACCTTCGACGTGTCCATCCTGA	TCCTCCACGAAGTGGTTCACCA
HSPB2	3316	ACCGCCGAGTACGAATTTG	GAGGCCGGACATAGTAGCCA
IFI44	10561	ATGGCAGTGACAACTCGTTTG	TCCTGGTAACTCTCTTCTGCATA
IFI44L	10964	AGCCGTCAGGGATGTACTATAAC	AGGGAATCATTTGGCTCTGTAGA
IGFBP7	3490	CGAGCAAGGTCCTTCCATAGT	GGTGTCGGGATTCCGATGAC
IGFL1	374918	CACAAGAGATGTGGGGACAAG	CACTGCGACAAAGCCTGTCA
IGFL3	388555	TGCTGTCCCGAGTCTTTTGG	ATGGGAGATAAGTGACACTGAGA
ITGA2	3673	CCTACAATGTTGGTCTCCCAGA	AGTAACCAGTTGCCTTTTGGATT
KCNB1	3745	GAGTCCTGGTGATTGCTCTTC	CTCTCGCCGTTTGATTGCTTT
LAMA4	3910	GTGTAGGAATTGCTTACGCAACA	GCTAACCGCAGGTCATCAGT
LAMC2	3918	GACAAACTGGTAATGGATTCCGC	TTCTCTGTGCCGGTAAAAGCC
LEMD1	93273	ATTGCAGAACCAACTTGAGAAGC	CGCGCAGTAGTCTCTCTCTT
LIMS2	55679	GCACCGGCACTATGAGAAGAA	ACGGGCTTCATGTCGAACTC
LIPH	200879	GTCAAGATCAGACGCAGAAGAA	TTTCCTTGTGTAGAGCATCAGC
LLGL2	3993	CGGGACCTGTTCCAGTTTAAC	CGTCACAGCGTTGTTCTCC
LMAN1	3998	AGTGTAGGAGATCGAGAGCTAAG	AGTTCTTGTTGAGTAATCTGCCC
LSP1	4046	AGGACCGAGTCCCTAAACCG	CTGGGTGTATTGTTCCAGCCA
LY6K	54742	ACGGACGAGGGTGACAATAGA	CCGCTATAACGCAGTATGGC
MAP2K6	5608	GAAGCATTTGAACAACCTCAGAC	CCTGGCTATTTACTGTGGCTC
MGST1	4257	ATTGGCCTCCTGTATTCCTTGA	GTGCTCCGACAAATAGTCTGAAG
MISP	126353	TCCCAGTCATCTGATCTGCTG	ATCTGGCGTTGGGGAGAAGA
MLLT3	4300	CAGATTCTGAAGAACTCTCAGCC	GGTGGTGCGCTAGAAAAACTTT
MOB3B	79817	CGGATCAACCTCATCTATGGC	CACCCACGCATGTTGGAAATA
MYL2	4633	TTGGGCGAGTGAACGTGAAAA	CCGAACGTAATCAGCCTTCAG
NAV1	89796	GCCTCAGACAATCTCAGTTCAG	ACCACTGTCGTACTCCAGTTTT
NOSTRIN	115677	CAGAAAGACACAGCAGCGTTA	CAGAAGATGCCTTGCTCACAATA
NOV	4856	CACGGCGGTAGAGGGAGATAA	TGGGCCACAGATCCACTTTTC
OSCAR	126014	CGCTTGGAGATTTGGACTTTTCA	GCAGCGGTAAATTCCCCCTT
PAM	5066	TACCACCAGACCCGTAGTTCC	GTTTAGGTGTAACCCCAGGCA
PAX7	5081	TCCAAGATTCTTTGCCGCTAC	GGTCACAGTGCCCATCCTTC
PBX1	5087	CATGCTGTTAGCGGAAGGC	CTCCACTGAGTTGTCTGAACC
PDE4B	5142	AGATGAGCCGATCAGGGAAC	CCTGTCTTTCTGGGTAGGAGA
PDGFA	5154	GCAAGACCAGGACGGTCATTT	GGCACTTGACACTGCTCGT
PDLIM1	9124	GACACACTTGGAAGCTCAGAAC	GTAAAGGGCATGGCACTTCG
PDLIM5	10611	AATCCCACCTAAACGCCCAC	GACGTGAAGGGGTATCTTTTCC
PLAC1	10761	AGTTCACCTACCGTGTTACTGA	AGCACATGACACTGGGATCAC
PLAC8	51316	GTGTGACTGTTTCAGCGACTG	CTGCAACTTGACACCCAAGG
PRR16	51334	ACAGCTCCAAAACGGACACG	AATAAGCGGTGCATTAGCCTG
PRSS33	260429	GCATGTCCAGTCGGATCGTT	GCACCCTTACTCCTTGTAGCG
RIPOR2	9750	GAAAATTCCTCCGCTCTCAAGA	TTCAAGGCCCTGTAGACTTCT
RGS4	5999	ACATCGGCTAGGTTTCCTGC	GTTGTGGGAAGAATTGTGTTCAC
RGS16	6004	ATCAGAGCTGGGCTGCGATA	CAGGTCGAACGACTCTCTCC
RIPOR2	9750	GAAAATTCCTCCGCTCTCAAGA	TTCAAGGCCCTGTAGACTTCT
RPS4Y1	6192	TGGATGCTTGACAAACTAACGG	AGGAAGACGATCAGAGGAAGAC

S100A4	6275	GATGAGCAACTTGGACAGCAA	CTGGGCTGCTTATCTGGGAAG
SEMA3A	10371	GTGCCAAGGCTGAAATTATCCT	CCCACTTGCATTCATCTCTTCT
SELENBP1	8991	TCATCTCCTCTCGCATCTATGTG	AAGGCCAGTTCGCACTTGG
SERPINF1	5176	TCATTCACCGGGCTCTCTACT	GGGCAGTGACCGTGTCAAG
SLC1A3	6507	AGCAGGGAGTCCGTAAACG	AGCATTCCGAAACAGGTAACTTT
SLC6A17	388662	CCTGGAGTGAATGTCCTGTCG	GAGGGAGCTGAAATACATCACC
SLC25A25	114789	TGACCATCGACTGGAACGAGT	ACATCAAAGATCGTGGAATGCTT
SLFN5	162394	GAGTGTGTTGTAGATGCAGGAA	ACTGCTCGCAGGATGATTTCA
SLITRK6	84189	ATCACGACCTTTCCAACTAAGC	ATAGCATTGGTAAGCCCAGAAAA
SNX13	23161	GGGGTTTAGTGGTTACTCTCCT	CCTGGCTTCCCGTTTCATTTC
SPANXB1	728695	AATGAGGCCAACAAGACGATG	CTCCTCCATTTGGTCGGGG
SPP1	6696	CTCCATTGACTCGAACGACTC	CAGGTCTGCGAAACTTCTTAGAT
SRGN	5552	AGGTTATCCTACGCGGAGAG	GTCTTTGGAAAAAGGTCAGTCCT
STARD5	80765	CCGGGAAGGCAATGGAGTTT	TCATCCCACTTCACTCGTAGG
SULT1A1	6817	GCCTTCTACGCCGGTATGAG	AGACCACCATATAGGTGTTCCA
SYT8	90019	GCACCACAGCTATACCTGGG	CCACGGACTCCTTGTCCCT
TGFB2	7042	CAGCACACTCGATATGGACCA	CCTCGGGCTCAGGATAGTCT
TMEM40	55287	CAGAGCAACCGGAAAACATCG	TCATCCTTCAAAACGTCAGGC
TMEM154	201799	GGTCCTCTTACTTTTATCCGTGG	ACTTTCACGTTTTCACTTCCCAG
TMEM200A	114801	GCAACTGGTGGAGTGATAACTG	TGCCACGAACAACCACAACA
TNFAIP6	7130	TTTCTCTTGCTATGGGAAGACAC	GAGCTTGTATTTGCCAGACCG
TOX	9760	CCCCATGAACCATAATGGCCT	CCCAGCATATTGGAGACTGTGA
TRABD2A	129293	CAAGCCCCAACAAAGCGAG	ACATGGATTGTGCCAAAGAAGTA
TRBC2	28638	CCCAGGATAGGGCCAAACC	TCATAGAGGATGGTGGCAGACA
UTSB2	257313	ATCTGTGCATGGACGACCATA	GGTCAGTGTTGAAAGGTCTTTGG
VGF	7425	GGAACTGCGAGATTTCAGTCC	GTGCGGGTTTCCGTCTCTG
XYLT1	64131	GAAGCCACCGAGTAGACAGAA	GGGCTGGTCATACTTGGTCTC
ZC4H2	55906	AGATCAAGGCTCGTTTGAAGG	GATCAGTCGGAGTTCCTCCAC
ZNF260	339324	ATGTGGTAAAGTGTGCTCTCG	GGTGTCTGATGATGGTTGGCA
ZNF419	79744	GTAGGACTGCTCAGTTCAAACAT	ACAGTTACTACACCCGTAAGGC
ZNF420	147923	ATGGCTCGGAAATTAGTGATGTT	AAGTCCTTACTTGCACACCTTG
ZNF605	100289635	AACATTGTTCATGTAGGACTGCG	TGGGTTCTGCCAGGTTTGATA
ZNF608	57507	AATTGATTTGGACGCTGATTTGG	CCGGACCTCCACAATCCTTG
ZNF615	284370	TCCTGCTGAAGCAAGATTGTG	GCAGAGTTCTTTAGGCCAGAG
ZNF618	114991	TGCCGAGCAAGGAACGATG	GCATTCGTAAGACCCAAGGG

Primer sequences originated from PrimerBank database (339) and primers were purchased from Eurofins Genomics GmbH (Ebersberg, Germany).

4.5 Cellular assays

4.5.1 Cell morphology

Possible influences of the 5-LO knockout on the cell morphology were evaluated after seeding $1*10^5$ cells in 6-well plates followed by an incubation period of 48 hours at 37°C, 5% CO_2 in a humidified atmosphere. Pictures were taken using a Zeiss Axio Vert.A1 microscope and examined using the Zen blue software.

4.5.2 Cell proliferation

The influence of the 5-LO knockout on cell proliferation rates was evaluated by seeding cells in complete growth medium with a density of $1*10^5$ cells per well (24-well plate) in technical triplicates followed by an incubation period of 24, 48, 72, and 96 hours at 37°C, 5% CO_2 in a humidified atmosphere. After the respective period, cells were detached using TE and counted manually using a Bürker counting chamber after staining with trypan blue solution [0.4% (w/v)].

4.5.3 Two-dimensional colony forming assay

The capacity to establish single-cell colonies in a two-dimensional environment was measured in 6-well plates. For this, 400 cells/well were seeded in complete growth medium and incubated at 37°C, 5% CO_2 in a humidified atmosphere as technical triplicates. After 7 days, the medium was discarded, wells were washed with PBS, and colonies were fixed with 100% methanol for 15 minutes. Methanol was then discarded, plates were dried for 5 minutes, and colonies were stained with Ponceau red [0.1% (w/v) Ponceau S in 5% acetic acid] for 10 minutes. The dye was removed and wells were washed with PBS until all free dye was gone. After that, plates were dried at room temperature, and colonies were counted manually.

4.5.4 Three-dimensional colony forming assay

2-fold concentrated DMEM was mixed with 1% agarose solution and the wells of a 24-well plate were covered with 300 µL of this mixture. Now, 5000 cells were diluted in 600 µL of 2-fold DMEM and mixed with 600 µL 0.6% agarose solution. 300 µL of the cell suspension were each transferred to 3 pre-covered wells. After 15 minutes agarose layers were covered with 0.5 mL of medium and kept at 37°C, 5% CO_2. After three weeks of incubation, the medium was discarded and 0.5 mL crystal violet solution [0.004% (w/v) crystal violet in 2% ethanol/PBS] were added to stain the colonies for a period of 24 hours. Colonies were counted manually.

4.5.5 Spheroid formation

Spheroid formation was carried out in Corning 96-well Spheroid Microplates. For this purpose, $1*10^5$ cells were suspended in 1 mL complete growth medium and 100 µL of this suspension were added to each well. The microplates were kept at 37°C, 5% CO_2 in a humidified atmosphere for a total of 15 days, and pictures were taken each day to monitor spheroid growth using a Zeiss Axio Vert.A1 microscope. The diameter of the spheroids was measured employing the Zen blue software (version 2.6).

4.5.5.1 Number of cells per spheroid

To elucidate the number of cells in each spheroid, 3 spheroids per cell line were harvested after 7 days of incubation from the low attachment plate, washed with PBS, and disaggregated by incubation in StemPro™ Accutase™ for 30 minutes at room temperature. Afterwards, spheroids were ultimately cleaved, and the suspension homogenised by pipetting up and down. Cells were counted manually with a Bürker counting chamber after staining with trypan blue solution [0.4% (w/v)].

4.5.5.2 Cell survival in spheroids

The viability of cells in spheroids was examined using the CellTiter-Glo® 3D Cell Viability Assay according to the manufacturer's protocol.

4.5.5.3 Spheroid outgrowth

Spheroids were formed as described in chapter **4.5.4** and kept for 4 days at 37°C, 5% CO_2 in a humidified atmosphere. Matrigel® was thawed overnight at 4°C and 100 µL of Matrigel® embedding the spheroids were added to each well using a frozen pipette tip. Plates were incubated for 15 minutes at 37°C for the gel to solidify and afterwards covered with 50 µL of fresh complete growth medium and further incubated at 37°C, 5% CO_2 in a humidified atmosphere. Pictures were taken daily for 19 days using a Zeiss Axio Vert.A1 microscope. The diameter of the spheroids was measured employing the Zen blue software (version 2.6).

4.5.6 FACS analysis

4.5.6.1 Tumour stem cell markers

For FACS analysis of cell surface markers, cells were seeded with a density of $1*10^6$ cells per well in a 6-well plate and incubated for 24 hours at 37°C, 5% CO_2 in a humidified atmosphere. In the next step, the medium was removed, and cells were washed with PBS followed by cell detachment with TE for 10 minutes. 2 mL medium were added and the cell suspension was transferred to a 15 mL reaction tube. The samples were now centrifuged (5 min, 2,000 x g), the supernatant was aspired, and the cells were resuspended in 1 mL of PBS and transferred to a FACS tube.

For cell surface staining, cells were resuspended in 30 µL of BSA/PBS [0.5% (w/v)] after another centrifugation step and incubated for 10 minutes at room temperature. Now, 20 µL of BSA/PBS containing a 1:200 dilution of the respective FACS antibodies (**Table 4.19**) were added and incubated for 30 minutes on ice. In the last step, 350 µL of the PBS/BSA mixture was added, all samples were centrifuged (5 min, 2,000 x g, 4°C) and the supernatants were discarded. Cells were suspended in 500 µL BSA/PBS and measured by flow cytometry using a BD FACSVerse™ flow cytometer. Data were analysed using the FlowJo software (version 10).

Table 4.19 *FACS antibodies*

Antigen	Company	Clonality	Species	Dilution
CD24-FITC	Miltenyi Biotec B.V. & Co. KG, Bergisch Gladbach, Germany	monoclonal	rec. human	1:200
CD44-VioBlue®		monoclonal	rec. human	1:200
CD133/2-APC		monoclonal	rec. human	1:200

4.5.6.2 Annexin V/PI staining

Cells were seeded in 6-well plates with a density of $2*10^5$ cells per well and incubated for 24 hours at 37°C, 5% CO_2 in a humidified atmosphere. After this period, the medium was changed and cells were incubated with 0.1% DMSO (as control), Actinomycin D (5, 10 nM), Etoposide (20, 40 µM), or 5-FU (50 µM) for 48 hours under given conditions. Next, the cell culture medium was removed and collected in tubes, cells were washed with PBS while collecting the washing buffer and detached using TE. Ice-cold PBS was added to the wells and the cell suspension was transferred to the respective tubes. The tubes were centrifuged (1,200 x g, 5 min, 4 °C) and the supernatant was discarded. Cells were resuspended in ice-cold PBS and transferred to a FACS tube. Again, the tubes were centrifuged (1,300 x g, 6 min, 4°C) and the supernatant was discarded. 100 µL of a binding buffer as well as 3.5 µL Annexin V reagent and 3.5 µL PI (50 µg/mL) were added to each tube and incubated for 15 minutes at room temperature in the dark. Afterwards, 400 µL of a binding buffer/PBS mix were added to each tube, and samples were measured immediately by flow cytometry using a BD FACSVerse™ flow cytometer. Data were analysed using the FlowJo software (version 10).

4.5.6.3 Cell cycle analysis

For cell cycle analysis, $3*10^6$ cells were seeded in 10 cm dishes in a serum starvation medium containing 0.5% FCS and incubated for 24 hours at 37°C, 5% CO_2 in a humidified atmosphere. After this period, the medium was replaced by complete growth medium. After another 6 hours of incubation, cells were detached, separated using a cell strainer, and fixed with 80% ethanol. $2*10^6$ cells were washed and resuspended in 500 µL staining buffer (PBS, 0.1% Triton-X-100), treated with 10 µg RNase A and 10 µg propidium iodide for 30 minutes, and measured by flow cytometry (BD FACSVerse™). Data were analysed using the FlowJo software (version 10).

4.5.6.4 Cytometric bead assay (CBA) for fractalkine and MCP-1

Secretion of fractalkine and MCP-1 from cells grown in monolayer was assessed by seeding $1*10^5$ cells in a 24-well plate. After 3 days of incubation at 37°C, 5% CO_2 in a humidified atmosphere, the medium was changed and a total volume of 1 mL starvation medium containing no FBS was added, followed by an incubation of 24 hours. After this period, 500 µL of the supernatants were transferred to a reaction tube and centrifuged for 5 minutes at 2000 x g to remove cells and debris from the supernatant. 100 µL of each sample were analysed using a bead-based immunoassay (cytometric bead array - CBA, BD Biosciences). Human fractalkine and MCP-1 Flex Sets were used, and the assay was performed according to the manufacturer‘s manual. Data analysis was performed with FCAP Array™ software (version 3.0, BD™ Biosciences).

4.5.7 Confocal microscopy

$8*10^4$ cells were seeded in an 8-well Nunc™ Lab-Tek™ II CC2™ Chamber Slide System and allowed to attach for 24 hours in complete growth medium at 37°C, 5% CO_2 in a humidified atmosphere. After this period, the supernatant was discarded, and cells were fixed using a 4% PFA/PBS solution for 30 minutes. After several washing steps with PBS, blocking/permeabilization solution (1% BSA, 0.2% Triton-X-100 in PBS) was added to each well and left for 1 hour at room temperature. Cells again were washed three times with PBS and incubated for 1 hour with the respective primary antibodies in PBS containing 0.1% BSA and 0.2% Triton-X-100 (antibodies see **Table 4.20**) and, after additional three washing steps with PBS, for another hour with secondary antibodies (also see **Table 4.20**). Nuclear staining was carried out with DAPI solution (1 mg/mL DAPI, diluted 1:1000 in PBS) and after the final washing steps, slides were covered with Mowiol® mounting solution (**Table 4.21** Composition of Mowiol® mounting solution) and capped with a cover slip that was sealed after additional 10 minutes. Images were acquired using a Zeiss LSM 780 confocal microscope under identical conditions for pinhole opening, laser power, photomultiplier tension, and layer number. During data elaboration with Zen black and Zen blue software, identical parameters were applied for all samples.

Table 4.20 *Antibodies for confocal microscopy*

Antigen	Company	Clonality	Species	Dilution
Ki-67	Santa Cruz Biotechnology, Dallas, USA	monoclonal	mouse	1:50
Cytokeratin-20		monoclonal	mouse	1:50
EpCAM [AUA-1]	Abcam, Cambridge, United Kingdom	polyclonal	rabbit	1:50
CDX1		monoclonal	rabbit	1:50
Anti-mouse Alexa Fluor® 647	Thermo Scientific™, Waltham, USA		donkey	1:2000
Anti-rabbit Alexa Fluor® 488			donkey	1:2000

Table 4.21 *Composition of Mowiol® mounting solution*

Mowiol® mounting solution	
Mowiol® 4-88	2.4 g
Glycerol	6 g
Tris-HCl (pH 8.5, 0.2 M)	12 mL
DABCO	0.1% (w/v)
Water	6 mL

4.5.8 WST-1 cell viability assay

To evaluate the influence of different conditions and the treatment with cytostatic drugs on cell viability of all cell lines a WST-1 assay was performed. To do so, cells were seeded with a density of $3*10^4$ cells per well each in a 96-well plate in 100 µL of complete growth medium and incubated at 37°C, 5% CO_2 in a humidified atmosphere for 24 hours. To assess the influence of cytostatic drugs, cells were treated with the cytostatics in different concentrations (Actinomycin D: 3.5, 7, 10, and 14 nM, Etoposide: 10, 20, 40, and 50 µM) using DMEM medium without phenol-red. Cells treated with DMSO served as a negative control. Plates were incubated for 48 hours at given conditions and then 10 µL of WST-1 reagent were added to each well. After one more hour of incubation at 37°C, absorbance was measured at 450 nm and 620 nm with a Tecan Infinite® M200 plate reader.

4.5.9 Transwell assay/directed cell migration

Cells were detached using TE, counted, and resuspended in a medium containing 0.5% FCS to receive a cell suspension of $1*10^6$ cells/mL. 400 µL of this cell suspension were transferred to the upper chamber of a Bio-One ThinCert™ Tissue Culture Insert for 12-well plates. The bottom chamber of the 12-well plate was filled with 1.2 mL of complete growth medium containing 10% FCS. After 3 hours (U-2 OS) or 24 hours (HCT-116 and HT-29) of incubation at 37°C, 5% CO_2 in a humidified atmosphere, the medium was removed from the lower chamber and replaced by 900 µL medium containing 0.5% FCS medium and 8 µM of Calcein-AM followed by an additional incubation of 45 minutes.

Subsequently, the cell suspension from the upper chamber was removed and the chambers were incubated in 1 mL TE for 10 minutes to detach all cells on the bottom side of the membrane. 200 µL of the cell suspension were transferred to a black 96-well plate and fluorescence was measured at 485 nm/520 nm using a Tecan Infinite® M200 plate reader.

4.5.10 Transwell invasion assay

The invasion assay was performed in the same manner as the transwell assay (**4.5.9**), only before the addition of the cell suspension, membranes were covered with 100 µL of Matrigel® (thawed overnight at 4°C and handled using frozen pipette tips) and incubated for 15 minutes at 37°C for the Matrigel® to solidify. For all three cell lines, plates were incubated for 24 hours at 37°C, 5% CO_2 in a humidified atmosphere.

4.5.11 Wound closure assay

$4.9*10^4$ cells were seeded in complete growth medium in both chambers of an ibidi® culture-insert 2-well system for 24-well plates and incubated at 37°C, 5% CO_2 in a humidified atmosphere. After 24 hours of adherence, inserts were removed, and cells were covered with medium. In the following, pictures were taken using a Zeiss Axio Vert.A1 microscope.

4.5.12 Enzyme-linked immunosorbent assay (ELISA) for TGF-β2 and PDGF-AA

Secretion of TGF-β2 from cells grown in monolayer was assessed by seeding $3*10^5$ cells in a 24-well plate in a total volume of 2 mL medium followed by incubation at 37°C, 5% CO_2 in a humidified atmosphere for 72 hours. After this incubation period, 500 µL of the supernatants were transferred to a reaction tube and centrifuged for 5 minutes at 2,000 x g to remove cells and debris from the supernatant. As TGF-β2 normally is expressed in a latent complexed form, it is necessary to cleave this bond to measure free TGF-β2 (340) (341). Therefore, 40 µL 1 M HCl was added to 200 µL of the purified supernatants and incubated for 10 minutes. Afterwards, the samples were neutralized by the addition of 40 µL NaOH (1 M), and 200 µL of each sample were transferred to the pre-coated ELISA plate of the TGF beta-2 Human ELISA Kit and incubated overnight at 4°C while gently shaking. The following assay was conducted as prescribed in the manufacturer's manual.

Secretion of PDGF-AA from cells grown in monolayer was assessed by seeding $1*10^5$ cells in a 24-well plate. After 3 days of incubation at 37°C, 5% CO_2 in a humidified atmosphere, the medium was changed and a total volume of 1 mL starvation medium containing no FBS was added, followed by an incubation of 24 hours. After this period, 500 µL of the supernatants were transferred to a reaction tube and centrifuged for 5 minutes at

2000 x g to remove cells and debris from the supernatant. 100 µL of each sample were used and the assay was conducted as prescribed in the manufacturer's manual.

4.6 Long-term treatment with 5-LO inhibitors

To evaluate whether possible effects of the knockout of 5-LO are due to enzymatic activity or other non-canonical functions, vector control cells were treated with the 5-LO inhibitors Zileuton and CJ-13610. As it is possible for mechanisms that take some time to carry out their functions to be involved, cells were pre-incubated with the inhibitors before the actual experiments. For this purpose, cells were split as usual but 5 different conditions were applied. While control cells were seeded as usual in 10 mL complete growth medium containing 0.1% DMSO, for inhibitor treatments 10 µL of the respective inhibitor dilutions (**Table 4.22**) were added. Cells were incubated as usual for 3 to 4 days at 37°C, 5% CO_2 in a humidified atmosphere. After this incubation cells were either harvested and lysed (RNA isolation and real-time qPCR, **4.5**) or seeded for proliferation assay (**4.5.1**), spheroid formation (**4.5.4**), or transwell migration assay (**4.5.8**). In case cells were seeded for further procedure, respective amounts of the inhibitors, or 0.1% DMSO respectively, were added to yield final concentrations of desire.

Table 4.22 *Long-term inhibitor treatment of cell culture*

Inhibitor	Concentration of dilution	Final concentration
Zileuton	10 mM	10 µM
	3 mM	3 µM
CJ-13610	3 mM	3 µM
	0.3 mM	0.3 µM

4.7 Re-expression of 5-LO in 5-LO knockout cells

4.7.1 Transfection

For re-expression of 5-LO in 5-LO knockout cells, cells were transiently transfected using Lipofectamine LTX with Plus Reagent with a sleeping beauty plasmid carrying a modified *ALOX5* gene (pSB-bi-GH-mod5LO, Addgene plasmid #60514, **Figure 4.3**), as well as a Hygromycin resistance sequence, and a second plasmid carrying the transposase (pSB100x_amp) friendly provided by Marius Kreiß as well as Eric Kowarz from the institute of pharmaceutical biology, Goethe University. An empty control plasmid lacking the *ALOX5* sequence (pSBbi-GH) served as a control for all experiments.

Single-cell clones from each cell line were chosen (HCT-116: F5 + G6, HT-29: F4 + G6, U-2 OS: C4) and cells carrying the vector control were used as controls. Next, cells were seeded in 6-well plates (HCT-116: $6.25*10^5$ cells/well, HT-29: $7.5*10^5$ cells/well,

6.7*10^5 cells/well). After 24 hours of adhesion, 1.9 µg/well pSB-bi plasmid and 0.1 µg transposase plasmid were added to plus reagent, mixed with equal amounts of LTX reagent, and left for 30 minutes. Cells were washed twice and incubated with the DNA/LTX-mix suspended in Opti-MEM™ Reduced Serum Medium for 16 hours.

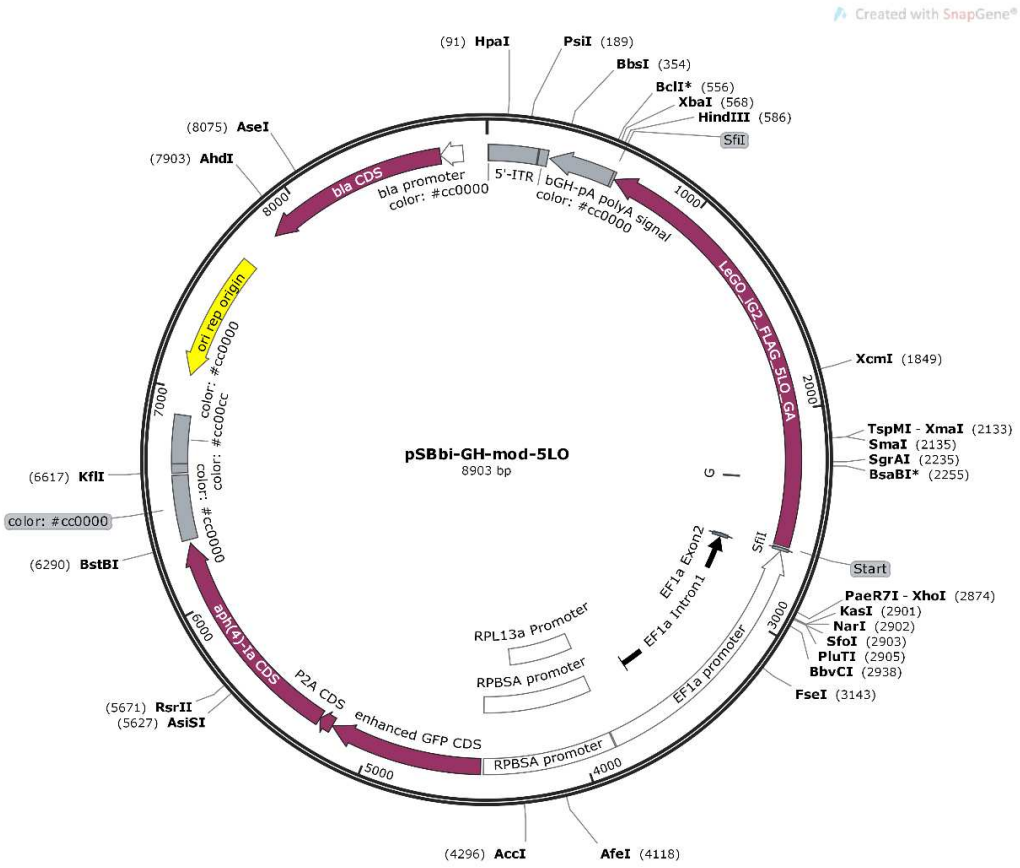

Figure 4.3 Plasmid map of pSB-bi-GH-mod5LO.

4.7.2 Hygromycin selection

The DNA/LTX mix was discarded and complete growth medium containing Hygromycin for selection purpose was added (HCT-116, U-2 OS: 500 µg/mL, HT-29: 1000 µg/mL). As control untransfected cells were seeded and treated with Hygromycin in the same manner. After 72 hours medium and dead cells were discarded and new medium containing Hygromycin was added. This procedure was repeated over the next two weeks. All left cells were detached using TE and transferred to cell culture flasks. Successful knock-in of 5-LO was evaluated via Western blotting.

4.8 Statistical analysis

All data are presented as mean + SEM or mean + SD depending on the performed assay. Statistical analysis was performed with GraphPad Prism version 8.00. Data were subjected to an unpaired t-test with Welsch correction or one-way ANOVA coupled with Dunnett's post-test for multiple comparisons.

5 Results

5.1 Generation and confirmation of the 5-LO knockout in HCT-116, HT-29, and U-2 OS cells

During preliminary work, the four cell lines HCT-116, HT-29, U-2 OS and Capan-2 were identified as 5-LO expressing solid tumour cell lines (**Figure 3.1**). Since transfection in Capan-2 cells was not successful, these cells were excluded from this study and only HCT-116, HT-29, and U-2 OS were further processed. The CRISPR/Cas system was used to eliminate 5-LO from different 5-LO-expressing tumour cell lines. Therefore, cells were transiently transfected with a plasmid coding for the CRISPR/Cas9 machinery. A specialized guide RNA directs the Cas9 enzyme to either exon 2 or exon 6 of the *ALOX5* gene. Here, the Cas9 enzyme cuts the DNA. Intracellular DNA polymerases try to rectify this problem, and by this, mistakes in the repair mechanism occur that lead to small mutations and in the best case to a frameshift resulting either in a premature stop codon and mRNA degradation or to a dysfunctional protein that also gets decomposed. As a control treatment, plasmids missing the guide RNA sequence were used. After transfection, cells were left for 72 hours to enable expression and work of the CRISPR/Cas9 system. Puromycin was used for selection purposes as the used plasmids also contained a Puromycin resistance sequence. Surviving cells were diluted and seeded in a 96-well plate to generate single-cell clones. This assured that only cells containing a complete knockout of the 5-LO were used for further consideration as for single-cell clones the knockout could be validated on the genomic level. After 3 weeks single-cell clones were picked, raised, and analysed.

For this purpose, cells were lysed, and protein expression was measured using Western blot technique (**Figure 5.1**). More than 25 single-cell clones from each of the three cell lines were picked and analysed. Of those, only about 20% showed no 5-LO band during Western blot analysis. Those clones were further analysed.

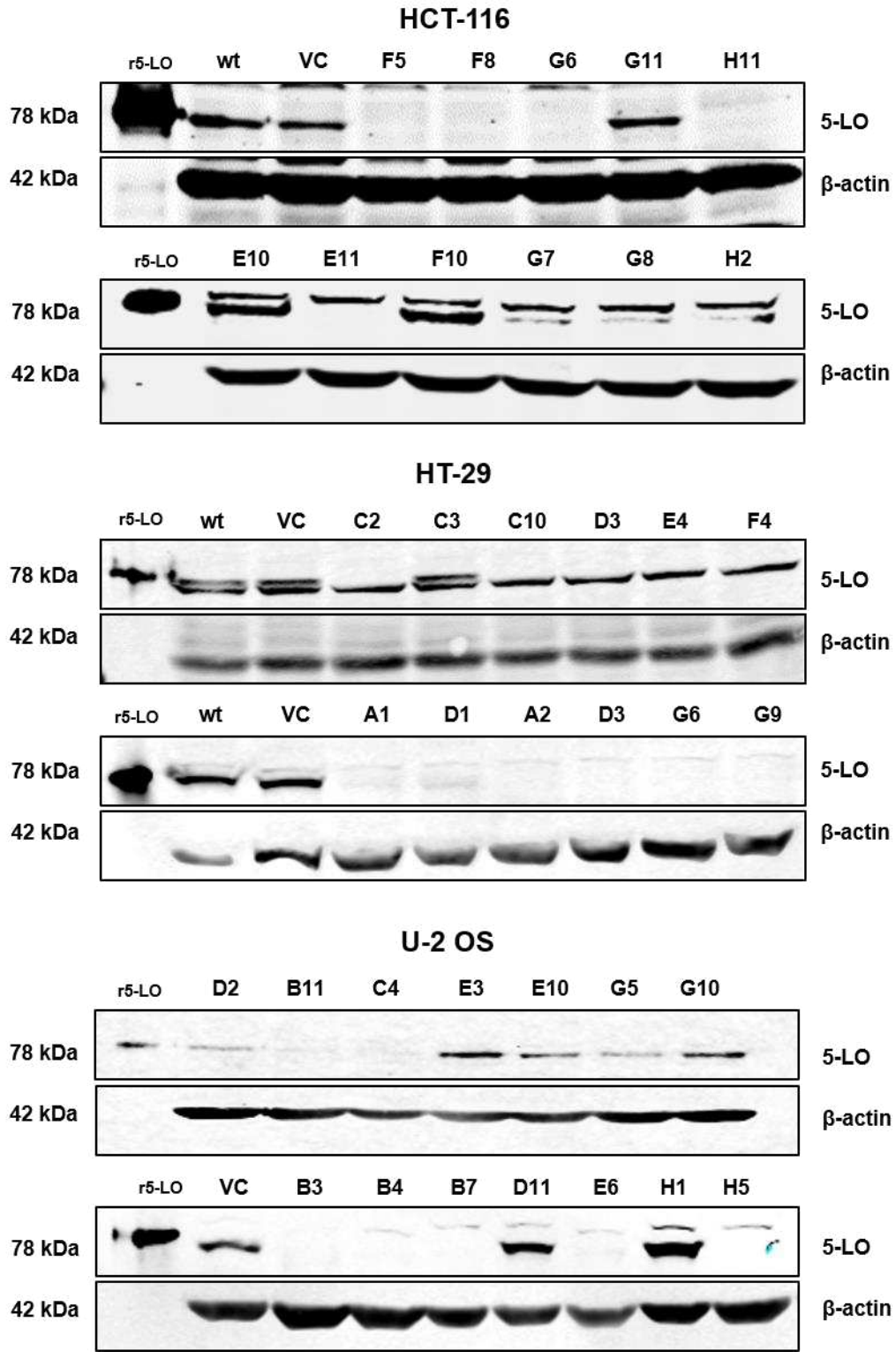

Figure 5.1 Investigation of 5-LO protein level in HCT-116, HT-29, and U-2 OS single-cell clones analysed by Western blotting. *Recombinant human 5-LO was used as a positive control. M: marker, r5-LO: recombinant human 5-LO, wt: wildtype cells VC: vector control. 5-LO antibodies from different manufacturers were used causing the band patterns.*

To validate the complete knockout of the *ALOX5* gene, single-cell clones showing no 5-LO band in Western blot analysis were lysed in TRIzol® and genomic DNA was isolated. For sequencing, a certain genomic section around the complementary guide RNA sequence was amplified using different primer pairs (**Figure 5.2**), purified by agarose gel electrophoresis, and sequenced using Sanger sequencing.

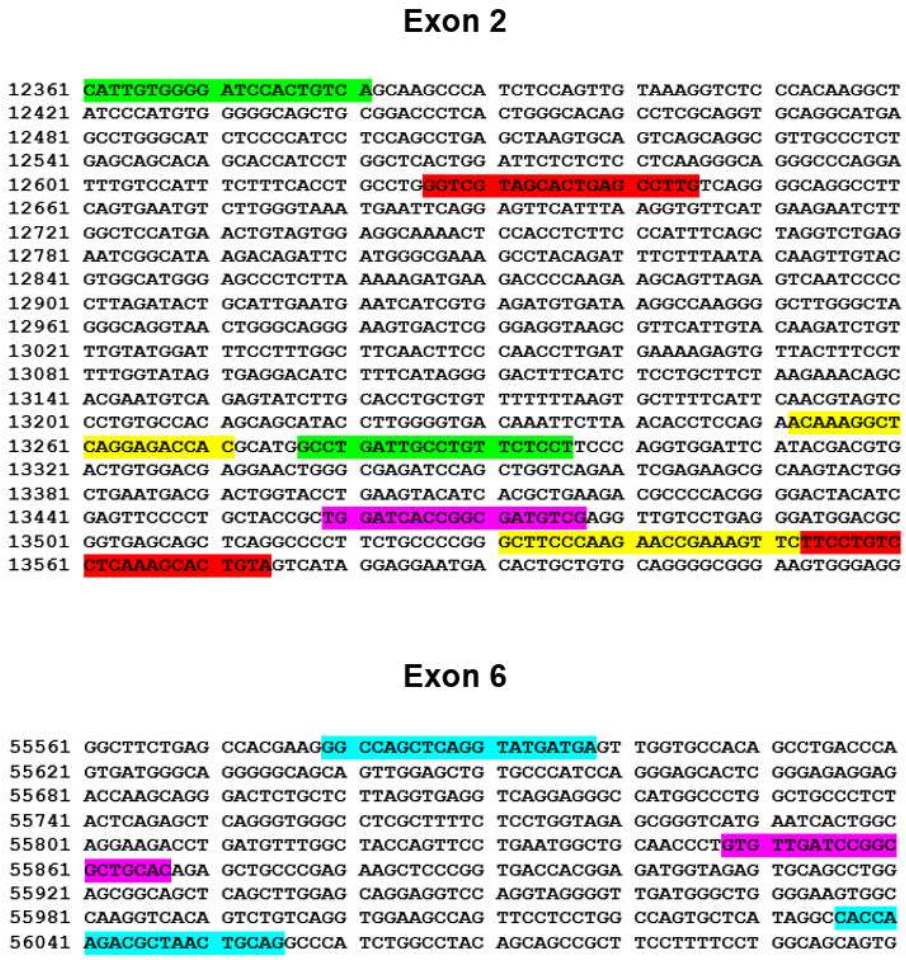

Figure 5.2 gRNA sequences in exon 2 and exon 6 and respective primer sequences. *gRNA sequences (purple) in exon 2 (top) and exon 6 (bottom), primer pairs 1/2 (exon 6, turquoise), 3/4 (exon 2, green), 5/6 (exon 2, yellow) and 7/8 (exon 2, red).*

All HCT-116 clones were transfected using the guide RNA binding in exon 2. Analysis of the DNA sequence of 5-LO knockout clone F5 showed the desired result of two overlapping signals, where neither resembled the wildtype sequence (**Figure 5.3 B**). On one allele, deletion of 19 bases could be ascertained while on the other allele 7 bases were substituted by 9 different ones. On both alleles, the mutations caused a frameshift, and the complete knockout could be proven.

For clone G6 also no wildtype sequence was detectable but nevertheless, validation of the sequencing data occurred to be a bit more difficult. After amplifying the DNA region of interest by PCR, products were analysed and purified using gel electrophoresis. Thereupon, it became obvious that for primer pair 7/8 two bands occurred from one sample with a big size difference (**Figure 5.3 D**) raising the assumption that on one allele a big part of the gene was missing. Both bands were purified and sequenced individually (**Figure 5.3 C**). In fact, on one allele 583 bases containing almost all of exon 2 were deleted probably leading to a missense protein. The second allele showed an alteration of 100 bases that were deleted and replaced by 3 different ones. Again, both cases resulted in a complete knockout of the 5-LO enzyme.

Analysis of the HCT-116 clone H11 (**Figure 5.3 E**) revealed a third possible outcome. Sequencing of the DNA did not show overlapping signals, but the single sequence was not the wildtype sequence anyway since 7 bases were missing. No matter which primers were used and how far from the gRNA binding site DNA was analysed, no second sequence was found. This leads to two different options, either both alleles are mutated in the same manner resulting in identical signals, or the missing part of DNA is even bigger than analysed. In both cases, no functional protein would result so a complete knockout can be considered certain.

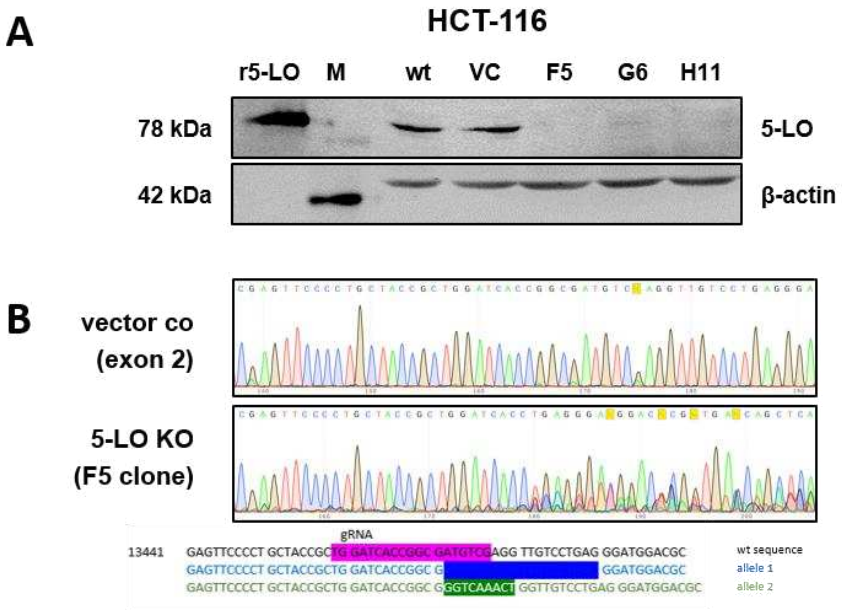

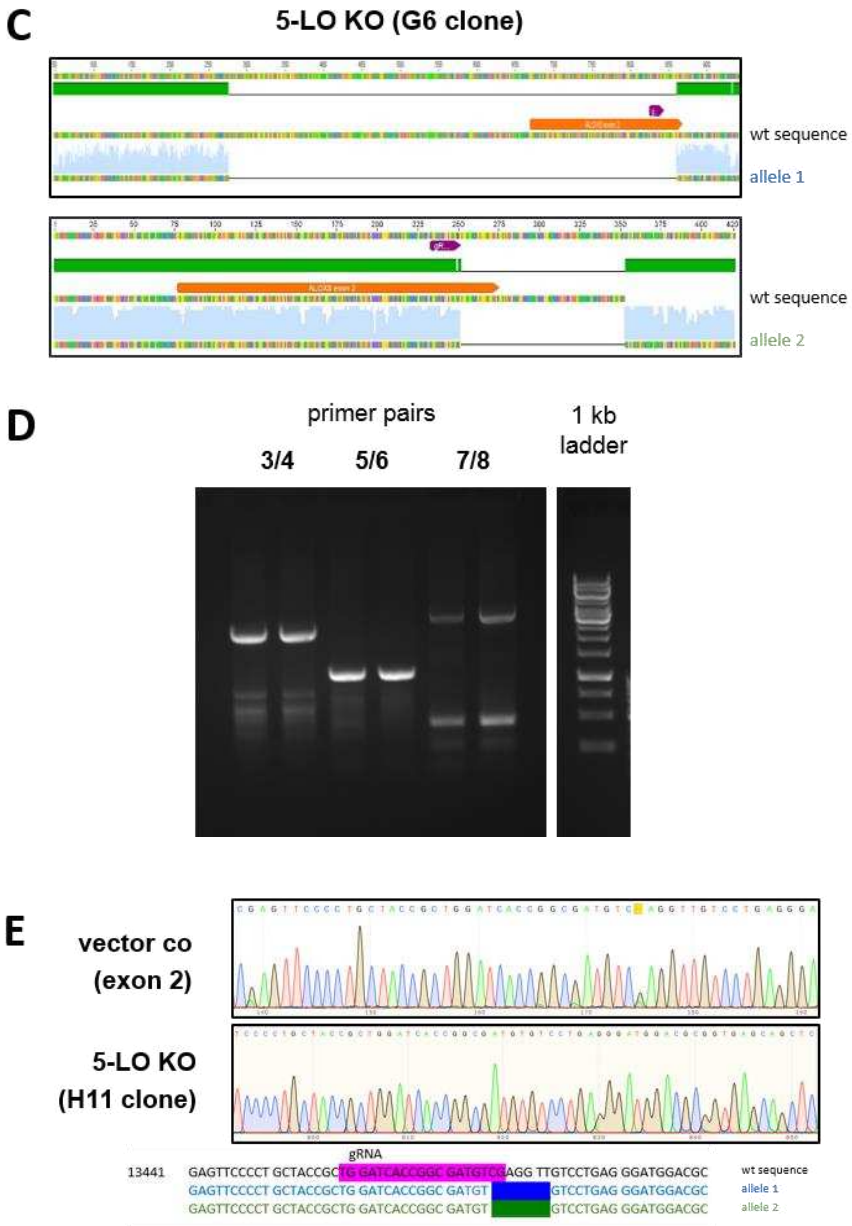

Figure 5.3 5-LO knockout in HCT-116 cells. *(A) Validation of 5-LO KO on protein level in HCT-116 single-cell clones analysed by Western blotting. Recombinant human 5-LO was used as a positive control. M: marker, r5-LO: recombinant human 5-LO, wt: wildtype cells, VC: vector control. (B) Top: Comparison of the sequencing data from vector control transfected HCT-116 cells with the HCT-116 KO clone F5 showing sequence alterations on both alleles. Bottom: Analogy of DNA wildtype sequence with both alleles of HCT-116 KO clone F5 carrying frameshift mutations. The gRNA binding site is marked in purple. Allele 1: Deletion of 19 bases (dark blue); Allele 2: Substitution of 7 bases (ATGTCGA) by 9 different bases (GGTCAAACT) (green). (C) Comparison of the sequencing data from vector control transfected HCT-116 cells with the HCT-116 KO clone G6 showing sequence alterations on both alleles. The gRNA binding site is marked in purple. Allele 1: Deletion of 583 bases (top); Allele 2: Substitution of 100 bases by 3 different bases (bottom). (D) Agarose gel of PCR products using HCT-116 clone G6 as a template with different primer pairs. (E) Top: Comparison of the sequencing data from vector control transfected HCT-116 cells with the HCT-116 KO clone H11 showing sequence alterations. Bottom: Analogy of DNA wildtype sequence with both alleles of HCT-116 KO clone H11 carrying frameshift mutations. The gRNA binding site is marked in purple. Allele 1: Deletion of 7 bases (dark blue); Allele 2: Deletion of 7 bases (green).*

Evaluation of HT-29 clones occurred to be more explicit (**Figure 5.4**). While single-cell clone F4 was generated directing the CRISPR/Cas9 machinery to exon 2, genomic sequences of clones A2 and G6 were altered in exon 6.

Sequencing of clone F4 (**Figure 5.4 B**) revealed a deletion of 2 bases on one allele and a deletion of 36 bases on the other allele. Even though this does not lead to a frameshift on the second allele, the complete absence of any 5-LO band on protein level led to the assumption that those 13 missing amino acids were enough to cause a probably misfolded or at least dysfunctional protein that gets degraded immediately.

For clone A2 (**Figure 5.4 C**) a deletion of 16 bases on one allele and a deletion of 5 bases on the other alleles could be ascertained while the two deletions of clone G6 (**Figure 5.4 D**) only covered 1 respectively 2 bases. In both cases, frameshifts were the result, assuring the complete knockout of the 5-LO gene.

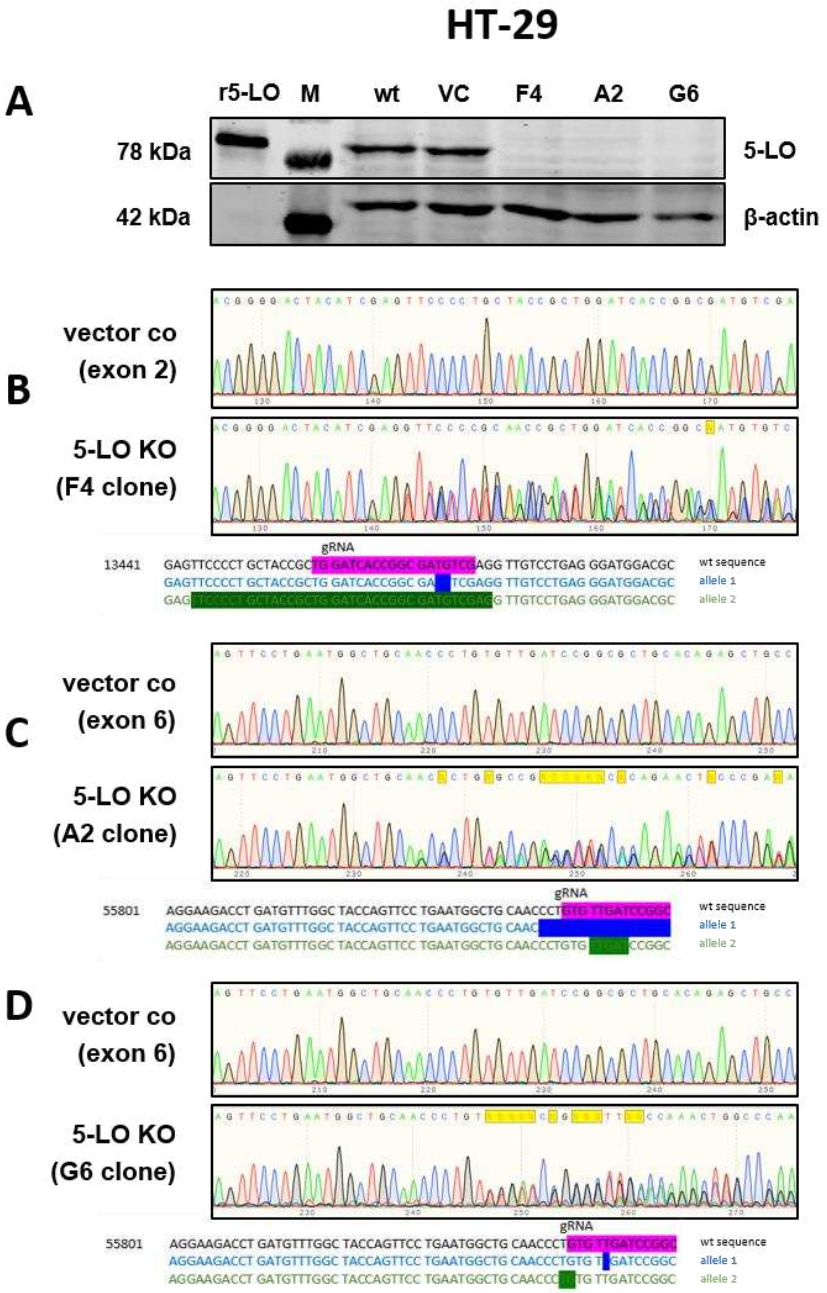

Figure 5.4 5-LO knockout in HT-29 cells. *(A) Validation of 5-LO KO on protein level in HT-29 single-cell clones analysed by Western blotting. Recombinant human 5-LO was used as a positive control. M: marker, r5-LO: recombinant human 5-LO, wt: wildtype cells, VC: vector control. (B) Top: Comparison of the sequencing data from vector control transfected HT-29 cells with the HT-29 KO clone F4 showing sequence alterations on both alleles. Bottom: Analogy of DNA wildtype sequence with both alleles of HT-29 KO clone F4 carrying mutations. The gRNA binding site is marked in purple. Allele 1: Deletion of 2 bases (dark blue); Allele 2: Deletion of 36 bases (green). (C) Top: Comparison of the sequencing data from vector control transfected HT-29 cells with the HT-29 KO clone A2 showing sequence alterations on both alleles. Bottom: Analogy of DNA wildtype sequence with both alleles of HT-29 KO clone A2 carrying frameshift mutations. The gRNA binding site is marked in purple. Allele 1: Deletion of 16 bases (dark blue); Allele 2: Deletion of 5 bases (green). (D) Top: Comparison of the sequencing data from vector control transfected HT-29 cells with the HT-29 KO clone G6 showing sequence alterations on both alleles. Bottom: Analogy of DNA wildtype sequence with both alleles of HT-29 KO clone G6 carrying frameshift mutations. The gRNA binding site is marked in purple. Allele 1: Deletion of 1 base (dark blue); Allele 2: Deletion of 2 bases (green).*

As U-2 OS cells are described to be hypertriploid, a successful knockout of the 5-LO on all three alleles was much harder to perform. Additionally, the validation of the knockouts could not be easily done with three overlapping sequences which resulted in poor quality of the sequencing and made the distinct assignment of the sequences hard to do. This resulted in only two 5-LO knockout single-cell clones. Anyway, it was assured that none of the resulting signals corresponds to the wildtype sequence (**Figure 5.5 B, C**).

For clone C4 a possible interpretation of the sequences hypothesizes a deletion on all three alleles of 18, 18, and 20 bases. Here again, the absence of any 5-LO protein in Western blot analysis led to the assumption that all resulting protein was degraded.

For clone H5 it is likely that on one allele 7 bases were deleted while on the second allele 34 bases were substituted by 19 different ones and on the third allele 28 bases were substituted by 26 different ones. In all cases, no functional protein was the result.

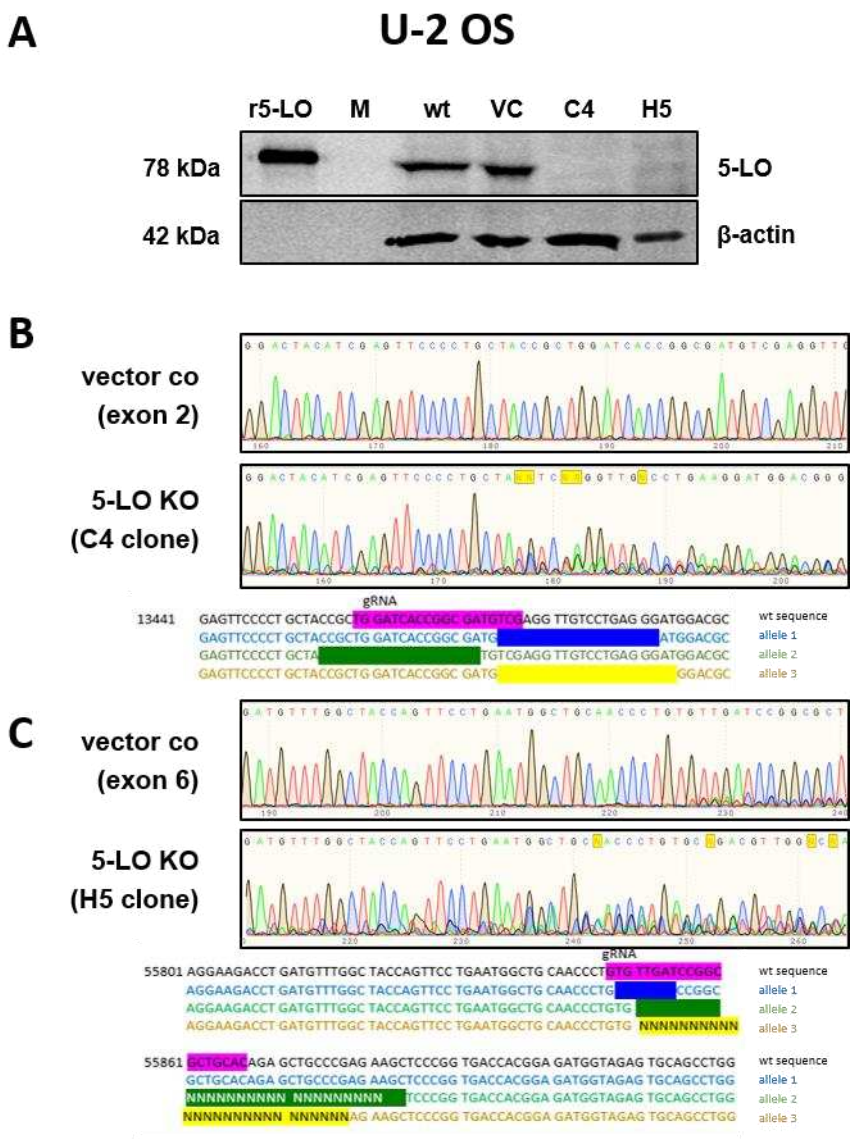

Figure 5.5 5-LO knockout in U-2 OS cells. *(A) Validation of 5-LO KO on protein level in U-2 OS single-cell clones analysed by Western blotting. Recombinant human 5-LO was used as a positive control. M: marker, r5-LO: recombinant human 5-LO, wt: wildtype cells, VC: vector control. (B) Top: Comparison of the sequencing data from vector control transfected U-2 OS cells with the U-2 OS KO clone C4 showing sequence alterations on all three alleles. Bottom: Analogy of DNA wildtype sequence with all three alleles of U-2 OS KO clone C4 carrying mutations. The gRNA binding site is marked in purple. Allele 1: Deletion of 18 bases (dark blue); Allele 2: Deletion of 18 bases (green); Allele 3: Deletion of 20 bases (yellow). (C) Top: Comparison of the sequencing data from vector control transfected U-2 OS cells with the U-2 OS KO clone H5 showing sequence alterations on all three alleles. Bottom: Analogy of DNA wildtype sequence with all three alleles of U-2 OS KO clone H5 carrying frameshift mutations. The gRNA binding site is marked in purple. Allele 1: Deletion of 7 bases (dark blue); Allele 2: Substitution of 34 bases by 20 different ones (green); Allele 3: Substitution of 28 bases by 28 different ones (yellow).*

5.2 Influence of 5-LO KO on cell morphology

The first step in the evaluation process of the newly generated 5-LO knockout cells was to investigate obvious changes in the cell morphology. Therefore, cells were grown under standard cell culture conditions and pictures were taken at about 70% confluency (**Figure 5.6**)**.** No visible differences in the cell morphology could be detected for any of the generated cell lines, but while passaging the cells over time, it became obvious that the confluency of the cells did differ although all cells from one cell line were split in the same manner. This was to be examined more closely by performing a cell proliferation assay.

Comparing the different cell lines revealed big differences in the cell phenotypes. HCT-116 cells were strongly proliferating with a doubling time of 25 hours and possessed a fibroblast-like phenotype with weak adherence to the culture flask (342) (343). HT-29 and U-2 OS, on the contrary, both had a doubling time of 40-60 hours with a more differentiated, epithelioid phenotype and adherence to the flask surface was stronger (344) (345) (346) (347).

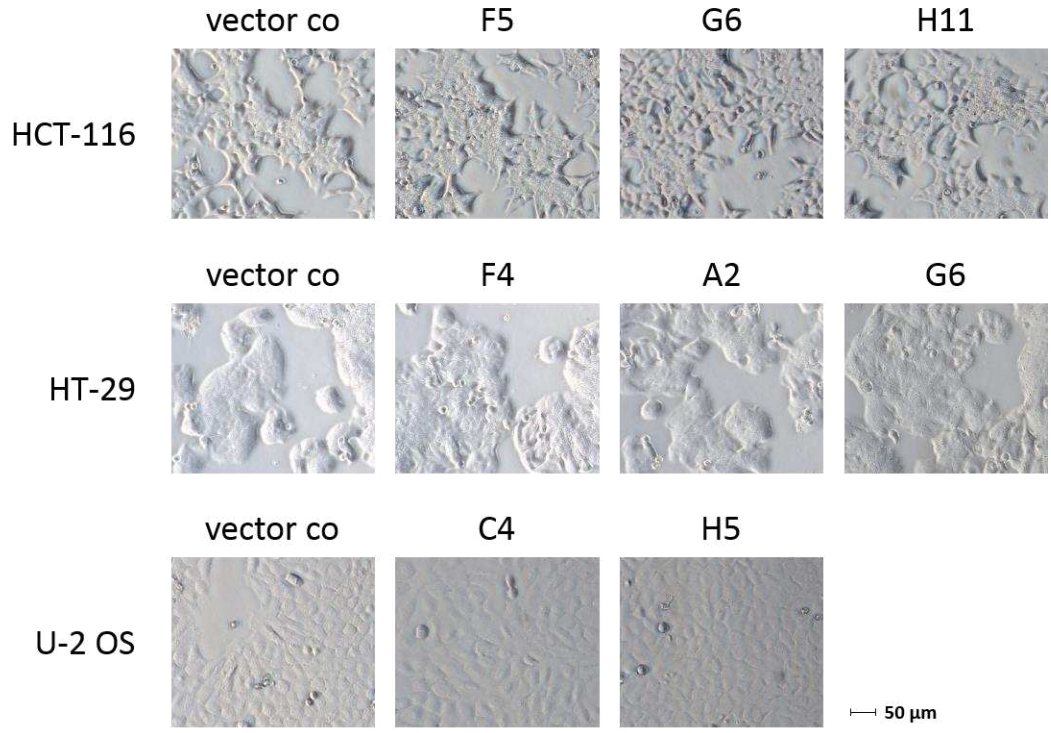

Figure 5.6 Cell morphology of HCT-116, HT-29, and U-2 OS vector control-treated cells and 5-LO knockout single-cell clones. *Cell morphology was evaluated after seeding 1*10^5 cells in 6-well plates followed by an incubation period of 48 hours at 37°C, 5% CO2 in a humidified atmosphere. Pictures were taken at 20x magnification using a Zeiss Axio Vert.A1 microscope and examined using the Zen blue software.*

5.3 Knockout of 5-LO alters gene expression in HCT-116, HT-29, and U-2 OS cells

To globally investigate gene expression and find possible differences between 5-LO positive and knockout cells, RNA sequencing was determined as the method of choice. RNA was isolated from the cells and a corresponding DNA library containing small parts of all mRNAs was produced. Short index sequences unique for all samples as well as adapter molecules necessary for binding the Illumina flow cell were attached to all library molecules. Libraries were amplified and mixed equimolarly to yield one sample that was loaded to the flow cell. 10 cycles each for both index sequences and 50 cycles sequencing the first 50 bases of each library molecule were carried out.

Sequencing data were aligned to the human genome (Hg38) and differential expression analysis (DEA) was performed using the Lexogen Bluebee platform as well as RSem platform to identify all genes that were up- or downregulated in 5-LO knockout cells compared to the 5-LO-containing counterparts. DEA results of all 3, respectively 2, knockout clones were compared and genes that occurred in all knockout clones were chosen for further investigations (**Figure 5.7 A**).

In HCT-116 cells, 28 genes were regulated by the 5-LO knockout in all clones (**Figure 5.7 B**). 15 of the genes that were altered by the 5-LO knockout were upregulated, 11 genes were downregulated and for the two genes *NPM1P21* and *SEMA3A* the type of regulation was depending on the single-cell clone.

In HT-29 cells, 18 genes were expressed differently when comparing 5-LO positive and negative cells and while most of the differentially expressed genes in the HT-29 cell line were downregulated, also clonal differences played a bigger role here as 6 of the investigated genes were downregulated in clone F4 and clone A2 clone but upregulated in clone G6.

In U-2 OS cells, the by far biggest number of differentially expressed genes was found with 234 genes occurring at the intersection of DEA results for the two 5-LO knockout clones. Of those, about 2/3 of the genes were downregulated by the 5-LO knockout. Also, clonal effects among the two single-cell clones played a role and resulted in a contrary regulation for 18 genes.

Interestingly none of the found genes occurred in more than one of the parental cell lines and regulation patterns differed as well.

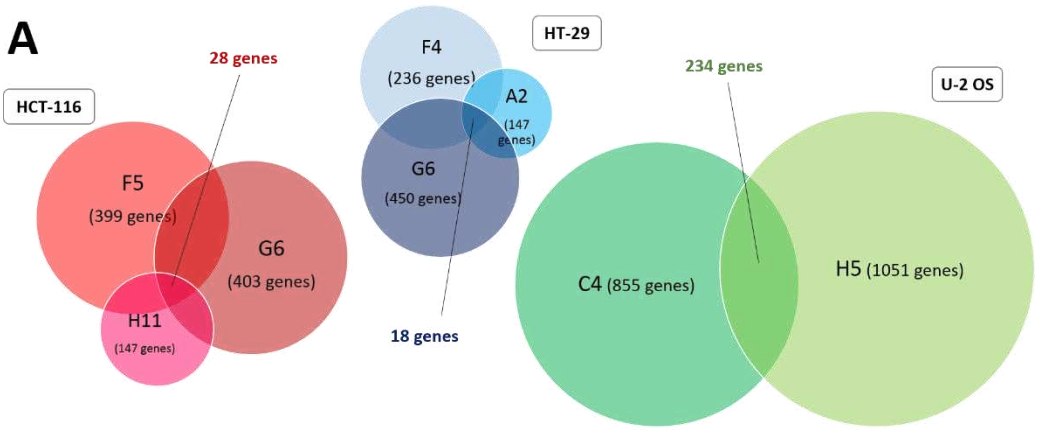
A
HCT-116
28 genes
F5
(399 genes)
G6
(403 genes)
H11
(147 genes)
HT-29
F4
(236 genes)
A2
(147 genes)
G6
(450 genes)
18 genes
234 genes
U-2 OS
C4 (855 genes)
H5 (1051 genes)

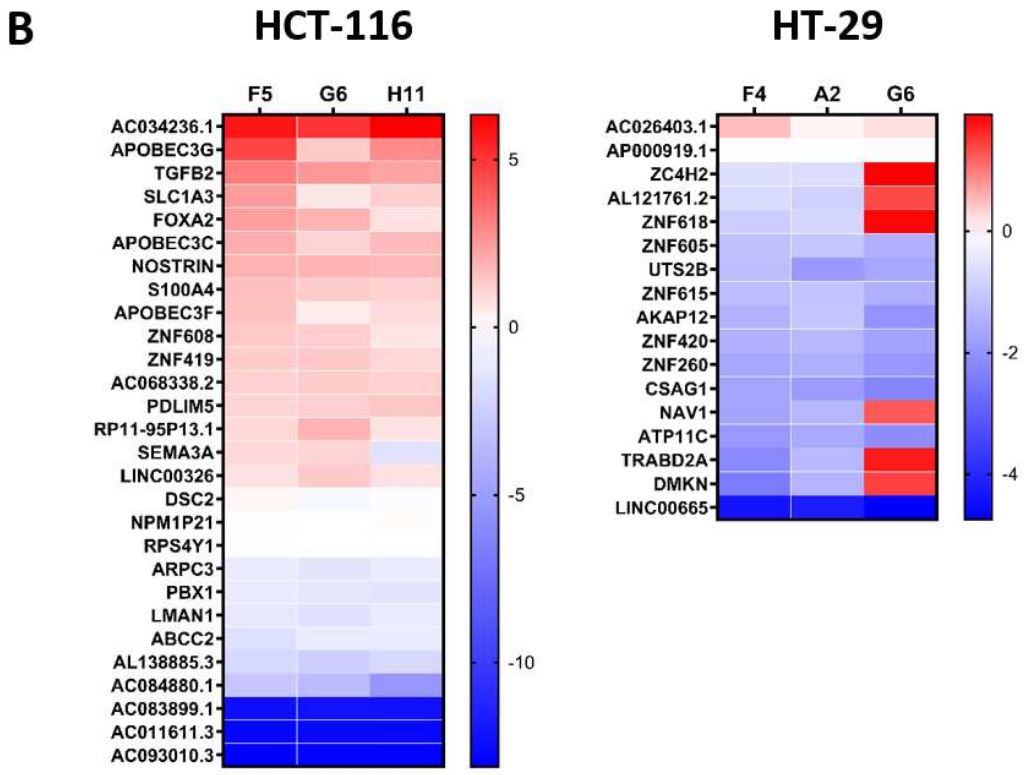
B
HCT-116
F5
G6
H11
AC034236.1
APOBEC3G
TGFB2
SLC1A3
FOXA2
APOBEC3C
NOSTRIN
S100A4
APOBEC3F
ZNF608
ZNF419
AC068338.2
PDLIM5
RP11-95P13.1
SEMA3A
LINC00326
DSC2
NPM1P21
RPS4Y1
ARPC3
PBX1
LMAN1
ABCC2
AL138885.3
AC084880.1
AC083899.1
AC011611.3
AC093010.3
5
0
-5
-10
HT-29
F4
A2
G6
AC026403.1
AP000919.1
ZC4H2
AL121761.2
ZNF618
ZNF605
UTS2B
ZNF615
AKAP12
ZNF420
ZNF260
CSAG1
NAV1
ATP11C
TRABD2A
DMKN
LINC00665
0
-2
-4

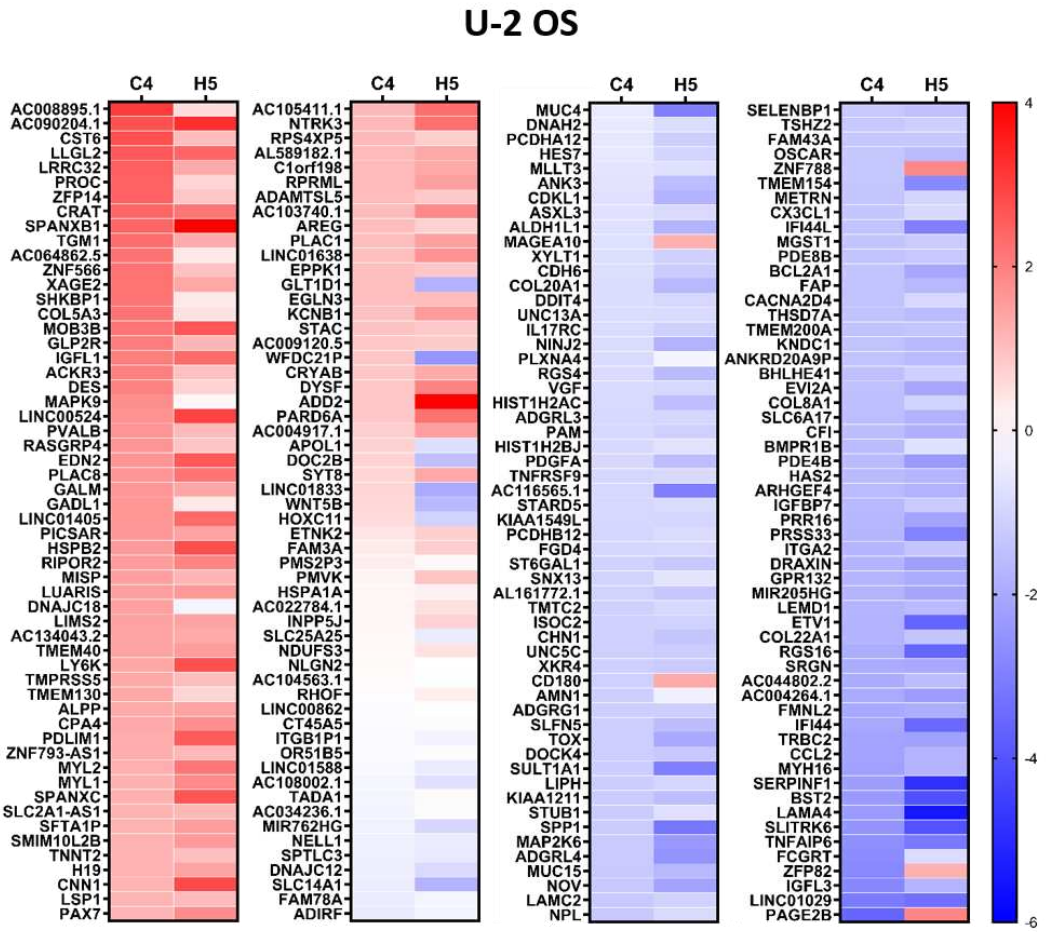

Figure 5.7 Genome-wide RNA sequencing and differential expression analysis after 5-LO KO. *(A) Venn diagrams of differentially expressed genes in HCT-116 (red), HT-29 (blue), and U-2 OS (green) single-cell clones. (B) Results of the RNA sequencing are depicted as heat maps that display the genes differentially expressed per cell line compared to the respective empty vector control: HCT-116 (top left), HT-29 (top right), U-2 OS (bottom). The genes upregulated compared to vector control cells are marked red while downregulated genes are marked in blue.*

Pathway analysis using the Enrichr platform was carried out, to find the first indication of the possible effects these gene alterations could have on the cell lines, and different pathways were suggested to be influenced (**Figure 5.8**). Depending on the used database HCT-116 gene expression alterations influence responses to hostile infections, different metabolic mechanisms, and angiogenesis. In HT-29 cells, transcription, as well as different signalling pathways, were most likely to be influenced. As the number of altered genes was the highest in U-2 OS cells, it is not surprising that the number of influenced pathways was the highest here as well. Prominent cancer-related mechanisms like regulation of extracellular matrix, adhesion, and epithelial-mesenchymal-transition occurred as hits for the pathway analysis. All those findings gave a first hint on the direction of further investigations. Additionally to the Enrichr pathway analysis, literature was searched for cellular mechanisms in which the differentially expressed genes played a role (**Table 5.1**).

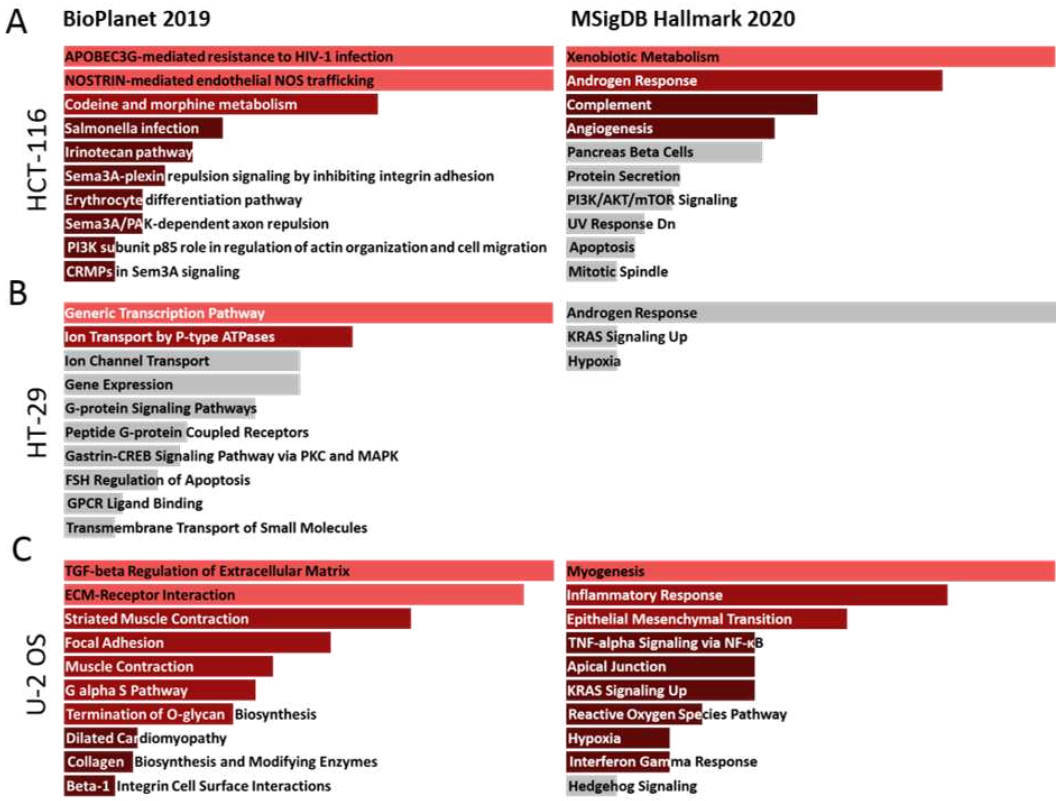

Figure 5.8 Enrichment pathway analyses after genome-wide RNA sequencing of 5-LO KO cells. *Gene set enrichment analysis of the sequencing data of HCT-116 (A), HT-29 (B), and U-2 OS (C) cells was performed employing the NCATS BioPlanet 2019 and GSEAs MSigDB Hallmark 2020 tools.*

Table 5.1 *Comprehensive overview of the differentially expressed genes per cell line grouped according to their involvement in cellular processes important for tumourigenesis. Genes involved in more than one process are listed several times.*

	Epithelial-mesenchymal-transition		**Migration**		
HCT-116	*DSC2* *FOXA2* *PBX1* *S100A4* *TGFB2*		*ARPC3* *DSC2* *FOXA2* *NOSTRIN*	*PBX1* *PDLIM5* *RPS4Y1*	*S100A4* *SEMA3A* *TGFB2*
HT-29	*AKAP12* *DMKN* *TRABD2A*		*AKAP12* *DMKN* *NAV1* *TRABD2A*		
U-2 OS	*ACKR3* *ADGRG1* *AREG* *BCL2A1* *BHLHE41* *CCL2* *CDH6* *CHN1* *CNN1* *CPA4* *CRYAB* *CST6* *CX3CL1* *DES* *DOC2B* *DRAXIN* *ETV1* *FAP* *FMNL2* *HAS2* *IGFBP7* *ITGA2* *LAMA4* *LAMC2* *LEMD1* *LIPH* *MAGEA10* *MAP2K6* *MGST1*	*MIR205HG* *MUC15* *MUC4* *NOV* *NTRK3* *PAM* *PARD6A* *PAX7* *PDE4B* *PDGFA* *PLAC1PLAC8* *PRR16* *RGS16* *RGS4* *RHOF* *SELENBP1* *SERPINF1* *SHKBP1* *SLC2A1-AS1* *SLFN5* *SPANXB1* *SPP1* *ST6GAL1* *STUB1* *TGM1* *THSD7A* *TNFAIP6* *VGF* *WNT5B*	*ACKR3* *ADD2* *ADGRG1* *AREG* *ARHGEF4* *BCL2A1* *BHLHE41* *BST2* *CCL2* *CDH6* *CDKL1* *CHN1* *CNN1* *CRYAB* *CST6* *CX3CL1* *DDIT4* *DES* *DOC2B* *DRAXIN* *DYSF* *EDN2* *EGLN3* *EPPK1* *ETNK2* *ETV1* *EVI2A* *FAM3A* *FAP* *FMNL2* *GADL1* *GPR132* *HAS2* *HOXC11*	*IFI44* *IFI44L* *IGFBP7* *IL17RC* *ITGA2* *ITGB1BP1* *KCNB1* *LAMA4* *LAMC2* *LEMD1* *LIPH* *LRRC32* *LSP1* *MAGEA10* *MAP2K6* *MAPK9* *METRN* *MGST1* *MIR205HG* *MUC15* *MUC4* *MYL2* *NDUFS3* *NELL1* *NINJ2* *NOV* *NTRK3* *PAM* *PARD6A* *PAX7* *PDE4B* *PDGFA* *PICSAR*	*PLAC1* *PLAC8* *PLXNA4* *PRR16* *RGS16* *RGS4* *RHOF* *RIPOR2* *SELENBP1* *SERPINF1* *SHKBP1* *SLC2A1-AS1* *SLFN5* *SPANXB1* *SPANXC* *SPP1* *SRGN* *ST6GAL1* *STUB1* *SYT8* *TADA1* *TGM1* *THSD7A* *TMEM130* *TNFAIP6* *TNFRSF9* *TOX* *TSHZ2* *UNC5C* *VGF* *WNT5B* *XKR4* *ZFP82*

	Extracellular matrix/adhesion	Transcription	G-protein signalling	Cytoskeleton organisation
HCT-116	*DSC2* *TGFB2* *S100A4*	*APOBEC3C* *APOBEC3G* *ZNF419* *ZNF608*		*ARPC3* *S100A4* *TGFB2*
HT-29	*DMKN*	*ZNF260* *ZNF420* *ZNF605* *ZNF615* *ZNF618*	*AKAP12*	*CSAG1* *NAV1*
U-2 OS	*ADAMTSL5* *BST2* *CDH6* *COL20A1* *COL22A1* *COL5A3* *COL8A1* *CST6* *FAP* *HAS2* *ITGA2* *ITGB1BP1* *LAMA4* *LAMC2* *MUC15* *MUC4* *NINJ2* *NOV* *PARD6A* *PCDHA12* *PCDHB12* *SPP1* *SRGN* *STUB1* *TGM1* *TMTC2* *TNFAIP6* *XYLT1*	*HES7* *MLLT3* *TSHZ2* *ZFP14* *ZFP82* *ZNF566* *ZNF788* *ZNF793-AS1*	*ADGRG1* *ADGRL3* *ADGRL4* *ARHGEF4* *CHN1* *DOCK4* *GLP2R* *KNDC1* *OR51B5* *PARD6A* *PMVK* *RASGRP4* *RGS16* *RGS4* *RHOF* *RIPOR2*	*ADD2* *AMN1* *ANK3* *ARHGEF4* *CNN1* *DES* *DNAH2* *DRAXIN* *EPPK1* *FGD4* *FMNL2* *KIAA1211* *LLGL2* *LSP1* *MISP* *MYH16* *MYL1* *MYL2* *PARD6A* *PLXNA4* *RHOF* *SNX13* *THSD7A* *TNNT2* *UNC5C*

To validate findings from RNA sequencing, isolated RNA from all knockout cells was reverse transcribed to cDNA and subjected to qPCR analysis investigating the expression of most of the identified genes. *ACTB* was used as a housekeeping gene and data were analysed using the $2^{-\Delta\Delta CT}$ method normalized to *ACTB* and the respective vector control cells.

As predicted from RNA sequencing results, most of the target genes regulated in HCT-116 cells were upregulated in the 5-LO knockout single-cell clones (**Figure 5.9**). The strongest upregulation occurred for gene *APOBEC3G* with a 10- (clone G6) to 60-fold (clones F5 and H11) upregulation of mRNA expression levels. *TGFB2* and *FOXA2* showed a moderate upregulation with a 10- to 20-fold increase of mRNA depending on the single-cell clone as well as *NOSTRIN* where mRNA amount was about 10-fold higher in all knockout clones than in the vector control-treated cells. Moderate upregulation of RNA levels in all clones was also detectable for *PDLIM5*, the two zinc finger protein-coding genes *ZNF608* and *ZNF419*, *S100A4*, the two *APOBEC* subfamilies *3C* and *3F*, and *SLC1A3*. An upregulation in clones F5 and G6 of *SEMA3A* mRNA levels but downregulation in clone H11 could be validated. While RNA expression of *DSC2*, *ABCC2*, and *ARPC3* was not altered in the knockout clones, about 2-fold downregulation of *PBX1* and *LMAN1* mRNA levels for all knockout clones could be detected. The strongest downregulation was measured for the gene expression of ribosomal protein S4 Y-linked 1 (*RPS4Y1*), a component of the 40S subunit of cytosolic ribosomes.

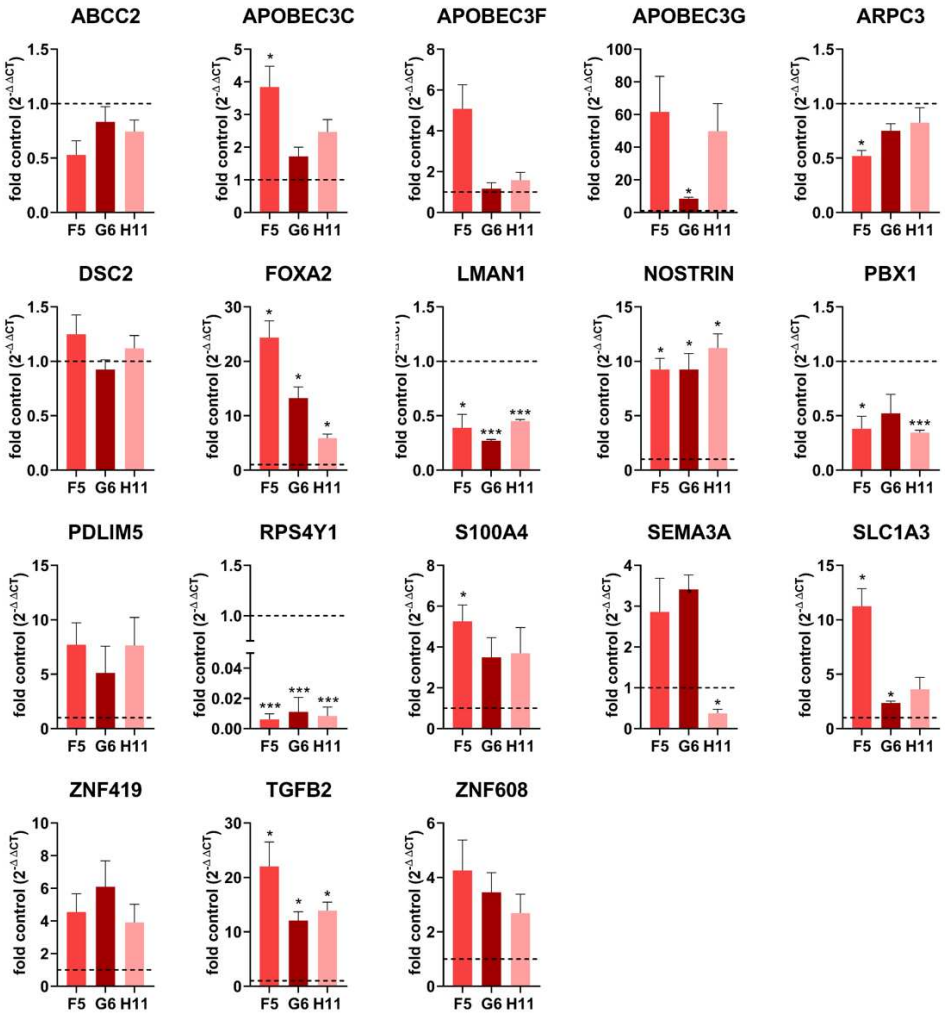

Figure 5.9 RT-qPCR analysis of differentially expressed genes in HCT-116 cells. *mRNA expression of differentially regulated genes in HCT-116 5-LO knockout clones. Gene expression was normalized to ACTB (housekeeping gene) and the corresponding vector control cells ($2^{-\Delta\Delta CT}$ method). Data are presented as mean + SEM of 3 independent experiments. Asterisks indicate significant changes vs. vector control cells *p ≤ 0.05, **p ≤ 0.01, ***p ≤ 0.001.*

In HT-29 cells, 2 different mRNA expression patterns were most prominent (**Figure 5.10**). Evaluation of gene expression for *NAV1*, *DMKN*, *AKAP12*, *TRABD2A*, *ZC4H2*, and *ZNF618* showed a decrease in mRNA expression in the knockout clones F4 and A2, while there was an increase in mRNA expression in clone G6. For the second pattern, very strong downregulation of mRNA expression for the four zinc finger protein-coding genes *ZNF605*, *ZNF615*, *ZNF420*, and *ZNF260* as well as for *CSAG1* and *ATP11C* in all three knockout clones could be detected. In that case, the mean mRNA level of the investigated genes was decreased from 74-fold (*CSAG1*) to more than 1000-fold (*ZNF260*). Expression of *LINC00665* and *UTS2B* RNA was only moderate but significantly downregulated in all knockout clones.

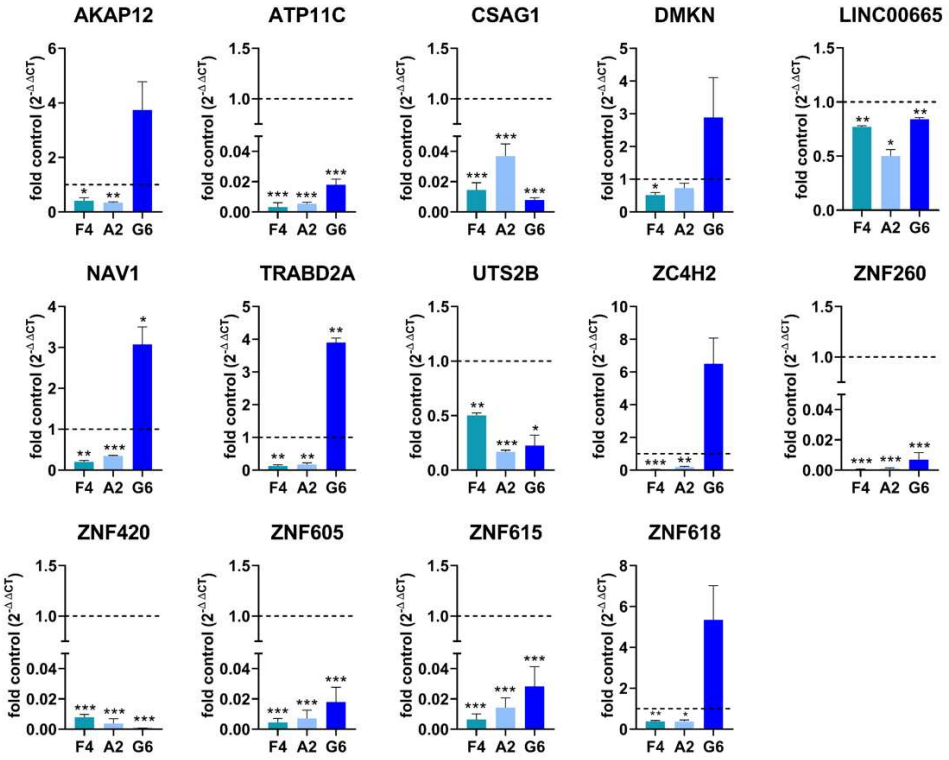

Figure 5.10 RT-qPCR analysis of differentially expressed genes in HT-29 cells. *mRNA expression of differentially regulated genes in HT-29 5-LO knockout clones. Gene expression was normalized to ACTB (housekeeping gene) and the corresponding vector control cells ($2^{-\Delta\Delta CT}$ method). Data are presented as mean + SEM of 3 independent experiments. Asterisks indicate significant changes vs. vector control cells *p ≤ 0.05, *p ≤ 0.01, ***p ≤ 0.001.*

234 genes were found for U-2 OS cells that were differentially expressed, but not all of them were validated by qPCR analysis (**Figure 5.11**). As already mentioned, about one-third of all genes that were differentially expressed were upregulated in the 5-LO knockout cells. The strongest upregulation of mRNA levels was measured for *EDN2*, *HSPB2*, *IGFL1*, and *LLGL2*. Here, depending on the single-cell clone, mRNA levels were up to 15- to 30- fold higher in cells lacking the 5-LO than in the 5-LO-containing counterparts. For *SPANXB1*, *CRAT*, *RIPOR2*, *MYL2*, *PLAC1*, and *PLAC8* mRNA expression was 5 to 10 times higher in the knockout cells and genes like *MISP*, *TMEM40* and *LIMS2* still showed a 2- to 5-fold increase in mRNA levels. However, a lot more genes were down- than upregulated in the knockout cells. While many genes were moderately downregulated by 2- to 5-fold like *BCL2A1*, *DRAXIN*, *CCL2*, or *CHN1*, for some genes stronger downregulation was investigated. Most prominent were *GPR132* and *SELENBP1*. Here mRNA expression in the knockout clones was 50-fold lower compared to the vector control carrying cells. A strong downregulation could also be examined for the genes *TNFAIP6*, *SLITRK6*, and *TRBC2* which showed average downregulation of about 20-fold. mRNA levels of the target genes *RGS16*, *CFI*, *BST2*, *SERPINF1*, *ETV1*, *IFI44*, *LAMA4*, *FMNL1*, and *SRGN* were at least 10 times lower than in 5-LO expressing cells.

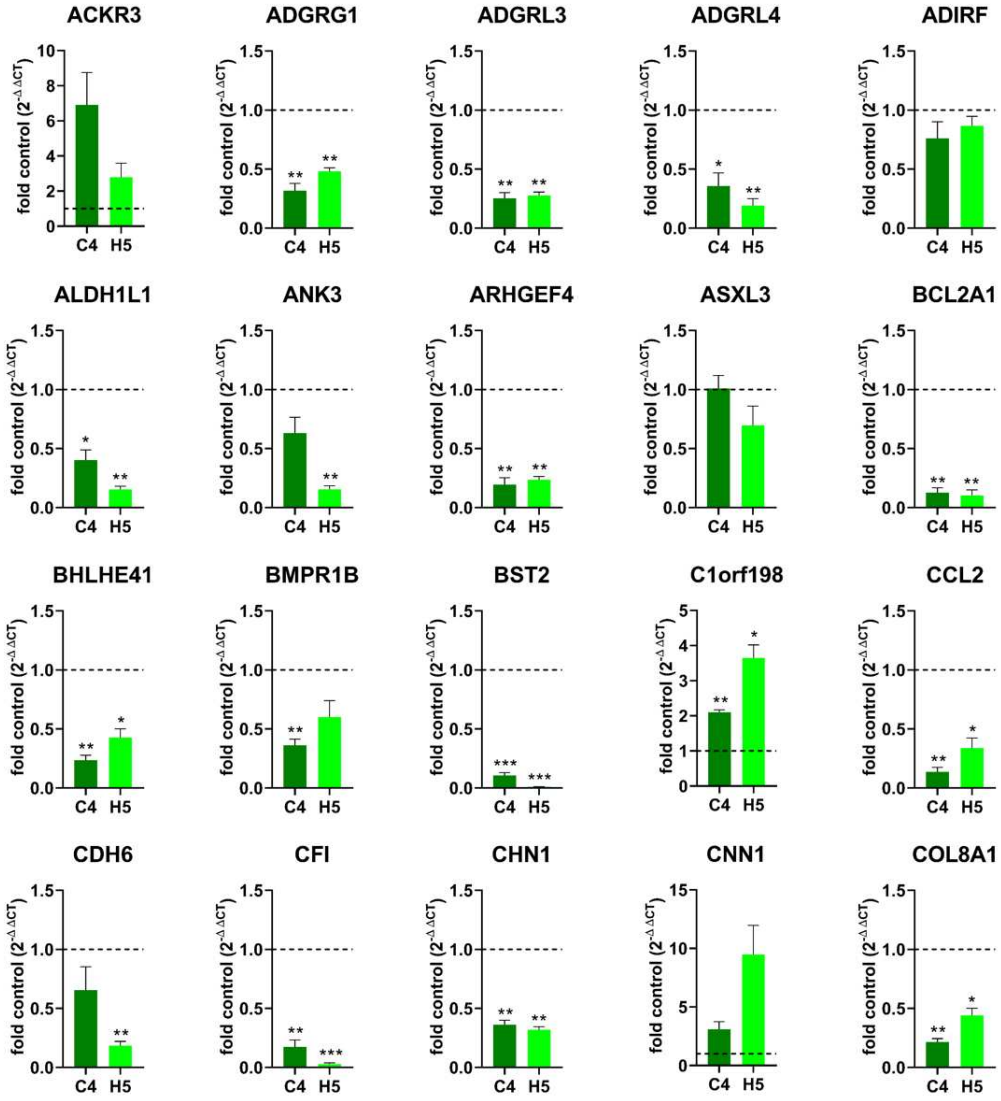

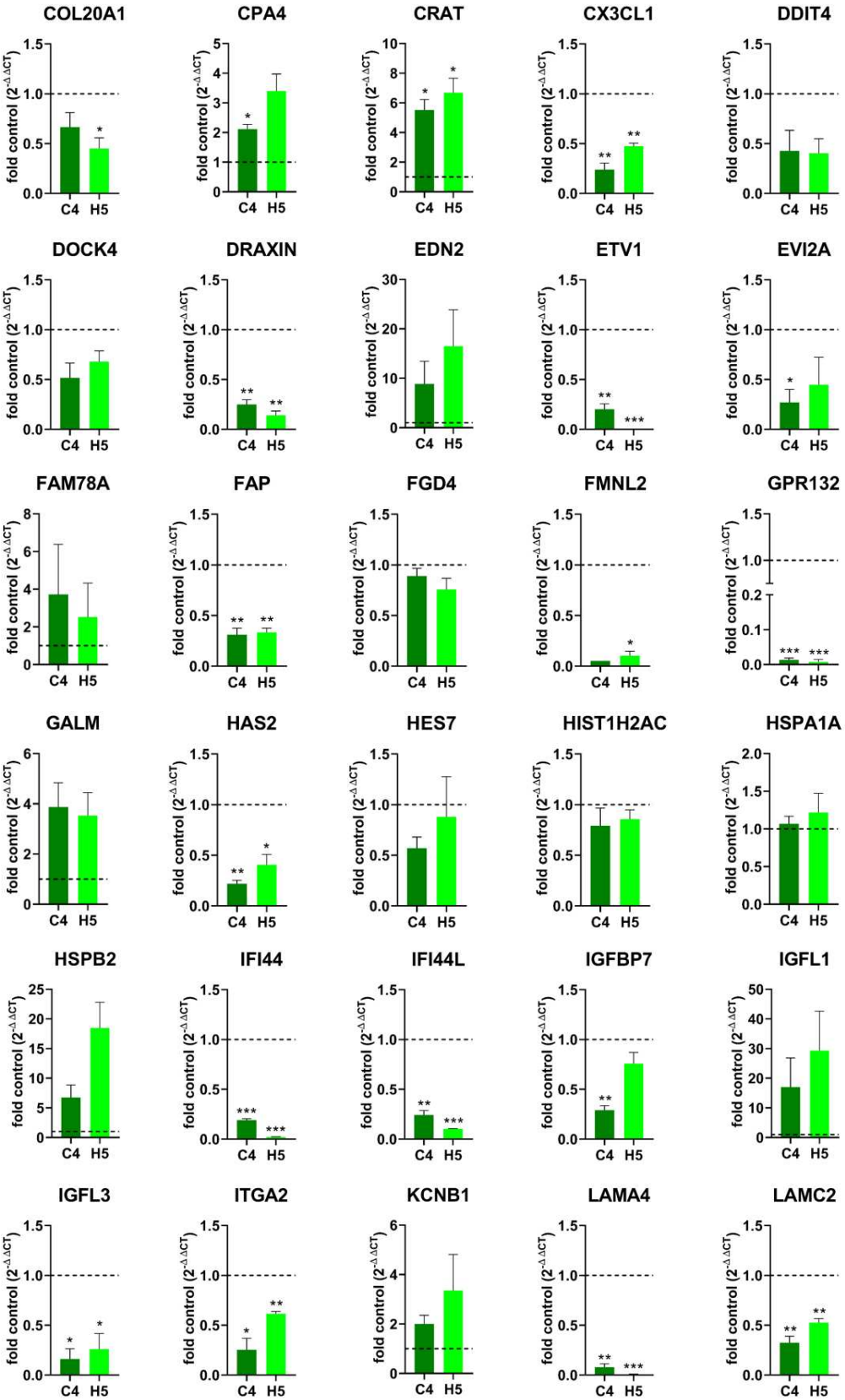
COL20A1
CPA4
CRAT
CX3CL1
DDIT4
DOCK4
DRAXIN
EDN2
ETV1
EVI2A
FAM78A
FAP
FGD4
FMNL2
GPR132
GALM
HAS2
HES7
HIST1H2AC
HSPA1A
HSPB2
IFI44
IFI44L
IGFBP7
IGFL1
IGFL3
ITGA2
KCNB1
LAMA4
LAMC2
fold control ($2^{-\Delta\Delta CT}$)
C4
H5

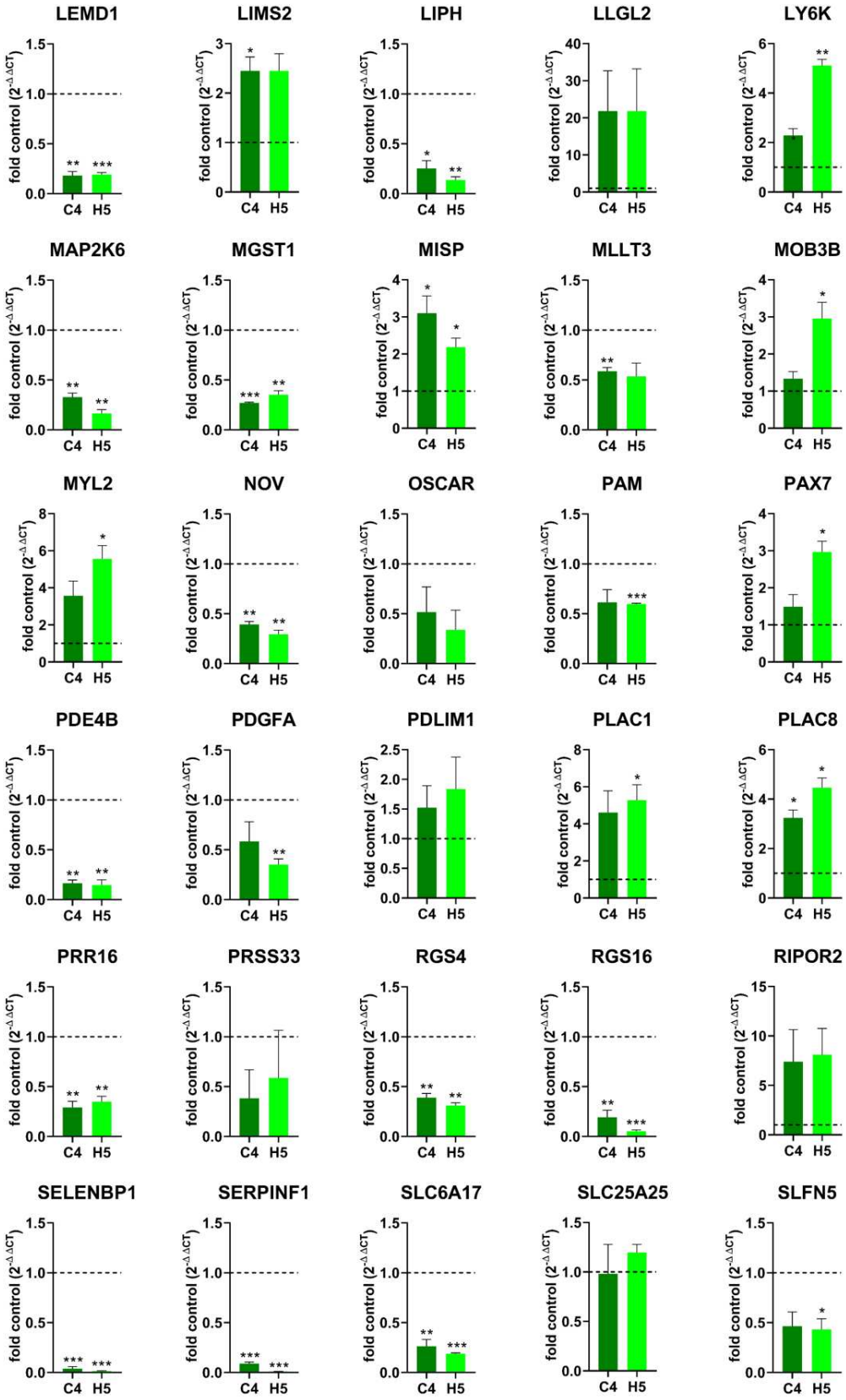
LEMD1
LIMS2
LIPH
LLGL2
LY6K
MAP2K6
MGST1
MISP
MLLT3
MOB3B
MYL2
NOV
OSCAR
PAM
PAX7
PDE4B
PDGFA
PDLIM1
PLAC1
PLAC8
PRR16
PRSS33
RGS4
RGS16
RIPOR2
SELENBP1
SERPINF1
SLC6A17
SLC25A25
SLFN5
fold control (2^-ΔΔCT)
C4
H5

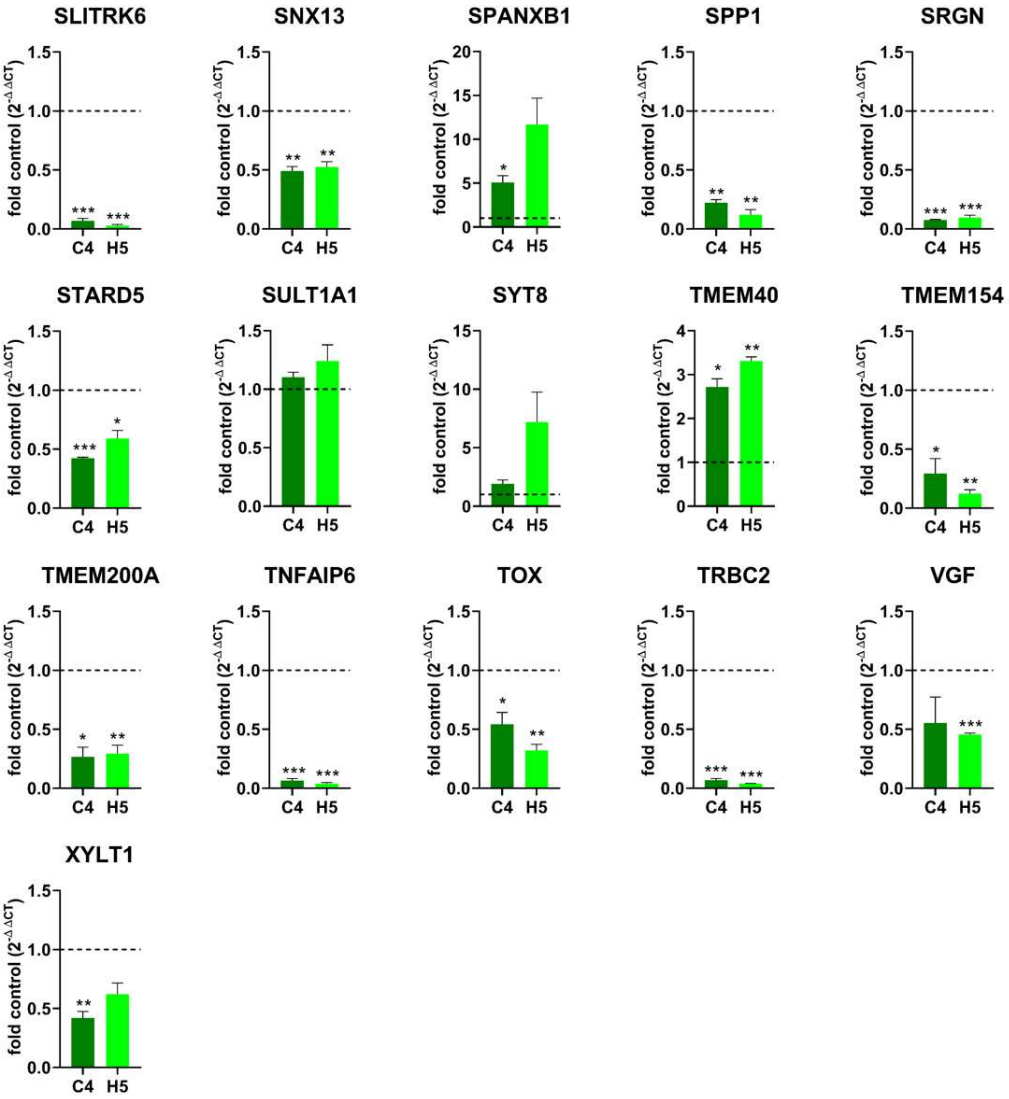

Figure 5.11 RT-qPCR analysis of differentially expressed genes in U-2 OS cells. *mRNA expression of differentially regulated genes in U-2 OS 5-LO knockout clones. Gene expression was normalized to ACTB (housekeeping gene) and the corresponding vector control cells ($2^{-\Delta\Delta CT}$ method). Data are presented as mean + SEM of 3 independent experiments. Asterisks indicate significant changes vs. vector control cells *p ≤ 0.05, **p ≤ 0.01, ***p ≤ 0.001.*

5.4 Knockout of 5-LO influences tumour cell proliferation, viability, and responsiveness to cytotoxic treatments

For investigation of the influence of the 5-LO knockout on the cell proliferation rate, cells were seeded, incubated, detached, and counted after 24, 48, 72, and 96 hours (**Figure 5.12**). While for HCT-116 cells no difference in cell numbers for 5-LO positive or negative cells was detectable, for HT-29, as well as for U-2 OS cells, a decrease in cell numbers for all knockout clones could be examined. HT-29 5-LO knockout cells in the mean showed a 50% decrease in the cell number already after 48 hours, a 55% decrease after 72 hours, and after 96 hours a decrease of around 65%. For U-2 OS cells, the cell number of 5-LO knockout cell clones was decreased on average to 75% of the respective control cells after 48 hours and to around 70% after 72 and 96 hours.

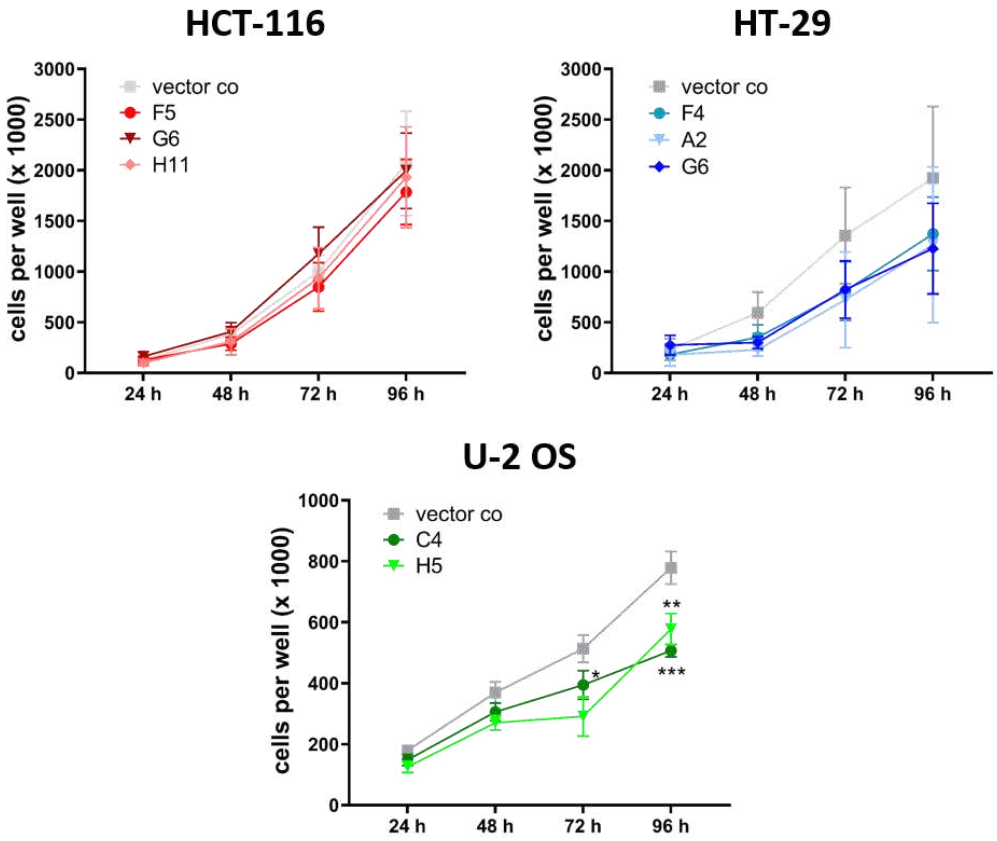

Figure 5.12 Influence of 5-LO knockout on cell proliferation. *Cell proliferation of 5-LO KO cells compared to vector controls in HCT-116, HT-29, and U-2 OS cells. Data are presented as mean ± SD from 3 independent experiments. Asterisks indicate significant changes vs. vector control-treated cells *p ≤ 0.05, **p ≤ 0.01, ***p ≤ 0.001.*

Several studies showed that 5-LO expressing tumours are distinguished by impaired responsiveness to the treatment with cytostatic drugs compared to 5-LO negative tumours (308) (264) (266). For this reason, the influence of 5-LO knockout on the overall cell viability as well as cell survival after the treatment with cytostatic drugs was tested. To investigate this, a WST-1 cell viability assay was performed. In addition, to analyse the cells more precisely FACS analysis after Annexin V/PI staining was conducted.

While untreated HT-29 cells showed no difference in the overall cell viability for any of the 5-LO knockout clones (**Figure 5.13**, middle left), in HCT-116 and U-2 OS cells, a large variability of the cell viability between the 5-LO knockout single-cell clones was determined, leading to the assumption that cell viability here underlies clonal regulation.

In HCT-116 cells, the same clonal effects could be detected after the treatment with the cytostatic drugs Actinomycin D (ActD) and Etoposide (Eto), resulting in a strong decrease in the cell viability for single-cell clone G6 after the treatment with low doses of ActD, while after the treatment with higher doses of ActD, the cell viability of clones H11 and F5 was strongly increased compared to the vector controls (**Figure 5.13**, top right). Interestingly the treatment of HCT-116 cells with higher doses of Eto lead to inverted results.

Treating HT-29 cells with higher doses of Eto seemed to affect 5-LO positive cells more as all three knockout clones showed a higher survival rate which was even significant in the case of clones A2 and G6.

Meanwhile, U-2 OS 5-LO knockout cells showed stronger responsiveness to the treatment with ActD resulting in significantly lower cell viability for both knockout clones.

However, determining the state of cell death by FACS analysis (**Figure 5.14**) suggested that in HCT-116 cells the knockout of 5-LO led to weaker responsiveness to the treatment with any of the cytostatic drugs as the number of living cells was always the smallest in the 5-LO positive vector control-treated cells. HT-29, as well as U-2 OS cells, showed no difference in the distribution between living, apoptotic and necrotic cells in this setup.

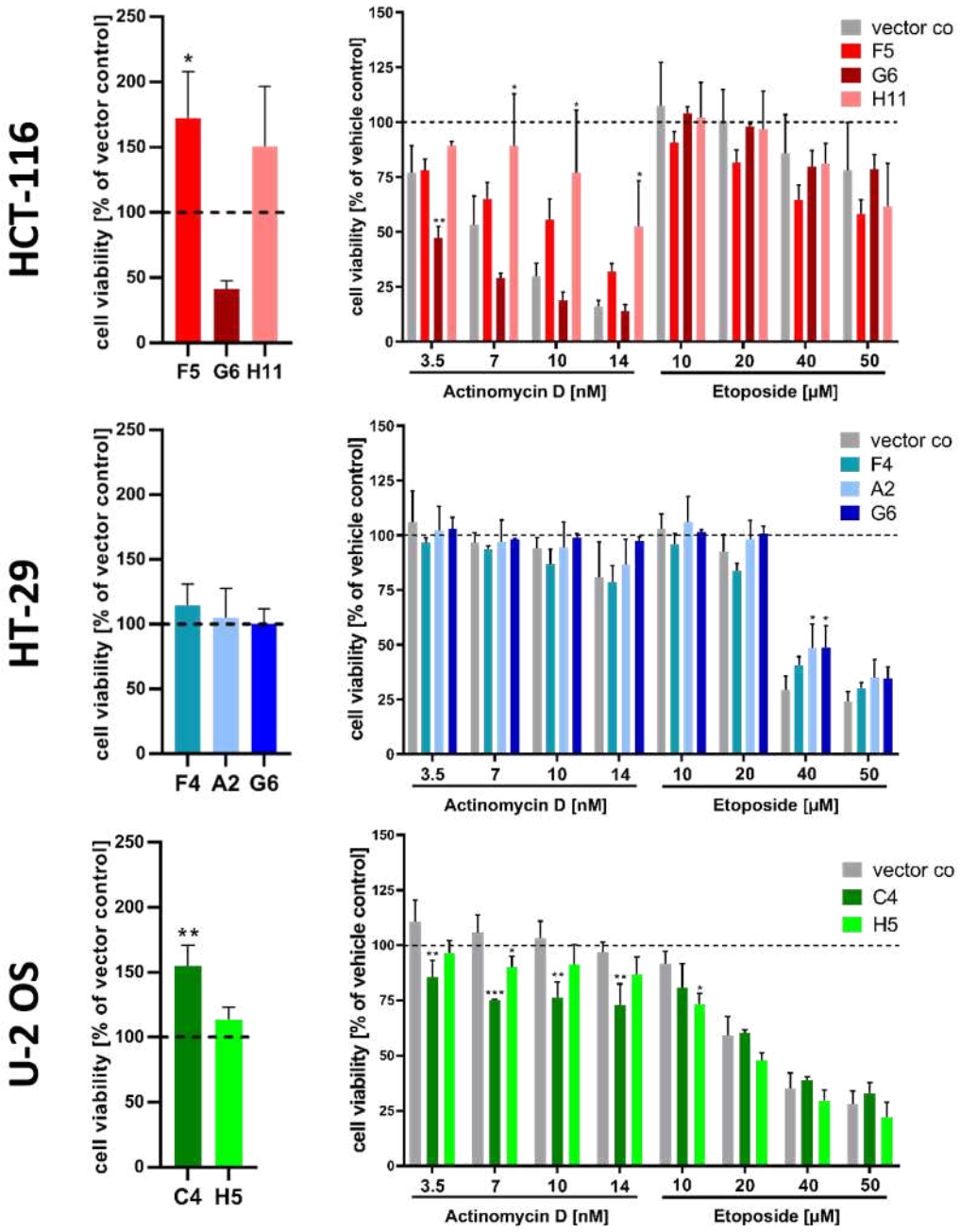

Figure 5.13 Influence of 5-LO knockout on cell viability and responsiveness to the treatment with cytostatic drugs. *(A) Cell viability of the 5-LO KO clones was assessed after 72 hours using the WST-1 assay. Viability is depicted as % of vector control. (B) Cell viability of 5-LO KO clones and vector control cells after treatment with the cytotoxic drugs Actinomycin D (3.5, 7, 10, 14 nM) and Etoposide (10, 20, 40, 50 µM) for 48 h. Cell viability was assessed using the WST-1 assay. Data are depicted as % of DMSO-treated control and presented as mean + SD from 3 independent experiments. Asterisks indicate significant changes vs. vector control-treated cells *p ≤ 0.05, **p ≤ 0.01, ***p ≤ 0.001.*

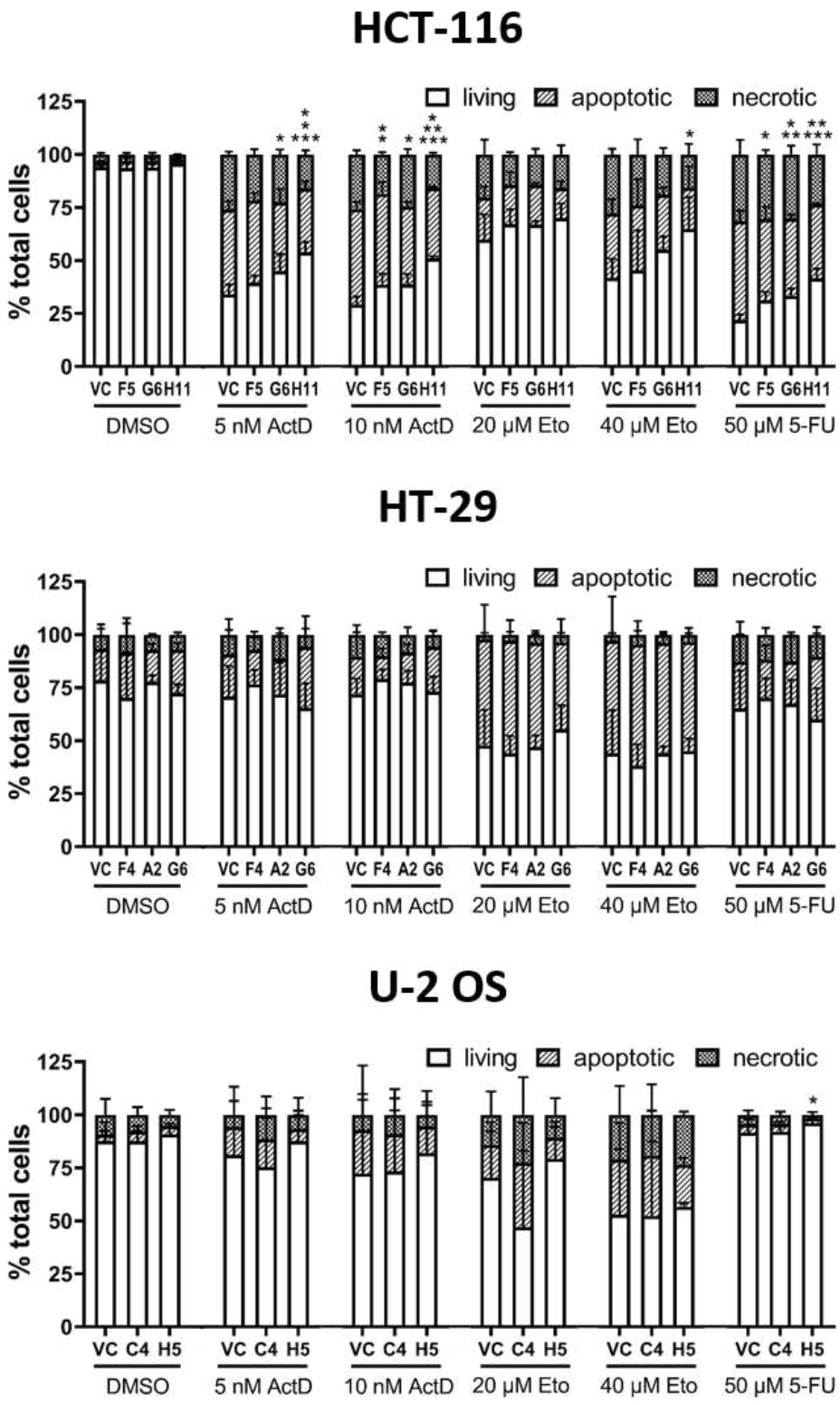

Figure 5.14 FACS analysis of HCT-116, HT-29, and U-2 OS cells after the treatment with cytostatic drugs. *Cell death analysis of 5-LO KO clones and vector control cells treated with Actinomycin D (5, 10 nM), Etoposide (20, 40 µM), or 5-fluorouracil (50 µM) after 48 hours. DMSO-treated samples were used as a negative control. Cell death was analysed via flow cytometry after Annexin V/propidium iodide staining. Data are presented as mean + SD from 3 independent experiments. Asterisks indicate significant changes vs. vector control-treated cells *p ≤ 0.05, **p ≤ 0.01, ***p ≤ 0.001. ActD: Actinomycin D, Eto: Etoposide, VC: vector control, 5-FU: 5-fluorouracil.*

5.5 Knockout of 5-LO alters colony formation and 3D growth of HCT-116, HT-29, and U-2 OS cells

The ability to form colonies when seeded at low density can also be used for the characterisation of tumour cells. Therefore, cells were seeded at low density in each well of a 6-well plate and incubated for one week. Next, colonies were fixed, stained using Ponceau red (HCT-116, HT-29) or crystal violet solution (U-2 OS) and the number of colonies was examined (**Figure 5.15**).

Despite the status of 5-LO, there was no difference in the number of colonies in HCT-116 and HT-29 cells.

In U-2 OS 5-LO knockout cells, the number of colonies formed in this setting was slightly but not significantly decreased to, depending on the single-cell clone, 60-80% of the respective 5-LO positive counterparts.

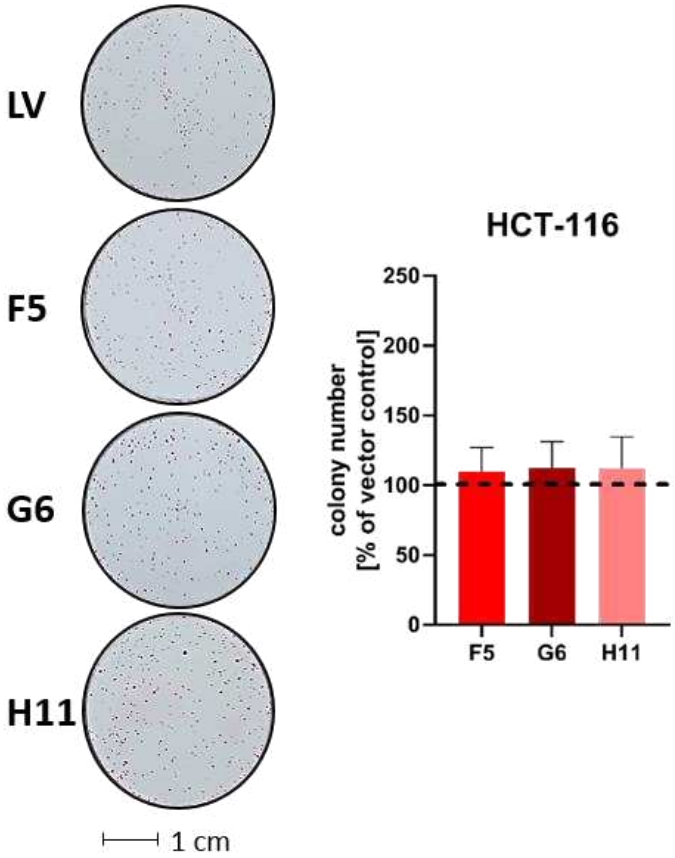

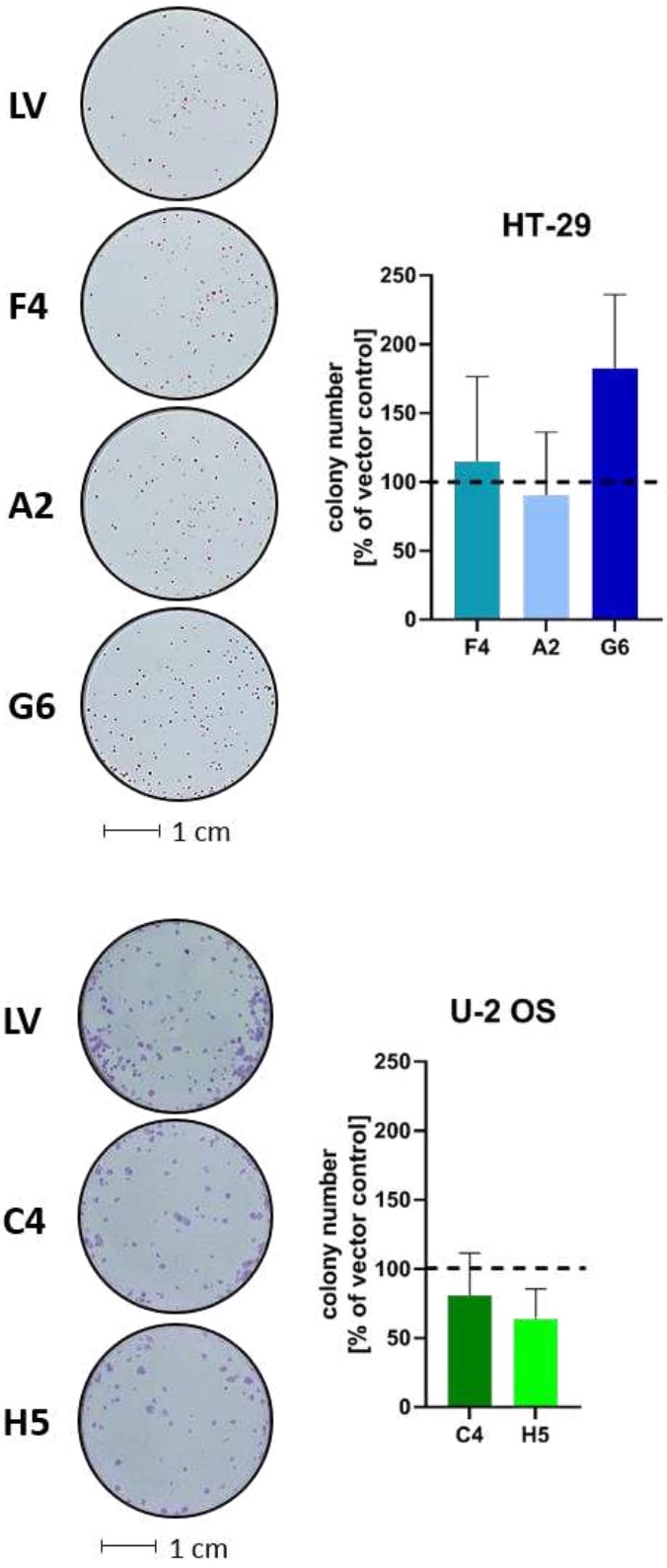

Figure 5.15 Two-dimensional colony formation of HCT-116, HT-29, and U-2 OS cells. *400 cells were seeded into 6-well plates and incubated at 37°C, 5% CO2 in a humidified atmosphere for one week. The number of colonies formed after 7 days was assessed after Ponceau red or crystal violet staining. Data are depicted as % of vector control and presented as + SD of 3 independent experiments.*

A similar setting was used for the soft agar 3D-colony-forming assay. Here the cells were seeded in liquefied agar solution and left for 3 weeks.

No U-2 OS cells - neither 5-LO positive nor 5-LO knockout cells - were able to grow in this environment.

HCT-116 5-LO knockout cells showed an increase in the number of colonies depending on the single-cell clone of 120 to 220% of the respective control but not in a significant manner (**Figure 5.16**).

In HT-29 cells no difference in the number of colonies formed in soft agar was detectable.

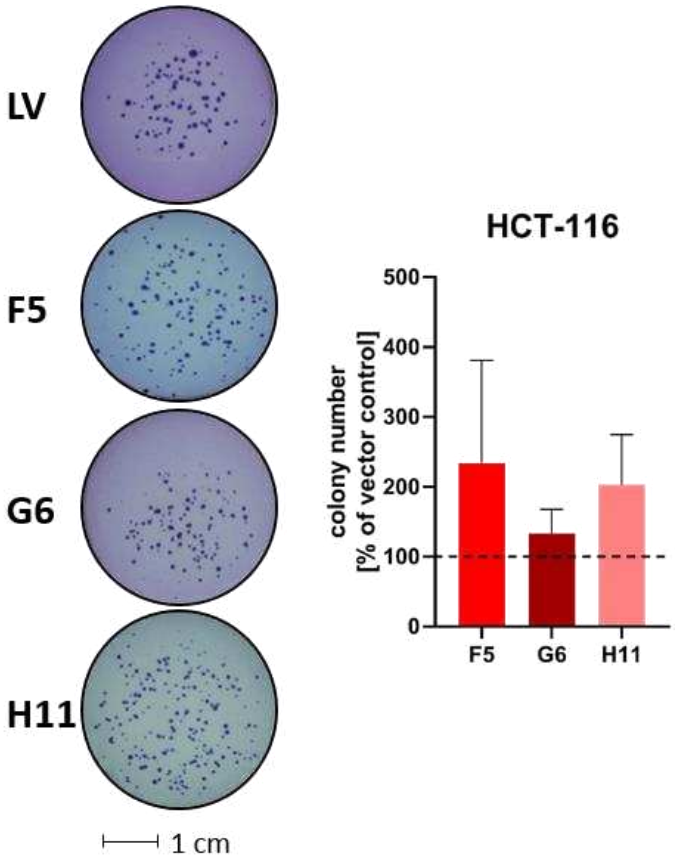

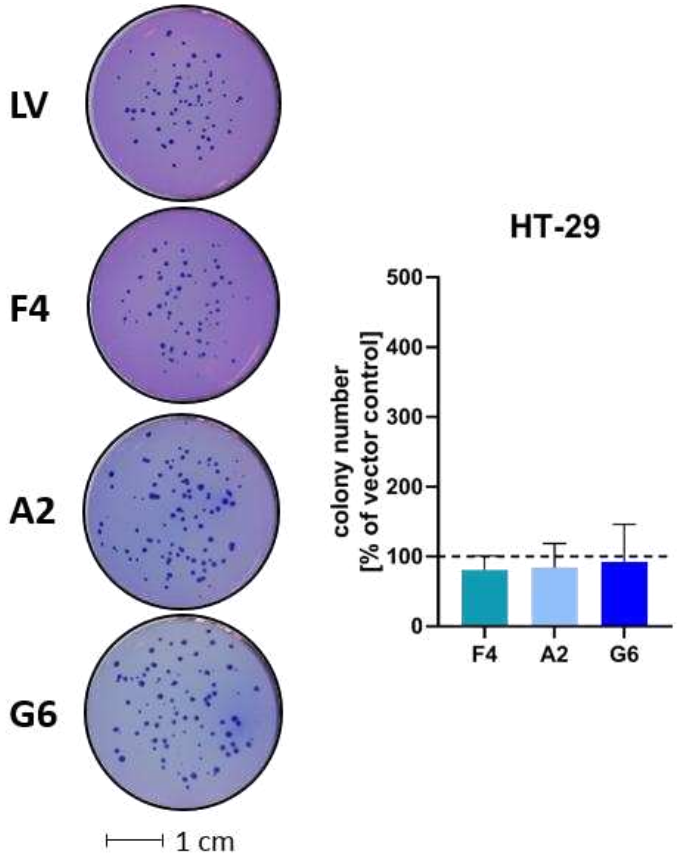

Figure 5.16 Soft agar three-dimensional colony formation of HCT-116 and HT-29 cells. *5,000 cells were seeded in 6-well plates in a layer of soft agar. After three weeks, the colonies formed were stained with crystal violet and counted. U-2 OS cells did not form any colonies under these conditions. Data are depicted as % of vector control and presented as mean + SD of 3 independent experiments.*

As conventional 2D cell culture shows limitations in transferability to physiological processes, effects of the 5-LO knockout on 3D growth and the ability to form spheroids were examined next. Cells were seeded in low-attachment plates to force the growth of multicellular spheroids. Now size, appearance, the number of cells per spheroid, and cell survival in spheroids were investigated.

Spheroids consisting of HCT-116 cells showed the largest size of all spheroids with a medium diameter of 900 µm on day 4. After 7 days it was detected that spheroid integrity was not maintained any longer as loose cells on the surface were spotted (**Figure 5.17 A**). This was observed for all types of HCT-116 cells.

HT-29 spheroids were slightly smaller but also more stable as cells on the surfaces merged to a more solid formation and it took at least 11 days for the spheroids to lose their compact round shape and release cells from the core part (**Figure 5.17 D**). In both cases, 5-LO positive cells did not show any difference in the behaviour compared to the 5-LO knockout cell clones.

However, for U-2 OS cells it was visible from day one that cells appeared differently. U-2 OS spheroids were by far the smallest and while 5-LO positive vector control cells formed a solid and denser spheroid, both knockout cell clones only were able to form loose cell gatherings with no distinct outline that were highly unstable (**Figure 5.17 G**). This can also be seen by assessing the spheroid diameters that are significantly larger for both knockout clones even though none of these cells are bigger nor did the spheroids consist of a larger number of cells (**Figure 5.17 H**).

7 days after the initial seeding of the cells, spheroids were disaggregated and the number of cells in each spheroid was counted. In HCT-116 cells neither the number of living nor the total number of cells was influenced by the knockout of 5-LO (**Figure 5.17 C**). This was different for HT-29 cells, where the number of living as well as the total number of cells was elevated in all 5-LO knockout clone spheroids from 120 to 160% of the control cells (**Figure 5.17 F**). In U-2 OS cells contrary effects of the 5-LO knockout could be detected as the number of cells per spheroid was decreased to about 50% of the 5-LO positive counterparts (**Figure 5.17 I**).

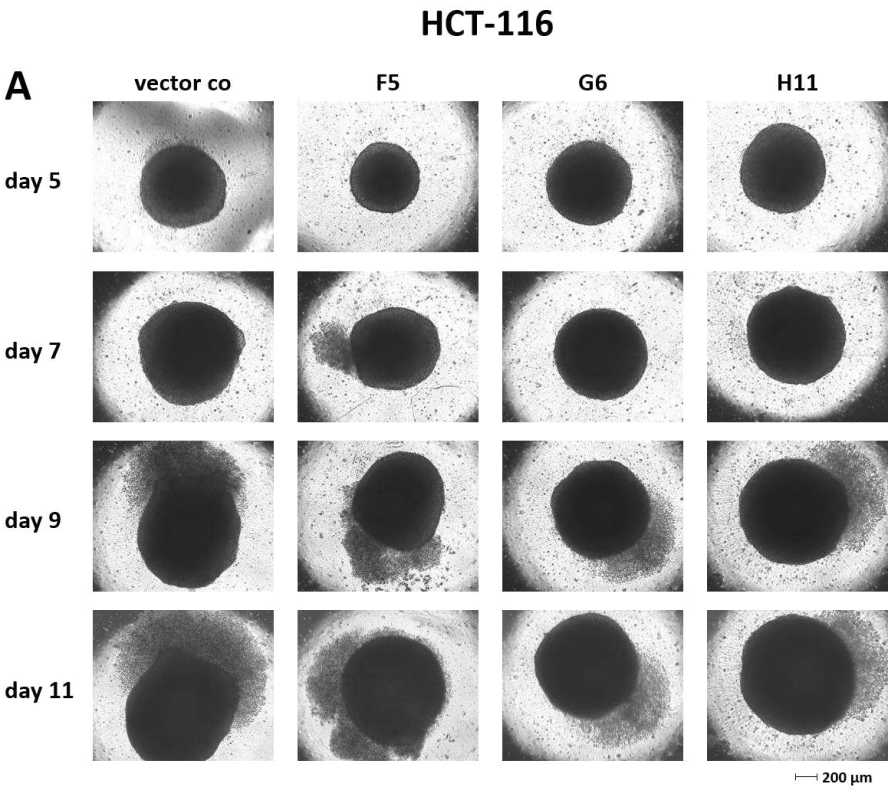
HCT-116
A
vector co
F5
G6
H11
day 5
day 7
day 9
day 11
200 µm

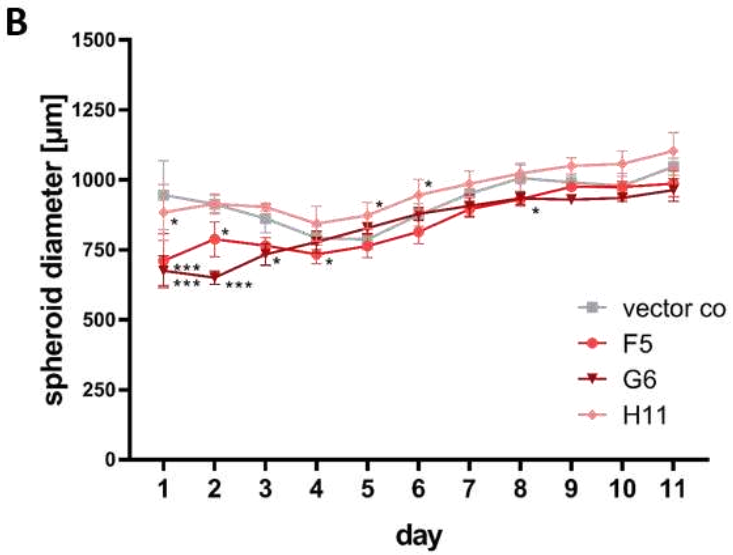
B
spheroid diameter [µm]
1500
1250
1000
750
500
250
0
1
2
3
4
5
6
7
8
9
10
11
day
vector co
F5
G6
H11

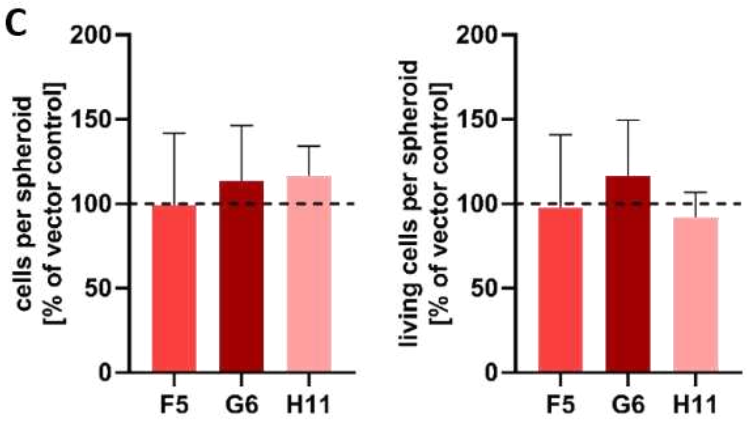
C
cells per spheroid [% of vector control]
living cells per spheroid [% of vector control]
200
150
100
50
0
F5
G6
H11

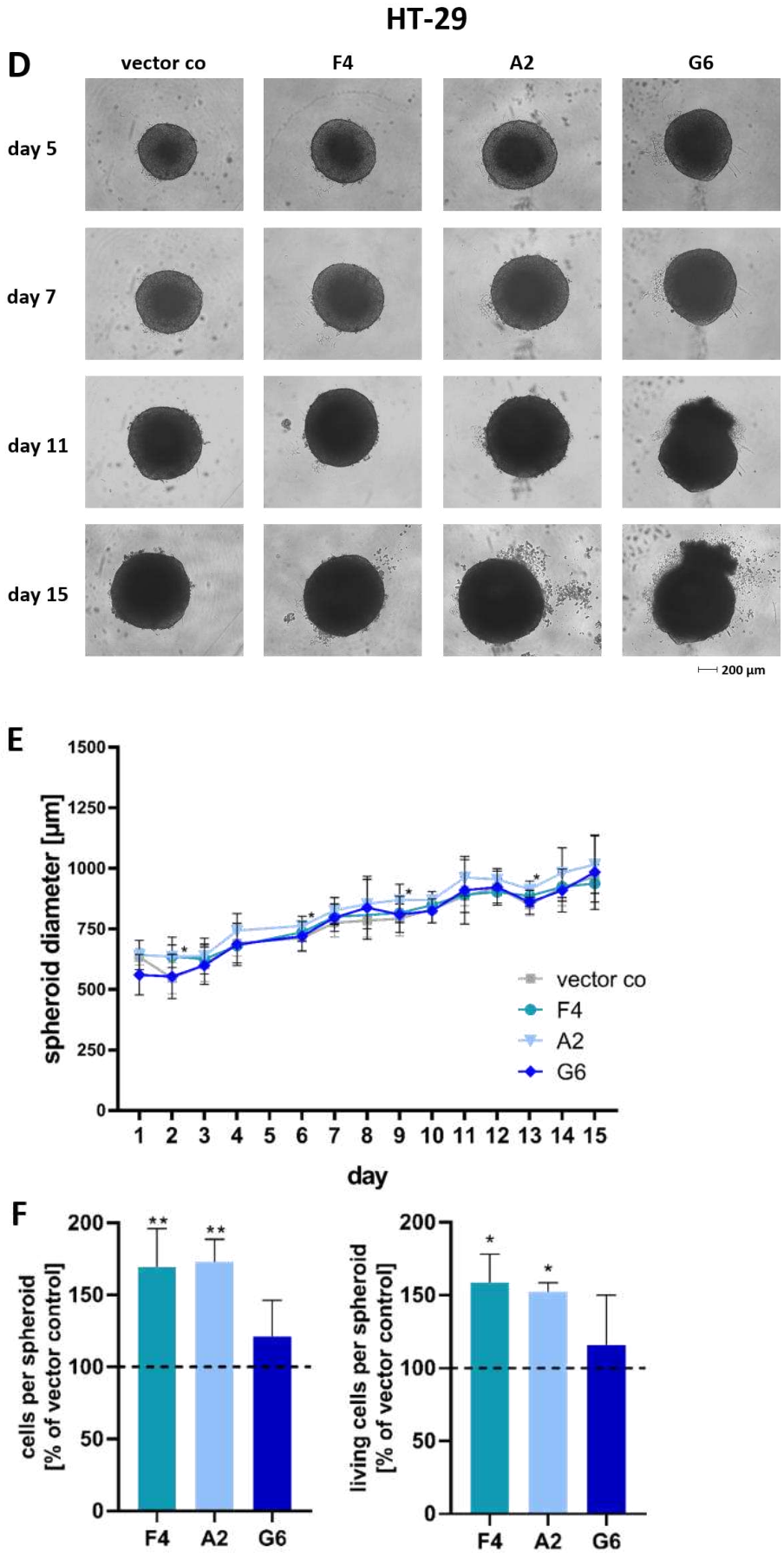
HT-29
D
vector co
F4
A2
G6
day 5
day 7
day 11
day 15
200 µm
E
spheroid diameter [µm]
1500
1250
1000
750
500
250
0
1 2 3 4 5 6 7 8 9 10 11 12 13 14 15
day
vector co
F4
A2
G6
F
cells per spheroid [% of vector control]
living cells per spheroid [% of vector control]
200
150
100
50
0
F4
A2
G6

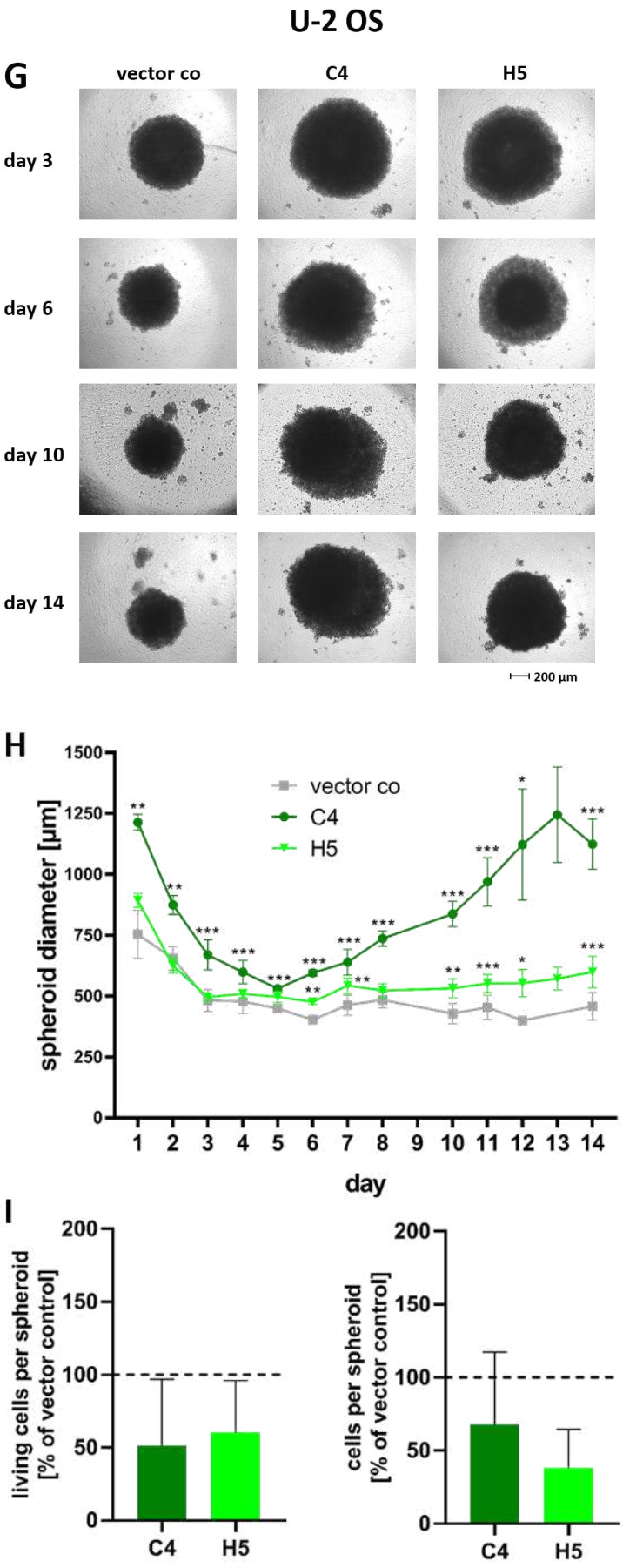
U-2 OS
G
vector co
C4
H5
day 3
day 6
day 10
day 14
200 µm
H
spheroid diameter [µm]
vector co
C4
H5
day
I
living cells per spheroid [% of vector control]
cells per spheroid [% of vector control]
C4
H5

Figure 5.17 Appearance, size, and composition of spheroids formed by HCT-116, HT-29, and U-2 OS cells. *For spheroid formation, $1*10^4$ cells were seeded in each well of a low-attachment 96-well plate and incubated at 37°C, 5% CO_2 in a humidified atmosphere. (A) HCT-116 spheroids incubated for 5, 7, 9, and 11 days. Pictures were taken at 5x magnification using a Zeiss Axio Vert.A1 microscope and examined using the Zen blue software. (B) Diameter of spheroids measured over a period of 11 days. Data are presented as mean ± SD of 3-9 independent experiments. (C) Number of living (left) and total (right) cells per spheroid depicted as % of the corresponding vector control. Data are presented as mean + SD of 3 independent experiments. (D) HT-29 spheroids incubated for 5, 7, 11, and 15 days. (E) Diameter of spheroids measured over a period of 15 days. Data are presented as mean ± SD of 3-9 independent experiments. (F) Number of living (left) and total (right) cells per spheroid depicted as % of the corresponding vector control. Data are presented as mean + SD of 3 independent experiments. (G) U-2 OS spheroids incubated for 3, 6, 10, and 14 days. (H) Diameter of spheroids measured over a period of 14 days. Data are presented as mean ± SD of 3-9 independent experiments. (I) Number of living (left) and total (right) cells per spheroid depicted as % of the corresponding vector control. Data are presented as mean + SD of 3 independent experiments. Asterisks indicate significant changes vs. vector control cells *p ≤ 0.05, **p ≤ 0.01, ***p ≤ 0.001.*

Overall cell viability using ATP as a surrogate parameter in spheroids was examined using the Promega CellTiter-Glo® 3D Cell Viability Assay. Here, a slight decrease in the cell viability in spheroids formed by HT-29 5-LO knockout cells compared to the vector control cells was revealed. In HCT-116 and U-2 OS 5-LO knockout cells, cell viability was determined by clonal effects as for HCT-116 clones F5 and G6, as well as U-2 OS clone H5 the viability was slightly decreased while an increase was detectable for the rest (**Figure 5.18**).

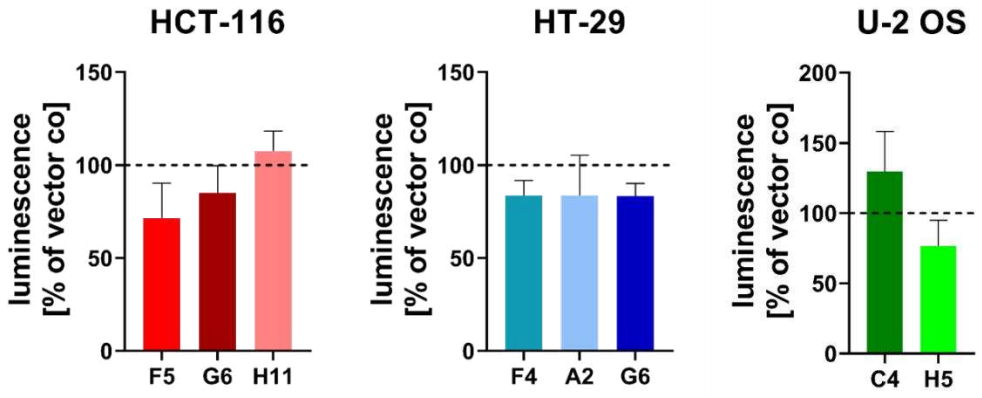

Figure 5.18 Cell viability in spheroids of HCT-116, HT-29, and U-2 OS cells. *Cell viability in spheroids was assessed by the CellTiter-Glo® 3D cell viability assay. Viability is depicted as % of vector control. Data are presented as mean + SD of 3 independent experiments*

To investigate the influence of the 5-LO knockout on spheroid outgrowth, spheroids incubated for four days were embedded in Matrigel®, an artificial extracellular matrix that allows an even more complex 3D growth of the cells. The size and appearance of the spheroids were examined over a period of 19 days.

Among the three parental cell lines, HCT-116 cells showed the highest increase in the size of the spheroids over time and embedding in Matrigel® led to the evolution of a spiked spheroid surface outgrowing into the extracellular matrix. Only knockout clone G6 showed a significantly increased size of the spheroids while clones F5 and H11 resembled the vector control-treated cells (**Figure 5.19 A, B**).

HT-29 cells evolved a bubble-shaped surface after the addition of an artificial extracellular matrix but no differences in shape and size among the 5-LO positive and negative cells were detectable (**Figure 5.19 C, D**).

Similar to the already assessed conventional spheroid formation, this was different for U-2 OS cells. By embedding the spheroids in Matrigel®, 5-LO positive, as well as 5-LO knockout cells, were able to evolve the typical spheroid structure, but 5-LO positive vector control cells formed spheroids of about twice the size of 5-LO knockout cells (**Figure 5.19 E, F**). Also, on the surface of spheroids formed by 5-LO-containing cells (wildtype as well as vector control-treated), tube-like structures started to emerge and grow into the extracellular matrix (**Figure 3.19 G**, marked by arrows). This effect was completely absent for both 5-LO knockout cell clones.

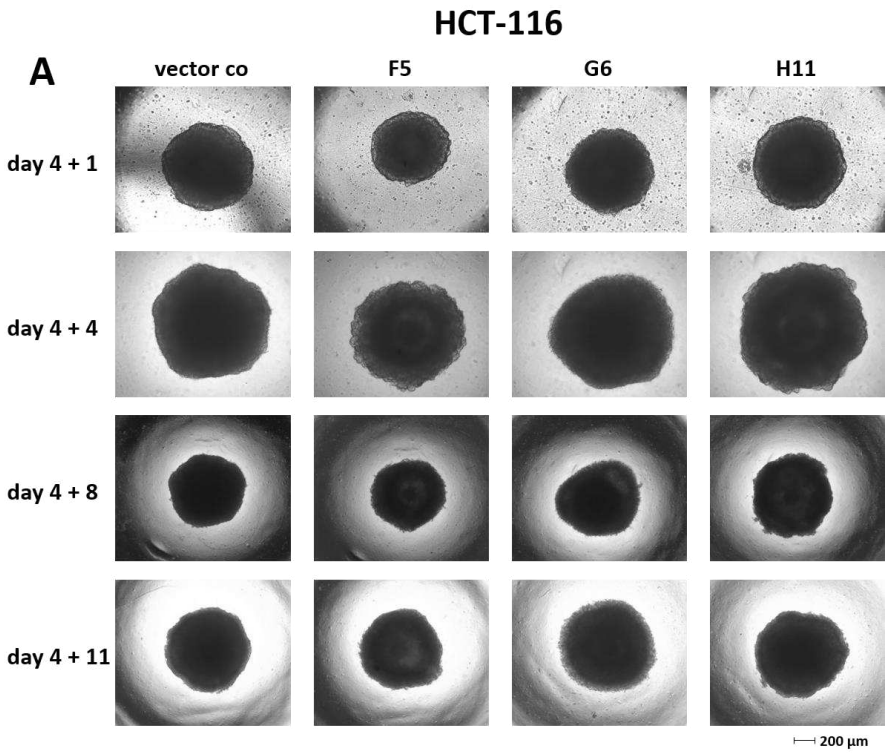
HCT-116
A
vector co
F5
G6
H11
day 4 + 1
day 4 + 4
day 4 + 8
day 4 + 11
200 µm

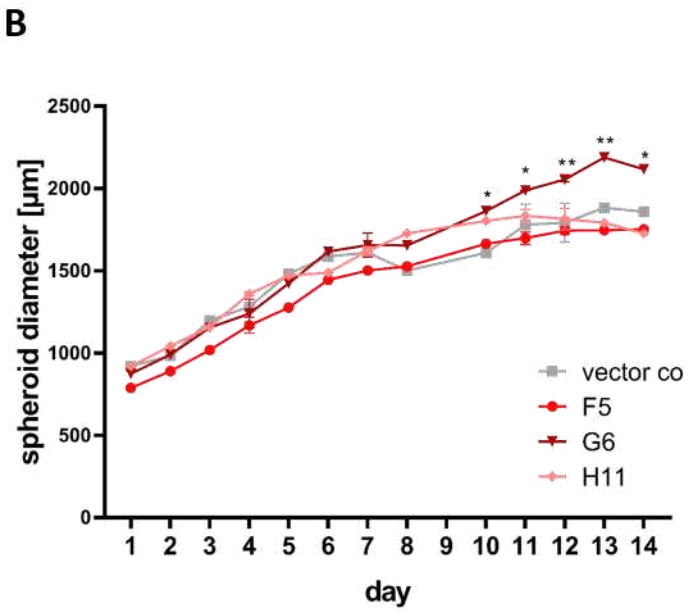
B
spheroid diameter [µm]
2500
2000
1500
1000
500
0
1 2 3 4 5 6 7 8 9 10 11 12 13 14
day
vector co
F5
G6
H11

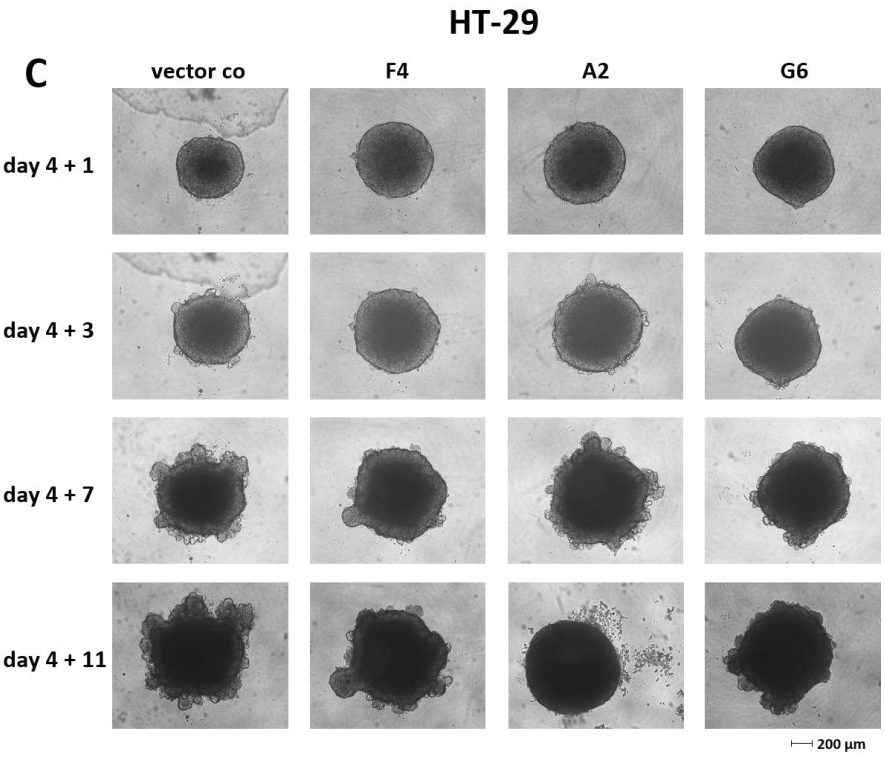
HT-29
C
vector co
F4
A2
G6
day 4 + 1
day 4 + 3
day 4 + 7
day 4 + 11
200 µm

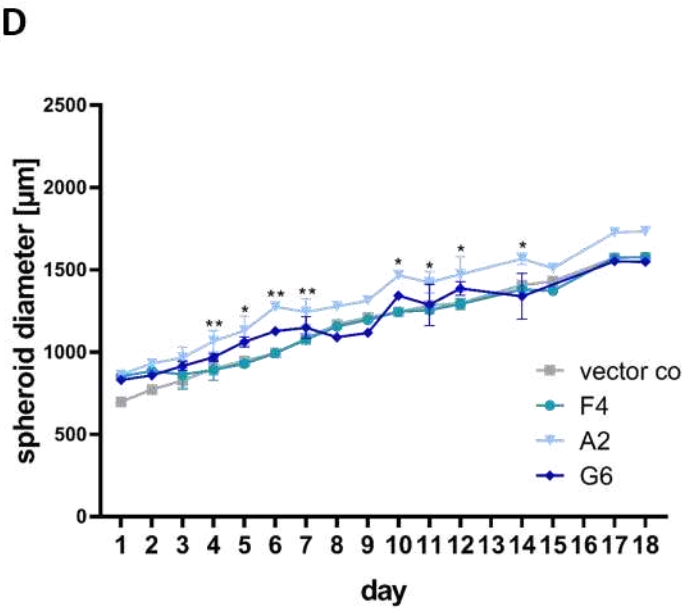
D
spheroid diameter [µm]
2500
2000
1500
1000
500
0
1 2 3 4 5 6 7 8 9 10 11 12 13 14 15 16 17 18
day
vector co
F4
A2
G6

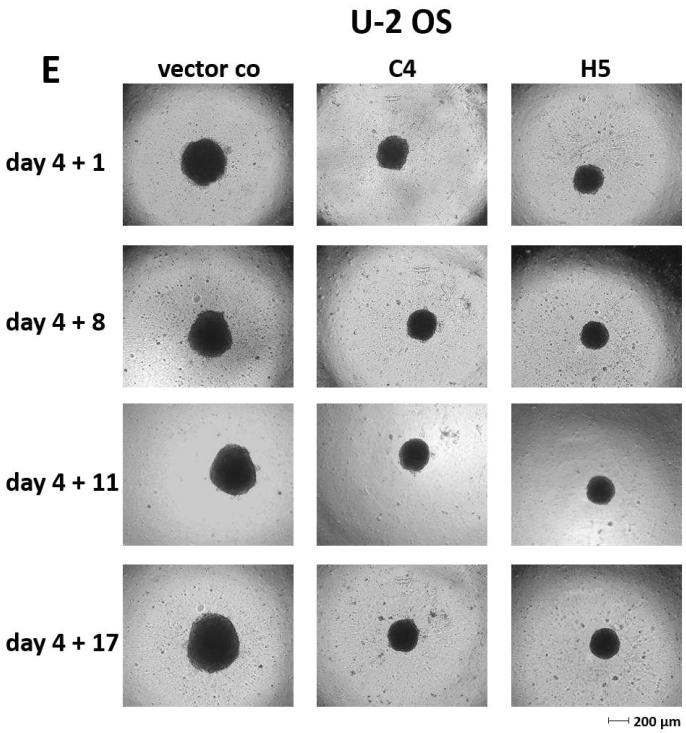
U-2 OS
E
vector co
C4
H5
day 4 + 1
day 4 + 8
day 4 + 11
day 4 + 17
200 µm

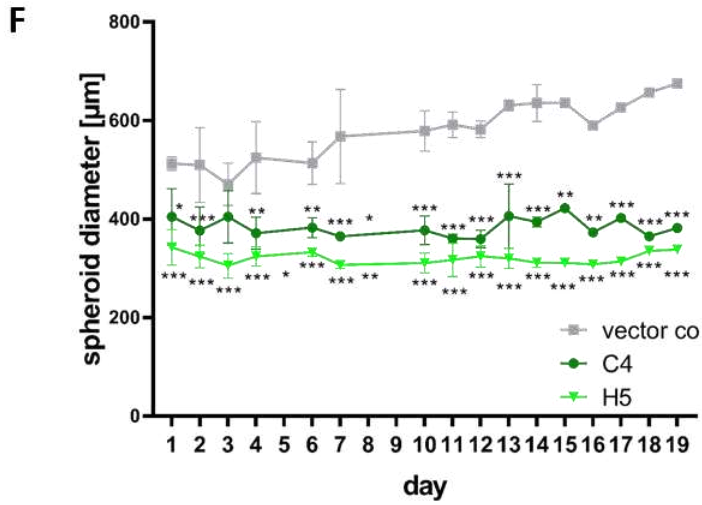
F
spheroid diameter [µm]
800
600
400
200
0
1 2 3 4 5 6 7 8 9 10 11 12 13 14 15 16 17 18 19
day
vector co
C4
H5

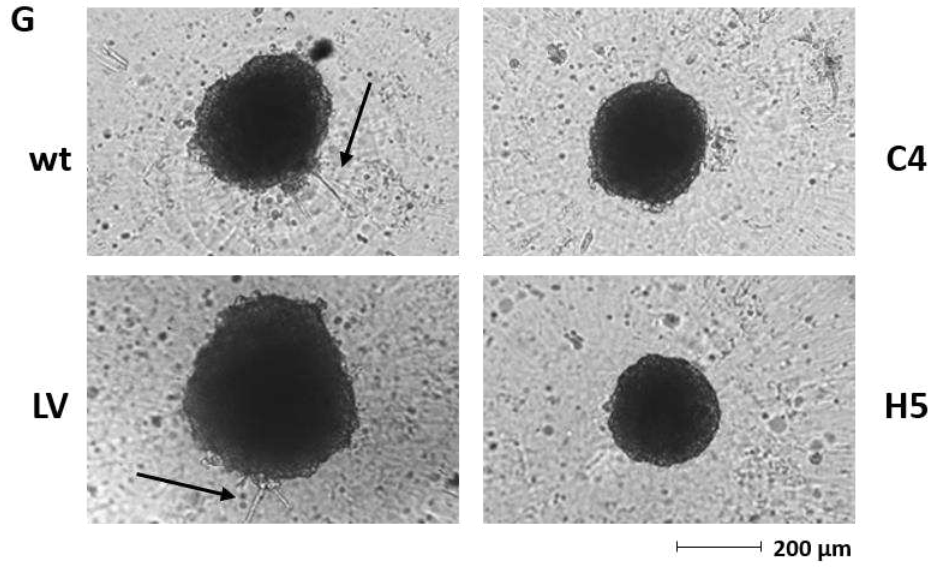
G
wt
C4
LV
H5
200 µm

Figure 5.19 Assessment of spheroid outgrowth into the extracellular matrix. *$1*10^4$ cells were seeded in low-attachment plates and incubated at 37°C, 5% CO_2 in a humidified atmosphere. After four days, Matrigel® was added and spheroids were further incubated. (A) HCT-116 Spheroids incubated in Matrigel® for 1, 4, 8, and 11 days. (B) Diameter of HCT-116 spheroids measured over a period of 14 days. (C) HT-29 spheroids incubated in Matrigel® for 1, 3, 7, and 11 days. (D) Diameter of HT-29 spheroids measured over a period of 18 days. (E) U-2 OS spheroids incubated in Matrigel® for 1, 8, 11, and 17 days. (F) Spheroids incubated in Matrigel® for 8 days, arrows mark the outgrowing structures from U-2 OS wildtype (wt) and vector control-treated cells. (G) Diameter of U-2 OS spheroids measured over a period of 14 days. Data are presented as mean ± SD of 3-9 independent experiments. Asterisks indicate significant changes vs. vector control cells *p ≤ 0.05, **p ≤ 0.01, ***p ≤ 0.001. Pictures were taken at 5x or 2.5x (only HCT-116, 8 + 11 days) magnification using a Zeiss Axio Vert.A1 microscope and examined using the Zen blue software.*

5.6 Knockout of 5-LO strongly increases directed cell migration in HCT-116 and U-2 OS cells

Many of the regulated genes that were found with RNA sequencing are known to be connected to epithelial-mesenchymal-transition (EMT). For this reason, the mRNA expression of genes that are used as common EMT markers was analysed by real-time qPCR (**Figure 5.20**).

In HCT-116 cells, only *SNAI2* expression was slightly altered. Here mRNA levels in all three 5-LO knockout clones were decreased to about 50% of the respective vector control cells.

In HT-29 cells, *CDH2* and *SNAI2* were upregulated in all knockout clones, even if this was not significant.

U-2 OS cells revealed contradictory regulation for *CDH2* and *SNAI1* for the two knockout clones and no regulation of the other two genes.

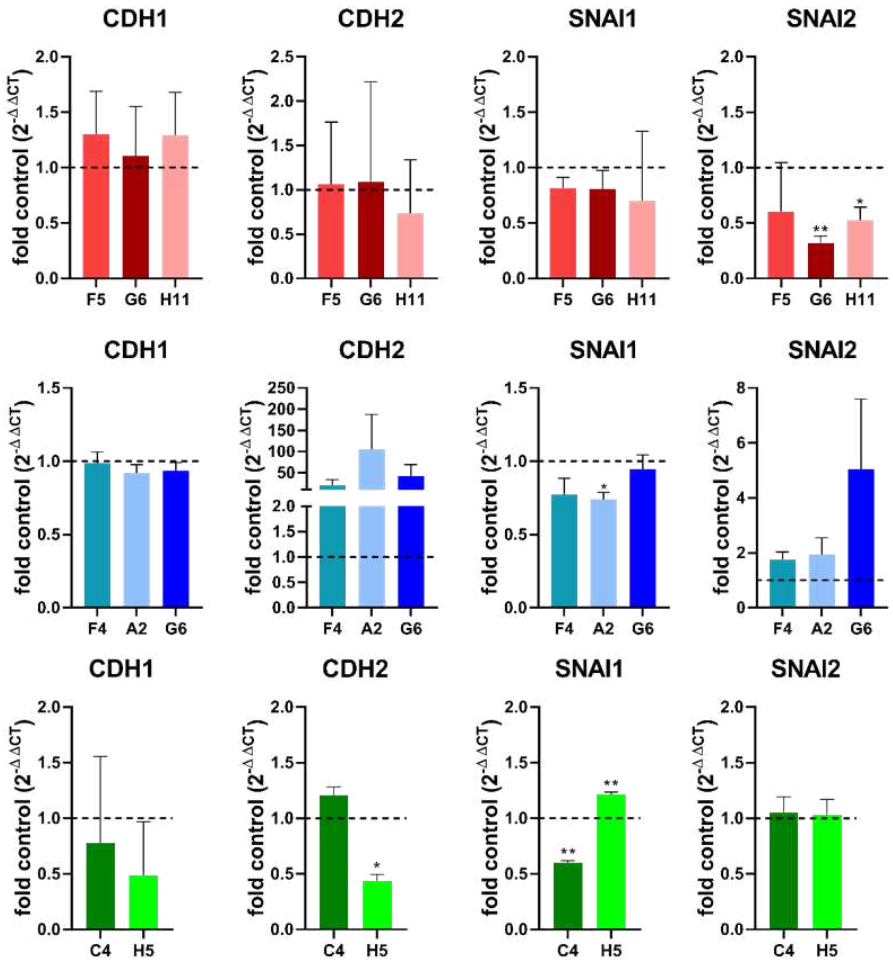

Figure 5.20 RT-qPCR analysis of CDH1, CDH2, SNAI1, and SNAI2 in HCT-116, HT-29, and U-2 OS cells. *mRNA expression of EMT marker genes in HCT-116, HT-29, and U-2 OS 5-LO knockout clones. Gene expression was normalized to ACTB (housekeeping gene) and the corresponding vector control cells ($2^{-\Delta\Delta CT}$ method). Data are presented as mean + SD of 3 independent experiments. Asterisks indicate significant changes vs. vector control cells *p ≤ 0.05, **p ≤ 0.01, ***p ≤ 0.001.*

Directed and undirected cell migration was explored next. For directed cell migration, cells were seeded in the upper compartment of a transwell chamber in a serum-deprived medium. The lower compartment contained 10% FCS and migration towards the serum gradient was assessed. After a defined period (HCT-116 + HT-29: 24 hours, U-2 OS: 3 hours) medium from the lower chamber was replaced by a serum-deprived medium containing the esterified fluorescent dye Calcein-AM and incubated for 45 minutes. Subsequently, cells that migrated through the membrane to the bottom side were detached using TE, and the fluorescence of the cell suspension was measured (**Figure 5.21 A**). Despite their 5-LO status, all U-2 OS cells were much more mobile than the two colorectal cancer cell lines and so incubation time was kept shorter.

Signal intensity in all three HCT-116 knockout clones was increased to 200 to 300% of the respective control, meaning that 2 to 3 times more cells were able to migrate towards the chemoattractant if they lacked 5-LO. While HT-29 cells showed no differences in the directed cell migration, also 50% more U-2 OS cells not expressing 5-LO were able to migrate through the membrane.

When a layer of Matrigel® on top of the membrane was added to the experimental setup to mimic invasion into the extracellular matrix, no differences in the migration ability of 5-LO positive and negative cells could be examined for any of the cell lines (**Figure 5.21 B**).

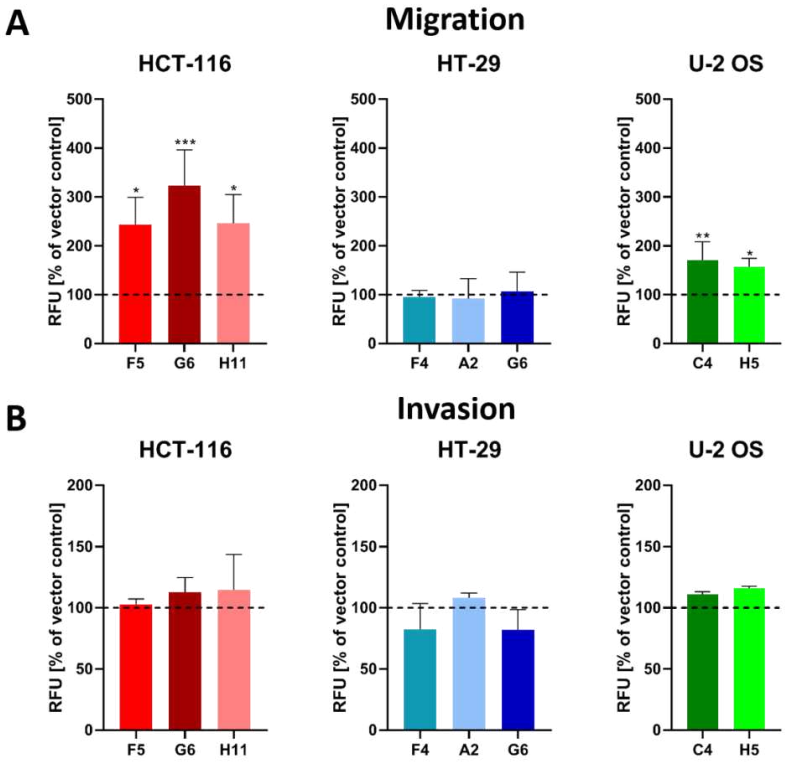

Figure 5.21 Directed cell migration and invasion of HCT-116, HT-29, and U-2 OS cells. *(A) Directed cell migration towards a serum gradient was measured in a transwell assay for 3 h (U-2 OS) or 24 h (HCT-116, HT-29). (B) For investigations on invasive properties of the cells, migration through Matrigel® was measured. Data are depicted as % of vector control and presented as mean + SD from 3-5 independent experiments. Asterisks indicate significant changes vs. vector control-treated cells *p ≤ 0.05, **p ≤ 0.01, ***p ≤ 0.001.*

The influence on undirected cell migration - known as haptotaxis - was assessed by performing a wound closure assay (**Figure 5.22**). For that, cells were seeded in both chambers of a cell culture insert and after reaching confluency the insert was removed resulting in a precise gap between the two cell fields. Now cells were able to close this gap by moving or growing toward each other. Interestingly, the time it took for the cells to close this gap was very different between the three cell lines.

As already learned from the transwell assay, U-2 OS cells are extremely mobile adherent cells and in a time course of 13 - 16 hours, the gap was closed. Nevertheless, this was true for all types of U-2 OS cells regardless of their 5-LO status.

For HCT-116 cells it took about 66 hours to close the gap again showing the enhanced motility for U-2 OS cells. Also, taking a closer look after this time course suggests that the closing of the gap for HCT-116 cells was rather due to proliferation than to active movement as the gap, even though it is closed, was still visible with cell masses surrounding it.

HT-29 cells are hardly moving at all as it took them more than 120 hours to close the gap. But here again, no difference could be detected for the 5-LO knockout clones compared to the vector control-treated cells.

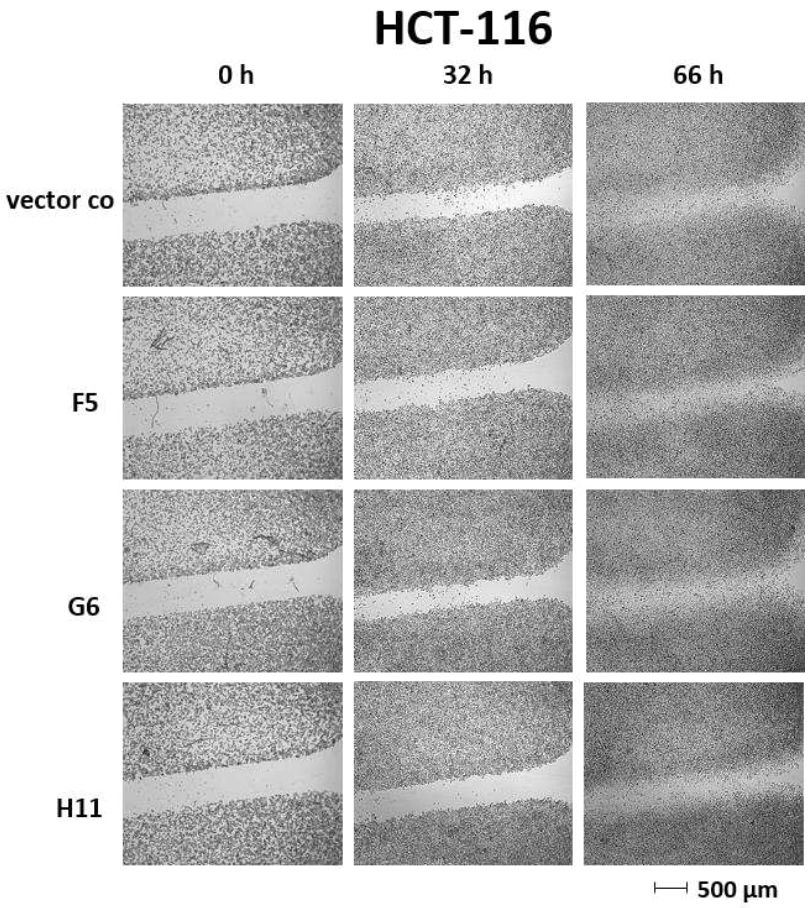

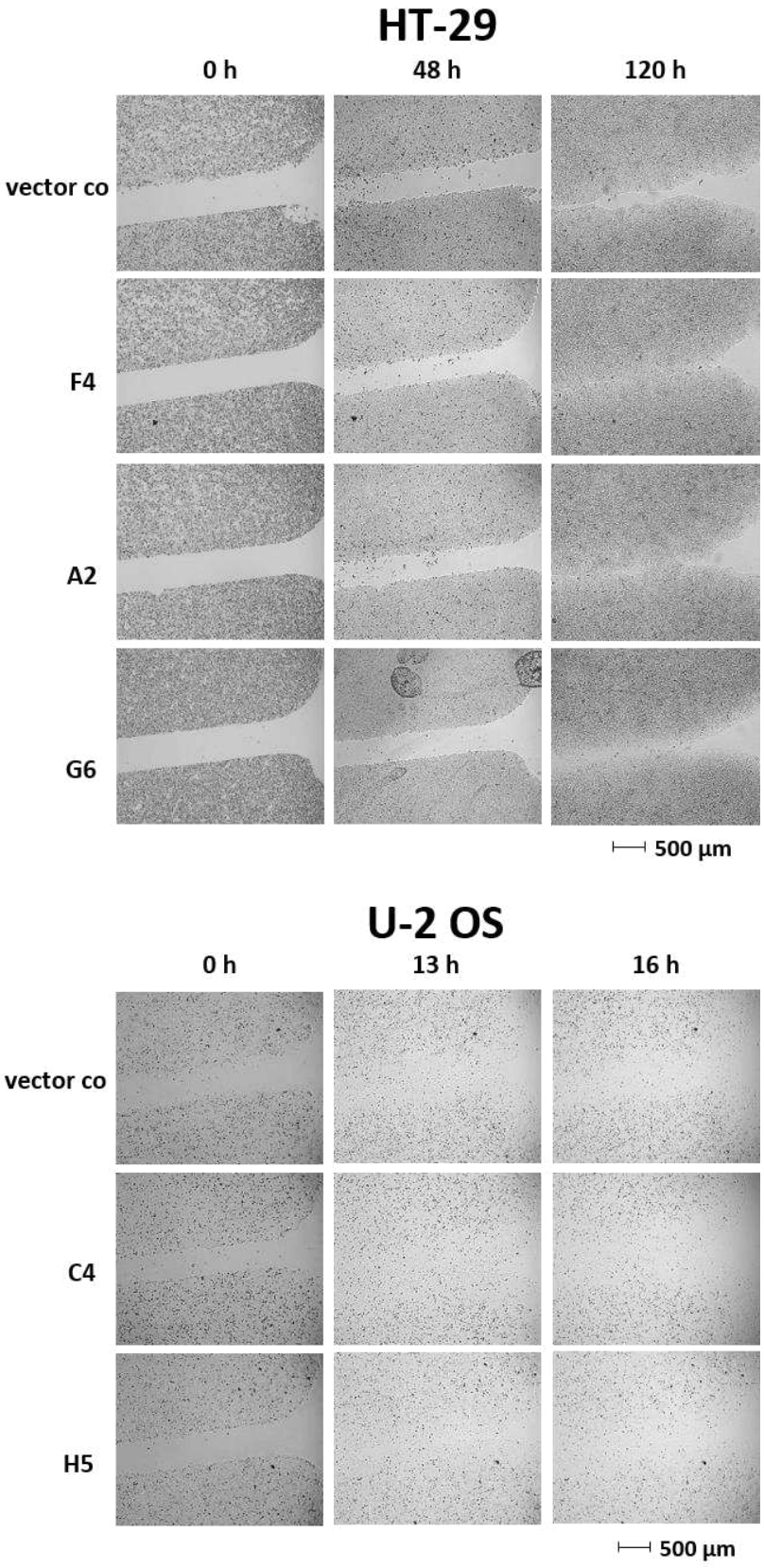

Figure 5.22 Wound closure in 5-LO KO cells. *Closing of an artificial wound gap yielded by seeding 4.9*10^4 cells in 2-well culture-inserts. Cells were allowed to attach for 24 h, inserts were removed, cells were washed carefully with PBS to remove all unattached cells, and finally covered with fresh medium. Pictures were taken at 2.5x magnification in the following using a Zeiss Axio Vert.A1 microscope and examined using the Zen blue software.*

5.7 Cell cycle analysis of 5-LO knockout HCT-116, HT-29, and U-2 OS cells

Dependency of the cell cycle on 5-LO KO was analysed in the different cell lines by incubating cells in a starvation medium for 24 hours followed by an incubation period of 6 hours in complete growth medium. After this time, cells were fixed, stained, and analysed by flow cytometry (**Figure 5.23**). For none of the three investigated cell lines, any difference in the distribution of the cells among the different phases of the cell cycle could be detected.

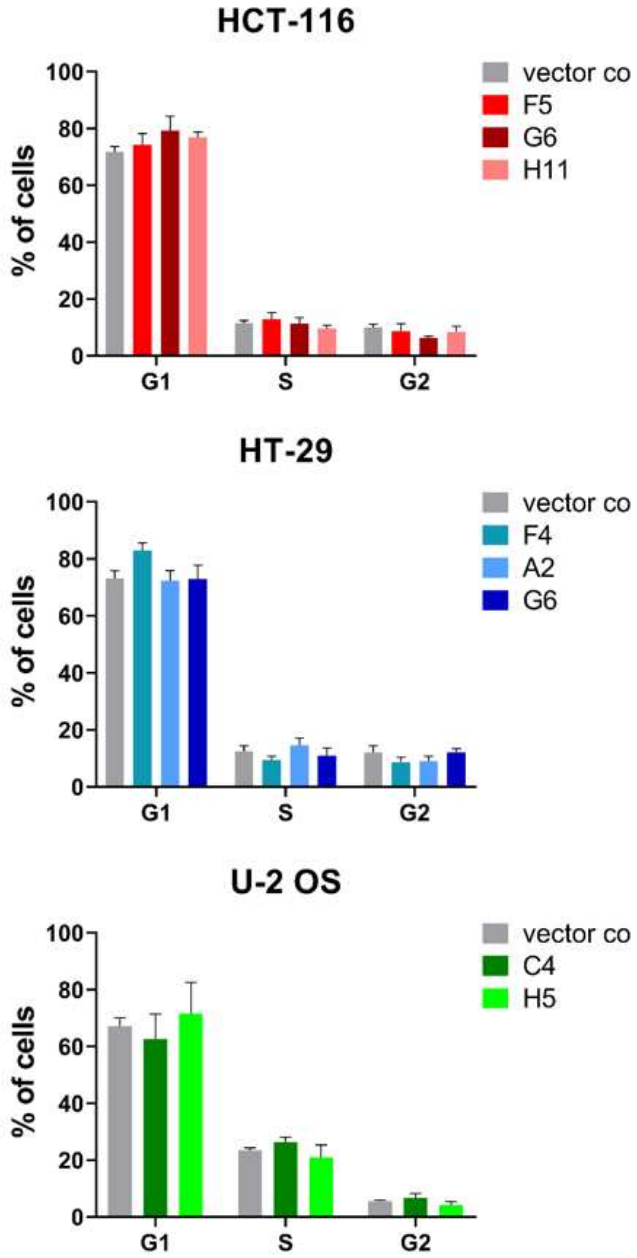

Figure 5.23 Cell cycle analysis of the 5-LO KO cells. *Cells were synchronised by serum starvation in a medium containing 0.5% FCS for 24 h. Subsequently, the medium was changed to complete growth medium containing 10% FCS. After another 6 h cells were harvested, fixed, and analysed via flow cytometry. Data are presented as mean + SD of 3 independent experiments.*

5.8 Influence of 5-LO knockout on mitogen and chemokine release from HCT-116, HT-29, and U-2 OS cells

During the evaluation of RNA sequencing results, gene expression levels of different mitogens and chemokines were found to be regulated by the 5-LO knockout on mRNA level. Among them were *TGFB2* (in HCT-116 cells) and *PDGFA*, *CXC3CL1*, and *CCL2* (in U-2 OS cells). To see whether these regulations were not only limited to mRNA amounts, protein expression of the respective mitogens and chemokines was measured by ELISA (TGF-β2 and PDGF-AA) and by cytokine bead assay (CBA) using FACS analysis (fractalkine and MCP-1).

5.8.1 TGF-β2

For measuring TGF-β2 secretion via ELISA, $7*10^5$ HCT-116 cells were seeded in a 24-well plate and incubated at standard cell culture conditions. After 72 hours, supernatants were collected, centrifuged to remove any leftover cells, and acid-activated. As TGF-β2 normally is expressed in a latent complexed form, it is necessary to cleave this bond to measure free TGF-β2 (340) (341). In all three single-cell 5-LO knockout clones, elevated levels of TGF-β2 compared to the vector control cells could be detected (**Figure 5.24**). While clone G6 only expressed 170% of the TGF-β2 amounts expressed by vector control cells, in clones H11 and F5 TGF-β2 levels were elevated to 286% which was in the case of clone F5 even significant.

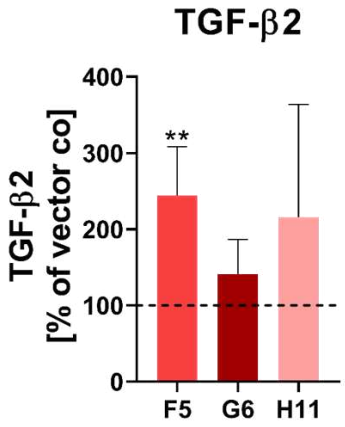

Figure 5.24 TGF-β2 secretion in HCT-116 cells. *Supernatants of HCT-116 5-LO knockout and control vector cells were acid-activated and TGF-β2 protein amounts were measured using ELISA method. Data are depicted as % of vector control and presented as mean + SD from 6 independent experiments. Asterisks indicate significant changes vs. vector control-treated cells *p ≤ 0.05, **p ≤ 0.01, ***p ≤ 0.001.*

5.8.2 Fractalkine, MCP-1, and PDGF-AA

The mitogen and chemokine expression from the different U-2 OS cell lines was measured in supernatants from confluent cells grown in monolayer (**Figure 5.25**). Besides the stress factor of confluent-grown cells, medium was replaced by new medium lacking FCS to increase cellular stress even more and cells were incubated for another 24 hours. Platelet-derived growth factor A (PDGF-AA) secretion was measured using ELISA method and fractalkine and monocyte chemoattractant protein 1 (MCP-1) were quantified by a cytometric bead assay. For all substances, a significant reduction of the expression in both 5-LO knockout clones was discovered. In the supernatants of clone H5, only 33-40% of the cytokine amounts secreted from vector control cells were measured and while only 14%, respectively 20%, of PDGF-AA and MCP-1 could be detected in the supernatants of clone C4, fractalkine expression was even below the limit of quantification.

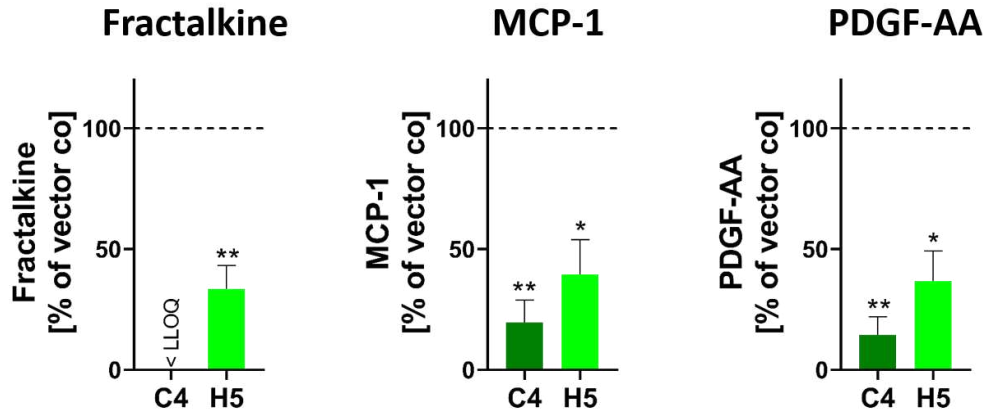

Figure 5.25 Fractalkine, MCP-1, and PDGF-AA secretion from U-2 OS cells. *Supernatants of U-2 OS 5-LO knockout and control vector cells were measured by ELISA (PDGF-AA) or by cytometric bead array (fractalkine, MCP-1). Data are depicted as % of vector control and presented as mean + SD from 3 independent experiments. Asterisks indicate significant changes vs. vector control-treated cells *p ≤ 0.05, **p ≤ 0.01, ***p ≤ 0.001.*

5.9 Regulation of cellular processes by 5-LO knockout presumably is not connected to cancer stem cells

Cancer stem cells play an important role in ongoing malignant processes as they are able, like normal stem cells, to give rise to a multitude of cell types important for tumour progression. In addition, they show stronger resistance to cytotoxic treatments and therefore play an important role in the relapse after such therapies. As cancer stem cells are strongly heterogenic, today a huge variety of cancer stem cell markers are known focussing on the different properties that support pathophysiological processes like elevated proliferation, lacking differentiation, or reinforced metabolism (348) (349). For this work, different types of markers were used to investigate possible incidents including cancer stem cells. In combination, CD24, CD44, and CD133 are common markers for cancer stem cells, especially used to characterise colorectal cancer (350).

The presence of the different cancer stem cell markers expressed on the cell surface was investigated using FACS analysis (**Figure 5.26**). Cells were stained with fluorophore-coupled antibodies and sorted by a BD FACSDiva™ in the following.

In HT-29 cells, no differences in the expression of cell surface markers comparing 5-LO knockout cells with vector control cells could be detected at all.

In HCT-116 cells, CD24 as well as CD44 expression levels were higher in two of three knockout clones (F5 + H11) but remained indifferent in the third clone (G6). CD133/2 showed a moderate elevation from 140 to 170% of the mean fluorescence measured in the vector control in all three knockout clones.

In U-2 OS cells, CD44 expression was only elevated in clone H5 while CD24, as well as CD133/2 both, were less present on the cell surfaces of both knockout clones although this decrease was not significant.

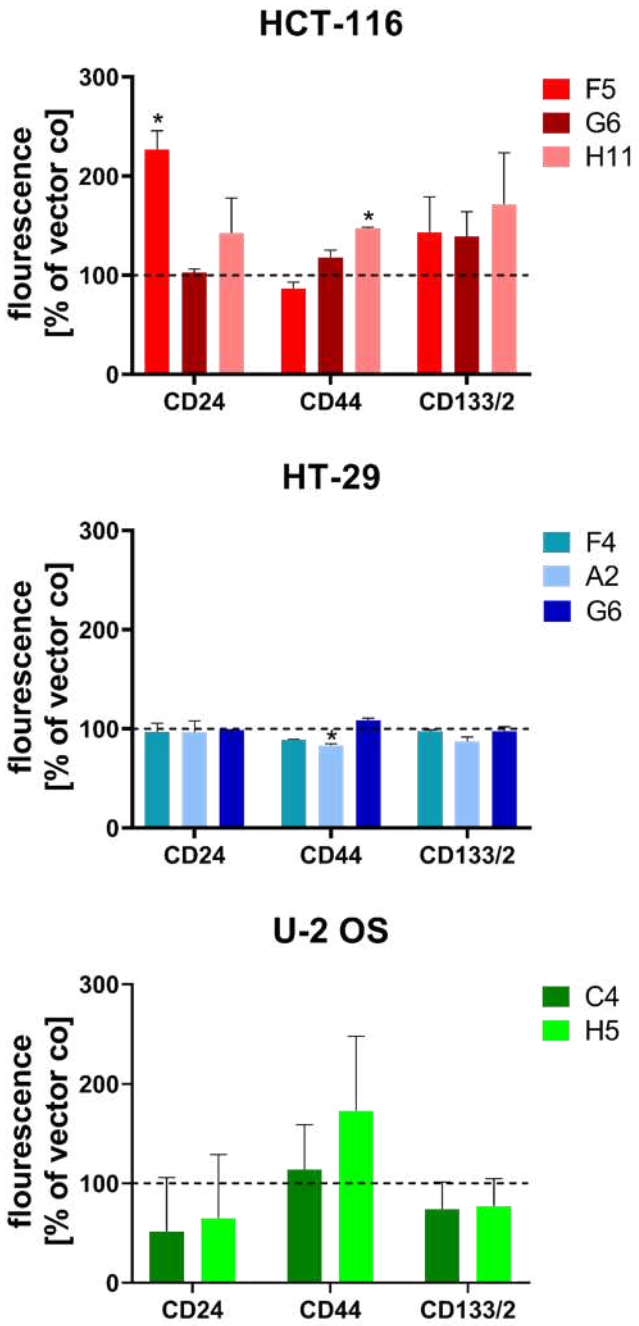

Figure 5.26 Expression of cancer cell stem markers in HCT-116, HT-29, and U-2 OS cells. *FACS analysis of CD24, CD44, and CD133/2 cell surface markers. Data are depicted as the mean of fluorescence as % of vector control and presented as mean + SD from 3 independent experiments. Asterisks indicate significant changes vs. vector control-treated cells *p ≤ 0.05, **p ≤ 0.01, ***p ≤ 0.001.*

Other markers characteristic of processes prominent in malignant cells were investigated by immunostainings analysed by confocal microscopy. Ki-67 is commonly used as a marker for proliferation since it is widely expressed during the G1-, G2-, S-, and M-phase in human cells but it is absent in resting cells in the G0-phase (351). Epithelial cell adhesion molecule (EpCAM) belongs to the superfamily of cell adhesion molecules (CAMs) and is expressed on epithelial cells. Here, it conveys cell-cell contacts and is an important tumour marker that serves as a target for antibody-mediated cancer therapy (352). Cytokeratin 20 (CK20) is a frequently used tumour marker for colorectal carcinomas and other malignancies of the gastrointestinal and urogenital tract as it is commonly expressed by the intestinal and urogenital mucosa. In combination with Ki-67, it serves as a strong prognostic marker for different types of cancers (353). Homeobox protein CdX-1 is a transcription factor exclusively expressed in the human intestine and can be used as a marker for enterocyte differentiation (354). To investigate the expression and distribution of these markers, cells were attached to microscopy slides, stained with the respective primary and fluorophore-coupled secondary antibodies, and examined using a confocal microscope (**Figures 5.27 – 5.29**).

Ki-67 expression was detected in all HCT-116 with some single cells transmitting a stronger signal indicating higher Ki-67 expression. This was true for vector control cells as well as for the knockout clones. EpCAM expression however revealed some differences between 5-LO positive and negative cells. The strongest signals were detected for vector control-treated cells. Clones G6 and H11 showed a moderate reduction of the signal intensity and expression in clone F5 was the lowest. CK20 and CdX-1 distribution however did not alter consistently between 5-LO positive and negative cells.

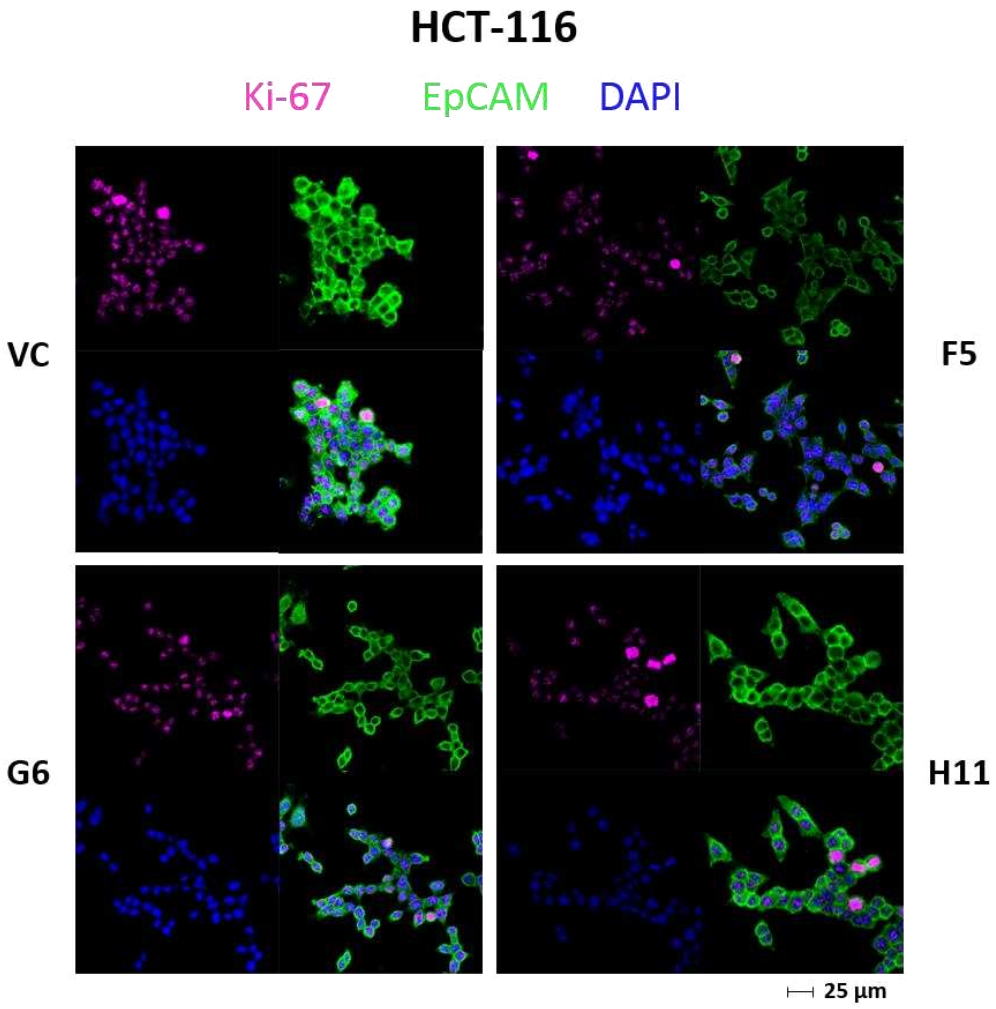

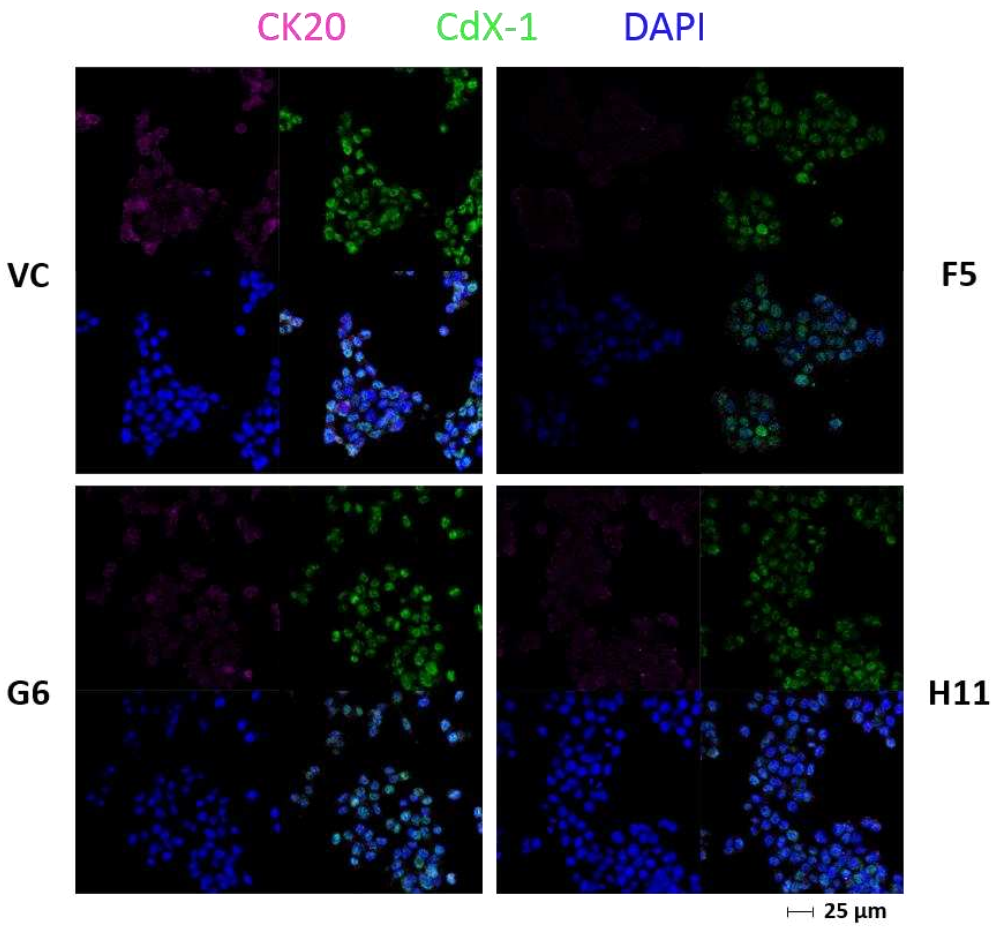

Figure 5.27 Immunostaining of Ki-67, EpCAM, CK20, and CdX-1 in HCT-116 vector control-treated and 5-LO KO cells. *PFA fixed cells were stained with antibodies against Ki-67, EpCAM, CK20, and CdX-1 and Alexa Fluor® coupled secondary antibodies. Nuclear counterstaining was performed with DAPI and images were acquired at 40x magnification using a Zeiss LSM 780 confocal microscope under identical conditions for pinhole opening, laser power, photomultiplier tension, and layer number. Results from one representative out of three independent experiments are shown.*

In HT-29 cells, Ki-67 showed an uneven distribution in the vector control cells with some cells highly positive for expressing the protein. This was true for clones A2 and G6 as well while clone F4 had a more uniform distribution with weaker signals. In contrast, EpCAM was evenly distributed in the vector control-treated cells with strong signals on the cell surfaces highlighting cell-cell contacts. This pattern looks the same for clone F4 but both single-cell clones A2 and G6 show a stronger overall signal for EpCAM expression and also single cells with a higher intensity. CK20 and CdX-1 signals were rather uniformly spread with some cells showing a stronger expression, but this was the same in all cell types independent of their 5-LO status.

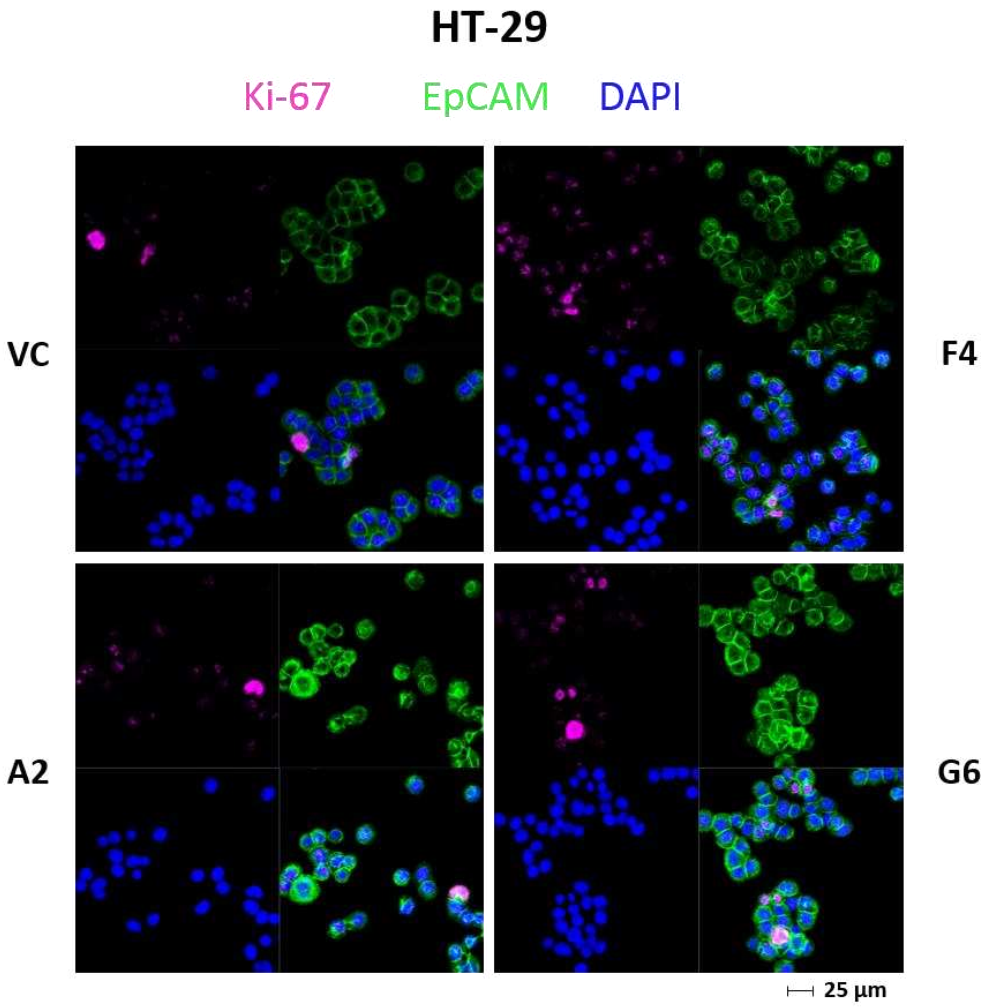

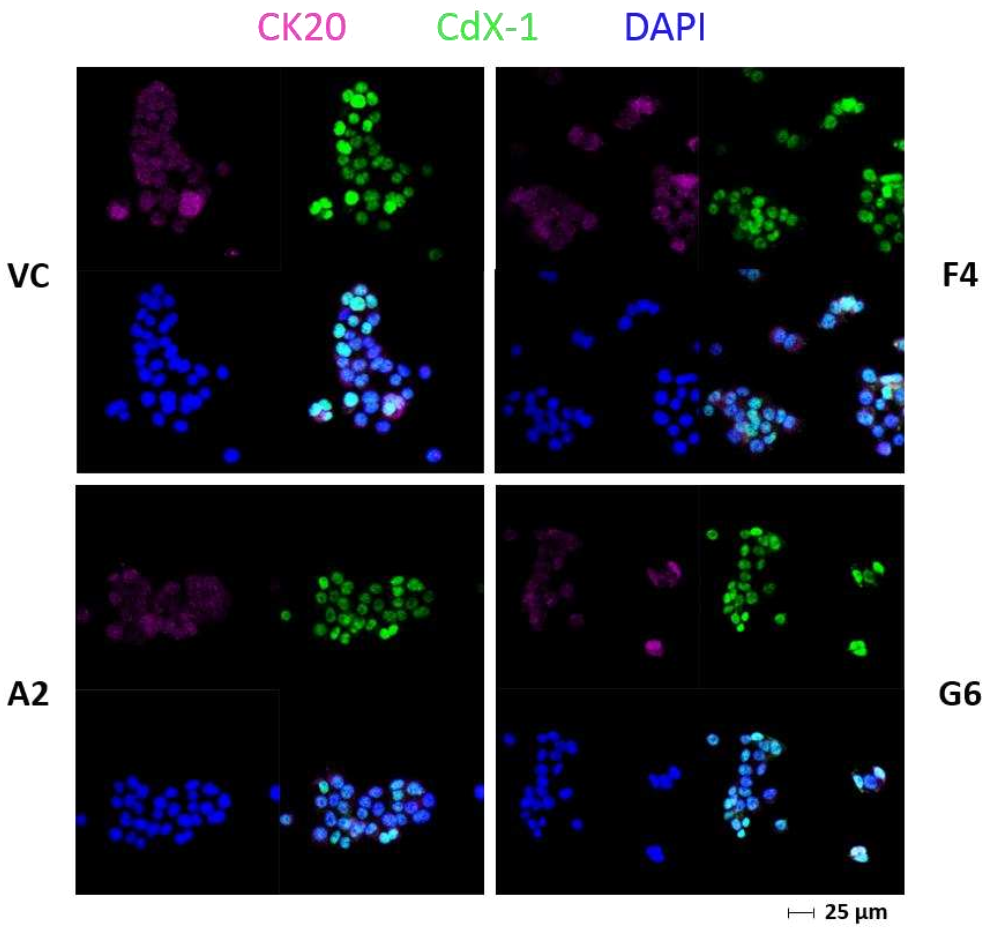

Figure 5.28 Immunostaining of Ki-67, EpCAM, CK20, and CdX-1 in HT-29 vector control-treated and 5-LO KO cells. *PFA fixed cells were stained with antibodies against Ki-67, EpCAM, CK20, and CdX-1 and Alexa Fluor® coupled secondary antibodies. Nuclear counterstaining was performed with DAPI and images were acquired at 40x magnification using a Zeiss LSM 780 confocal microscope under identical conditions for pinhole opening, laser power, photomultiplier tension, and layer number. Results from one representative out of three independent experiments are shown.*

Interestingly, in U-2 OS cells EpCAM was not located at the cell surface but within the cytosol around the nucleus of the cells. While single-cell clone C4 showed an overall stronger signal for EpCAM expression in all cells compared to the 5-LO positive counterparts, in clone H5 only some cells were highlighted by higher EpCAM expression. For the other three investigated markers no differences in the expression patterns were visible for any of the different U-2 OS cell types.

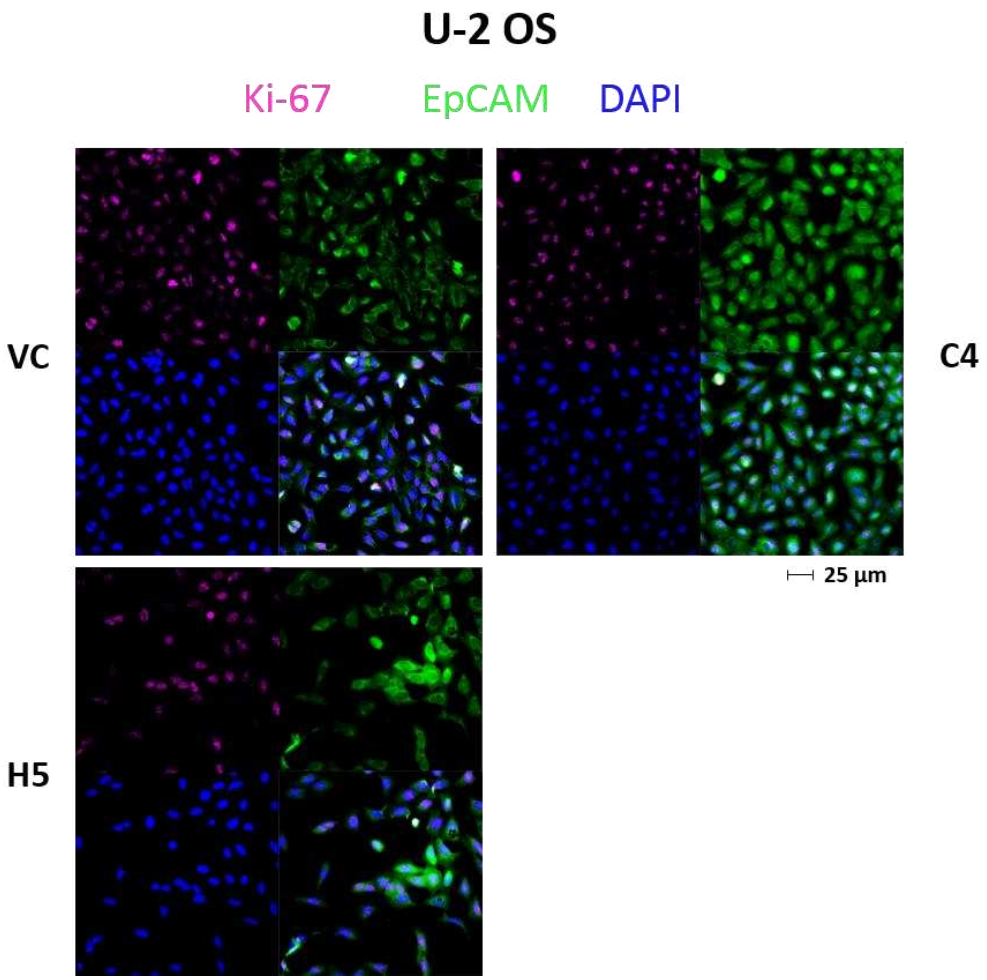

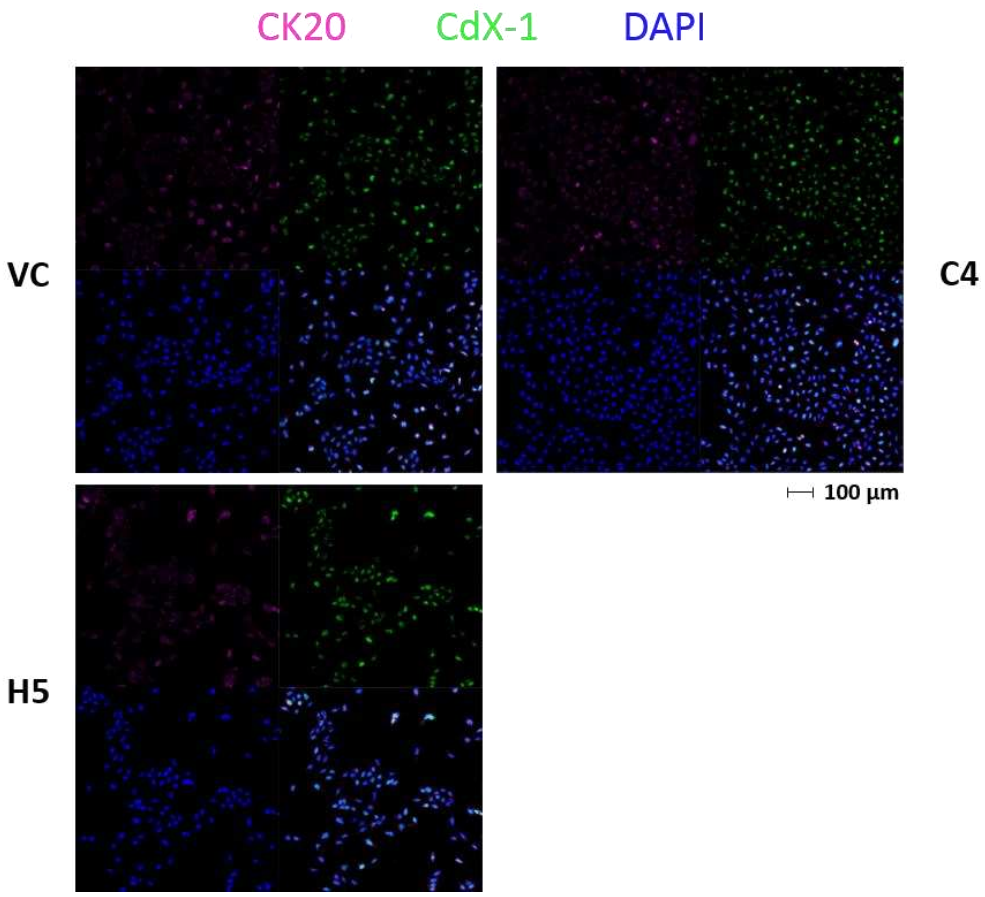

Figure 5.29 Immunostaining of Ki-67, EpCAM, CK20, and CdX-1 in U-2 OS vector control-treated and 5-LO KO cells. *PFA fixed cells were stained with antibodies against Ki-67, EpCAM, CK20, and CdX-1 and Alexa Fluor® coupled secondary antibodies. Nuclear counterstaining was performed with DAPI and images were acquired at 40x (top) or 10x (bottom) magnification using a Zeiss LSM 780 confocal microscope under identical conditions for pinhole opening, laser power, photomultiplier tension, and layer number. Results from one representative out of three independent experiments are shown.*

5.10 Pharmacological inhibition of 5-LO only partly mimicked the 5-LO KO

The influence of 5-LO inhibition on mRNA expression in HCT-116, HT-29, and U-2 OS cells was investigated by isolating RNA from vector control cells incubated for 3 days with Zileuton (3 + 10 µM) and CJ-13610 (0.3 + 3 µM) in complete growth medium at 37°C, 5% CO_2 in a humidified atmosphere. mRNA was reverse transcribed to cDNA and subjected to qPCR analysis investigating the expression of some of the - due to 5-LO knockout - differentially expressed genes. *ACTB* was used as a housekeeping gene and data were analysed using the $2^{-\Delta\Delta CT}$ method normalized to *ACTB* and the respective vector control cells.

In HCT-116 cells, several genes were found to be differentially regulated by knocking out the 5-LO. The expression of some of these genes was measured after the long-term treatment with the 5-LO inhibitory drugs Zileuton and CJ-13610 (**Figure 5.30**). While gene expression of *APOBEC3C*, *FOXA2*, *S100A4*, *SLC1A3*, and *ZNF608* was upregulated after the knockout of 5-LO, pharmacological inhibition of 5-LO did not lead to altered mRNA expression of those genes. Zinc finger protein coding gene *ZNF419* was even 2-fold downregulated after the inhibition of 5-LO even though complete knockout of the enzyme led to 4-fold upregulation of *ZNF419* mRNA. The same contrary effects could be detected for a high dose of CJ-13610 leading to downregulation of *APOBEC3G* mRNA levels and upregulation of *LMAN1* expression even though results in 5-LO knockout cells were inverted. Also, *PBX1* gene expression was increased by inhibiting 5-LO but decreased after knocking it out. But on the other side, for some genes effects yielded by genomic 5-LO knockout could be - at least to some extent - reproduced by enzymatic inhibition. *NOSTRIN*, *PDLIM5*, and *TGFB2* mRNA levels all were upregulated around 5- to 20-fold in 5-LO knockout cells, depending on the single-cell clone, and for *NOSTRIN* and *TGFB2* a 3- to 5-fold increase in mRNA expression after the treatment with both inhibitors could be detected which was not dose-dependent. For *PDLIM5* high doses of CJ-13610 could even completely mimic the effects of the 5-LO knockout. The strongest downregulation of gene expression in HCT-116 5-LO knockout cells was detected for *RPS4Y1*, in the mean to more than 100-fold and by inhibition of the enzyme for all concentrations of the inhibitors a decreased mRNA level of up to 16-fold could be reproduced.

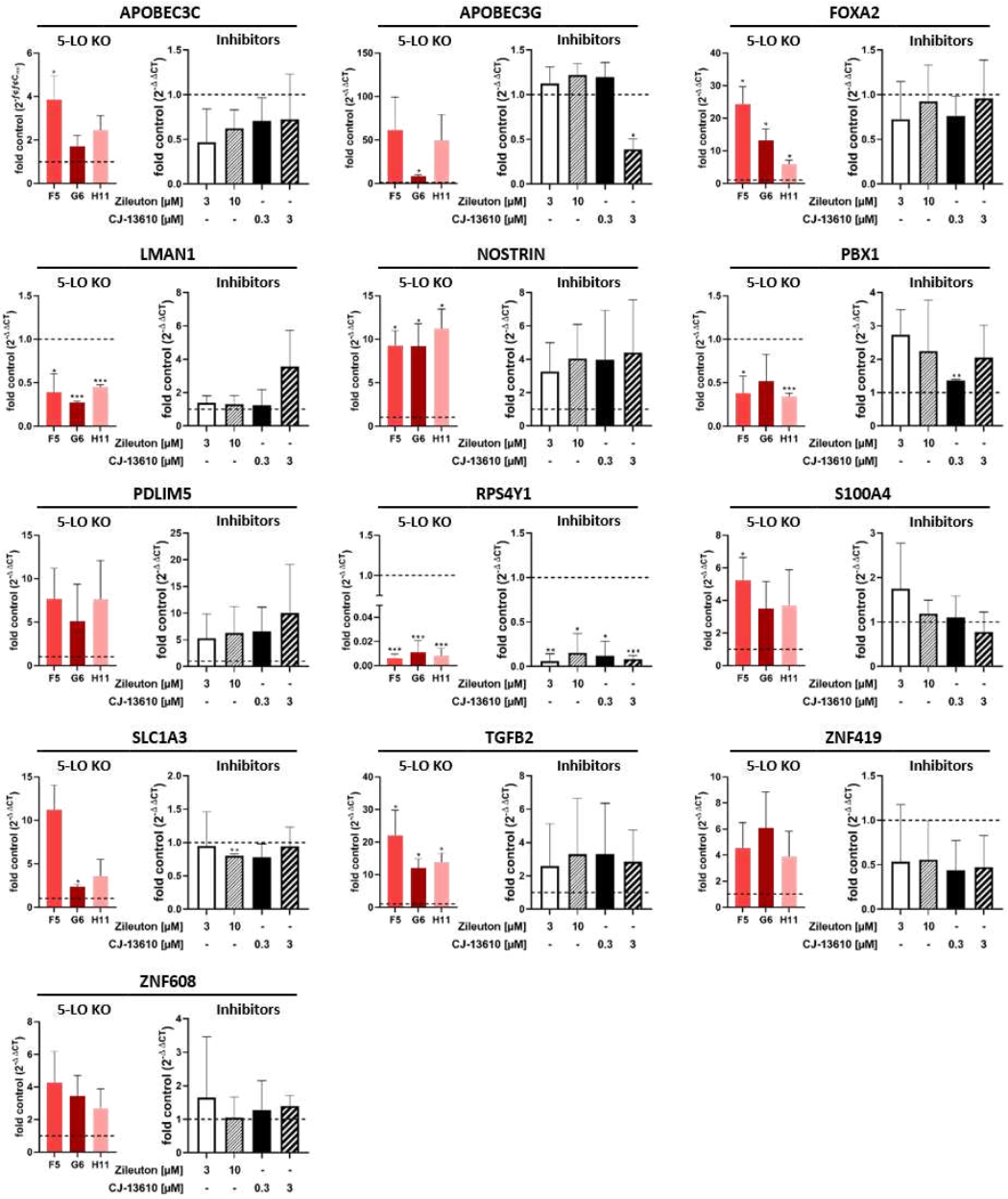

Figure 5.30 RT-qPCR analysis of selected differentially expressed genes in HCT-116 cells treated with 5-LO inhibitors in comparison to results of complete knockout of 5-LO. *mRNA expression of differentially regulated genes in HCT-116 cells treated with Zileuton (3 + 10 µM) and CJ-13610 (0.3 + 3 µM) for 3 days (black and white) compared to 5-LO knockout data (red). Gene expression of inhibitor-treated cells was normalized to ACTB (housekeeping gene) and the corresponding DMSO-treated vector control cells ($2^{-\Delta\Delta CT}$ method). Data are presented as mean + SD of 3 independent experiments. Asterisks indicate significant changes vs. vector control cells *p ≤ 0.05, **p ≤ 0.01, ***p ≤ 0.001.*

In HT-29 cells, two different patterns of mRNA regulation in the knockout clones could be detected. *AKAP12*, *DMKN*, *NAV1*, *TRABD2A*, *ZC4H2*, and *ZNF618* were downregulated in single-cell clones F4 and A2 but upregulated in clone G6. For the majority of those genes, no differential expression was measured by inhibition of the 5-LO (**Figure 5.31**). Only

AKAP12 and *DMKN* gene expression could be increased by the treatment with Zileuton dose-dependently. The second cluster of genes was strongly downregulated in all three knockout single-cell clones. For those genes, no inhibitory treatment led to comparable results. While pharmacological inhibition of 5-LO did not alter *LINC00665* gene expression, high doses of CJ-13610 exhibited the same effects for regulation of *UTS2B* mRNA levels as the complete genomic knockout of the enzyme did.

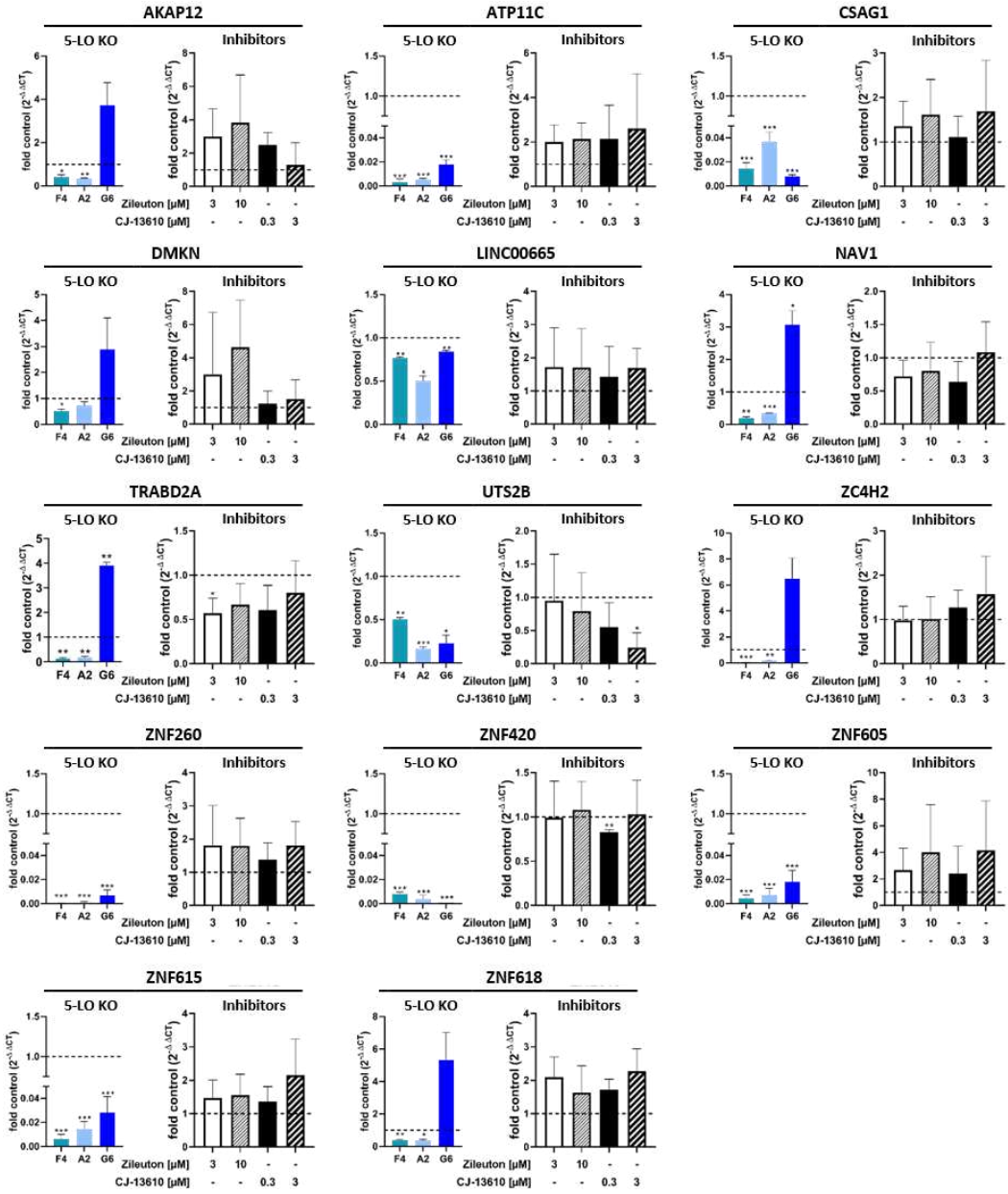

Figure 5.31 RT-qPCR analysis of selected differentially expressed genes in HT-29 cells treated with 5-LO inhibitors in comparison to results of complete knockout of 5-LO. *mRNA expression of differentially regulated genes in HT-29 cells treated with Zileuton (3 + 10 µM) and CJ-13610 (0.3 + 3 µM) for 3 days (black and white) compared to 5-LO knockout data (blue). Gene expression of inhibitor-treated cells was normalized to ACTB (housekeeping gene) and the corresponding DMSO-treated vector control cells ($2^{-\Delta\Delta CT}$ method). Data are presented as mean + SD of 3 independent experiments. Asterisks indicate significant changes vs. vector control cells *p ≤ 0.05, **p ≤ 0.01, ***p ≤ 0.001.*

In U-2 OS cells, only some of the genes that were differentially regulated by 5-LO knockout were investigated after the treatment with the inhibitory drugs (**Figure 5.32**). While gene expression of *BCL2A1*, *BHLHB41*, *CX3CL1*, *DRAXIN*, *LAMA4*, *LIMS2*, and *SSP1* was hardly influenced by long-term treatment with Zileuton and CJ-13610, some knockout effects could also be depicted under these conditions. *CCL2* gene expression was decreased in 5-LO knockout cells and higher doses of both inhibitors could mimic these effects which could also be achieved for *HAS2* and at least to some extent for *ITGA2*. A moderate upregulation of mRNA expression of *PLAC1* after the inhibitory treatment could be shown as well as for *COL8A1*, in this case being contradictory to the knockout data.

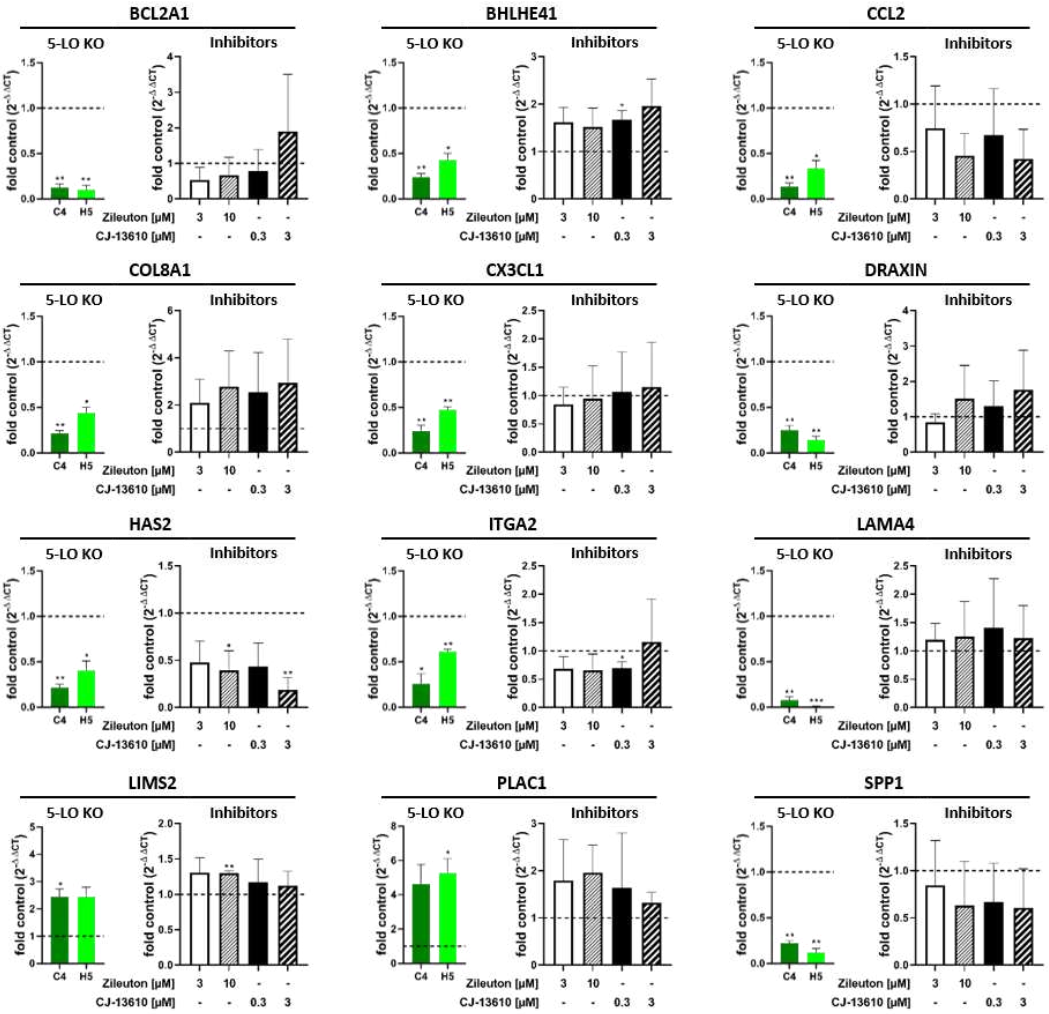

Figure 5.32 RT-qPCR analysis of selected differentially expressed genes in U-2 OS cells treated with 5-LO inhibitors in comparison to results of complete knockout of 5-LO. *mRNA expression of differentially regulated genes in U-2 OS cells treated with Zileuton (3 + 10 µM) and CJ-13610 (0.3 + 3 µM) for 3 days (black and white) compared to 5-LO knockout data (green). Gene expression of inhibitor-treated cells was normalized to ACTB (housekeeping gene) and the corresponding DMSO-treated vector control cells ($2^{-\Delta\Delta CT}$ method). Data are presented as mean + SD of 3 independent experiments. Asterisks indicate significant changes vs. vector control cells *p ≤ 0.05, **p ≤ 0.01, ***p ≤ 0.001.*

The next aim was to investigate whether the attenuated cell proliferation in 5-LO knockout cells from both HT-29 and U-2 OS cell lines could also be achieved by inhibiting the 5-LO. Therefore, vector control-treated cells were incubated for 3 days with Zileuton (3 + 10 µM) and CJ-13610 (0.3 + 3 µM) in complete growth medium at 37°C, 5% CO_2 in a humidified atmosphere. After this time, cells were seeded in 24-well plates with additional inhibitor treatment, detached using TE after 24, 48, 72, and 96 hours and counted manually after trypan-blue staining (**Figure 5.33**).

In HT-29 cells a decrease in cell numbers for all knockout clones could be examined after 48, 72, and 96 hours. In this new setting, only the cell number of HT-29 vector control cells treated with 3 µM CJ-13610 was significantly decreased after 96 hours of incubation. In U-2 OS cells as well, only high dose CJ-13610 treatment affected the cell proliferation, in this case already after 72 hours of incubation, leading to a decreased cell number of 60% of the DMSO-treated control for 72- and 96-hour time points.

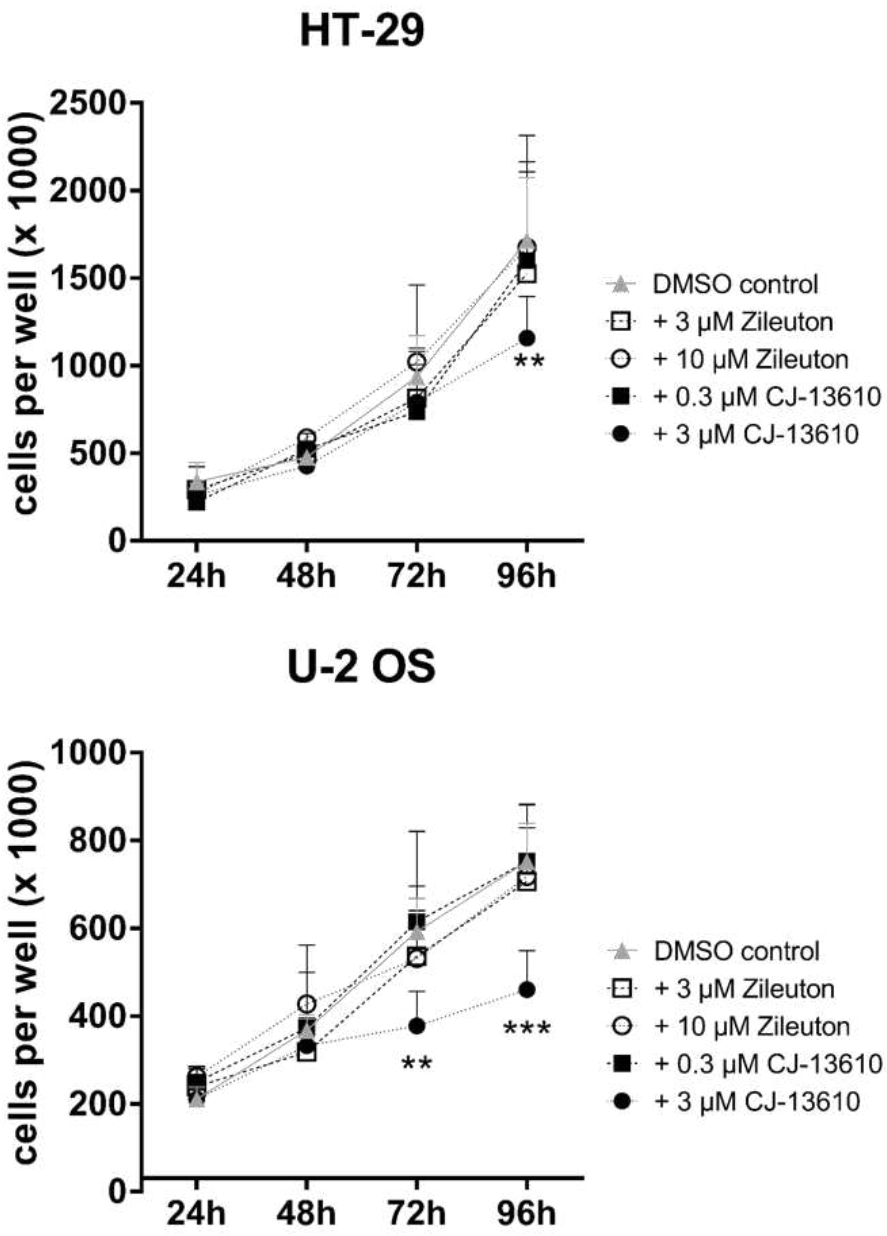

Figure 5.33 Cell proliferation in HT-29 and U-2 OS vector control cells treated with 5-LO inhibitors. *Cell proliferation in cells treated with the 5-LO inhibitors Zileuton (3, 10 µM) or CJ-13610 (0.3, 3 µM) compared to DMSO-treated controls in HT-29 (top) and U-2 OS (bottom) cells. Data are presented as mean ± SD from 3 independent experiments. Asterisks indicate significant changes vs. vector control-treated cells *p ≤ 0.05, **p ≤ 0.01, ***p ≤ 0.001.*

The influence of 5-LO inhibition on spheroid formation was assessed as well. HT-29 and U-2 OS vector control-treated cells, incubated for 3 days with Zileuton (3 + 10 µM) and CJ-13610 (0.3 + 3 µM) in complete growth medium at 37°C, 5% CO_2 in a humidified atmosphere, were seeded with additional inhibitor treatment in ultra-low-attachment plates.

The size and appearance of HT-29 spheroids did not differ whether the cells were treated with inhibitors or not (**Figure 5.34 A**). 7 days after initial seeding, spheroids were digested using Accutase® and the number of cells per spheroid was counted manually using a Bürker chamber after trypan-blue staining. All inhibitor concentrations led to a slightly increased number of living as well as total cells per spheroid and again high dose CJ-13610 treatment resulted in the strongest effects (**Figure 5.34 B**).

In U-2 OS cells the biggest differences in spheroid formation in 5-LO knockout cells compared to 5-LO positive cells were detected. While 5-LO knockout cells were not able to form any kind of compact spheroid, 5-LO inhibitor-treated cells did not show any different behaviour compared to mock control after the seeding for spheroid formation (**Figure 5.34 C**). Contrary to HT-29 cells, the number of cells per spheroid was slightly decreased for the inhibitor treatments, resembling results from 5-LO knockout cells, where the number of cells per spheroid was also decreased in both knockout single-cell clones (**Figure 5.34 D**).

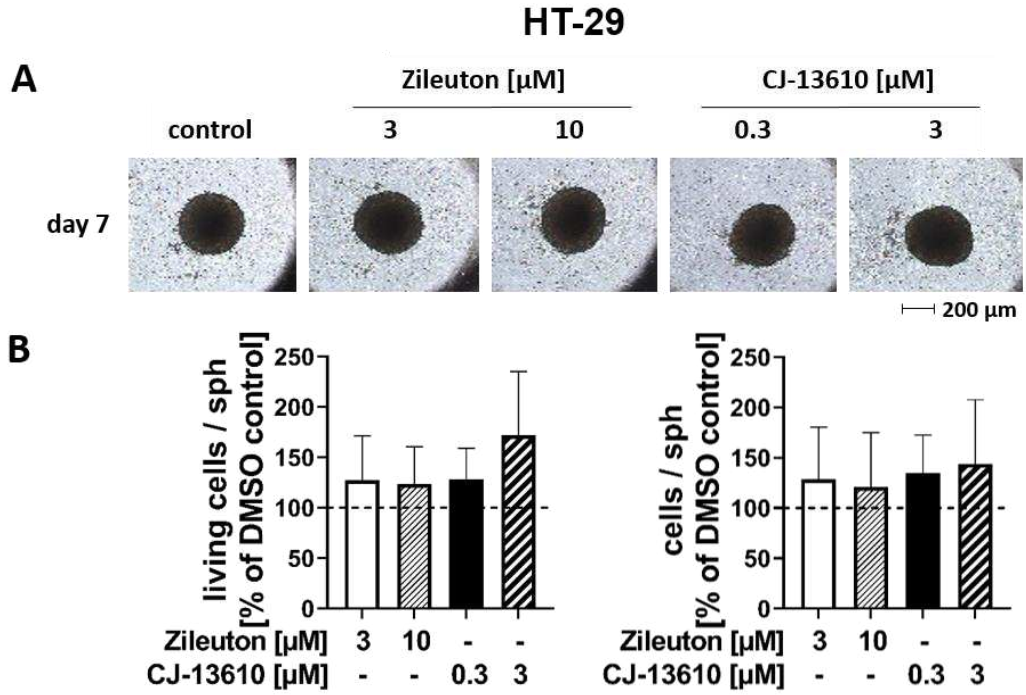

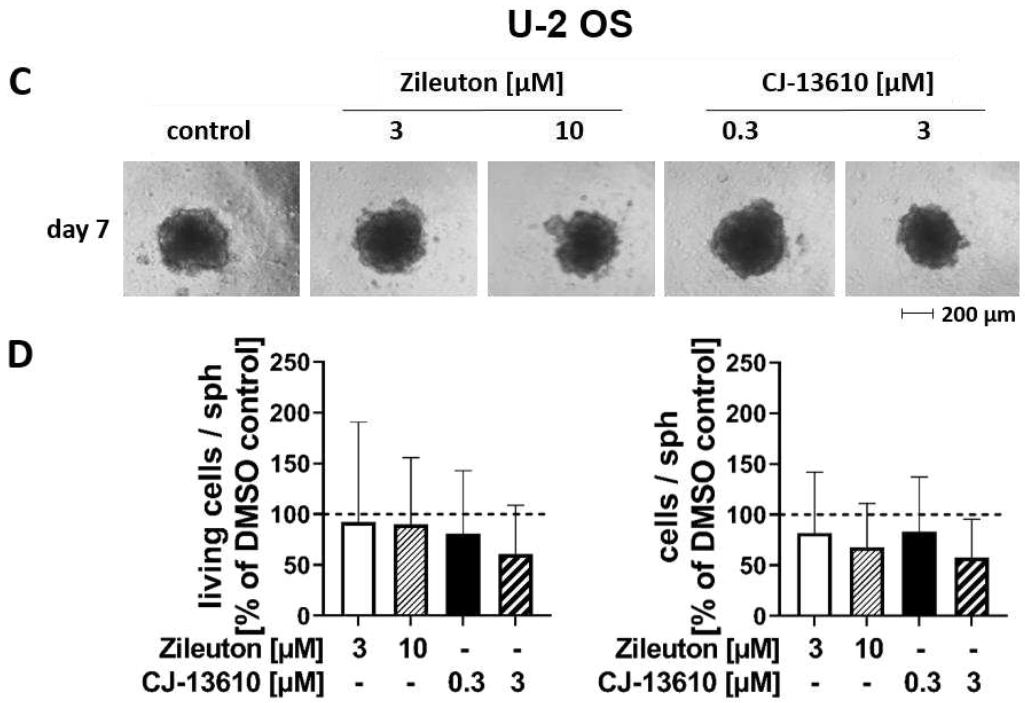

Figure 5.34 Spheroid formation after pharmacological inhibition of 5-LO. *Three-dimensional growth of HT-29 and U-2 OS vector control cells treated with Zileuton (3, 10 µM) or CJ-13610 (0.3, 3 µM) was assessed by seeding 1*10^4 cells in each well of a low-attachment plate and incubation at 37°C, 5% CO_2 in a humidified atmosphere. (A) HT-29 spheroids incubated for 7 days. Pictures were taken at 5x magnification using a Zeiss Axio Vert.A1 microscope and examined using the Zen blue software. (B) Number of living and total HT-29 cells per spheroid depicted as % of the corresponding DMSO-treated vector control. (C) U-2 OS spheroids incubated for 7 days. Pictures were taken at 5x magnification using a Zeiss Axio Vert.A1 microscope and examined using the Zen blue software. (D) Number of living and total U-2 OS cells per spheroid depicted as % of the corresponding DMSO-treated vector control. Data are presented as mean + SD of 3 independent experiments.*

The strongest differences from all experiments conducted with the 5-LO knockout cells were found in the transwell assay. Therefore, directed cell migration was examined in HCT-116 and U-2 OS vector control cells incubated for 3 days with Zileuton (3 + 10 µM) or CJ-13610 (0.3 + 3 µM) in complete growth medium at 37°C, 5% CO_2 in a humidified atmosphere. After this initial incubation, cells were seeded in the upper chamber of a transwell system with an additional inhibitor treatment in a starvation medium containing only 0.5% FBS while the bottom chamber was filled with complete growth medium creating a serum gradient as a chemoattractant (**Figure 5.35**).

In HCT-116 vector control-treated cells, cell motility was dose-dependently increased by inhibiting 5-LO with both inhibitors. While 3 µM Zileuton treatment had no effects on cell motility, 10 µM treatment increased the number of migrated cells to 120% of the control cells. CJ-13610 treatment for both concentrations elevated the level of cells in the lower chamber to 190% (0.3 µM) and even 220% (3 µM). Nevertheless, the whole extent of the 5-LO knockout mediated effect could not be achieved.

Interestingly, in U-2 OS cells none of the treatments led to an upregulation of the cell number in the lower compartment, while 0.3 µM of CJ-13610 even decreased the number of migrated cells to 80% of the mock control.

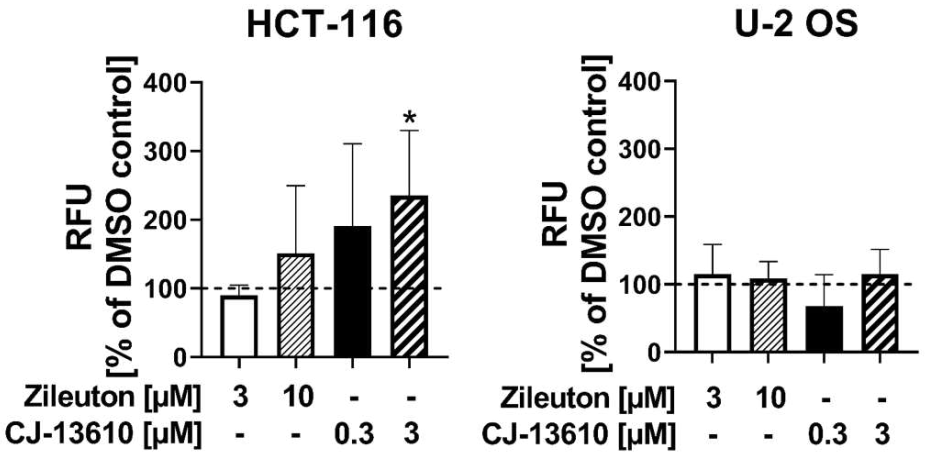

Figure 5.35 Directed cell migration of HCT-116 and U-2 OS vector control cells during treatment with Zileuton (3, 10 µM) or CJ-13610 (0.3, 3 µM). *After 3 h (U-2 OS) or 24 h (HCT-116), migrated cells were stained, and fluorescence of the cell suspension was measured. Data are presented as mean + SD from 3-5 independent experiments. Asterisks indicate significant changes vs. DMSO control *p ≤ 0.05, **p ≤ 0.01, ***p ≤ 0.001.*

To exclude possible cytotoxic effects of the two 5-LO inhibitors, HCT-116, HT-29, and U-2 OS vector control cells, incubated for 3 days with Zileuton (3 + 10 µM) and CJ-13610 (0.3 + 3 µM) in complete growth medium at 37°C, 5% CO_2 in a humidified atmosphere were seeded for WST-1 assay again treated with an additional dose of the respective inhibitors (**Figure 5.36**). In all three cell lines, Zileuton treatment led to a dose-dependent increase in cell viability and while 0.3 µM treatment of CJ-13610 also slightly increased cell viability in all three cell lines, treatment with 3 µM of CJ-13610 decreased the viability in HT-29 cells to 90% and in U-2 OS cells to 75% of the DMSO treated control.

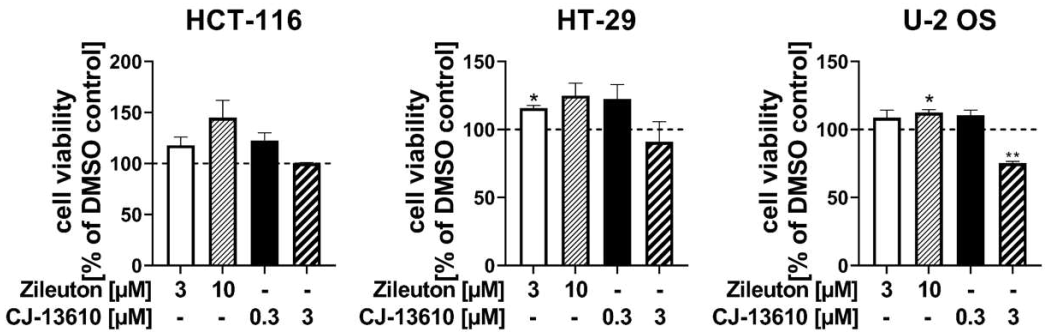

Figure 5.36 Influence of 5-LO inhibitors on cell viability. *Cell viability of the 5-LO inhibitor-treated vector control cells was assessed after 72 hours using the WST-1 assay. Viability is depicted as % of DMSO-treated vector control and presented as mean + SD from 3 independent experiments. Asterisks indicate significant changes vs. DMSO-treated cells *p ≤ 0.05, **p ≤ 0.01, ***p ≤ 0.001.*

5.11 Re-expression of 5-LO did not reverse the knockout-mediated effects

One of the most common ways to validate knockout effects is to re-express the target of interest in the knockout cells and to see whether knockout-mediated effects can be reversed by this. For this purpose, 5-LO knockout clones (HCT-116: F5, G6; HT-29: F4, G6; U-2 OS: C4) and their respective vector control-treated cells were transfected using a sleeping beauty plasmid carrying the coding sequence of the *ALOX5* gene. For control purposes, the same plasmid only missing the coding sequence of 5-LO was used for all cell types. Hygromycin was used to select the transfected cells and the knock-in was validated via Western blot analysis (**Figure 5.37**). In all three cell lines, the re-expression of 5-LO could be validated for all used cell types, but by comparing 5-LO knock-in cells with wildtype-carrying vector control-treated cells, it becomes obvious that the amount of 5-LO by far exceeds the physiological amount present in the tumour cells. Nevertheless, further experiments were conducted.

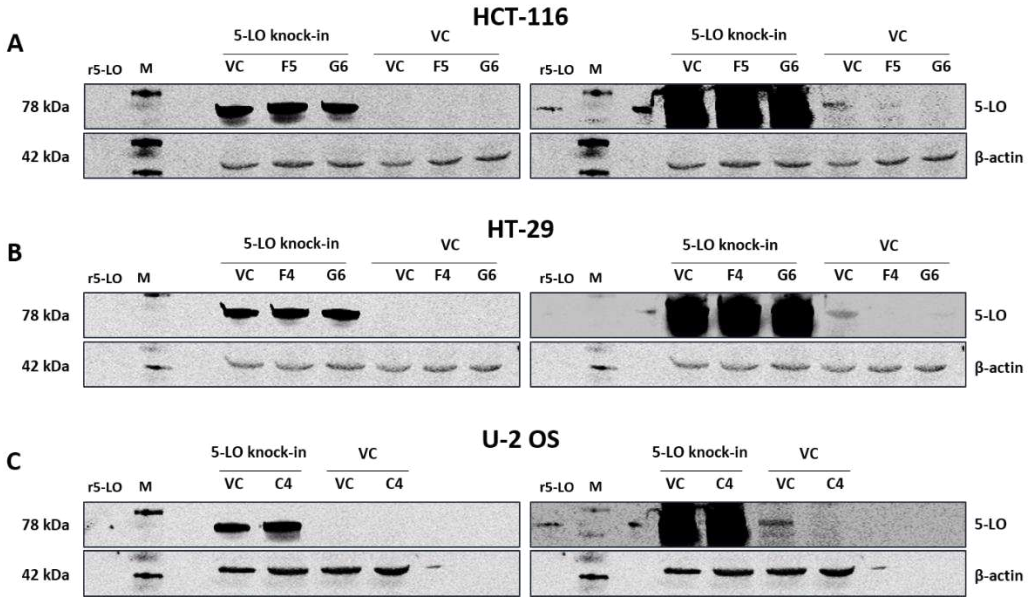

Figure 5.37 Re-expression of 5-LO in HCT-116, HT-29, and U-2 OS 5-LO knockout cells and vector controls. *Validation of 5-LO knock-in on protein level in HCT-116 (A), HT-29 (B), and U-2 OS (C) single-cell clones and vector controls analysed by Western blotting. Left: Low intensity showing successful knock-in of 5-LO. Right: High intensity showing physiological 5-LO expression in vector control-treated cells. Recombinant human 5-LO was used as a positive control. M: marker, r5-LO: recombinant human 5-LO, VC: vector control.*

For each cell line, four, respectively five, representative genes were chosen to be validated via RT-qPCR. RNA from 5-LO knock-in and vector control-treated cells was isolated, reverse transcribed to cDNA, and subjected to qPCR analysis. *ACTB* was used as a housekeeping gene and data were analysed using the $2^{-\Delta\Delta CT}$ method normalized to *ACTB* and the respective vector control cells.

In HCT-116 cells (**Figure 5.38**) the re-expression of 5-LO could neither reverse the upregulation of *NOSTRIN* mRNA levels, nor the downregulation of *LMAN1*. Expression of *TGFB2* and *FOXA2* could be completely normalized in knock-in clone G6 but interestingly this was also true for the vector control-treated knockout clone. Expression of *TGFB2* in knock-in clone F5 was reduced from 22-fold in the 5-LO knockout to 2.5-fold in the mock control but the same was true for the respective control. For *FOXA2,* mRNA expression in knock-in clone F5 was 3 times lower than in the vector control-treated cells but still comparable to the levels in the pure knockout.

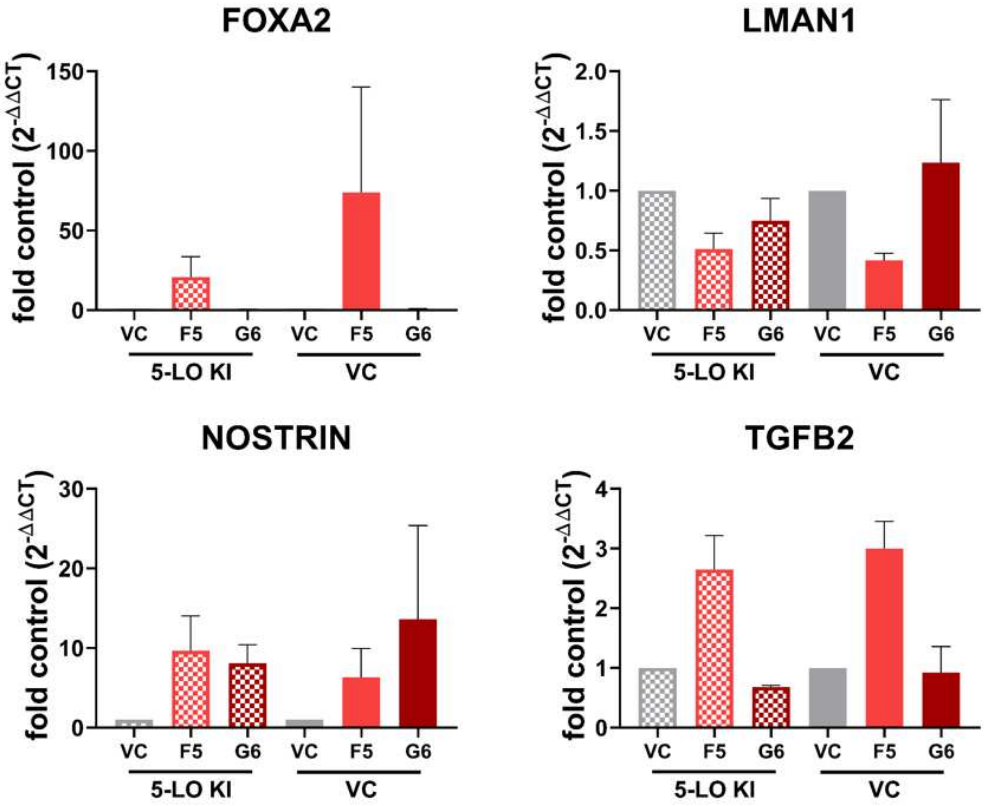

Figure 5.38 RT-qPCR analysis of selected differentially expressed genes in HCT-116 5-LO knock-in cells and the respective controls. *mRNA expression of differentially regulated genes in HCT-116 5-LO knock-in and the respective control cells. Gene expression was normalized to ACTB (housekeeping gene) and the corresponding vector control cells ($2^{-\Delta\Delta CT}$ method). Data are presented as mean + SD of 3 independent experiments. Asterisks indicate significant changes vs. vector control cells *p ≤ 0.05, **p ≤ 0.01, ***p ≤ 0.001.*

The knock-in of 5-LO in HT-29 cells could only partly reverse some effects yielded by the knockout (**Figure 5.39**). For *ATP11C,* gene expression in single-cell clone G6 could be elevated from 30-fold downregulation to 12-fold compared to the respective controls. The same was true for the gene expression of *ZNF420* in clone F4. Here, an increase from 400-fold to 15-fold downregulation could be detected by comparing knock-in cells to the respective vector control-treated cells. *UTS2B* expression was slightly elevated in both knockout clones but still not normalized to the expression in vector control-treated cells. For *TRABD2A* no alteration in the expression after the re-expression of 5-LO could be detected.

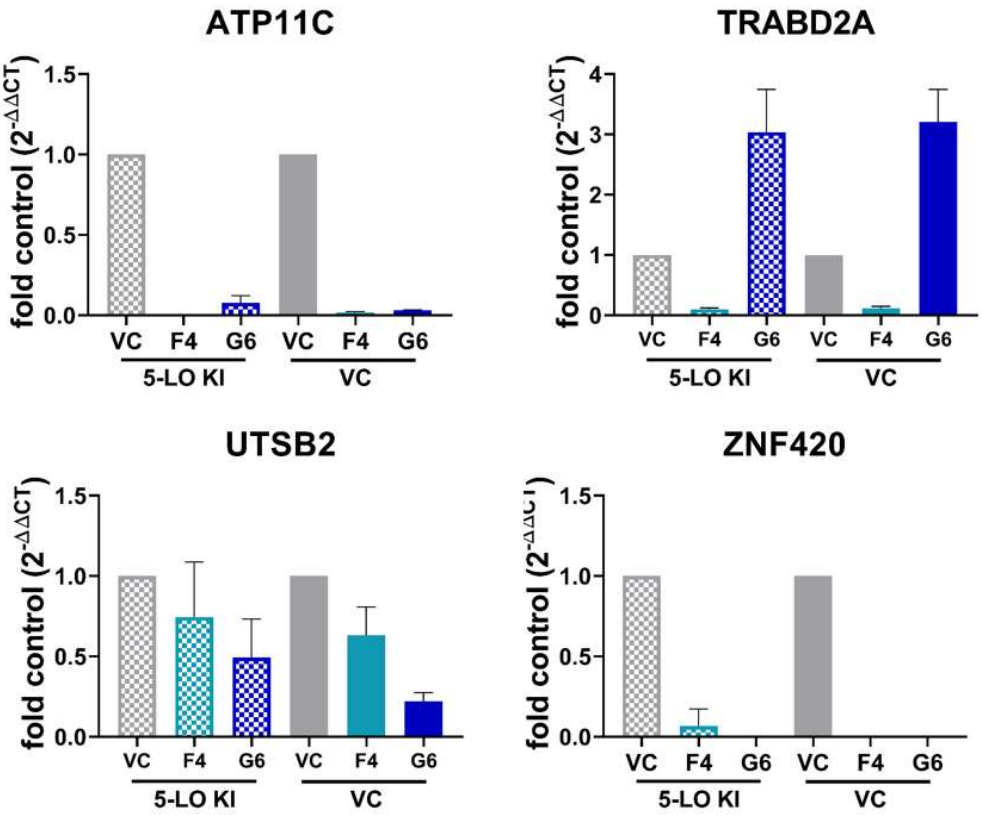

Figure 5.39 RT-qPCR analysis of selected differentially expressed genes in HT-29 5-LO knock-in cells and the respective controls. *mRNA expression of differentially regulated genes in HT-29 5-LO knock-in and the respective control cells. Gene expression was normalized to ACTB (housekeeping gene) and the corresponding vector control cells ($2^{-\Delta\Delta CT}$ method). Data are presented as mean + SD of 3 independent experiments. Asterisks indicate significant changes vs. vector control cells *p ≤ 0.05, **p ≤ 0.01, ***p ≤ 0.001.*

Although in U-2 OS cells gene expression of *CCL2*, *CX3CL1* and *ITGA2* could be raised closer to expression in vector control cells (**Figure 5.40**), the same effects were visible in vector control-treated knockouts, suggesting that other processes might play a role in this regulation. Gene expression of *LAMA4* and *COL8A1* was not altered by re-expression of 5-LO.

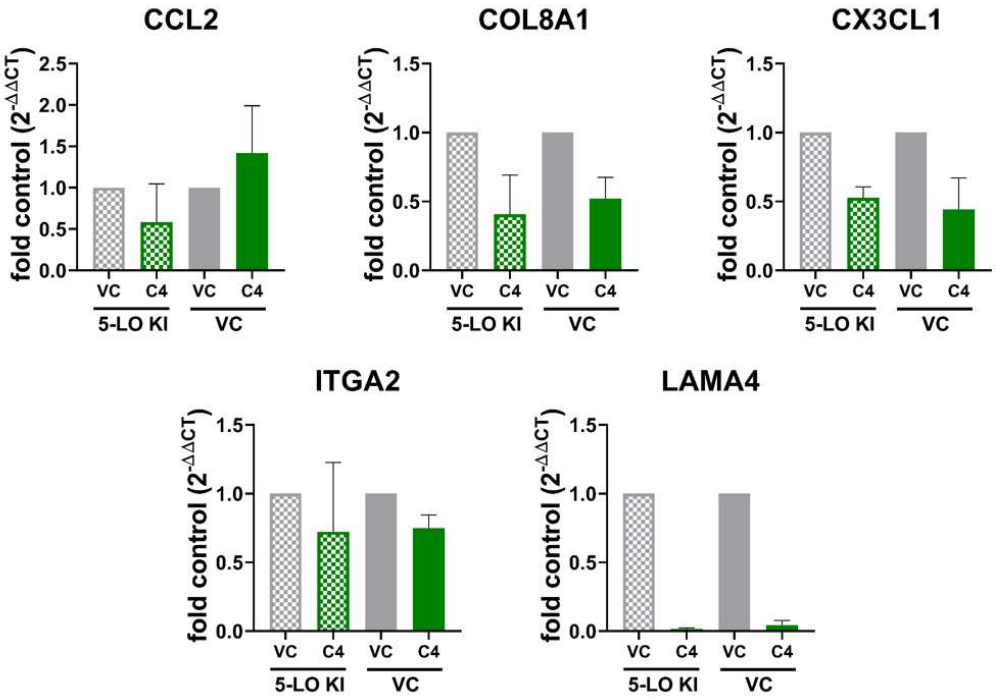

Figure 5.40 RT-qPCR analysis of selected differentially expressed genes in U-2 OS 5-LO knock-in cells and the respective controls. *mRNA expression of differentially regulated genes in U-2 OS 5-LO knock-in and the respective control cells. Gene expression was normalized to ACTB (housekeeping gene) and the corresponding vector control cells ($2^{-\Delta\Delta CT}$ method). Data are presented as mean + SD of 3 independent experiments. Asterisks indicate significant changes vs. vector control cells *p ≤ 0.05, **p ≤ 0.01, ***p ≤ 0.001.*

Cell proliferation was impaired after knocking out the 5-LO in HT-29 and U-2 OS cells. For this reason, the same experiment was conducted in all generated knock-in and control cell lines (**Figure 5.41**).

In HCT-116 cells the knockout of 5-LO did not affect proliferation, so it was not surprising that the over-expression of 5-LO as well did not result in altered proliferation rates.

In HT-29 cells the retarded proliferation achieved by knocking out 5-LO could be completely reversed. Single-cell clone F4 even showed the highest cell number at each time point after re-expressing 5-LO.

Contrary results were detected in U-2 OS cells. Here, re-expression of 5-LO in clone C4 did not lead to reinforced proliferation compared to the vector control-treated cells.

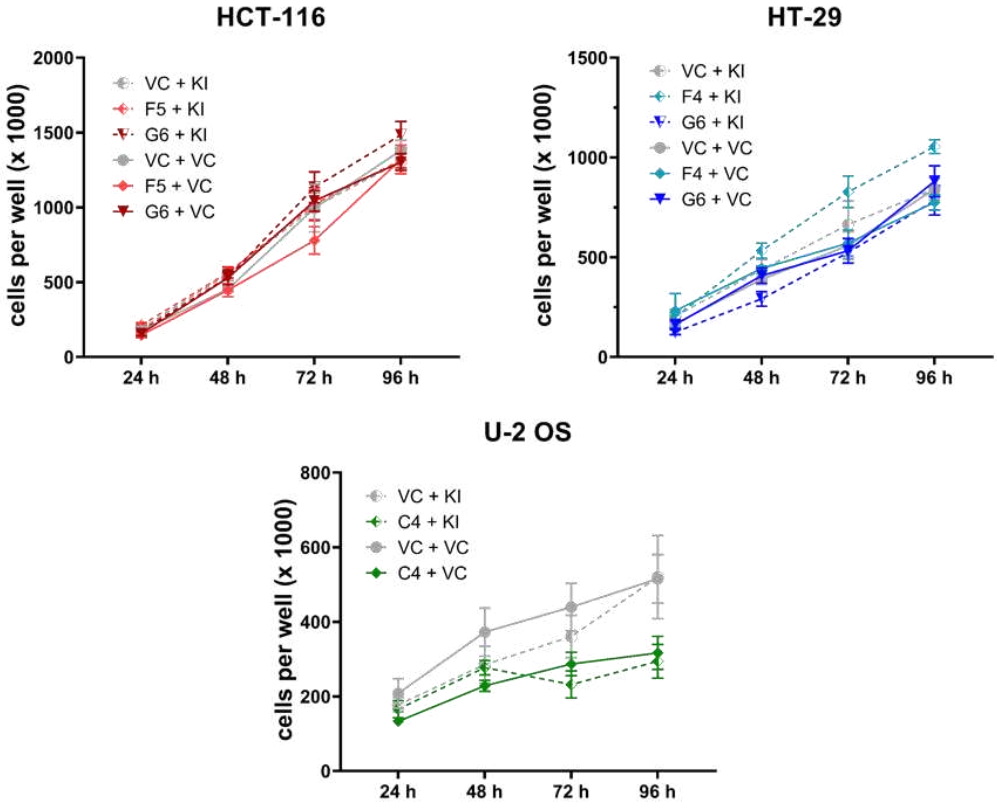

Figure 5.41 Cell proliferation in HCT-116, HT-29, and U-2 OS 5-LO knock-in and vector control-treated cells. *Cell proliferation in HCT-116 (top left), HT-29 (top right), and U-2 OS (bottom) cells over a time-course of 96 hours. Data are presented as mean ± SD from 3 independent experiments. Asterisks indicate significant changes vs. vector control-treated cells *p ≤ 0.05, **p ≤ 0.01, ***p ≤ 0.001.*

Directed cell migration was investigated in HCT-116 and U-2 OS cells as only here the knockout of 5-LO increased cell motility (**Figure 5.42**). In both HCT-116 5-LO knockout clones now over-expressing the 5-LO, a slight decrease in the number of migrated cells could be detected compared to the vector control-treated counterparts. In U-2 OS cells, cell migration was not altered by the re-expression of 5-LO.

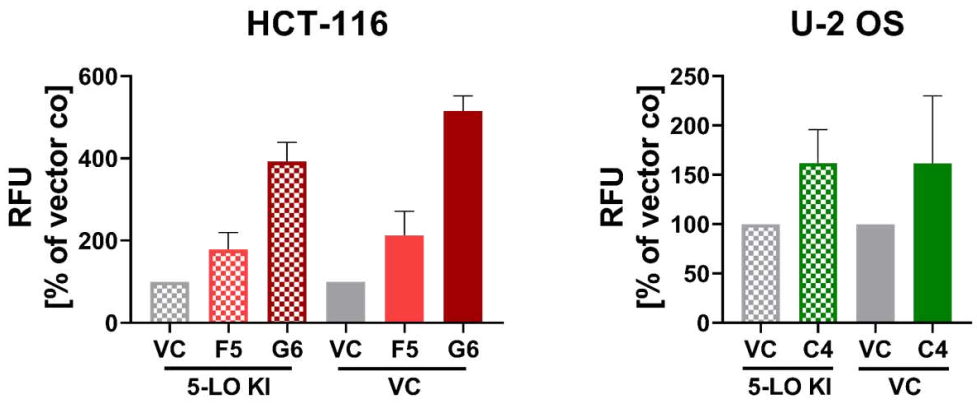

Figure 5.42 Directed cell migration of HCT-116 and U-2 OS 5-LO knock-in and vector control cells. *After 3 hours (U-2 OS) or 24 hours (HCT-116), migrated cells were stained, and fluorescence of the cell suspension was measured. Data are presented as mean + SD from 3-5 independent experiments. Asterisks indicate significant changes vs. DMSO control *p ≤ 0.05, **p ≤ 0.01, ***p ≤ 0.001.*

6 Discussion, conclusion and perspective

6.1 Discussion

6.1.1 5-LO expressing tumour cells produce only small amounts of lipid mediators

In the present work, the influence of the complete genomic knockout of 5-lipoxygenase (5-LO) from different solid, 5-LO expressing tumour cell lines was studied. Until now it has only been known, that 5-LO expression in solid tumours results in enhanced proliferation and tumour progression but the mechanisms that lie behind these effects have remained to be unclear so far (269) (305) (307). For this reason, three different 5-LO knockout cell lines, two colorectal cancer cell lines (HCT-116 and HT-29) and one osteosarcoma cell line (U-2 OS) were established. The knockout was performed employing CRISPR/Cas technology, to give new insights into the canonical and non-canonical functions of 5-LO in solid tumours. The three selected cell lines show strong differences in their phenotype concerning their differentiation and proliferation status and also in the expression of 5-LO. While HCT-116 cells possess a rather undifferentiated but strongly proliferative, fibroblast-like phenotype, HT-29 and U-2 OS cells are more of the contrary type with a lower replication rate (see **5.2**). HT-29 cells were described as rather differentiated goblet-like colon cancer cells while HCT-116 cells resemble more the stem-like subtype (355). On mRNA as well as on protein level, HCT-116 cells showed the weakest 5-LO expression (**Figure 3.2**) while HT-29 cells and U-2 OS cells both expressed higher levels of 5-LO. This led to the assumption that 5-LO expression might be a feature of a rather differentiated cell phenotype in adherent tumour cells.

Beyond expression levels, it remains of question why the 5-LO enzyme - whose presence is under physiological conditions limited to different types of immune cells - is expressed in the tumour cells, since the enzymatic function seems to be only, if at all, a side function. Previous work (performed by Tamara Göbel) to this study could show, that in all three investigated cell lines the complete machinery of enzymes involved in the leukotriene biosynthesis is expressed. Measuring the 5-LO activity revealed that, compared to PMNL, only small amounts of the two main products 5-HETE and LTB_4 were synthesised in all three cell lines independent of the amount of expressed enzyme (**Figure 3.3**). The by far strongest activity of 5-LO was detected in pancreas carcinoma cell line Capan-2. Unfortunately, the knockout of 5-LO in those cells was not successful. Therefore, they were excluded from this study. Destroying cell integrity by homogenising the cells and additionally utilising the 100,000 x g supernatants increased the amounts of produced 5-HETE about 5- to 10-fold in all cell lines and in U-2 OS cells also LTB_4 levels, indicating that in the cellular context of intact tumour cells 5-LO activity is inhibited by an unknown mechanism. Since it is known that cellular localisation is one regulator of 5-LO activity (52), confocal microscopy was used to investigate the cellular distribution of 5-LO in the used cell lines (**Figure 3.4**). In HCT-116 and HT-29 cells, 5-LO was found almost exclusively in the cytosolic fraction providing an explanation for the rather low enzymatic activity. In

U-2 OS cells, 5-LO was evenly distributed between the cytosol and the nucleus. This could be a possible explanation for the elevated LTB_4 and 5-HETE production that was 2-5-fold higher in U-2 OS cells than in the two colorectal cancer cell lines. Leukotrienes and other lipid mediators like 5-HETE and 5-oxo-ETE are potent lipid mediators that perform a wide range of tasks in biological processes. Additionally, the enzymatic machinery responsible for the production of such mediators is able to produce highly reactive oxygen species that are known to impair nucleotide structures and induce cell death via different ways (308) (356) (357) (358) (359). Therefore, it is of no surprise that cancer cells tightly regulate the enzymatic activity of 5-LO to prevent cell damage. Also, LTB_4 and 5-oxo-ETE act as chemotactic molecules for immune cells, which could induce the body's own defence mechanisms against neoplasia that is of no interest to the tumour cells. All in all, it seems reasonable for the tumour cells to reduce 5-LO activity, which leaves the question of why 5-LO is expressed in those cells in the first place and what other non-canonical functions it could exert.

6.1.2 Gene expression is cell line dependently altered by 5-LO

To get a global overview of the possible effects induced by the total knockout of the 5-LO, RNA sequencing was picked as the method of choice. Here it became obvious that the influence of the 5-LO knockout is cell line dependent. While for HCT-116 and HT-29 cells only 28, respectively 18, genes were influenced, in U-2 OS cells 234 genes were discovered to be differentially expressed in 5-LO knockout single-cell clones compared to their 5-LO positive counterparts (**Figure 5.7 A**). Pathway analysis of the particular genes that was performed to evaluate which cellular processes are influenced led to interesting results. Although the genes that were altered in expression were different in each cell line, the linked processes were overlapping. Clustering the differentially expressed genes revealed that the epithelial-mesenchymal-transition (EMT) was most prominent as several genes known to be involved in EMT were regulated by the 5-LO knockout in each cell line (**Table 5.1**). Other processes that overlapped in the three cell lines were ECM modulation and cytoskeleton formation, cell adhesion and migration, as well as GPCR signalling and transcription, leading to the assumption that even though the way the 5-LO knockout alters cellular processes is individual, the outcome is similar. Considering how heterogenic tumours are in general, this seems to be plausible after all. As mentioned before, the three investigated cell lines strongly differ in their origin and status of differentiation, so one can assume that the transcriptome, as well as the proteasome of the cells, differ which generates multiple possible sites of action for the 5-LO.

Different cytokines were found to be regulated in 5-LO knockout cells. In HCT-116 cells, mRNA levels of *TGFB2* were 10- to 20-fold increased in all three 5-LO knockout single-cell clones compared to the respective control (**Figure 5.9**). These findings were congruent with the performed TGF-β2 ELISA where up to 3 times more protein was secreted by the 5-LO knockout clones (**Figure 5.24**). TGF-β can exhibit various functions in tumours but it was shown that in the early stages of tumours TGF-β can inhibit the cell cycle and induce apoptosis (360) (361). It is therefore beneficial for the developing tumours to suppress

TGF-β expression possibly via 5-LO. In U-2 OS cells TGF-β-signaling was targeted as well. Here, *LRRC32*, an activator of TGF-β, was found to be differentially expressed via RNA sequencing with an upregulation in both 5-LO-knockout clones, giving another way to suppress TGF-β activity (**Figure 5.7**, bottom left). This is one example of the diverse regulatory mechanisms of similar processes. In U-2 OS cells the three cytokine-coding genes *CCL2*, *CX3CL1* and *PDGFA* were found to be differentially expressed in the 5-LO knockout single-cell clones (**Figure 5.11**). In both knockout clones, all three genes were downregulated compared to the control cells. Performing an ELISA and a cytometric bead assay (CBA) revealed that cytokine expression of platelet-derived growth factor A (PDGF-AA), monocyte chemoattractant protein 1 (MCP-1) and fractalkine was in fact reduced in 5-LO knockout single-cell clones (**Figure 5.25**). Those cytokines are known to regulate tumour proliferation and progression. MCP-1 mediates its effects via PI3K/Akt/mTOR and other prominent signalling pathways, promotes angiogenesis and metastasis in tumours and recruits macrophages to the tumour environment - all resulting in poor prognosis (362). Fractalkine can have different effects on cancer cells but was shown to stimulate cancer cell proliferation, increase resistance to apoptotic signals and induce EMT leading to promoted migration and metastasis (363). PDGF-A on its part can induce various growth signals mediating proliferation and enhanced survival of tumour cells (364). As all of those cytokines promote desirable features for tumour cells, an over-expression that positively correlates with the 5-LO status is advantageous for U-2 OS cells.

Besides mentioned cytokines, expression levels of different genes responsible for cell adhesion and migration were found to be altered in U-2 OS cells (**Figure 5.11**). Transcript levels of genes encoding collagens (*COL5A3*, *COL8A1*, *COL20A1*, *COL22A1*), laminins and laminin regulators (*LAMA4*, *LAMC2*, *DRAXIN*) were decreased in 5-LO cells, giving a hint that 5-LO enhances those processes. In fact, 5-LO itself, as well as its products LTB_4 and LTD_4, were already shown to promote the expression of collagens and laminins (365) (366) (367). In Mono Mac 6 cells, knockout of 5-LO was recently shown to increase cell adhesion to human umbilical vein endothelial cells (HUVEC), proving the relevance of this enzyme for said processes (320).

Additionally, the secretion and expression of the before mentioned cytokines and cell adhesion molecules like laminins modified in the presence of 5-LO, are linked to altering the attraction of other components of the multicellular tumour environment (368) (369) (370) (371) (372). Cancer-associated fibroblasts as well as infiltrating immune cells exhibit important functions mediating tumour growth, metastasis, and angiogenesis and are crucial for communication within the tumour environment (373) (374). In fact, it was shown that 5-LO - upregulated by hypoxia - recruits tumour-associated macrophages in ovarian cancer supporting the assumption that 5-LO participates in organising the tumour microenvironment (375).

6.1.3 5-LO promotes cancer cell proliferation in 2D and 3D cell culture

With this knowledge, different cellular assays were conducted. At first, the influence on cell proliferation was evaluated which is one characteristic property important for tumour progression (**Figure 5.12**). For the already fast proliferating HCT-116 cells no difference in the proliferation rate could be seen independent of the 5-LO status, while for both HT-29 and U-2 OS cells the 5-LO knockout resulted in impaired cell growth visible already after 48 hours. These findings lead to the assumption that in rather differentiated cells the 5-LO can support cell proliferation while for already strongly proliferating cells the presence of 5-LO makes no difference in their growth behaviour. Another feature crucial for tumour progression is the ability of one single cell to proliferate and form a new growing colony. This was investigated by 2D, as well as 3D, colony-forming assays. While in both HCT-116 and HT-29 cells no difference in colony growth neither in number nor in size could be found, in U-2 OS cells a slight downregulation in the number of colonies was detectable, again supporting the assumption that the 5-LO - at least in some cells - can help the tumour cells to proliferate even in hostile surroundings (**Figure 5.15**). Embedding the cells in a layer of agar revealed that HCT-116 5-LO knockout clones possessed a slight advantage in the growing ability compared to the control cells (**Figure 5.16**). So here again, the mechanisms in which 5-LO influences the tumour cells are cell line dependent.

As 2D cell culture shows limitations in transferability to physiological conditions, spheroid formation is always a good way to go if a more physiological environment is needed (376). Different aspects of the spheroids were investigated: appearance, size, viability, and proliferation of cells in the spheroids. Most interesting was the behaviour of U-2 OS cells. Taking a closer look at the spheroid appearance indicates that while control vector-treated cells show a distinct outer rim with merging cells on the surface, distinctive for tumour spheroids, this rim is completely absent in both 5-LO knockout single-cell clones (**Figure 5.17 G**). Here cells form a more or less loose cell clump with no distinct contour resulting in significant bigger spheroid diameters. As it is important for developing tumours to form a well-defined separated area to keep out immune cells searching for malignancies this could be another tumour supporting property of 5-LO. Despite being of bigger size, the 5-LO knockout spheroids contain about 50% fewer cells - living and total - than the control spheroids containing 5-LO (**Figure 5.17 I**), so like already investigated in cells growing in monolayer 5-LO supports cell proliferation in U-2 OS cells. An explanation for the impaired tumour cell proliferation in the 5-LO knockout spheroids is the cell-cell contacts that are - contrary to the 5-LO positive cells - not sufficiently developed. Besides its relevance for building a solid and robust tumour body, intercellular adhesion is also relevant for communication and induction of different processes like the proliferation of the tumour cells (377) (378). Only if tumour spheroids grow too dense, the proliferation rate of the cells is impaired. Interestingly, cell proliferation in spheroids of the different types of HT-29 cells was reinforced in cells lacking the 5-LO (**Figure 5.17 F**). But since 5-LO positive and negative cells formed perfectly round-shaped spheroids with tight cell-cell interactions (**Figure 5.17 D**), different mechanisms appear to be involved in those cells. Since digesting the spheroids and counting the living and dead cells only gives limited information about the actual situation inside the spheroid, a 3D cell viability assay was

performed to get more information about the condition of the spheroids. Here, a bioluminescent reagent penetrates the spheroid and is converted by ATP, which is used as a surrogate parameter for cell viability. In most of the 5-LO knockout single-cell clones, a slight decrease in the viability of cells in the spheroids was detected (**Figure 5.18**), again giving a hint that 5-LO is supportive of 3D tumour cell survival.

6.1.4 Drug resistance, directed cell migration and invasion of tumour cells are regulated by 5-LO

The resistance to cytotoxic agents achievable by different processes is a much-desired aspect of tumour cells. Possible ways of resistance are decreased uptake or enhanced efflux of the cytotoxic agent, disposing or depletion of the drug and mutation of the elements targeted by the cytotoxic substance (379). By any means, a decreased responsiveness to cytostatic drugs is causing many problems in today's cancer treatment options and it was described that 5-LO expressing tumours are distinguished by poor responsiveness to the treatment with cytostatic drugs (308) (264) (266). Hence, it was decided to evaluate if the genomic knockout of 5-LO influences cell viability and the responsiveness to cytostatic drugs. Overall cell viability was measured using a WST-1-assay while FACS analysis after staining with Annexin V/propidium iodide was used to distinguish the different cellular states after the treatment. While the presence of 5-LO gave an advantage to U-2 OS cells treated with the DNA intercalating drug Actinomycin D (**Figure 5.13**, bottom), the knockout of 5-LO in HT-29 cells resulted in increased resistance to the treatment with high doses of the topoisomerase II inhibitor etoposide (**Figure 5.13**, middle). Moreover, Actinomycin D treatment of HCT-116 cells increased the population of living cells in the absence of 5-LO (**Figure 5.14**, top). Although the investigated effects were not too pronounced, it remains in question, why 5-LO increases sensitivity to cytostatic drugs in both colon carcinoma cell lines but administers resistance to the very same drugs in U-2 OS cells. Certainly, the individual endowment of active pathways and cellular processes is decisive for this feature.

RNA sequencing revealed that epithelial-to-mesenchymal transition, as well as cell adhesion and cytoskeleton rearrangement, might be the most interesting processes affected by the 5-LO knockout. EMT - and adverse MET - are important processes for tumour progression in solid tumours (238). While in the initiation phase of the tumour, EMT needs to be inhibited for the tumour to form a solid and encapsulated body consisting of stationary, polarized epithelial-like cells, in later stages EMT is necessary for developing agile mesenchymal-like cells able to migrate to the surrounding area and eventually to distant hospitable locations (380). At the new locus, they undergo MET and change back to the epithelial subtype to proliferate and form a new tumourigenic body. This highlights the fact, that under certain conditions EMT is much desired by tumour cells, while in other situations the suppression of EMT becomes crucial. From literature, various genes are known as markers for EMT but the most frequently mentioned are *CDH1*, *CDH2*, *SNAI1* and *SNAI2* (381). *CDH1* is the gene encoding E-cadherin (cadherin-1), a cell-cell adhesion protein that is strongly expressed on epithelial cell surfaces and gets

downregulated by cells undergoing EMT. N-cadherin (cadherin-2), encoded by *CDH2*, on the contrary, is important for trans-endothelial cell migration and by this is an important driver of tumour metastasis (382). *SNAI1* and *SNAI2* encode the two transcription factors Snail and Slug responsible for the transcriptional repression of E-cadherin and promoted migration of tumour cells (383). In HCT-116 5-LO knockout single-cell clones, *SNAI2* is 2-fold downregulated (**Figure 5.20**), generating the assumption that EMT is promoted by 5-LO in those cells. On the other side, in HT-29 cells the strong upregulation of *CDH2* and the moderate upregulation of *SNAI2* in all 5-LO knockout clones indicate the suppression of EMT by 5-LO. The same is true for U-2 OS cells where a slight downregulation of *CDH1* in both 5-LO knockout clones could be examined. These differences between HCT-116 cells and - on the other hand - HT-29 and U-2 OS cells fit the assumption, that the status of differentiation of the cells might interfere with the 5-LO status and function. Anyways, as it is known that multiple effectors are involved in EMT and also the cellular setting is important, further investigation of the possible effects of 5-LO on EMT in functional assays was conducted. As nutrient deprivation is one hallmark of tumours and a strong driver for tumour spreading, a transwell assay was used to determine directed cell migration toward serum used as a chemoattractant. In both, HCT-116 and U-2 OS cells, cell motility was increased by knocking out 5-LO (**Figure 5.21 A**), proving that direct cell migration toward a serum gradient is enhanced if 5-LO is absent in both cell lines cells. In contrast, undirected cell migration assessed by a wound closure assay was not influenced by 5-LO. Invasion into ECM is another feature of metastatic tumour cells. While adding a layer of artificial ECM to the transwell chamber to mimic invasion into the tumour surroundings did not reveal any difference in the behaviour between 5-LO positive and negative cells (**Figure 5.21 B**), differences for the U-2 OS subtypes became obvious by embedding the tumour spheroids in Matrigel®. Cells lacking the 5-LO formed significantly smaller spheroids that were not able to invade the surrounding matrix (**Figure 5.19 E, F**). For both, U-2 OS wildtype and control vector-treated cells, a typical evolution of tube-like structures on the surface of the spheroids could be detected (**Figure 5.19 G**). This unequivocally highlights that in U-2 OS cells 5-LO provides features enabling spheroid growth and invasion into ECM, both desirable during tumour progression, but to examine those effects a more physiological setting of tumour spheroids is needed. The fact that - kept in complete growth medium without adding ECM - U-2 OS cells were hardly able to form spheroids, but by embedding the cells in Matrigel® spheroids were generated from all types of U-2 OS cells, shows the relevance of ECM providing cells with growth signals from the environment already described in chapter 1.4.

6.1.5 Pharmacological inhibition of 5-LO partly reproduces the effects mediated by the 5-LO knockout

To evaluate whether canonical or non-canonical functions of the 5-LO mediated the investigated effects, several experiments were repeated with control vector cells carrying wildtype 5-LO that were treated with two different 5-LO inhibitors. Zileuton is the only approved 5-LO inhibitor for pharmaceutical use on the market and CJ-13610 is an *in vitro* used non-redox type 5-LO inhibitor. To include the possibility that long-term processes

are involved, cells were pre-incubated for 3 days with the inhibitors and re-treated on the day of seeding for the respective experiment.

Investigation of gene expression of selected genes via RT-qPCR revealed that enzymatic 5-LO activity is only partly responsible for the effects achieved by the complete 5-LO knockout. Regulation of the genes *NOSTRIN*, *PDLIM5*, *TGFB2* and *RPS4Y1* seen in HCT-116 5-LO KO cells could be at least partly mimicked by the inhibition of 5-LO (**Figure 5.30**) while most other genes were not affected by any of the two inhibitors or even showed opposite regulation (*PBX1*, *LMAN1*, *ZNF419*). The same was true in HT-29 and U-2 OS cells. Only the 5-LO knockout mediated regulation of *UTS2B* (**Figure 5.31),** respectively *CCL2*, *HAS2*, *PLAC1* and *SPP1* (**Figure 5.32**) was also dose-dependently achieved by pharmacological inhibition of the enzyme while all other regulations remained to be knockout-specific.

High doses of CJ-13610 (3 µM) also attenuated cell proliferation in both, HT-29 and U-2 OS cells (**Figure 5.33**), again only partly imitating the impact of the 5-LO knockout. But measuring overall cell viability in inhibitor-treated cells revealed impaired cell viability in both cell lines treated with 3 µM CJ-13619 assuming that attenuated proliferation is dependent on decreased cell viability caused by high doses of the inhibitor.

The formation of cell spheroids under the influence of 5-LO inhibitors lead to no difference in size and appearance of the spheroids but a slight increase in the number of cells per spheroid was detected (**Figure 5.34**), again showing similar tendencies to the results of the 5-LO knockout single-cell clones. The most interesting results were achieved by conducting the transwell migration assay with inhibited 5-LO activity (**Figure 5.35**). While enhanced cell migration was not detected for inhibitor-treated U-2 OS cells, in HCT-116 cells indeed an increase in cell motility after the treatment with higher doses of Zileuton as well as low and high doses of CJ-13610 was detectable.

To sum this up, inhibiting the enzymatic function of 5-LO only partly reproduced the 5-LO KO effects. Thus, it seems reasonable, that canonical, as well as non-canonical functions of the 5-LO, affect tumour cells. This was verified for functional assays, as well as for gene expression. The known non-canonical functions of 5-LO are its interaction with p53, β-catenin and DICER, as well as direct DNA binding and transcriptional regulation (chapter 1.6). All of those are known to directly and indirectly - via microRNA processing - influence DNA transcription as well as processes like cell viability, adhesion, and motility. Interaction with those partners is a possible explanation for the examined effects but it remains also possible that other unknown, non-canonical mechanisms are involved here (262) (310) (316) (320).

A possible explanation for the canonical function and thereby the effects mimicked by inhibiting 5-LO could be that oxygenated lipids produced by 5-LO are integrated into phospholipids of the cell membrane thereby altering membrane fluidity resulting in more static and immobile cells (384). Supporting this hypothesis are the levels of LTB_4 and 5-HETE that are produced and secreted by the tumour cells which are surprisingly low regarding the amount of expressed enzyme. Additionally, it is known that 5-LO only oxygenates PUFAs liberated from the membrane by $cPLA_2$ but regardless, 5-HETE and

5-oxo-ETE esterified in membranes of primary and activated neutrophils could be detected (385). Besides influencing the sheer membrane condition, oxidized membrane lipids are also known to regulate processes like cellular signalling, ferroptosis and apoptosis and strongly shape innate as well as adaptive immune responses (386). Direct integration of the different 5-LO products (5-HETE and 5-oxo-ETE) is a conceivable explanation for the low levels of lipid mediators measured in the cell supernatants as well as for some functional consequences of 5-LO. Additionally, effects beyond the classical leukotriene pathways are known for some 5-LO products, providing another explanation for the results of inhibitor-treated cells. Tumour development, cell viability and proliferation plus PPAR-activation and recruitment of immune cells are only a few to mention (387) (388) (389).

Validation of knockout experiments is usually conducted by re-expression of the knocked-out protein. Therefore, 5-LO knockout and control vector carrying cells were transfected with a sleeping-beauty plasmid containing the *ALOX5* sequence. Unfortunately, due to limited time, only some of the expressive experiments were repeated with the knock-in cells. Western Blot analysis of the transfected cells confirmed the successful knock-in of 5-LO but also indicated an increased 5-LO expression of 3000-4000% of the wildtype level (**Figure 5.37**). As this is far beyond physiological expression, the results of the conducted experiments should be handled with care. Effects of 5-LO knockout on gene expression of some selected genes like *FOXA2*, *ATP11C*, *UTS2B* and *ZNF420* could be at least partly reversed by 5-LO knock-in but expression levels of none of those genes correspond to physiological levels (**Figures 5.38 - 5.40**). Congruent effects were examined for directed cell migration that was slightly attenuated in 5-LO knock-in cells compared to the respective knockout clone (**Figure 5.42**). Still, those data are not sufficient to validate the described findings of this work due to unphysiological over-expression of the enzyme. For future studies, these experiments should be repeated after re-expressing 5-LO under more physiological conditions for example by using the CRISPR/Cas technique as a genome editing method and inserting the gene at its original genomic location.

6.2 Conclusion and perspective

In this work, I investigated the influence of the knockout of 5-lipoxygenase on 5-LO expressing tumour cells. I could show that in all chosen cell lines knockout of 5-LO influences different properties essential for tumour cell viability, proliferation, motility, and invasiveness. Based on the previously presented data, I infer that 5-LO affects gene expression of all used cell lines, even though the individual genetic profile remains cell line dependent. Nevertheless, similar cellular functions are altered by the knockout of 5-LO, proving that besides tumour cell survival and proliferation 5-LO also influences cell motility and invasiveness into extracellular compartments. Therefore, it is reasonable to conclude that 5-LO influences EMT and most probably inhibits - at least in the investigated cell lines - this process to form a solid primary tumour body. Additionally, 5-LO alters the secretion and expression of different cytokines and cell adhesion molecules which, among other things, participate in attracting immune cells and cancer-associated fibroblasts. By this, 5-LO might be involved in shaping the tumour microenvironment.

What remains to be clarified in further studies is:

- How are 5-LO expression and activity controlled in 5-LO expressing tumour cells?
- Which mechanisms administrate the regulation of gene expression mediated by 5-LO?
- Do canonical and/or non-canonical 5-LO functions influence functional properties of the cancer cells like proliferation, motility, and invasiveness?
- How is the tumour-microenvironment involved in the regulatory processes initiated by 5-LO?

7 Zusammenfassung

Die 5-Lipoxygenase ist das Schlüsselenzym in der Biosynthese von Leukotrienen. Nach Aktivierung durch unterschiedliche Stimuli transloziert die 5-LO an die Kernmembran, wo sie einen Komplex mit der zytosolischen Phospholipase A_2 und dem 5-LO aktivierenden Protein (FLAP) bildet. Dieser aktivierte Komplex setzt die mehrfach ungesättigte Fettsäure Arachidonsäure aus der Membran frei. In einer Zweischritt-Reaktion wird diese anschließend über das Intermediat 5-HpETE (5(*S*)-Hydroperoxy-6,8,11,14-eicosatetraensäure) zum instabilen Epoxid Leukotrien A_4 (LTA_4) oxidiert. Leukotrien A_4 kann dann entweder durch die LTA_4-Hydrolase zu Leukotrien B_4 umgesetzt werden, oder es wird durch die LTC_4-Synthase an Glutathion gekoppelt, wobei die sogenannten Cysteinyl-Leukotriene C_4, D_4 und E_4 entstehen.

Leukotriene vermitteln entzündliche Reaktionen und tragen zum allergischen Geschehen bei Asthma bronchiale und der allergischen Rhinitis entscheidend bei. LTB_4 wirkt als potentes Chemokin, wobei Leukozyten rekrutiert werden und deren Anheften an das Gefäßendothel erhöht wird. LTB_4 fördert die Erkennung und Beseitigung von Erregern durch Leukozyten und ist somit ein wichtiger Teil des angeborenen Immunsystems. Die Cysteinyl-Leukotriene gehören zu den potentesten bisher bekannten Bronchokonstriktoren und sind maßgeblich am pathologischen Umbau der Atemwege bei entzündlichen Erkrankungen beteiligt. Hier agieren sie wie LTB_4 als chemische Lockstoffe und vermitteln das Einwandern von Immunzellen, wodurch das entzündliche Geschehen vorangetrieben wird.

Die 5-Lipoxygenase wird vorrangig in verschiedenen Zellen des Immunsystems wie Makrophagen, Mastzellen oder dentritischen Zellen exprimiert. Zusätzlich konnte in den letzten Jahren aber auch die Expression von 5-LO in soliden Tumoren unterschiedlichen Ursprungs, wie Brust-, Pankreas-, Prostata- oder Kolonkarzinomen, gezeigt werden, obwohl all diese Gewebe unter physiologischen Bedingungen keine 5-LO exprimieren.

5-LO-exprimierende Tumore sind charakterisiert durch eine schlechte Prognose hinsichtlich der Überlebensrate der Patient*innen und ein geringeres Ansprechen auf die Behandlung mit zytostatischen Wirkstoffen. Neben der 5-LO selbst, konnten auch die unterschiedlichen Produkte der 5-LO in Tumoren nachgewiesen werden und durch die Inhibition der 5-LO konnten Zellzyklusarrest und Apoptose ausgelöst werden. Die in den unterschiedlichen Studien verwendeten Konzentrationen der Inhibitoren lagen jedoch teilweise weit über dem IC_{50} Wert für die 5-LO, was es fraglich macht, ob diese Effekte allein durch die Hemmung der 5-LO zustande kamen.

Nichtsdestotrotz stellt sich bis heute die Frage, warum diese soliden Tumore 5-LO exprimieren. Neben ihrer eigentlichen Produktion von Lipidmediatoren, kann die 5-LO auch weitere Strukturen oxidieren, wobei reaktive Sauerstoffspezies entstehen, die die

Zelle erheblich schädigen können. Es birgt also ein gewisses Risiko, dieses Enzym zu exprimieren, wodurch es nur logisch erscheint, dass die 5-LO diesen Tumorzellen einen Vorteil verschaffen muss und die Aktivität der 5-LO streng reguliert wird.

Neben ihrer gewöhnlichen kanonischen, also der enzymatischen, Funktion sind noch weitere nicht-kanonische Funktionen der 5-LO bekannt. So konnten Interaktionen mit p53, β-Cathenin und dem microRNA prozessierenden Protein DICER, sowie die Regulation der Transkription in Mono Mac 6 Zellen gezeigt werden. Über diese nicht-kanonischen Funktionen ist es denkbar, dass die 5-LO weitere zelluläre Prozesse jenseits der Synthese von Lipidmediatoren beeinflusst.

In vorherigen Arbeiten, größtenteils durchgeführt durch Tamara Göbel, wurde die Expression der 5-LO in Tumorzelllinien, die von soliden Tumoren unterschiedlichen Ursprungs entstammen, untersucht, wobei HCT-116, HT-29 (Kolonkarzinom), Capan-2 (Pankreaskarzinom) und U-2 OS (Osteosarkom) Zellen allesamt die 5-LO exprimierten. Zusätzlich wurde die Expression weiterer Proteine, die an der Biosynthese der Lipidmediatoren beteiligt sind (FLAP, $cPLA_2$, LTA_4-Hydrolase und LTC_4-Synthase), auf Protein- oder mRNA-Ebene bestätigt. Bei Aktivitätsmessungen wurde die Bildung von 5-HETE und LTB_4 durch intakte Zellen, Zellhomogenate und zusätzlich den S100 (100.000 x g) Überständen der Homogenate untersucht. Hier konnte gezeigt werden, dass die Lipidmediatorproduktion in allen 4 Zelllinien in intakten Zellen sehr gering ist und durch das Homogenisieren der Zellen erhöht werden kann. In HT-29, HCT-116 und U-2 OS Zellen bleibt die Menge der gebildeten Substrate jedoch trotzdem deutlich unter derer, die von PMNL unter vergleichbaren Bedingungen gebildet wurde. Dies legt die Vermutung nahe, dass die Aktivität der 5-LO in den Tumorzellen gehemmt wird. Da bekannt ist, dass die Lokalisation der 5-LO einen starken Einfluss auf deren Aktivität hat, wurde mittels Konfokal-Mikroskopie die zelluläre Verteilung der 5-LO untersucht. Hier konnte gezeigt werden, dass in HT-29 und HCT-116 Zellen die 5-LO fast ausschließlich zytosolisch vorliegt, während in U-2 OS und Capan-2 Zellen eine gleichmäßige Verteilung zwischen Zytosol und Zellkern zu beobachten ist. Da die 5-LO-abhängige Lipidmediatorproduktion durch nukleäre Lokalisation in der Regel begünstigt wird, stellt diese Verteilung eine mögliche Erklärung für die verminderte Aktivität der 5-LO in den beiden Kolonkarzinomzellen dar, wobei trotzdem die Frage bleibt, wodurch diese vermittelt wird und wofür die 5-LO in den Tumorzellen benötigt wird, wenn die enzymatische Funktion offenbar gehemmt ist.

Um zu untersuchen, welchen Zweck die 5-LO in den Tumorzellen erfüllt, wurden in der vorliegenden Arbeit nun die Einflüsse des CRISPR/Cas vermittelten Knockouts der 5-Lipoxygenase auf die unterschiedlichen Tumorzelllinien untersucht. Dafür wurden HCT-116, HT-29 und U-2 OS Zellen mit einem CRISPR/Cas Plasmid transfiziert, welches den Cas9-Komplex zu Exon 2 oder Exon 6 der 5-LO navigiert, wodurch dort ein Doppelstrangbruch verursacht wird. Durch kleine Fehler der Reparaturmechanismen kommt es zu Rasterschub-Mutationen, die darin resultieren, dass kein funktionsfähiges Protein mehr gebildet werden kann. Um den vollständigen genomischen Knockout zu validieren, wurden die Zellen anschließend mit Puromycin selektioniert, Einzelzellklone generiert und diese mittels Western Blot und DNA-Sequenzierung untersucht. Für die

beiden Kolonkarzinomzellen HCT-116 und HT-29 wurden jeweils drei Klone für die weiteren Untersuchungen ausgewählt, während nur zwei der U-2 OS Einzelzellklone den geforderten Kriterien entsprachen. Als Kontrolle für alle Experimente dienten Leervektor-behandelte Zellen, die ebenfalls mit Puromycin selektioniert wurden. Da die Transfektion der Capan-2 Zellen nach mehreren Versuchen nicht erfolgreich war, wurden diese aus der weiteren Arbeit ausgeschlossen.

Um einen breiten Überblick über die möglichen Einflüsse des 5-LO Knockouts auf die Ziellinien zu bekommen, wurde ein Next-Generation-Sequencing (RNAseq) durchgeführt und dadurch die durch den Knockout bedingten, differentiell exprimierten Gene ermittelt. Dabei wurden für die HCT-116 Zelllinie 28 Gene ermittelt, deren Expression in allen 3 Einzelzellklonen verändert war, in den HT-29 Zellen waren es 18 und in den U-2 OS Zellen 234 Gene. Die Expression dieser Gene wurde nun mittels real-time qPCR genauer untersucht, um die 5-LO abhängige Regulation zu bestätigen und genauer quantifizieren zu können. Um die beeinflussten biologischen Prozesse genauer zu betrachten, wurden die differenziell exprimierten Gene nach ihren bekannten Funktionen geordnet. Obwohl keines der ermittelten Gene in mehr als einer Zelllinie reguliert war, zeigten die beeinflussten zellulären Prozesse hier jedoch eine große Überschneidung. So waren in allen Zelllinien Prozesse wie Zelladhäsion und -migration, die epithelial-mesenchymale Transition, Gentranskription und G-Protein gekoppelte Signalkaskaden beeinflusst.

Diese Prozesse sollten nun funktionell untersucht werden. In einem Proliferation-Assay konnte gezeigt werden, dass sowohl HT-29, also auch U-2 OS Zellen langsamer wuchsen, wenn die 5-LO nicht exprimiert wurde. In diesen beiden Zelllinien unterstütz das Enzym also scheinbar das Zellwachstum. Da 5-LO über-exprimierende Tumore oft eine erhöhte Resistenz gegen die Behandlung mit zytostatischen Wirkstoffen zeigen, wurde das Ansprechen auf unterschiedliche Wirkstoffe mittels WST-Assay und durch FACS-Analyse untersucht. Hier lieferten die einzelnen Zelllinien gegenteilige Ergebnisse. Während in HCT-116 Zellen der 5-LO Knockout zu einem besseren Überleben während der Behandlung mit Actinomycin D, Etoposid und 5-Fluorouracil führt, zeigten die beiden U-2 OS Einzelzellklone eine verringerte Lebensrate nach der Behandlung mit Actinomycin D, in Abwesenheit der 5-LO. Diese Unterschiede zwischen den einzelnen Zelllinien konnten auch bei weiteren Versuchen beobachtet werden und legen die Vermutung nahe, dass der Effekt, den die 5-LO in Tumorzellen vermittelt, stark von der zellulären Umgebung abhängt.

Während sowohl zwei- als auch dreidimensionale Koloniebildungs-Assays nur wenige Unterschiede im Wachstumsverhalten der 5-LO positiven und negativen Zellen aufdeckten, konnten gerade in den U-2 OS Zellen große Unterschiede im dreidimensionalen Wachstumsverhalten in Sphären gezeigt werden. Hier wurden Zellen in speziell beschichtete Platten mit abgerundetem Boden ausgesät, sodass keine Adhäsion an die Platten stattfinden kann und verstärkt Zell-Zell-Kontakte ausgebildet werden, die dafür sorgen, dass sich dreidimensionale Tumorsphären formen. Erscheinung, Größe und die Anzahl an Zellen pro Sphäre wurden im Folgenden untersucht. HCT-116 Zellen waren dabei am wenigsten durch den Knockout der 5-LO

beeinflusst, da weder Unterschiede in der Größe noch in der Zusammensetzung der Sphären beobachtet werden konnten. In HT-29 Zellen war jedoch auffällig, dass, obwohl Größe und Aussehen sich nicht zwischen 5-LO positiven und negativen Zellen unterschieden, bei allen drei 5-LO Knockout Klonen eine erhöhte Anzahl an Zellen pro Sphäre zu finden war. Dieser Umstand ließe sich dadurch erklären, dass entweder die Zellen in diesem Kontext kleiner waren, wenn sie keine 5-LO exprimieren, oder, dass die Sphären dichter gepackt und der Hohlraum, der sich klassischerweise im Inneren dieser Gebilde befindet, kleiner ist in Sphären, die von 5-LO Knockout Zellen gebildet wurden. In U-2 OS Zellen konnten offensichtliche Unterschiede zwischen 5-LO positiven und negativen Zellen in der Erscheinung der Sphären beobachtet werden. So konnte unter dem Mikroskop gesehen werden, dass keine kompakten Sphären gebildet wurden, sondern nur lose Zellansammlungen entstanden. Das resultierte in einem deutlich größeren Radius der 5-LO Knockout Sphären, obwohl die Sphären aus weniger Zellen als die entsprechenden Kontrollen bestanden.

Auch das Einbetten der Sphären in Matrigel® - einer artifiziellen extrazellulären Matrix (ECM) - um die physiologische Tumorumgebung zu imitieren, lieferte interessante Ergebnisse. In HCT-116 und HT-29 Zellen konnte zwar das typische Hinauswachsen der Sphären in die extrazelluläre Matrix beobachtet werden, wobei sich gerade in den HT-29 Zellen komplexe, dreidimensionale Gebilde formten, jedoch waren diese Effekte nicht abhängig vom 5-LO Status der Zellen. In U-2 OS Zellen verursachte das Einbetten in ECM jedoch, dass auch die 5-LO Knockout Zellen Sphären bildeten, diese jedoch signifikant kleiner waren, als die der Kontrollvektor-behandelten Zellen, möglicherweise auf der Tatsache beruhend, dass das Zellwachstum in den 5-LO Knockout Sphären - wie bereits gezeigt - vermindert war. Zusätzlich bildeten beide 5-LO positiven Zellen - Wildtyp und Kontrollvektor-behandelter Wildtyp - nadelförmige Auswüchse in die Matrix, die typischerweise in einem Spheroid-Outgrowth-Assay erwartet werden. Diese waren in beiden 5-LO Knockout Einzelzellklonen nicht zu sehen.

Da die epithelial-mesenchymale Transition als einer der am stärksten beeinflussten Prozesse in der Auswertung des Next-Generation-Sequencing auftauchte, wurde die Expression von klassischen EMT-Markern untersucht. Diese Untersuchung lieferte allerdings keine eindeutigen Ergebnisse und stattdessen wurden die funktionellen Einflüsse des 5-LO Knockouts auf die Zellmigration untersucht. Während die ungerichtete Zellmigration in einem Wound-Healing-Assay nicht durch den Knockout der 5-LO beeinflusst wurde, waren starke Einflüsse des 5-LO Knockouts auf die gerichtete Zellmigration zu beobachten. In einem Transwell-Assay wurden Zellen in Serum-reduziertem Medium auf die Oberseite einer porösen Membran ausgesät und die untere Kammer des Systems wurde mit gewöhnlichem Wachstumsmedium gefüllt, wodurch ein Gradient hin zu höherer Serumkonzentration gebildet wurde. HCT-116 sowie U-2 OS Zellen, aus denen die 5-LO ausgeknockt wurde, zeigten hier eine deutlich verstärkte Wanderung der Zellen hin zum Serumgradienten. Dieser Effekt konnte vollständig ausgelöscht werden, wenn die Membran vorher mit Matrigel® beschichtet wurde, um die Invasion in ECM zu imitieren.

Die differentielle Expressionsanalyse der RNAseq zeigte ebenfalls, dass auch einige Cytokine und Mitogene durch den Knockout der 5-LO beeinflusst wurden. In HCT-116 Zellen war die Expression des Gens *TGFB2* in 5-LO Knockout Zellen 10-20-fach hochreguliert, während in U-2 OS 5-LO KO-Zellen die Genexpression von *CCL2*, *CX3CL1* und *PDGFA* signifikant reduziert war. Die Sekretion dieser Mediatoren wurde deswegen mittels Cytometric bead array (CBA) und ELISA aus Zellüberständen gemessen, wobei für alle Mediatoren die Regulation auf Genebene auch auf Proteinebene gezeigt werden konnte. TGF-β erfüllt vielfältige Funktionen in Zellen, jedoch konnte gerade in frühen Stadien der Tumorentwicklung gezeigt werden, dass der Zellzyklus inhibiert und Apoptose vermittelt durch TGF-β ausgelöst werden kann. Unter diesen Umständen bietet die 5-LO regulierte Unterdrückung der TGF-β-Expression also einen Überlebensvorteil für die Tumorzellen. Auch in U-2 OS Zellen konnte eine Regulation des TGF-β-Signalwegs gezeigt werden. Hier wurde die Genexpression von *LRRC32*, eines TGF-β Aktivators, durch den Knockout der 5-LO gesteigert, sodass also auch hier eine 5-LO vermittelte Unterdrückung der TGF-β-Signalkaskade vorliegt. MCP-1, codiert von dem Gen *CCL2*, initiiert Angiogenese und Metastasierung in Tumoren. Fraktalkin (*CX3CL1*) kann proliferationssteigernd wirken und vermittelt sowohl anti-apoptotische als auch EMT-induzierende Signale. Der Platelet-Derived Growth Factor A (*PDGFA*) ist hingegen ein klassischer Wachstumsfaktor, der Tumorzellproliferation begünstigt. Da der Knockout der 5-LO für alle dieser Gene zu einer Reduktion der Genexpression führte, ist davon auszugehen, dass die 5-LO hierdurch unterschiedliche Effekte ausüben kann, die die Tumorprogression begünstigen.

Weitere Experimente wurden durchgeführt, die jedoch keine oder zumindest keine eindeutige Regulation durch die 5-LO zeigen konnten. So wurde der Zellzyklus der unterschiedlichen Zelllinien untersucht, Tumorstammzellenmarker quantifiziert und unterschiedliche Tumormarker, die Prozesse wie Proliferation oder Differenzierung anzeigen können, mittels Immunofärbungen und Konfokalmikroskopie untersucht.

Interessant an den 5-LO-exprimierenden Tumorzellen ist die Tatsache, dass zwar die komplette Maschinerie für die Leukotrienbiosynthese exprimiert wird, die Menge der gebildeten Lipidmediatoren im Vergleich zu Leukozyten jedoch eher gering ist. Trotzdem stellt sich die Frage, ob diese Restaktivität ausreicht, um einige der vorher untersuchten 5-LO vermittelten Effekte zu verursachen, oder ob es gänzlich nicht-kanonische Funktionen sind, die hier eine Rolle spielen. Dafür wurden Leervektor-behandelte Zellen mit den beiden 5-LO Inhibitoren Zileuton und CJ-13610 in zwei unterschiedlichen Konzentrationen über einen Zeitraum von 3 Tagen behandelt und anschließenden die entsprechenden Experimente erneut durchgeführt. Hier konnten einige der Effekte, die durch den Knockout der 5-LO verursacht wurden, zumindest teilweise imitiert werden, während die Behandlung mit Inhibitoren in anderen Experimenten keine Ergebnisse zeigte, oder sogar zu gegenteiligen Ergebnissen führten. Die Genexpression von ausgewählten Genen wurde unter dem Einfluss der Inhibitoren in allen drei Zelllinien untersucht. Hier zeigte ein Teil der Gene, wie *NOSTRIN*, *TGFB2* und *PDLIM5* (HCT-116), *UTS2B* (HT-29) und *CCL2*, *HAS2* und *ITGA2* (U-2 OS) eine ähnliche Regulation durch die Inhibition der 5-LO wie durch deren Knockout, während andere Gene gar nicht oder sogar invers durch die Inhibitorbehandlung reguliert wurden. Der Knockout der 5-LO führte in

HT-29 und U-2 OS Zellen zu einer verringerten Proliferationsrate. Dieser Effekt konnte durch höhere Dosen des nicht-redox-Inhibitors CJ-13610 ebenfalls erreicht werden, wobei mittels eines WST-Assays gezeigt wurde, dass, zumindest in U-2 OS Zellen, 3 µM CJ-13610 ausreichten, um die Zellviabilität zu verringern, wodurch die verminderte Proliferationsrate zu erklären ist. Die Sphärenbildung unter Inhibitorbehandlung wurde ebenfalls in HT-29 und U-2 OS Zellen überprüft, allerdings wurden in keiner der Zelllinien Unterschiede im Wachstumsverhalten der Sphären durch die Behandlung hervorgerufen. Die direkte Zellmigration, die durch den Knockout der 5-LO in HCT-116 und U-2 OS Zellen signifikant gesteigert werden konnte, wurde zumindest in den HCT-116 Zellen auch durch die Inhibitorbehandlung dosisabhängig gesteigert, während in U-2 OS Zellen kein Effekt sichtbar war. Die Auswertung dieser Experimente legt also die Vermutung nahe, dass die Funktion der 5-LO in den Tumorzellen sowohl kanonischer als auch nicht-kanonischer Natur ist. Eine mögliche Erklärung hierfür liegt darin, dass bei den Aktivitätsuntersuchungen der 5-LO nur die sezernierten Produkte der 5-LO in den Zellüberständen gemessen wurden. Da in den Phospholipiden der Zellmembranen jedoch auch oxidierte Fettsäuren zu finden sind, die 5-LO aber ausschließlich freie Fettsäuren als Substrate akzeptiert, ist es denkbar, dass die entstanden Produkte nachträglich in die Zellmembranen integriert werden, wo sie die Fluidität der Membranen verändern, sowie Signalkaskaden beeinflussen können.

Klassischerweise wird die Re-Expression des ausgeknockten Gens genutzt, um die Ergebnisse von Knockout-Studien zu bestätigen. Genexpression ausgewählter Gene, Proliferation und direkte Zellmigration wurden deswegen auch mit Knockout Zellen, in die nachträglich die 5-LO mittels Sleeping-Beauty-Technologie wieder eingebracht wurde, untersucht. Hier konnte ein Teil der durch den Knockout vermittelten Effekte durch den Knock-In umgekehrt werden, während ein Großteil der Effekte jedoch nur leicht oder gar nicht durch den Knock-In beeinflusst wurde. Da der Knock-In in den Zellen durch den verwendeten hochaktiven Promotor allerdings zu einer mehr als 300-fach erhöhten 5-LO-Expression verglichen zu den Wildtyp-Zellen führte, müssen diese Ergebnisse mit Vorsicht betrachtet werden.

Nichtsdestotrotz konnte durch die vorliegende Arbeit gezeigt werden, dass die 5-LO in soliden Tumoren unterschiedliche Prozesse wie die Genexpression, Zellproliferation, das dreidimensionales Wachstum sowie die Zellmigration reguliert. Diese Regulation ist streng Zelltyp-spezifisch und hängt von vielen Faktoren wie dem Proteom der Zellen und der Tumormikroumgebung ab.

8 List of references

1. Ivanov I, Heydeck D, Hofheinz K, Roffeis J, O'Donnell VB, Kuhn H, Walther M. Molecular enzymology of lipoxygenases. *Arch Biochem Biophys.* 503(2):161-74, 2010 Nov 15.

2. Funk CD, Chen XS, Johnson EN, Zhao L. Lipoxygenase genes and their targeted disruption. *Prostaglandins Other Lipid Mediat.* 68-69:303-12, 2002 Aug.

3. Haeggström JZ, Funk CD. Lipoxygenase and leukotriene pathways: biochemistry, biology, and roles in disease. *Chem Rev.* 111(10):5866-98, 2011 Oct 12.

4. Mancini AD, Di Battista JA. The cardinal role of the phospholipase A2/cyclooxygenase-2/prostaglandin E synthase/prostaglandin E2 (PCPP) axis in inflammostasis. *Inflamm. Res.* 60, 1083–1092, 2011.

5. Kuhn H, Banthiya S, van Leyen K. Mammalian lipoxygenases and their biological relevance. *Biochim Biophys Acta.* 1851(4):308-30, 2015 Apr.

6. Hamberg M, Samuelsson B. Prostaglandin endoperoxides. Novel transformations of arachidonic acid in human platelets. *Proc Natl Acad Sci U S A.* 71(9), 3400–3404, 1974.

7. Funk CD, Furci L, FitzGerald GA. Molecular cloning, primary structure, and expression of the human platelet/erythroleukemia cell 12-lipoxygenase. *Proc Natl Acad Sci U S A.* 87(15):5638-42, 1990 Aug.

8. Virmani J, Johnson EN, Klein-Szanto AJ, Funk CD. Role of 'platelet-type' 12-lipoxygenase in skin carcinogenesis. *Cancer Letters.* 162(2):161-5, 2001.

9. Boeglin WE, Kim RB, Brash AR. A 12R-lipoxygenase in human skin: mechanistic evidence, molecular cloning, and expression. *Proc Natl Acad Sci U S A.* 1998 Jun 9, pp. 95(12):6744-9.

10. Krieg P, Fürstenberger G. The role of lipoxygenases in epidermis. *Biochim Biophys Acta.* 1841(3):390-400, 2014 Mar.

11. Zheng Y, Yin H, Boeglin WE, Elias PM, Crumrine D, Beier DR, Brash AR. Lipoxygenases mediate the effect of essential fatty acid in skin barrier formation: a proposed role in releasing omega-hydroxyceramide for construction of the corneocyte lipid envelope. *J Biol Chem.* 286(27):24046-56, 2011 Jul 8.

12. Conrad DJ, Kuhn H, Mulkins M, Highland E, Sigal E. Specific inflammatory cytokines regulate the expression of human monocyte 15-lipoxygenase. *Proc Natl Acad Sci U S A.* 89(1):217-21, 1992 Jan 1.

13. Sigal E, Grunberger D, Cashman JR, Craik CS, Caughey GH, Nadel JA. Arachidonate 15-lipoxygenase from human eosinophil-enriched leukocytes: partial purification and properties. *Biochem Biophys Res Commun.* 150(1):376-83, 1988 Jan 15.

14. Sigal E, Dicharry S, Highland E, Finkbeiner WE. Cloning of human airway 15-lipoxygenase: identity to the reticulocyte enzyme and expression in epithelium. *Am J Physiol.* 262(4 Pt 1):L392-8, 1992 Apr.

15. Ebert R, Cumbana R, Lehmann C, Kutzner L, Toewe A, Ferreirós N, Parnham MJ, Schebb NH, Steinhilber D, Kahnt AS. Long-term stimulation of toll-like receptor-2 and -4 upregulates 5-LO and 15-LO-2 expression thereby inducing a lipid mediator shift in human monocyte-derived macrophages. *Biochim Biophys Acta Mol Cell Biol Lipids.* 1865(9):158702, 2020 Sep.

16. Brash AR, Boeglin WE, Chang MS. Discovery of a second 15S-lipoxygenase in humans. *Proc Natl Acad Sci U S A.* 94(12):6148-52, 1997 Jun 10.

17. Samuelsson B, Dahlén SE, Lindgren JA, Rouzer CA, Serhan CN. Leukotrienes and lipoxins: structures, biosynthesis, and biological effects. *Science.* 237(4819):1171-6, 1987.

18. Powell WS, Gravelle F, Gravel S. Metabolism of 5(S)-hydroxy-6,8,11,14-eicosatetraenoic acid and other 5(S)-hydroxyeicosanoids by a specific dehydrogenase in human polymorphonuclear leukocytes. *J Biol Chem.* 267, 19233–19241, 1992.

19. Serhan CN, Hamberg M, Samuelsson B. Lipoxins: novel series of biologically active compounds formed from arachidonic acid in human leukocytes. *Proc Natl Acad Sci U S A.* 81, 5335–5339, 1984.

20. Luo M, Jones SM, Phare SM, Coffey MJ, Peters-Golden M, Brock TG. Protein kinase A inhibits leukotriene synthesis by phosphorylation of 5-lipoxygenase on serine 523. *J Biol Chem.* 2004, pp. 279(40):41512-20.

21. Werz O, Szellas D, Steinhilber D, Rådmark O. Arachidonic acid promotes phosphorylation of 5-lipoxygenase at Ser-271 by MAPK-activated protein kinase 2 (MK2). *J Biol Chem.* 277(17):14793-800, 2002.

22. Rådmark O, Werz O, Steinhilber D, Samuelsson B. 5-Lipoxygenase: regulation of expression and enzyme activity. *Trends Biochem Sci.* 32(7):332-41, 2007.

23. Ochs MJ, Suess B, Steinhilber D. 5-lipoxygenase mRNA and protein isoforms. *Basic Clin Pharmacol Toxicol.* 114(1):78-82, 2014 Jan.

24. Ochs MJ, Sorg BL, Pufahl L, Grez M, Suess B, Steinhilber D. Post-transcriptional regulation of 5-lipoxygenase mRNA expression via alternative splicing and nonsense-mediated mRNA decay. *PLoS One.* 7(2):e31363, 2012.

25. Silverman, E.S., Du, J., Sanctis, G.T.D., Rådmark, O., Samuelsson, B., Drazen, J.M. and Collins, T. Egr-1 and Sp1 interact functionally with the 5-lipoxygenase promoter and its naturally occurring mutants. *Am. J. Respir. Cell Mol. Biol.,.* 1998, pp. 19(2), 316–323.

26. Uhl J, Klan N, Rose M, Entian KD, Werz O, Steinhilber D. The 5-lipoxygenase promoter is regulated by DNA methylation. *J Biol Chem.* 277(6):4374-9, 2002 Feb 8.

27. Kalayci O, Birben E, Sackesen C, Keskin O, Tahan F, Wechsler ME, Civelek E, Soyer OU, Adalioglu G, Tuncer A, Israel E, Lilly C. ALOX5 promoter genotype, asthma severity and LTC production by eosinophils. *Allergy.* 61(1):97-103, 2006 Jan.

28. Dwyer JH, Allayee H, Dwyer KM, Fan J, Wu H, Mar R, Lusis AJ, Mehrabian M. Arachidonate 5-lipoxygenase promoter genotype, dietary arachidonic acid, and atherosclerosis. *N Engl J Med.* 350(1):29-37, 2004 Jan 1.

29. Sorg BL, Klan N, Seuter S, Dishart D, Rådmark O, Habenicht A, Carlberg C, Werz O, Steinhilber D. Analysis of the 5-lipoxygenase promoter and characterization of a vitamin D receptor binding site. *Biochim Biophys Acta.* 1761(7):686-97, 2006 Jul.

30. Steinhilber, D. 5-Lipoxygenase: a target for antiinflammatory drugs revisited. *Curr Med Chem.* 6(1):71-85, 1999 Jan.

31. Seuter, S., Sorg, B.L. and Steinhilber, D. The coding sequence mediates induction of 5-lipoxygenase expression by Smads3/4. *Biochem. Biophys. Res. Commun.* 2006, pp. 348(4), 1403–1410.

32. Hoshiko S, Rådmark O, Samuelsson B. Characterization of the human 5-lipoxygenase gene promoter. *Proc Natl Acad Sci U S A.* 87 (23) 9073-9077, 1990.

33. In KH, Asano K, Beier D, Grobholz J, Finn PW, Silverman EK, Silverman ES, Collins T, Fischer AR, Keith TP, Serino K, Kim SW, De Sanctis GT, Yandava C, Pillari A, Rubin P, Kemp J, Israel E, Busse W, Ledford D, Murray JJ, Segal A, Tinkleman D, Drazen JM. Naturally occurring mutations in the human 5-lipoxygenase gene promoter that modify transcription factor binding and reporter gene transcription. *J Clin Invest.* 99(5), 1130–1137, 1997.

34. Steinhilber D, Brungs M, Werz O, Wiesenberg I, Danielsson C, Kahlen JP, Nayeri S, Schräder M, Carlberg C. The nuclear receptor for melatonin represses 5-lipoxygenase gene expression in human B lymphocytes. *J. Biol. Chem.* 270(13), 7037–7040, 1995.

35. Silverman ES, Drazen JM. The biology of 5-lipoxygenase: function, structure, and regulatory mechanisms. *Proc Assoc Am Physicians.* 111(6), 525–536, 1999.

36. Gillmor SA, Villaseñor A, Fletterick R, Sigal E, Browner MF. The structure of mammalian 15-lipoxygenase reveals similarity to the lipases and the determinants of substrate specificity. *Nat. Struct. Biol.* 4(12), 1003–1009, 1997.

37. Aparoy P, Reddy RN, Guruprasad L, Reddy MR, Reddanna P. Homology modeling of 5-lipoxygenase and hints for better inhibitor design. *J. Comput. Aided Mol. De.* 22(9), 611–619, 2008.

38. Gilbert NC, Bartlett SG, Waight MT, Neau DB, Boeglin WE, Brash AR, Newcomer ME. The structure of human 5-lipoxygenase. *Science.* 331(6014), 217–219, 2011.

39. Hammarberg T, Provost P, Persson B, Rådmark O. The N-terminal domain of 5-lipoxygenase binds calcium and mediates calcium stimulation of enzyme activity. *J Biol Chem.* 275(49), 38787–38793, 2000.

40. Hemak J, Gale D, Brock TG. Structural characterization of the catalytic domain of the human 5-lipoxygenase enzyme. *J Mol Model.* 8(4), 102–112, 2002.

41. Pande AH, Qin S, Tatulian SA. Membrane fluidity is a key modulator of membrane binding, insertion, and activity of 5-lipoxygenase. *Biophys J.* 88(6), 4084–4094, 2005.

42. Kulkarni S, Das S, Funk CD, Murray D, Cho W. Molecular basis of the specific subcellular localization of the C2-like domain of 5-lipoxygenase. *J Biol Chem.* 277(15), 13167–13174, 2002.

43. Hammarberg T, Zhang YY, Lind B, Radmark O, Samuelsson B. Mutations at the C-terminal isoleucine and other potential iron ligands of 5-lipoxygenase. *Eur J Biochem.* 230(2):401-7, 1995 Jun 1.

44. Zhang YY, Hammarberg T, Radmark O, Samuelsson B, Ng CF, Funk CD, Loscalzo J. Analysis of a nucleotide-binding site of 5-lipoxygenase by affinity labelling: binding characteristics and amino acid sequences. *Biochem J.* 351 (Pt 3), 697–707, 2000.

45. Peters-Golden M, McNish RW. Redistribution of 5-lipoxygenase and cytosolic phospholipase A2 to the nuclear fraction upon macrophage activation. *Biochem Biophys Res Commun.* 196(1):147-53, 1993 Oct 15.

46. Brock TG, Anderson JA, Fries FP, Peters-Golden M, Sporn PH. Decreased leukotriene C4 synthesis accompanies adherence dependent nuclear import of 5-lipoxygenase in human blood eosinophils. *J Immunol.* 162(3),1669–1676, 1999.

47. Chen XS, Naumann TA, Kurre U, Jenkins NA, Copeland NG, Funk CD. cDNA cloning, expression, mutagenesis, intracellular localization, and gene chromosomal assignment of mouse 5-lipoxygenase. *J Biol Chem.* 270(30):17993-9, 1995 Jul 28.

48. Woods JW, Coffey MJ, Brock TG, Singer II, Peters-Golden M. 5-Lipoxygenase is located in the euchromatin of the nucleus in resting human alveolar macrophages and translocates to the nuclear envelope upon cell activation. *J Clin Invest.* 95(5):2035-46, 1995 May.

49. Brock TG, McNish RW, Peters-Golden M. Translocation and leukotriene synthetic capacity of nuclear 5-lipoxygenase in rat basophilic leukemia cells and alveolar macrophages. *J Biol Chem.* 270(37):21652-8, 1995 Sep 15.

50. Brock TG, McNish RW, Bailie MB, Peters-Golden M. Rapid import of cytosolic 5-lipoxygenase into the nucleus of neutrophils after in vivo recruitment and in vitro adherence. *J Biol Chem.* 272(13), 8276–8280, 1997.

51. Hsieh FH, Lam BK, Penrose JF, Austen KF, Boyce JA. T helper cell type 2 cytokines coordinately regulate immunoglobulin E dependent cysteinyl leukotriene production by human cord blood-derived mast cells: profound induction of leukotriene C(4) synthase expression by interleukin 4. *J Exp Med.* 193(1), 123–133, 2001.

52. Luo, M., Jones, S.M., Peters-Golden, M. and Brock, T.G. Nuclear localization of 5-lipoxygenase as a determinant of leukotriene B4 synthetic capacity. *Proc. Natl. Acad. Sci. U. S. A.,.* 2003, pp. 100(21), 12165–12170.

53. Newcomer ME, Gilbert NC. Location, location, location: compartmentalization of early events in leukotriene biosynthesis. *The Journal of biological chemistry.* 285(49):38740, 2010.

54. Jones SM, Luo M, Healy AM, Peters-Golden M, Brock TG. Structural and functional criteria reveal a new nuclear import sequence on the 5-lipoxygenase protein. *J Biol Chem.* 277(41), 38550–38556, 2002.

55. Jones SM, Luo M, Peters-Golden M, Brock TG. Identification of two novel nuclear import sequences on the 5-lipoxygenase protein. *J Biol Chem.* 278(12), 10257–10263, 2003.

56. Luo M, Pang CW, Gerken AE, Brock TG. Multiple nuclear localization sequences allow modulation of 5-lipoxygenase nuclear import. *Traffic.* 5(11), 847–854, 2004.

57. Flamand N, Luo M, Peters-Golden M, Brock TG. Phosphorylation of serine 271 on 5-lipoxygenase and its role in nuclear export. *J Biol Chem.* 284(1), 306–313, 2009.

58. Hanaka H, Shimizu T, Izumi T. Stress-induced nuclear export of 5-lipoxygenase. *Biochem Biophys Res Commun.* 338(1):111-6, 2005 Dec 9.

59. Luo M, Jones SM, Flamand N, Aronoff DM, Peters-Golden M, Brock TG. Phosphorylation by protein kinase a inhibits nuclear import of 5-lipoxygenase. *J Biol Chem.* 2005 Dec 9, pp. 280(49):40609-16.

60. Markoutsa S, Sürün D, Karas M, Hofmann B, Steinhilber D, Sorg BL. Analysis of 5-lipoxygenase phosphorylation on molecular level by MALDI-MS. *FEBS J.* 281(8):1931-47., 2014 Apr.

61. McDonald PP, McColl SR, Naccache PH, Borgeat P. Studies on the activation of human neutrophil 5-lipoxygenase induced by natural agonists and Ca2+ ionophore A23187. *Biochem. J.* 280 (Pt 2), 379–385, 1991.

62. Hörnig C, Albert D, Fischer L, Hörnig M, Rådmark O, Steinhilber D, Werz O. 1-Oleoyl-2-acetylglycerol stimulates 5-lipoxygenase activity via a putative (phospho)lipid binding site within the N-terminal C2-like domain. *J Biol Chem.* 280(29):26913-21, 2005 Jul 22.

63. Fettel J, Kühn B, Guillen NA, Sürün D, Peters M, Bauer R, Angioni C, Geisslinger G, Schnütgen F, Meyer Zu Heringdorf D, Werz O, Meybohm P, Zacharowski K, Steinhilber D, Roos J, Maier TJ. Sphingosine-1-phosphate (S1P) induces potent anti-inflammatory effects in vitro and in vivo by S1P receptor 4-mediated suppression of 5-lipoxygenase activity. *FASEB J.* 33(2):1711-1726, 2019 Feb.

64. Funk, CD. Prostaglandins and leukotrienes: advances in eicosanoid biology. *Science.* 294(5548):1871-5, 2001.

65. Gijón MA, Leslie CC. Regulation of arachidonic acid release and cytosolic phospholipase A2 activation. *J Leukoc Biol.* 65(3):330-6, 1999 Mar.

66. Rybina IV, Liu H, Gor Y, Feinmark SJ. Regulation of leukotriene A4 hydrolase activity in endothelial cells by phosphorylation. *J Biol Chem.* 272(50):31865-71, 1997 Dec 12.

67. Ahmad S, Ytterberg AJ, Thulasingam M, Tholander F, Bergman T, Zubarev R, Wetterholm A, Rinaldo-Matthis A, Haeggström JZ. Phosphorylation of Leukotriene C4 Synthase at Serine 36 Impairs Catalytic Activity. *J Biol Chem.* 291(35), 18410-18418, 2016.

68. Skerrett SJ, Henderson WR, Martin TR. Alveolar macrophage function in rats with severe protein calorie malnutrition. Arachidonic acid metabolism, cytokine release, and antimicrobial activity. *J Immunol.* 144(3),1052–1061, 1990.

69. Cederholm T, Lindgren JA, Palmblad J. Impaired leukotriene C4 generation in granulocytes from protein-energy malnourished chronically ill elderly. *J Intern Med.* 247(6),715–722, 2000.

70. Thorsen S, Busch-Sørensen M, Søndergaard, J. Reduced neutrophil production of leukotriene B4 associated with AIDS. *AIDS.* 3(10),651–653, 1989.

71. Coffey MJ, Phare SM, Kazanjian PH, Peters-Golden M. 5-Lipoxygenase metabolism in alveolar macrophages from subjects infected with the human immunodeficiency virus. *J Immunol.* 157(1), 393–399, 1996.

72. Coffey MJ, Phare SM, Cinti S, Peters-Golden M, Kazanjian PH. Granulocyte-macrophage colony-stimulating factor upregulates reduced 5-lipoxygenase metabolism in peripheral blood monocytes and neutrophils in acquired immunodeficiency syndrome. *Blood.* 94(11), 3897–3905, 1999.

73. Dahlén SE, Hansson G, Hedqvist P, Björck T, Granström E, Dahlén B. Allergen challenge of lung tissue from asthmatics elicits bronchial contraction that correlates with the release of leukotrienes C4, D4, and E4. *Proc Natl Acad Sci U S A.* 80(6), 1712–1716, 1983.

74. Drazen JM, Lilly CM, Sperling R, Rubin P, Israel E. Role of cysteinyl leukotrienes in spontaneous asthmatic responses. *Adv Prostaglandin Thromboxane Leukot Res.* 22, 251–262, 1994.

75. Busse W, Kraft M. Cysteinyl leukotrienes in allergic inflammation: strategic target for therapy. *Chest.* 127(4),1312–1326, 2005.

76. Peters-Golden, M. Expanding roles for leukotrienes in airway inflammation. *Curr Allergy Asthma Rep.* 8(4), 367–373, 2008.

77. Voelkel NF, Tuder RM, Wade K, Höper M, Lepley RA, Goulet JL, Koller BH, Fitzpatrick F. Inhibition of 5-lipoxygenase-activating protein (FLAP) reduces pulmonary vascular reactivity and pulmonary hypertension in hypoxic rats. *J Clin Invest.* 97(11), 2491–2498, 1996.

78. Wilborn J, Bailie M, Coffey M, Burdick M, Strieter R, Peters-Golden M. Constitutive activation of 5-lipoxygenase in the lungs of patients with idiopathic pulmonary fibrosis. *J Clin Invest.* 97(8), 1827–1836, 1996.

79. Griffiths RJ, Pettipher ER, Koch K, Farrell CA, Breslow R, Conklyn MJ, Smith MA, Hackman BC, Wimberly DJ, Milici AJ, et al. Leukotriene B4 plays a critical role in the progression of collagen-induced arthritis. *Proc Natl Acad Sci U S A.* 92(2), 517–521, 1995.

80. Sharon P, Stenson WF. Enhanced synthesis of leukotriene B4 by colonic mucosa in inflammatory bowel disease. *Gastroenterology.* 86(3),453–460, 1984.

81. Meghji S, Sandy JR, Scutt AM, Harvey W, Harris M. Stimulation of bone resorption by lipoxygenase metabolites of arachidonic acid. *Prostaglandins.* 36(2), 139–149, 1988.

82. Meier F, Gross E, Klotz KN, Ruzicka T. Leukotriene B4 receptors on neutrophils in patients with psoriasis and atopic eczema. *Skin Pharmacol.* 2(2), 61–67, 1989.

83. Spanbroek R, Grabner R, Lotzer K, Hildner M, Urbach A, Ruhling K, Moos MP, Kaiser B, Cohnert TU, Wahlers T, Zieske A, Plenz G, Robenek H, Salbach P, Kuhn H, Radmark O, Samuelsson B, Habenicht AJ. Expanding expression of the 5-lipoxygenase pathway within the arterial wall during human atherogenesis. *Proc Natl Acad Sci U S A.* 100(3), 1238–1243, 2003.

84. Bäck, M. Inflammatory signaling through leukotriene receptors in atherosclerosis. *Curr Atheroscler Rep.* 10(3):244-51, 2008.

85. Yoshimura, R., Matsuyama, M., Tsuchida, K., Kawahito, Y., Sano, H. and Nakatani, T. Expression of lipoxygenase in human bladder carcinoma and growth inhibition by its inhibitors. *J. Urol.* 2003, pp. 170(5), 1994–1999.

86. Wächtershäuser A, Steinhilber D, Loitsch SM, Stein J. Expression of 5-lipoxygenase by human colorectal carcinoma Caco-2 cells during butyrate-induced cell differentiation. *Biochem Biophys Res Commun.* 268(3), 778–783, 2000.

87. Avis I, Martínez A, Tauler J, Zudaire E, Mayburd A, Abu-Ghazaleh R, Ondrey F, Mulshine JL. Inhibitors of the arachidonic acid pathway and peroxisome proliferator-activated receptor ligands have superadditive effects on lung cancer growth inhibition. *Cancer Res.* 65(10),4181–4190, 2005.

88. Ding XZ, Iversen P, Cluck MW, Knezetic JA, Adrian TE vvv. Lipoxygenase inhibitors abolish proliferation of human pancreatic cancer cells. *Biochem Biophys Res Commun.* 261(1), 218–223, 1999.

89. Hennig R, Ding XZ, Tong WG, Schneider MB, Standop J, Friess H, Büchler MW, Pour PM, Adrian TE. 5-Lipoxygenase and leukotriene B(4) receptor are expressed in human pancreatic cancers but not in pancreatic ducts in normal tissue. *Am J Pathol.* 161(2):421-8, 2002.

90. Myers CE, Ghosh J. Lipoxygenase inhibition in prostate cancer. *Eur Urol.* 35(5-6), 395–398, 1999.

91. Chen, Y., Hu, Y., Zhang, H., Peng, C. and Li, S. Loss of the Alox5 gene impairs leukemia stem cells and prevents chronic myeloid leukemia. *Nat. Genet.* 2009, pp. 41(7), 783–792.

92. DeKelver RC, Lewin B, Lam K, Komeno Y, Yan M, Rundle C, Lo MC, Zhang DE. Cooperation between RUNX1-ETO9a and novel transcriptional partner KLF6 in upregulation of Alox5 in acute myeloid leukemia. *PLoS Genet.* 9(10):e1003765, 2013.

93. Ford-Hutchinson AW, Bray MA, Doig MV, Shipley ME, Smith MJ. Leukotriene B, a potent chemokinetic and aggregating substance released from polymorphonuclear leukocytes. *Nature.* 286, 264–265, 1980.

94. Dahlén SE, Björk J, Hedqvist P, Arfors KE, Hammarström S, Lindgren JA, Samuelsson B. Leukotrienes promote plasma leakage and leukocyte adhesion in postcapillary venules: in vivo effects with relevance to the acute inflammatory response. *roc Natl Acad Sci U S A.* 78(6),3887–3891, 1981.

95. Palmer RM, Stepney RJ, Higgs GA, Eakins KE. Chemokinetic activity of arachidonic and lipoxygenase products on leuocyctes of different species. *Prostaglandins.* 20(2):411-8, 1980.

96. Bray MA, Ford-Hutchinson AW, Smith MJ. Leukotriene B4: an inflammatory mediator in vivo. *Prostaglandins.* 22(2), 213–222, 1981.

97. Hafstrom I, Palmblad J, Malmsten CL, Rådmark O, Samuelsson B. Leukotriene B4–a stereospecific stimulator for release of lysosomal enzymes from neutrophils. *FEBS Lett.* 130(1), 146–148, 1981.

98. Rae SA, Smith MJ. The stimulation of lysosomal enzyme secretion from human polymorphonuclear leucocytes by leukotriene B4. *J Pharm Pharmacol.* 33(9), 616–617, 1981.

99. Yamaoka KA, Claésson HE, Rosén A. Leukotriene B4 enhances activation, proliferation, and differentiation of human B lymphocytes. *J Immunol.* 143(6), 1996–2000, 1989.

100. Yamaoka, K.A., Dugas, B., Paul-Eugene, N., Mencia-Huerta, J.M., Braquet, P. and Kolb, J.P. Leukotriene B4 enhances IL-4-induced IgE production from normal human lymphocytes. *Cell. Immunol.* 1994, pp. 156(1), 124–134.

101. Claesson HE, Odlander B, Jakobsson PJ. Leukotriene B4 in the immune system. *Int J Immunopharmacol.* 14(3),441–449, 1992.

102. Narala VR, Adapala RK, Suresh MV, Brock TG, Peters-Golden M, Reddy RC. Leukotriene B4 is a physiologically relevant endogenous peroxisome proliferator-activated receptor-alpha agonist. *J Biol Chem.* 285(29), 22067–22074, 2010.

103. Yokomizo T, Izumi T, Chang K, Takuwa Y, Shimizu T. A G-protein-coupled receptor for leukotriene B4 that mediates chemotaxis. *Nature.* 1997, pp. 387(6633):620-4.

104. Yokomizo T, Kato K, Terawaki K, Izumi T, Shimizu T. A second leukotriene B(4) receptor, BLT2. A new therapeutic target in inflammation and immunological disorders. *J Exp Med.* 192(3):421-32, 2000.

105. Owman C, Nilsson C, Lolait SJ. Cloning of cDNA encoding a putative chemoattractant receptor. *Genomics.* 37(2), 187–194, 1996.

106. Okuno T, Yokomizo T, Hori T, Miyano M, Shimizu T. Leukotriene B4 receptor and the function of its helix 8. *J Biol Chem.* 280(37), 32049–32052, 2005.

107. Haribabu B, Verghese MW, Steeber DA, Sellars DD, Bock CB, Snyderman R. Targeted disruption of the leukotriene B(4) receptor in mice reveals its role in inflammation and platelet-activating factor-induced anaphylaxis. *J Exp Med.* 192(3), 433–438, 2000.

108. Tager AM, Dufour JH, Goodarzi K, Bercury SD, von Andrian UH, Luster AD. BLTR mediates leukotriene B(4)-induced chemotaxis and adhesion and plays a dominant role in eosinophil accumulation in a murine model of peritonitis. *J Exp Med.* 192(3), 439–446, 2000.

109. Yokomizo, T., Kato, K., Hagiya, H., Izumi, T. and Shimizu, T. Hydroxyeicosanoids bind to and activate the low affinity leukotriene B4 receptor, BLT2. *Biol. Chem.,.* 2001, pp. 276(15), 12454–12459.

110. Okuno T, Iizuka Y, Okazaki H, Yokomizo T, Taguchi R, Shimizu T. 12(S)-Hydroxyheptadeca-5Z, 8E, 10E-trienoic acid is a natural ligand for leukotriene B4 receptor 2. *J Exp Med.* 205(4):759-66, 2008 Apr 14.

111. Dahlén SE, Hedqvist P, Hammarström S, Samuelsson B. Leukotrienes are potent constrictors of human bronchi. *Nature.* 288(5790),484–486, 1980.

112. Hanna CJ, Bach MK, Pare PD, Schellenberg RR. Slow-reacting substances (leukotrienes) contract human airway and pulmonary vascular smooth muscle in vitro. *Nature.* 290(5804), 343–344, 1981.

113. Jones TR, Davis C, Daniel EE. Pharmacological study of the contractile activity of leukotriene C4 and D4 on isolated human airway smooth muscle. *Can. J. Physiol. Pharmacol.* 60(5), 638–643, 1982.

114. Marom Z, Shelhamer JH, Bach MK, Morton DR, Kaliner M. Slow-reacting substances, leukotrienes C4 and D4, increase the release of mucus from human airways in vitro. *Am Rev Respir Dis.* 126(3):449-51, 1982.

115. Peatfield AC, Piper PJ, Richardson PS. The effect of leukotriene C4 on mucin release into the cat trachea in vivo and in vitro. *Br J Pharmacol.* 77(3), 391–393, 1982.

116. Coles SJ, Neill KH, Reid LM, Austen KF, Nii Y, Corey EJ, Lewis RA. Effects of leukotrienes C4 and D4 on glycoprotein and lysozyme secretion by human bronchial mucosa. *Prostaglandins.* 25(2),155–170, 1983.

117. Mehrotra AK, Henderson WR Jr. The role of leukotrienes in airway remodeling. *Curr Mol Med.* 9(3), 383–391, 2009.

118. Lynch KR, O'Neill GP, Liu Q, Im DS, Sawyer N, Metters KM, Coulombe N, Abramovitz M, Figueroa DJ, Zeng Z, Connolly BM, Bai C, Austin CP, Chateauneuf A, Stocco R, Greig GM, Kargman S, Hooks SB, Hosfield E, Williams DL Jr, Ford-Hutchinson AW, Caskey CT, Evan. Characterization of the human cysteinyl leukotriene CysLT1 receptor. *Nature.* 399(6738):789-93, 1999.

119. Heise CE, O'Dowd BF, Figueroa DJ, Sawyer N, Nguyen T, Im DS, Stocco R, Bellefeuille JN, Abramovitz M, Cheng R, Williams DL Jr, Zeng Z, Liu Q, Ma L, Clements MK, Coulombe N, Liu Y, Austin CP, George SR, O'Neill GP, Metters KM, Lynch KR, Evans JF. Characterization of the human cysteinyl leukotriene 2 receptor. *J Biol Chem.* 275(39):30531-6, 2000.

120. Rovati GE, Capra V. Cysteinyl-leukotriene receptors and cellular signals. *ScientificWorldJournal.* 7, 1375–1392, 2007.

121. Sarau HM, Ames RS, Chambers J, Ellis C, Elshourbagy N, Foley JJ, Schmidt DB, Muccitelli RM, Jenkins O, Murdock PR, Herrity NC, Halsey W, Sathe G, Muir AI, Nuthulaganti P, Dytko GM, Buckley PT, Wilson S, Bergsma DJ, Hay DW. Identification, molecular cloning, expression, and characterization of a cysteinyl leukotriene receptor. *Mol Pharmacol.* 56(3), 657–663, 1999.

122. Figueroa DJ, Breyer RM, Defoe SK, Kargman S, Daugherty BL, Waldburger K, Liu Q, Clements M, Zeng Z, O'Neill GP, Jones TR, Lynch KR, Austin CP, Evans JF. Expression of

the cysteinyl leukotriene 1 receptor in normal human lung and peripheral blood leukocytes. *Am J Respir Crit Care Med.* 163(1), 226–233, 2001.

123. Evans, JF. Cysteinyl leukotriene receptors. *Prostaglandins Other Lipid Mediat.* 68-69, 587–597, 2002.

124. Lötzer K, Spanbroek R, Hildner M, Urbach A, Heller R, Bretschneider E, Galczenski H, Evans JF, Habenicht AJ. Differential leukotriene receptor expression and calcium responses in endothelial cells and macrophages indicate 5-lipoxygenase-dependent circuits of inflammation and atherogenesis. *Arterioscler Thromb Vasc Biol.* 23(8),e32–e36, 2003.

125. Sjöström M, Johansson AS, Schröder O, Qiu H, Palmblad J, Haeggström JZ. Dominant expression of the CysLT2 receptor accounts for calcium signaling by cysteinyl leukotrienes in human umbilical vein endothelial cells. *Arterioscler Thromb Vasc Biol.* 23(8), e37–e41, 2003.

126. Kanaoka Y, Boyce JA. Cysteinyl leukotrienes and their receptors: cellular distribution and function in immune and inflammatory responses. *J Immunol.* 173(3), 1503–1510, 2004.

127. Takasaki J, Kamohara M, Matsumoto M, Saito T, Sugimoto T, Ohishi T, Ishii H, Ota T, Nishikawa T, Kawai Y, Masuho Y, Isogai T, Suzuki Y, Sugano S, Furuichi K. The molecular characterization and tissue distribution of the human cysteinyl leukotriene CysLT(2) receptor. *Biochem Biophys Res Commun.* 274(2), 316–322, 2000.

128. Nothacker HP, Wang Z, Zhu Y, Reinscheid RK, Lin SH, Civelli O. Molecular cloning and characterization of a second human cysteinyl leukotriene receptor: discovery of a subtype selective agonist. *Mol. Pharmacol.* 58(6), 1601–1608, 2000.

129. RE, Goldstein. Involvement of leucocytes and leukotrienes in ischaemic dysfunction of the coronary microcirculation. *Eur Heart J.* 11 Suppl B:16-26, 1990 Apr.

130. Powell WS, Rokach J. Biochemistry, biology and chemistry of the 5-lipoxygenase product 5-oxo-ETE. *Prog Lipid Res.* 44(2-3):154-83, 2005 Mar-May.

131. Powell WS, Zhang Y, Gravel S. Effects of phorbol myristate acetate on the synthesis of 5-oxo-6,8,11,14-eicosatetraenoic acid by human polymorphonuclear leukocytes. *Biochemistry.* 5;33(13):3927-33, 1994 Apr.

132. Hosoi T, Koguchi Y, Sugikawa E, Chikada A, Ogawa K, Tsuda N, Suto N, Tsunoda S, Taniguchi T, Ohnuki T. Identification of a novel human eicosanoid receptor coupled to G(i/o). *J Biol Chem.* 277(35), 31459–31465, 2002.

133. Takeda S, Yamamoto A, Haga T. Identification of a G protein-coupled receptor for 5-oxo-eicosatetraenoic acid. *Biomedical Research Tokyo.* 23(2), 101–108, 2002.

134. Jones CE, Holden S, Tenaillon L, Bhatia U, Seuwen K, Tranter P, Turner J, Kettle R, Bouhelal R, Charlton S, Nirmala NR, Jarai G, Finan P. Expression and characterization of a 5-oxo-6E,8Z,11Z,14Zeicosatetraenoic acid receptor highly expressed on human eosinophils and neutrophils. *Mol. Pharmacol.* 63(3), 471–477, 2003.

135. Brink C, Dahlén SE, Drazen J, Evans JF, Hay DW, Rovati GE, Serhan CN, Shimizu T, Yokomizo T. International Union of Pharmacology XLIV. Nomenclature for the oxoeicosanoid receptor. *Pharmacol. Rev.* 56(1), 149–157, 2003.

136. Tateson JE, Randall RW, Reynolds CH, Jackson WP, Bhattacherjee P, Salmon JA, Garland LG. Selective inhibition of arachidonate 5-lipoxygenase by novel acetohydroxamic acids: biochemical assessment in vitro and ex vivo. *Br J Pharmacol.* 94(2), 528–539, 1988.

137. Carter GW, Young PR, Albert DH, Bouska J, Dyer R, Bell RL, Summers JB, Brooks DW. 5-lipoxygenase inhibitory activity of zileuton. *J Pharmacol Exp Ther.* 256(3), 929–937, 1991.

138. McMillan RM, Walker ER. Designing therapeutically effective 5-lipoxygenase inhibitors. *Trends Pharmacol Sci.* 13(8), 323–330, 1992.

139. Kusner EJ, Buckner CK, Dea DM, DeHaas CJ, Marks RL, Krell RD. The 5-lipoxygenase inhibitors ZD2138 and ZM230487 are potent and selective inhibitors of several antigen-induced guinea-pig pulmonary responses. *Eur J Pharmacol.* 257(3), 285–292, 1994.

140. Ford-Hutchinson AW, Gresser M, Young RN. 5-Lipoxygenase. *Annu Rev Biochem.* 63, 383–417, 1994.

141. Werz O, Steinhilber D. Development of 5-lipoxygenase inhibitors–lessons from cellular enzyme regulation. *Biochem Pharmacol.* 70(3), 327–333, 2005.

142. Pergola C, Werz O. 5-Lipoxygenase inhibitors: a review of recent developments and patents. *Expert Opin Ther Pat.* 20(3), 355–375, 2010.

143. Reiss TF, Sorkness CA, Stricker W, Botto A, Busse WW, Kundu S, Zhang J. Effects of montelukast (MK-0476); a potent cysteinyl leukotriene receptor antagonist, on bronchodilation in asthmatic subjects treated with and without inhaled corticosteroids. *Thorax.* 52(1), 45–48, 1997.

144. Dahlén SE, Dahlén B, Eliasson E, Johansson H, Björck T, Kumlin M, Boo K, Whitney J, Binks S, King B, et al. Inhibition of allergic bronchoconstriction in asthmatics by the leukotriene-antagonist ICI-204,219. *Adv .Prostaglandin Thromboxane Leukot. Res.* 21A, 461–464, 1991.

145. Kelloway, JS. Zafirlukast: the first leukotriene-receptor antagonist approved for the treatment of asthma. *Ann Pharmacother.* 31(9):1012-21, 1997 Sep.

146. Taki F, Suzuki R, Torii K, Matsumoto S, Taniguchi H, Takagi K. Reduction of the severity of bronchial hyperresponsiveness by the novel leukotriene antagonist 4-oxo-8-[4-(4-phenyl-butoxy)benzoylamino]-2-(tetrazol-5-yl)-4H-1-benzopyran hemihydrate. *Arzneimittelforschung.* 44(3),330–333, 1994.

147. Barnes NC, Pujet JC. Pranlukast, a novel leukotriene receptor antagonist: results of the first European, placebo controlled, multicentre clinical study in asthma. *Thorax.* 52(6):523-7, 1997 Jun.

148. Koeberle A, Siemoneit U, Northoff H, Hofmann B, Schneider G, Werz O. MK-886, an inhibitor of the 5-lipoxygenase-activating protein, inhibits cyclooxygenase-1 activity and suppresses platelet aggregation. *Eur J Pharmacol.* 608(1-3):84-90, 2009 Apr 17.

149. Depré M, Friedman B, Van Hecken A, de Lepeleire I, Tanaka W, Dallob A, Shingo S, Porras A, Lin C, de Schepper PJ. Pharmacokinetics and pharmacodynamics of multiple oral doses of MK-0591, a 5-lipoxygenase-activating protein inhibitor. *Clin. Pharmacol. Ther.* 56(1),22–30, 1994.

150. Fruchtmann R, Mohrs KH, Hatzelmann A, Raddatz S, Fugmann B, Junge B, Horstmann H, Müller-Peddinghaus R. In vitro pharmacology of BAY X1005, a new inhibitor of leukotriene synthesis. *Agents Actions.* 38(3-4), 188–195, 1993.

151. Cooper, GM. The Development and Causes of Cancer. *The Cell: A Molecular Approach. 2nd edition.* s.l. : Sunderland (MA): Sinauer Associates, 2000.

152. www.cancer.gov. [Online] NIH National cancer Institute, 5 May 2021. [Cited: 20 June 2022.] https://www.cancer.gov/about-cancer/understanding/what-is-cancer.

153. Metayer C, Dahl G, Wiemels J, Miller M. Childhood Leukemia: A Preventable Disease. *Pediatrics.* 138(Suppl 1):S45-S55, 2016.

154. Krebsregisterdaten, ZfKD - Zentrum für. https://www.rki.de/DE/Content/Gesundheitsmonitoring/Krebsregisterdaten/krebs_node.html. [Online] Robert-Koch-Institut, 2021. [Cited: 22 06 2022.]

155. Sung H, Ferlay J, Siegel RL, Laversanne M, Soerjomataram I, Jemal A, Bray F. Global Cancer Statistics 2020: GLOBOCAN Estimates of Incidence and Mortality Worldwide for 36 Cancers in 185 Countries. *CA Cancer J Clin.* 71(3):209-249, 2021 May.

156. Hanahan D, Weinberg RA. The hallmarks of cancer. *Cell.* 100(1):57-70, 2000 Jan 7.

157. Weinberg, RA. How cancer arises. *Sci Am.* 275(3):62-70, 1996 Sep.

158. Negrini S, Gorgoulis VG, Halazonetis TD. Genomic instability--an evolving hallmark of cancer. *Nat Rev Mol Cell Biol.* 11(3):220-8, 2010 Mar.

159. Aaronson, SA. Growth factors and cancer. *Science.* 254(5035):1146-53, 1991 Nov 22.

160. Nazarenko I, Hede SM, He X, Hedrén A, Thompson J, Lindström MS, Nistér M. PDGF and PDGF receptors in glioma. *Ups J Med Sci.* 117(2):99-112, 2012 May.

161. Tang P, Steck PA, Yung WK. The autocrine loop of TGF-alpha/EGFR and brain tumors. *J Neurooncol.* 35(3):303-14, 1997 Dec.

162. Schrevel M, Gorter A, Kolkman-Uljee SM, Trimbos JB, Fleuren GJ, Jordanova ES. Molecular mechanisms of epidermal growth factor receptor overexpression in patients with cervical cancer. *Mod Pathol.* 24(5):720-8, 2011 May.

163. Kersemaekers AM, Fleuren GJ, Kenter GG, Van den Broek LJ, Uljee SM, Hermans J, Van de Vijver MJ. Oncogene alterations in carcinomas of the uterine cervix: overexpression of the epidermal growth factor receptor is associated with poor prognosis. *Clin Cancer Res.* 5(3):577-86, 1999 Mar.

164. Zyzak LL, MacDonald LM, Batova A, Forand R, Creek KE, Pirisi L. Increased levels and constitutive tyrosine phosphorylation of the epidermal growth factor receptor contribute to autonomous growth of human papillomavirus type 16 immortalized human keratinocytes. *Cell Growth Differ.* 5(5):537-47, 1994 May.

165. Yun S, Kwak Y, Nam SK, Seo AN, Oh HK, Kim DW, Kang SB, Lee HS. Ligand-Independent Epidermal Growth Factor Receptor Overexpression Correlates with Poor Prognosis in Colorectal Cancer. *Cancer Res Treat.* 50(4):1351-1361, 2018 Oct.

166. Bianconi D, Unseld M, Prager GW. Integrins in the Spotlight of Cancer. *Int J Mol Sci.* 17(12):2037, 2016 Dec 6.

167. Hamidi H, Ivaska J. Every step of the way: integrins in cancer progression and metastasis. *Nat Rev Cancer.* 18(9):533-548, 2018 Sep.

168. Łasiñska I, Mackiewicz J. Integrins as A New Target for Cancer Treatment. *Anticancer Agents Med Chem.* 19(5):580-586, 2019.

169. Gilmore AP, Metcalfe AD, Romer LH, Streuli CH. Integrin-mediated survival signals regulate the apoptotic function of Bax through its conformation and subcellular localization. *J Cell Biol.* 149(2):431-46, 2000 Apr 17.

170. Aoudjit F, Vuori K. Integrin signaling inhibits paclitaxel-induced apoptosis in breast cancer cells. *Oncogene.* 20(36):4995-5004, 2001 Aug 16.

171. Yousefi H, Vatanmakanian M, Mahdiannasser M, Mashouri L, Alahari NV, Monjezi MR, Ilbeigi S, Alahari SK. Understanding the role of integrins in breast cancer invasion, metastasis, angiogenesis, and drug resistance. *Oncogene.* 40(6):1043-1063, 2021 Feb.

172. Avraamides CJ, Garmy-Susini B, Varner JA. Integrins in angiogenesis and lymphangiogenesis. *Nat Rev Cancer.* 8(8):604-17, 2008 Aug.

173. De Luca A, Maiello MR, D'Alessio A, Pergameno M, Normanno N. The RAS/RAF/MEK/ERK and the PI3K/AKT signalling pathways: role in cancer pathogenesis and implications for therapeutic approaches. *Expert Opin Ther Targets.* 16 Suppl 2:S17-27, 2012 Apr.

174. Wan PT, Garnett MJ, Roe SM, Lee S, Niculescu-Duvaz D, Good VM, Jones CM, Marshall CJ, Springer CJ, Barford D, Marais R. Cancer Genome Project. Mechanism of activation of the RAF-ERK signaling pathway by oncogenic mutations of B-RAF. *Cell.* 116(6):855-67, 2004.

175. Dankner M, Rose AAN, Rajkumar S, Siegel PM, Watson IR. Classifying BRAF alterations in cancer: new rational therapeutic strategies for actionable mutations. *Oncogene.* 37(24):3183-3199, 2018 Jun.

176. McCubrey JA, Steelman LS, Chappell WH, Abrams SL, Montalto G, Cervello M, Nicoletti F, Fagone P, Malaponte G, Mazzarino MC, Candido S, Libra M, Bäsecke J, Mijatovic S, Maksimovic-Ivanic D, Milella M, Tafuri A, Cocco L, Evangelisti C, Chiarini F, Martelli. Mutations and deregulation of Ras/Raf/MEK/ERK and PI3K/PTEN/Akt/mTOR cascades which alter therapy response. *Oncotarget.* 3(9):954-87, 2012 Sep.

177. Marescal O, Cheeseman IM. Cellular Mechanisms and Regulation of Quiescence. *Dev Cell.* 55(3):259-271, 2020 Nov 9.

178. Coller HA, Sang L, Roberts JM. A new description of cellular quiescence. *PLoS Biol.* 4(3):e83, 2006 Mar.

179. Stengel KR, Thangavel C, Solomon DA, Angus SP, Zheng Y, Knudsen ES. Retinoblastoma/p107/p130 pocket proteins: protein dynamics and interactions with target gene promoters. *J Biol Chem.* 284(29):19265-71, 2009 Jul 17.

180. Mandigo AC, Tomlins SA, Kelly WK, Knudsen KE. Relevance of pRB Loss in Human Malignancies. *Clin Cancer Res.* 28(2):255-264, 2022 Jan 15.

181. Hu X, Cress WD, Zhong Q, Zuckerman KS. Transforming growth factor beta inhibits the phosphorylation of pRB at multiple serine/threonine sites and differentially regulates the formation of pRB family-E2F complexes in human myeloid leukemia cells. *Biochem Biophys Res Commun.* 276(3):930-9, 2000 Oct 5.

182. Robson CN, Gnanapragasam V, Byrne RL, Collins AT, Neal DE. Transforming growth factor-beta1 up-regulates p15, p21 and p27 and blocks cell cycling in G1 in human prostate epithelium. *J Endocrinol.* 160(2):257-66, 1999 Feb.

183. Vander Ark A, Cao J, Li X. TGF-β receptors: In and beyond TGF-β signaling. *Cell Signal.* 52:112-120, 2018 Dec.

184. Matsushita M, Matsuzaki K, Date M, Watanabe T, Shibano K, Nakagawa T, Yanagitani S, Amoh Y, Takemoto H, Ogata N, Yamamoto C, Kubota Y, Seki T, Inokuchi H, Nishizawa M, Takada H, Sawamura T, Okamura A, Inoue K. Down-regulation of TGF-beta receptors in human colorectal cancer: implications for cancer development. *Br J Cancer.* 80(1-2):194-205, 1999 Apr.

185. Jonson T, Albrechtsson E, Axelson J, Heidenblad M, Gorunova L, Johansson B, Höglund M. Altered expression of TGFB receptors and mitogenic effects of TGFB in pancreatic carcinomas. *Int J Oncol.* 19(1):71-81, 2001 Jul.

186. Venkatasubbarao K, Ahmed MM, Mohiuddin M, Swiderski C, Lee E, Gower WR Jr, Salhab KF, McGrath P, Strodel W, Freeman JW. Differential expression of transforming growth factor beta receptors in human pancreatic adenocarcinoma. *Anticancer Res.* 20(1A):43-51, 2000 Jan-Feb.

187. Zhao M, Mishra L, Deng CX. The role of TGF-β/SMAD4 signaling in cancer. *Int J Biol Sci.* 14(2):111-123, 2018 Jan 12.

188. Matsumura Y, Nishigori C, Yagi T, Imamura S, Takebe H. Mutations of p16 and p15 tumor suppressor genes and replication errors contribute independently to the pathogenesis of sporadic malignant melanoma. *Arch Dermatol Res.* 290(4):175-80, 1998 Apr.

189. Robinson WA, Elefanty AG, Hersey P. Expression of the tumour suppressor genes p15 and p16 in malignant melanoma. *Melanoma Res.* 6(4):285-9, 1996 Aug.

190. Giacinti C, Giordano A. RB and cell cycle progression. *Oncogene.* 25(38):5220-7, 2006 Aug 28.

191. Buttitta LA, Edgar BA. Mechanisms controlling cell cycle exit upon terminal differentiation. *Curr Opin Cell Biol.* 19(6):697-704, 2007 Dec.

192. Hoffman B, Amanullah A, Shafarenko M, Liebermann DA. The proto-oncogene c-myc in hematopoietic development and leukemogenesis. *Oncogene.* 21(21):3414-21, 2002 May 13.

193. Grandori C, Cowley SM, James LP, Eisenman RN. The Myc/Max/Mad network and the transcriptional control of cell behavior. *Annu Rev Cell Dev Biol.* 16:653-99, 2000.

194. Wang YH, Liu S, Zhang G, Zhou CQ, Zhu HX, Zhou XB, Quan LP, Bai JF, Xu NZ. Knockdown of c-Myc expression by RNAi inhibits MCF-7 breast tumor cells growth in vitro and in vivo. *Breast Cancer Res.* 7(2):R220-8, 2005.

195. Tashiro H, Miyazaki K, Okamura H, Iwai A, Fukumoto M. c-myc over-expression in human primary ovarian tumours: its relevance to tumour progression. *Int J Cancer.* 50(5):828-33, 1992 Mar 12.

196. Christoph F, Schmidt B, Schmitz-Dräger BJ, Schulz WA. Over-expression and amplification of the c-myc gene in human urothelial carcinoma. *Int J Cancer.* 84(2):169-73, 1999 Apr 20.

197. Kuzyk A, Mai S. c-MYC-induced genomic instability. *Cold Spring Harb Perspect Med.* 4(4):a014373, 2014 Apr 1.

198. Taylor RC, Cullen SP, Martin SJ. Apoptosis: controlled demolition at the cellular level. *Nat Rev Mol Cell Biol.* 9(3):231-41, 2008 Mar.

199. Waring P, Müllbacher A. Cell death induced by the Fas/Fas ligand pathway and its role in pathology. *Immunol Cell Biol.* 77(4):312-7, 1999 Aug.

200. Rath PC, Aggarwal BB. TNF-induced signaling in apoptosis. *J Clin Immunol.* 19(6):350-64, 1999 Nov.

201. Almasan A, Ashkenazi A. Apo2L/TRAIL: apoptosis signaling, biology, and potential for cancer therapy. *Cytokine Growth Factor Rev.* 14(3-4):337-48, 2003 Jun-Aug.

202. Marsters SA, Sheridan JP, Pitti RM, Brush J, Goddard A, Ashkenazi A. Identification of a ligand for the death-domain-containing receptor Apo3. *Curr Biol.* 8(9):525-8, 1998 Apr 23.

203. Füllsack S, Rosenthal A, Wajant H, Siegmund D. Redundant and receptor-specific activities of TRADD, RIPK1 and FADD in death receptor signaling. *Cell Death Dis.* 10(2):122, 2019 Feb 11.

204. Balkwill, F. Tumour necrosis factor and cancer. *Nat Rev Cancer.* 9(5):361-71, 2009 May.

205. Marín-Rubio JL, Vela-Martín L, Fernández-Piqueras J, Villa-Morales M. FADD in Cancer: Mechanisms of Altered Expression and Function, and Clinical Implications. *Cancers (Basel).* 11(10):1462, 2019 Sep 29.

206. Cao X, Wen P, Fu Y, Gao Y, Qi X, Chen B, Tao Y, Wu L, Xu A, Lu H, Zhao G. Radiation induces apoptosis primarily through the intrinsic pathway in mammalian cells. *Cell Signal.* 62:109337, 2019 Oct.

207. Wu CC, Bratton SB. Regulation of the intrinsic apoptosis pathway by reactive oxygen species. *Antioxid Redox Signal.* 19(6):546-58, 2013 Aug 20.

208. Tesh, VL. The induction of apoptosis by Shiga toxins and ricin. *Curr Top Microbiol Immunol.* 357:137-78, 2012.

209. Wu L, Chen Y, Chen Y, Yang W, Han Y, Lu L, Yang K, Cao J. Effect of HIF-1α/miR-10b-5p/PTEN on Hypoxia-Induced Cardiomyocyte Apoptosis. *J Am Heart Assoc.* 8(18):e011948, 2019 Sep 17.

210. Goyeneche AA, Harmon JM, Telleria CM. Cell death induced by serum deprivation in luteal cells involves the intrinsic pathway of apoptosis. *Reproduction.* 131(1):103-11, 2006 Jan.

211. Ananiev J, Tchernev G, Patterson JW, Gulubova M, Ganchev G. p53 - "The Guardian of Genome,". *Acta Medica Bulg.* 38;72–82, 2011.

212. Duffy MJ, Synnott NC, Crown J. Mutant p53 as a target for cancer treatment. *Eur J Cancer.* 83:258-265, 2017 Sep.

213. Trapani JA, Smyth MJ. Functional significance of the perforin/granzyme cell death pathway. *Nat Rev Immunol.* 2(10):735-47, 2002 Oct.

214. Díaz-Basabe A, Burrello C, Lattanzi G, Botti F, Carrara A, Cassinotti E, Caprioli F, Facciotti F. Human intestinal and circulating invariant natural killer T cells are cytotoxic against colorectal cancer cells via the perforin-granzyme pathway. *Mol Oncol.* 15(12):3385-3403, 2021 Dec.

215. Hodge G, Barnawi J, Jurisevic C, Moffat D, Holmes M, Reynolds PN, Jersmann H, Hodge S. Lung cancer is associated with decreased expression of perforin, granzyme B and interferon (IFN)-γ by infiltrating lung tissue T cells, natural killer (NK) T-like and NK cells. *Clin Exp Immunol.* 178(1):79-85, 2014 Oct.

216. Shay JW, Wright WE. Hayflick, his limit, and cellular ageing. *Nat Rev Mol Cell Biol.* 1(1):72-6, 2000 Oct.

217. Saretzki, G. Telomeres, Telomerase and Ageing. *Subcell Biochem.* 90:221-308, 2018.

218. Shay JW, Bacchetti S. A survey of telomerase activity in human cancer. *Eur J Cancer.* 33(5):787-91, 1997 Apr.

219. Wang S, Zhao Y, Hu C, Zhu J. Differential repression of human and mouse TERT genes during cell differentiation. *Nucleic Acids Res.* 37(8):2618-29, 2009 May.

220. Yuan X, Larsson C, Xu D. Mechanisms underlying the activation of TERT transcription and telomerase activity in human cancer: old actors and new players. *Oncogene.* 38(34):6172-6183, 2019 Aug.

221. Alberts B, Johnson A, Lewis J, et al. Blood Vessels and Endothelial Cells. [book auth.] New York: Garland Science. *Molecular Biology of the Cell. 4th edition.* 2002.

222. Kieran MW, Kalluri R, Cho YJ. The VEGF pathway in cancer and disease: responses, resistance, and the path forward. *Cold Spring Harb Perspect Med.* 2(12):a006593, 2012 Dec 1.

223. Iruela-Arispe ML, Lombardo M, Krutzsch HC, Lawler J, Roberts DD. Inhibition of angiogenesis by thrombospondin-1 is mediated by 2 independent regions within the type 1 repeats. *Circulation.* 100(13):1423-31, 1999 Sep 28.

224. Jiménez B, Volpert OV, Crawford SE, Febbraio M, Silverstein RL, Bouck N. Signals leading to apoptosis-dependent inhibition of neovascularization by thrombospondin-1. *Nat Med.* 6(1):41-8, 2000 Jan.

225. Kazerounian S, Lawler J. Integration of pro- and anti-angiogenic signals by endothelial cells. *J Cell Commun Signal.* 12(1):171-179, 2018 Mar.

226. Hicklin DJ, Ellis LM. Role of the vascular endothelial growth factor pathway in tumor growth and angiogenesis. *J Clin Oncol.* 23(5):1011-27, 2005 Feb 10.

227. Costache MI, Ioana M, Iordache S, Ene D, Costache CA, Săftoiu A. VEGF Expression in Pancreatic Cancer and Other Malignancies: A Review of the Literature. *Rom J Intern Med.* 53(3):199-208, 2015 Jul-Sep.

228. Dore-Savard L, Lee E, Kakkad S, Popel AS, Bhujwalla ZM. The Angiogenic Secretome in VEGF overexpressing Breast Cancer Xenografts. *Sci Rep.* 6:39460, 2016 Dec 20.

229. Choi SB, Han HJ, Kim WB, Song TJ, Choi SY. VEGF Overexpression Predicts Poor Survival in Hepatocellular Carcinoma. *Open Med (Wars).* 12:430-439, 2017 Dec 9.

230. Masoud GN, Li W. HIF-1α pathway: role, regulation and intervention for cancer therapy. *Acta Pharm Sin B.* 5(5):378-89, 2015 Sep.

231. Bianco R, Rosa R, Damiano V, Daniele G, Gelardi T, Garofalo S, Tarallo V, De Falco S, Melisi D, Benelli R, Albini A, Ryan A, Ciardiello F, Tortora G. Vascular endothelial growth factor receptor-1 contributes to resistance to anti-epidermal growth factor receptor drugs in human cancer cells. *Clin Cancer Res.* 14(16):5069-80, 2008 Aug 15.

232. Tsourlakis MC, Khosrawi P, Weigand P, Kluth M, Hube-Magg C, Minner S, Koop C, Graefen M, Heinzer H, Wittmer C, Sauter G, Krech T, Wilczak W, Huland H, Simon R, Schlomm T, Steurer S. VEGFR-1 overexpression identifies a small subgroup of aggressive prostate cancers in patients treated by prostatectomy. *Int J Mol Sci.* 16(4):8591-606, 2015 Apr 16.

233. Ceci C, Atzori MG, Lacal PM, Graziani G. Role of VEGFs/VEGFR-1 Signaling and its Inhibition in Modulating Tumor Invasion: Experimental Evidence in Different Metastatic Cancer Models. *Int J Mol Sci.* 21(4):1388, 2020 Feb 18.

234. Kaur S, Bronson SM, Pal-Nath D, Miller TW, Soto-Pantoja DR, Roberts DD. Functions of Thrombospondin-1 in the Tumor Microenvironment. *Int J Mol Sci.* 22(9):4570, 2021 Apr 27.

235. Wang P, Zeng Z, Lin C, Wang J, Xu W, Ma W, Xiang Q, Liu H, Liu SL. Thrombospondin-1 as a Potential Therapeutic Target: Multiple Roles in Cancers. *Curr Pharm Des.* 26(18):2116-2136, 2020.

236. Koten JW, Neijt JP, Zonnenberg BA, Den Otter W. The difference between benign and malignant tumours explained with the 4-mutation paradigm for carcinogenesis. *Anticancer Res.* 13(4):1179-82, 1993 Jul-Aug.

237. Dillekås H, Rogers MS, Straume O. Are 90% of deaths from cancer caused by metastases? *Cancer Med.* 8(12):5574-5576, 2019 Sep.

238. Mittal, V. Epithelial Mesenchymal Transition in Tumor Metastasis. *Annu Rev Pathol.* 13:395-412, 2018 Jan 24.

239. Albelda SM, Buck CA. Integrins and other cell adhesion molecules. *FASEB J.* 4(11):2868-80, 1990 Aug.

240. Na TY, Schecterson L, Mendonsa AM, Gumbiner BM. The functional activity of E-cadherin controls tumor cell metastasis at multiple steps. *Proc Natl Acad Sci U S A.* 117(11):5931-5937, 2020 Mar 17.

241. Loh CY, Chai JY, Tang TF, Wong WF, Sethi G, Shanmugam MK, Chong PP, Looi CY. The E-Cadherin and N-Cadherin Switch in Epithelial-to-Mesenchymal Transition: Signaling, Therapeutic Implications, and Challenges. *Cells.* 8(10):1118, 2019 Sep 20.

242. Paolillo M, Schinelli S. Extracellular Matrix Alterations in Metastatic Processes. *Int J Mol Sci.* 20(19):4947, 2019 Oct 7.

243. Duffy, MJ. The role of proteolytic enzymes in cancer invasion and metastasis. *Clin Exp Metastasis.* 10(3):145-55, 1992 May.

244. Werb, Z. ECM and cell surface proteolysis: regulating cellular ecology. *Cell.* 91(4):439-42, 1997 Nov 14.

245. Johnsen M, Lund LR, Rømer J, Almholt K, Danø K. Cancer invasion and tissue remodeling: common themes in proteolytic matrix degradation. *Curr Opin Cell Biol.* 10(5):667-71, 1998 Oct.

246. Hanahan D, Weinberg RA. Hallmarks of cancer: the next generation. *Cell.* 144(5):646-74., 2011 Mar 4.

247. SY, Kim. Cancer Energy Metabolism: Shutting Power off Cancer Factory. *Biomol Ther (Seoul).* 26(1):39-44, 2018 Jan 1.

248. Zambrano A, Molt M, Uribe E, Salas M. Glut 1 in Cancer Cells and the Inhibitory Action of Resveratrol as A Potential Therapeutic Strategy. *Int J Mol Sci.* 20(13):3374, 2019 Jul 9. 10.3390/ijms20133374.

249. Lunt SY, Vander Heiden MG. Aerobic glycolysis: meeting the metabolic requirements of cell proliferation. *Annu Rev Cell Dev Biol.* 27:441-64, 2011. 10.1146/annurev-cellbio-092910-15423.

250. O, Feron. Pyruvate into lactate and back: from the Warburg effect to symbiotic energy fuel exchange in cancer cells. *Radiother Oncol.* 92(3):329-33, 2009 Sep.

251. Dagogo-Jack I, Shaw A. Tumour heterogeneity and resistance to cancer therapies. *Nat Rev Clin Oncol.* 15, 81–94, 2018.

252. Reitman ZJ, Yan H. Isocitrate dehydrogenase 1 and 2 mutations in cancer: alterations at a crossroads of cellular metabolism. *J Natl Cancer Inst.* 102(13):932-4, 2010 Jul 7.

253. Murata and M. Inflammation and cancer. *Environ Health Prev Med.* 20;23(1):50, 2018 Oct.

254. Loose D, Van de Wiele C. The immune system and cancer. *Cancer Biother Radiopharm.* 24(3):369-76, 2009 Jun.

255. Wieczorek M, Abualrous ET, Sticht J, Álvaro-Benito M, Stolzenberg S, Noé F, Freund C. Major Histocompatibility Complex (MHC) Class I and MHC Class II Proteins: Conformational Plasticity in Antigen Presentation. *Front Immunol.* 8:292, 2017 Mar 17. 10.3389/fimmu.2017.00292 .

256. Beatty GL, Gladney WL. Immune escape mechanisms as a guide for cancer immunotherapy. *Clin Cancer Res.* 21(4):687-92, 2015 Feb 15. 10.1158/1078-0432.CCR-14-1860.

257. Munari E, Mariotti FR, Quatrini L, Bertoglio P, Tumino N, Vacca P, Eccher A, Ciompi F, Brunelli M, Martignoni G, Bogina G, Moretta L. PD-1/PD-L1 in Cancer: Pathophysiological, Diagnostic and Therapeutic Aspects. *Int J Mol Sci.* 22(10):5123, 2021 May 12. 10.3390/ijms22105123.

258. Mocellin S, Marincola FM, Young HA. Interleukin-10 and the immune response against cancer: a counterpoint. *J Leukoc Biol.* 78(5):1043-51, 2005 Nov. 10.1189/jlb.0705358.

259. Ghahremanifard P, Chanda A, Bonni S, Bose P. TGF-β Mediated Immune Evasion in Cancer-Spotlight on Cancer-Associated Fibroblasts. *Cancers (Basel).* 12(12):3650, 2020 Dec 5. 10.3390/cancers12123650.

260. Rutkowski MR, Stephen TL, Conejo-Garcia JR. Anti-tumor immunity: myeloid leukocytes control the immune landscape. *Cell Immunol.* 278(1-2):21-6, 2012 Jul-Aug. 10.1016/j.cellimm.2012.06.014.

261. Fürstenberger G, Krieg P, Müller-Decker K, Habenicht AJ. What are cyclooxygenases and lipoxygenases doing in the driver's seat of carcinogenesis? *Int J Cancer.* 119(10):2247-54, 2006.

262. Roos J, Oancea C, Heinssmann M, Khan D, Held H, Kahnt AS, Capelo R, la Buscató E, Proschak E, Puccetti E, Steinhilber D, Fleming I, Maier TJ, Ruthardt M. 5-Lipoxygenase is a candidate target for therapeutic management of stem cell-like cells in acute myeloid leukemia. *Cancer Res.* 74(18):5244-55, 2014 Sep 15.

263. Ma D, Liu P, Wang P, Zhou Z, Fang Q, Wang J. PKC-β/Alox5 axis activation promotes Bcr-Abl-independent TKI-resistance in chronic myeloid leukemia. *J Cell Physiol.* 236(9):6312-6327, 2021 Sep.

264. Chen X, Sood S, Yang CS, Li N, Sun Z. Five-lipoxygenase pathway of arachidonic acid metabolism in carcino-genesis and cancer chemoprevention. *Curr Cancer Drug Targets.* 6(7):613-22, 2006 Nov.

265. Boado RJ, Pardridge WM, Vinters HV, Black KL. Differential expression of arachidonate 5-lipoxygenase transcripts in human brain tumors: evidence for the expression of a multitranscript family. *Proc Natl Acad Sci U S A.* 1992 Oct 1;, pp. 89(19):9044-8.

266. Hong SH, Avis I, Vos MD, Martínez A, Treston AM, Mulshine JL. Relationship of arachidonic acid metabolizing enzyme expression in epithelial cancer cell lines to the growth effect of selective biochemical inhibitors. *Cancer Res.* 59(9):2223-8, 1999 May 1.

267. Avis I, Hong SH, Martinez A, Moody T, Choi YH, Trepel J, Das R, Jett M, Mulshine JL. Five-lipoxygenase inhibitors can mediate apoptosis in human breast cancer cell lines through complex eicosanoid interactions. *FASEB J.* 2001 Sep;, pp. 15(11):2007-9. .

268. Hennig R, Ding XZ, Adrian TE. On the role of the islets of Langerhans in pancreatic cancer. *Histol Histopathol.* 19(3):999-1011, 2004 Jul.

269. Romano M, Catalano A, Nutini M, D'Urbano E, Crescenzi C, Claria J, Libner R, Davi G, Procopio A. 5-lipoxygenase regulates malignant mesothelial cell survival: involvement of vascular endothelial growth factor. *FASEB J.* 15(13):2326-36, 2001.

270. Jiang WG, Douglas-Jones AG, Mansel RE. Aberrant expression of 5-lipoxygenase-activating protein (5-LOXAP) has prognostic and survival significance in patients with breast cancer. *Prostaglandins Leukot Essent Fatty Acids.* 74(2):125-34, 2006.

271. Ohd JF, Nielsen CK, Campbell J, Landberg G, Löfberg H, Sjölander A. Expression of the leukotriene D4 receptor CysLT1, COX-2, and other cell survival factors in colorectal adenocarcinomas. *Gastroenterology.* 124(1):57-70, 2003.

272. Sun Z, Sood S, Li N, Ramji D, Yang P, Newman RA, Yang CS, Chen X. Involvement of the 5-lipoxygenase/leukotriene A4 hydrolase pathway in 7,12-dimethylbenz[a]anthracene (DMBA)-induced oral carcinogenesis in hamster cheek pouch, and inhibition of carcinogenesis by its inhibitors. *Carcinogenesis.* 27(9):1902-8, 2006.

273. Runarsson G, Feltenmark S, Forsell PK, Sjöberg J, Björkholm M, Claesson HE. The expression of cytosolic phospholipase A2 and biosynthesis of leukotriene B4 in acute myeloid leukemia cells. *Eur J Haematol.* 79(6):468-76, 2007.

274. Sjölinder M, Stenke L, Näsman-Glaser B, Widell S, Doucet J, Jakobsson PJ, Lindgren JA. Aberrant expression of active leukotriene C(4) synthase in CD16(+) neutrophils from patients with chronic myeloid leukemia. *Blood.* 15;95(4):1456-64, 2000.

275. Sveinbjörnsson B, Rasmuson A, Baryawno N, Wan M, Pettersen I, Ponthan F, Orrego A, Haeggström JZ, Johnsen JI, Kogner P. Expression of enzymes and receptors of the leukotriene pathway in human neuroblastoma promotes tumor survival and provides a target for therapy. *FASEB J.* 22(10):3525-36, 2008 Oct.

276. Ding XZ, Tong WG, Adrian TE. Multiple signal pathways are involved in the mitogenic effect of 5(S)-HETE in human pancreatic cancer. *Oncology.* 65(4):285-94, 2003.

277. Tong WG, Ding XZ, Talamonti MS, Bell RH, Adrian TE. LTB4 stimulates growth of human pancreatic cancer cells via MAPK and PI-3 kinase pathways. *Biochem Biophys Res Commun.* 30;335(3):949-56, 2005.

278. Mezhybovska M, Wikström K, Ohd JF, Sjölander A. The inflammatory mediator leukotriene D4 induces beta-catenin signaling and its association with antiapoptotic Bcl-2 in intestinal epithelial cells. *J Biol Chem.* 281(10):6776-84, 2006.

279. Paruchuri S, Broom O, Dib K, Sjölander A. The pro-inflammatory mediator leukotriene D4 induces phosphatidylinositol 3-kinase and Rac-dependent migration of intestinal epithelial cells. *J Biol Chem.* 280(14):13538-44, 2005.

280. Qiao L, Kozoni V, Tsioulias GJ, Koutsos MI, Hanif R, Shiff SJ, Rigas B. Selected eicosanoids increase the proliferation rate of human colon carcinoma cell lines and mouse colonocytes in vivo. *Biochim Biophys Acta.* 1258(2):215-23, 1995.

281. Bortuzzo C, Hanif R, Kashfi K, Staiano-Coico L, Shiff SJ, Rigas B. The effect of leukotrienes B and selected HETEs on the proliferation of colon cancer cells. *Biochim Biophys Acta.* 1300(3):240-6, 1996.

282. Kim EY, Seo JM, Cho KJ, Kim JH. Ras-induced invasion and metastasis are regulated by a leukotriene B4 receptor BLT2-linked pathway. *Oncogene.* 29(8):1167-78, 2010 Feb 25.

283. Tong WG, Ding XZ, Witt RC, Adrian TE. Lipoxygenase inhibitors attenuate growth of human pancreatic cancer xenografts and induce apoptosis through the mitochondrial pathway. *Mol Cancer Ther.* 1(11):929-35, 2002.

284. Tsukada T, Nakashima K, Shirakawa S. Arachidonate 5-lipoxygenase inhibitors show potent antiproliferative effects on human leukemia cell lines. *Biochem Biophys Res Commun.* 140(3):832-6, 1986.

285. Shimakura S, Boland CR. Eicosanoid production by the human gastric cancer cell line AGS and its relation to cell growth. *Cancer Res.* 52(7):1744-9, 1992.

286. Ghosh J, Myers CE. Inhibition of arachidonate 5-lipoxygenase triggers massive apoptosis in human prostate cancer cells. *Proc Natl Acad Sci USA.* 95(22):13182-7, 1998.

287. Bishayee K, Khuda-Bukhsh AR. 5-lipoxygenase antagonist therapy: a new approach towards targeted cancer chemotherapy. *Acta Biochim Biophys Sin (Shanghai).* 45(9):709-19, 2013 Sep.

288. Hoque A, Lippman SM, Wu TT, Xu Y, Liang ZD, Swisher S, Zhang H, Cao L, Ajani JA, Xu XC. Increased 5-lipoxygenase expression and induction of apoptosis by its inhibitors in esophageal cancer: a potential target for prevention. *Carcinogenesis.* 26(4):785-91, 2005 Apr.

289. Hayashi T, Nishiyama K, Shirahama T. Inhibition of 5-lipoxygenase pathway suppresses the growth of bladder cancer cells. *Int J Urol.* 13(8):1086-91, 2006 Aug.

290. Schuller HM, Zhang L, Weddle DL, Castonguay A, Walker K, Miller MS. The cyclooxygenase inhibitor ibuprofen and the FLAP inhibitor MK886 inhibit pancreatic carcinogenesis induced in hamsters by transplacental exposure to ethanol and the tobacco carcinogen NNK. *J Cancer Res Clin Oncol.* 128(10):525-32, 2002.

291. Gugliucci A, Ranzato L, Scorrano L, Colonna R, Petronilli V, Cusan C, Prato M, Mancini M, Pagano F, Bernardi P. Mitochondria are direct targets of the lipoxygenase inhibitor MK886. A strategy for cell killing by combined treatment with MK886 and cyclooxygenase inhibitors. *J Biol Chem.* 277(35):31789-95, 2002.

292. Fan XM, Tu SP, Lam SK, Wang WP, Wu J, Wong WM, Yuen MF, Lin MC, Kung HF, Wong BC. Five-lipoxygenase-activating protein inhibitor MK-886 induces apoptosis in

gastric cancer through upregulation of p27kip1 and bax. *J Gastroenterol Hepatol.* 19(1):31-7, 2004 Jan.

293. Titos E, Clària J, Planagumà A, López-Parra M, Villamor N, Párrizas M, Carrió A, Miquel R, Jiménez W, Arroyo V, Rivera F, Rodés J. Inhibition of 5-lipoxygenase induces cell growth arrest and apoptosis in rat Kupffer cells: implications for liver fibrosis. *FASEB J.* 17(12):1745-7, 2003 Sep.

294. Melstrom LG, Bentrem DJ, Salabat MR, Kennedy TJ, Ding XZ, Strouch M, Rao SM, Witt RC, Ternent CA, Talamonti MS, Bell RH, Adrian TA. Overexpression of 5-lipoxygenase in colon polyps and cancer and the effect of 5-LOX inhibitors in vitro and in a murine model. *Clin Cancer Res.* 14(20):6525-30, 2008 Oct 15.

295. Ding XZ, Talamonti MS, Bell RH Jr, Adrian TE. A novel anti-pancreatic cancer agent, LY293111. *Anticancer Drugs.* 16(5):467-73, 2005.

296. Tong WG, Ding XZ, Talamonti MS, Bell RH, Adrian TE. Leukotriene B4 receptor antagonist LY293111 induces S-phase cell cycle arrest and apoptosis in human pancreatic cancer cells. *Anticancer Drugs.* 18(5):535-41, 2007 Jun.

297. Kahnt AS, Angioni C, Göbel T, Hofmann B, Roos J, Steinbrink SD, Rörsch F, Thomas D, Geisslinger G, Zacharowski K, Grösch S, Steinhilber D, Maier TJ. Inhibitors of Human 5-Lipoxygenase Potently Interfere With Prostaglandin Transport. *Front Pharmacol.* 12:782584, 2022 Jan 21.

298. Göbel T, Diehl O, Heering J, Merk D, Angioni C, Wittmann SK, Buscato E, Kottke R, Weizel L, Schader T, Maier TJ, Geisslinger G, Schubert-Zsilavecz M, Steinhilber D, Proschak E, Kahnt AS. Zafirlukast Is a Dual Modulator of Human Soluble Epoxide Hydrolase and Peroxisome Proliferator-Activated Receptor γ. *Front Pharmacol.* 10:263, 2019 Mar 20.

299. Kahnt AS, Rörsch F, Diehl O, Hofmann B, Lehmann C, Steinbrink SD, Angioni C, Geisslinger G, Grösch S, Steinhilber D, Maier TJ. Cysteinyl leukotriene-receptor-1 antagonists interfere with PGE2 synthesis by inhibiting mPGES-1 activity. *Biochem Pharmacol.* 86(2):286-96, 2013 Jul 15.

300. Fischer AS, Metzner J, Steinbrink SD, Ulrich S, Angioni C, Geisslinger G, Steinhilber D, Maier TJ. 5-Lipoxygenase inhibitors induce potent anti-proliferative and cytotoxic effects in human tumour cells independently of suppression of 5-lipoxygenase activity. *Br J Pharmacol.* 161(4):936-49, 2010 Oct.

301. Riendeau D, Aspiotis R, Ethier D, Gareau Y, Grimm EL, Guay J, Guiral S, Juteau H, Mancini JA, Méthot N, Rubin J, Friesen RW. Inhibitors of the inducible microsomal prostaglandin E2 synthase (mPGES-1) derived from MK-886. *Bioorg Med Chem Lett.* 15(14):3352-5, 2005 Jul 15.

302. Rossi A, Pergola C, Koeberle A, Hoffmann M, Dehm F, Bramanti P, Cuzzocrea S, Werz O, Sautebin L. The 5-lipoxygenase inhibitor, zileuton, suppresses prostaglandin biosynthesis by inhibition of arachidonic acid release in macrophages. *Br J Pharmacol.* 161(3):555-70, 2010 Oct.

303. Theron AJ, Steel HC, Tintinger GR, Gravett CM, Anderson R, Feldman C. Cysteinyl leukotriene receptor-1 antagonists as modulators of innate immune cell function. *J Immunol Res.* 2014:608930, 2014.

304. Li L, Xiao Y, Xu Z, Wang S. Zileuton inhibits arachidonate-5-lipoxygenase to exert antitumor effects in preclinical cervical cancer models. *Cancer Chemother Pharmacol.* 88(6):953-960, 2021 Dec.

305. Monga J, Subramani D, Bharathan A, Ghosh J. Pharmacological and genetic targeting of 5-lipoxygenase interrupts c-Myc oncogenic signaling and kills enzalutamide-resistant prostate cancer cells via apoptosis. *Sci Rep.* 10(1):6649, 2020 Apr 20.

306. Woo SM, Min KJ, Seo SU, Kim S, Park JW, Song DK, Lee HS, Kim SH, Kwon TK. Up-regulation of 5-lipoxygenase by inhibition of cathepsin G enhances TRAIL-induced apoptosis through down-regulation of survivin. *Oncotarget.* 8(63):106672-106684, 2017 Nov 20.

307. Ding X, Zhou X, Zhang H, Qing J, Qiang H, Zhou G. Triptolide augments the effects of 5-lipoxygenase RNA interference in suppressing pancreatic tumor growth in a xenograft mouse model. *Cancer Chemother Pharmacol.* 69(1):253-61, 2012 Jan.

308. Catalano A, Caprari P, Soddu S, Procopio A, Romano M. 5-lipoxygenase antagonizes genotoxic stress-induced apoptosis by altering p53 nuclear trafficking. *FASEB J.* 18(14):1740-2, 2004 Nov.

309. Torosyan Y, Dobi A, Naga S, Mezhevaya K, Glasman M, Norris C, Jiang G, Mueller G, Pollard H, Srivastava M. Distinct effects of annexin A7 and p53 on arachidonate lipoxygenation in prostate cancer cells involve 5-lipoxygenase transcription. *Cancer Res.* 66(19):9609-16, 2006 Oct 1.

310. Gilbert B, Ahmad K, Roos J, Lehmann C, Chiba T, Ulrich-Rückert S, Smeenk L, van Heeringen S, Maier TJ, Groner B, Steinhilber D. 5-Lipoxygenase is a direct p53 target gene in humans. *Biochim Biophys Acta.* 1849(8):1003-16, 2015 Aug.

311. Häfner AK, Kahnt AS, Steinhilber D. Beyond leukotriene formation-The noncanonical functions of 5-lipoxygenase. *Prostaglandins Other Lipid Mediat.* 142:24-32, 2019 Jun.

312. Clevers, H. Wnt/beta-catenin signaling in development and disease. *Cell.* 127(3):469-80, 2006 Nov 3.

313. Clevers H, Nusse R. Wnt/β-catenin signaling and disease. *Cell.* 149(6):1192-205, 2012 Jun 8.

314. Roos J, Grösch S, Werz O, Schröder P, Ziegler S, Fulda S, Paulus P, Urbschat A, Kühn B, Maucher I, Fettel J, Vorup-Jensen T, Piesche M, Matrone C, Steinhilber D, Parnham MJ, Maier TJ. Regulation of tumorigenic Wnt signaling by cyclooxygenase-2, 5-lipoxygenase and their pharmacological inhibitors: A basis for novel drugs targeting cancer cells? *Pharmacol Ther.* 157:43-64, 2016 Jan.

315. Provost P, Samuelsson B, Rådmark O. Interaction of 5-lipoxygenase with cellular proteins. *Proc Natl Acad Sci U S A.* 96(5):1881-5, 1999 Mar 2.

316. Uebbing S, Kreiß M, Scholl F, Häfner AK, Sürün D, Garscha U, Werz O, Basavarajappa D, Samuelsson B, Rådmark O, Suess B, Steinhilber D. Modulation of microRNA processing by 5-lipoxygenase. *FASEB J.* 35(2):e21193, 2021 Feb.

317. Carissimi C, Fulci V, Macino G. MicroRNAs: novel regulators of immunity. *Autoimmun Rev.* 8(6):520-4, 2009 May.

318. Baltimore D, Boldin MP, O'Connell RM, Rao DS, Taganov KD. MicroRNAs: new regulators of immune cell development and function. *Nat Immunol.* 9(8):839-45, 2008 Aug.

319. Dincbas-Renqvist V, Pépin G, Rakonjac M, Plante I, Ouellet DL, Hermansson A, Goulet I, Doucet J, Samuelsson B, Rådmark O, Provost P. Human Dicer C-terminus functions as a 5-lipoxygenase binding domain. *Biochim Biophys Acta.* 1789(2):99-108, 2009 Feb.

320. Kreiß M, Oberlis JH, Seuter S, Bischoff-Kont I, Sürün D, Thomas D, Göbel T, Schmid T, Rådmark O, Brandes RP, Fürst R, Häfner AK, Steinhilber D. Human 5-lipoxygenase regulates transcription by association to euchromatin. *Biochem Pharmacol.* 203:115187, 2022 Jul 22.

321. Doudna JA, Charpentier E. Genome editing. The new frontier of genome engineering with CRISPR-Cas9. *Science.* 346(6213):1258096, 2014 Nov 28.

322. Charpentier E, Marraffini LA. Harnessing CRISPR-Cas9 immunity for genetic engineering. *Curr Opin Microbiol.* 19:114-119, Jun 2014.

323. Pourcel C, Salvignol G, Vergnaud G. CRISPR elements in Yersinia pestis acquire new repeats by preferential uptake of bacteriophage DNA, and provide additional tools for evolutionary studies. *Microbiology.* 151(Pt 3):653-663, 2005 Mar.

324. Bolotin A, Quinquis B, Sorokin A, Ehrlich SD. Clustered regularly interspaced short palindrome repeats (CRISPRs) have spacers of extrachromosomal origin. *Microbiology.* 151(Pt 8):2551-2561, 2005, Aug.

325. Deltcheva E, Chylinski K, Sharma CM, Gonzales K, Chao Y, Pirzada ZA, Eckert MR, Vogel J, Charpentier E. CRISPR RNA maturation by trans-encoded small RNA and host factor RNase III. *Nature.* 471, 602–607, 2011.

326. Mojica FJM, Díez-Villaseñor C, García-Martínez J, Almendros C. Short motif sequences determine the targets of the prokaryotic CRISPR defence system. *Microbiology.* 155(Pt 3):733-740, 2009 Mar.

327. Garneau JE, Dupuis MÈ, Villion M, Romero DA, Barrangou R, Boyaval P, Fremaux C, Horvath P, Magadán AH, Moineau S. The CRISPR/Cas bacterial immune system cleaves bacteriophage and plasmid DNA. *Nature.* 468(7320):67-71, 2010 Nov 4.

328. Jinek M, Chylinski K, Fonfara I, Hauer M, Doudna JA, Charpentier E. A programmable dual-RNA-guided DNA endonuclease in adaptive bacterial immunity. *Science.* 337(6096), 816–821, 2012.

329. Jinek M, Jiang F, Taylor DW, Sternberg SH, Kaya E, Ma E, Anders C, Hauer M, Zhou K, Lin S, Kaplan M, Iavarone AT, Charpentier E, Nogales E, Doudna JA. Structures of Cas9

endonucleases reveal RNA-mediated conformational activation. *Science.* 343(6176):1247997, 2014 Mar 14.

330. Rothkamm K, Krüger I, Thompson LH, Löbrich M. Pathways of DNA double-strand break repair during the mammalian cell cycle. *Mol Cell Biol.* 23(16):5706-15, 2003 Aug.

331. Lieber MR, Ma Y, Pannicke U, Schwarz K. Mechanism and regulation of human non-homologous DNA end-joining. *Nat Rev Mol Cell Biol.* 4(9):712-20, 2003 Sep.

332. Sander J, Joung J. CRISPR-Cas systems for editing, regulating and targeting genomes. *Nat Biotechnol.* 32, 347–355, 2014.

333. Jiang F, Doudna JA. CRISPR-Cas9 Structures and Mechanisms. *Annu Rev Biophys.* 46:505-529, 2017 May 22.

334. Wang H, Yang H, Shivalila CS, Dawlaty MM, Cheng AW, Zhang F, Jaenisch R. One-step generation of mice carrying mutations in multiple genes by CRISPR/Cas-mediated genome engineering. *Cell.* 153(4), 910–918, 2013.

335. Bortesi L, Fischer R. The CRISPR/Cas9 system for plant genome editing and beyond. *Biotechnol Adv.* 33(1):41-52, 2015 Jan-Feb.

336. Zhang, YT., Jiang, JY., Shi, TQ. et al. Application of the CRISPR/Cas system for genome editing in microalgae. *Appl Microbiol Biotechnol.* 2019, pp. 103, 3239–3248.

337. Hsu PD, Lander ES, Zhang F. Development and applications of CRISPR-Cas9 for genome engineering. *Cell.* 157(6), 1262–1278, 2014.

338. Uhlén M, Björling E, Agaton C, Szigyarto CA, Amini B, Andersen E, Andersson AC et al. A human protein atlas for normal and cancer tissues based on antibody proteomics. *Mol Cell Proteomics.* 4(12):1920-32, 2005.

339. Wang X, Spandidos A, Wang H, Seed B. PrimerBank: a PCR primer database for quantitative gene expression analysis, 2012 update. *Nucleic Acids Res.* 40(Database issue):D1144-9, 2012 Jan.

340. Shi M, Zhu J, Wang R, Chen X, Mi L, Walz T, Springer TA. Latent TGF-β structure and activation. *Nature.* 474(7351):343-9, 2011 Jun 15.

341. Brown PD, Wakefield LM, Levinson AD, Sporn MB. Physicochemical activation of recombinant latent transforming growth factor-beta's 1, 2, and 3. *Growth Factors.* 3(1):35-43, 1990.

342. Collection, ATCC - American Type Culture. https://www.atcc.org/atcc/productsheetpdf/generatehtmlpdf/ccl-247. [Online] 17 03 2022. [Cited: 27 06 2022.]

343. GmbH, DSMZ - German Collection of Microorganisms and Cell Cultures. https://www.dsmz.de/collection/catalogue/details/culture/ACC-581. [Online] 2022. [Cited: 27 06 2022.]

344. https://www.atcc.org/atcc/productsheetpdf/generatehtmlpdf/htb-38. ATCC - American Type Culture Collection. [Online] 13 03 2022. [Cited: 27 06 2022.]

345. Collection, ATCC - American Type Culture. https://www.atcc.org/atcc/productsheetpdf/generatehtmlpdf/htb-96. [Online] 16 03 2022. [Cited: 27 06 2022.]

346. GmbH, DSMZ - German Collection of Microorganisms and Cell Cultures. https://www.dsmz.de/collection/catalogue/details/culture/ACC-299. [Online] [Cited: 27 06 2022.]

347. —. https://www.dsmz.de/collection/catalogue/details/culture/ACC-785. [Online] [Cited: 27 06 2022.]

348. Cherciu I, Bărbălan A, Pirici D, Mărgăritescu C, Săftoiu A. Stem cells, colorectal cancer and cancer stem cell markers correlations. *Curr Health Sci J.* 40(3):153-61, 2014 Jul-Sep.

349. Najafi M, Farhood B, Mortezaee K. Cancer stem cells (CSCs) in cancer progression and therapy. *J Cell Physiol.* 234(6):8381-8395, 2019 Jun.

350. Sahlberg SH, Spiegelberg D, Glimelius B, Stenerlöw B, Nestor M. Evaluation of cancer stem cell markers CD133, CD44, CD24: association with AKT isoforms and radiation resistance in colon cancer cells. *PLoS One.* 9(4):e94621, 2014 Apr 23.

351. Scholzen T, Gerdes J. The Ki-67 protein: from the known and the unknown. *J Cell Physiol.* 182(3):311-22, 2000 Mar.

352. Went PT, Lugli A, Meier S, Bundi M, Mirlacher M, Sauter G, Dirnhofer S. Frequent EpCam protein expression in human carcinomas. *Hum Pathol.* 35(1):122-8, 2004 Jan.

353. Moll R, Löwe A, Laufer J, Franke WW. Cytokeratin 20 in human carcinomas. A new histodiagnostic marker detected by monoclonal antibodies. *Am J Pathol.* 140(2):427-47, 1992 Feb.

354. Silberg DG, Furth EE, Taylor JK, Schuck T, Chiou T, Traber PG. CDX1 protein expression in normal, metaplastic, and neoplastic human alimentary tract epithelium. *Gastroenterology.* 113(2):478-86, 1997 Aug.

355. Sadanandam A, Lyssiotis CA, Homicsko K, Collisson EA, Gibb WJ, Wullschleger S, Ostos LC, Lannon WA, Grotzinger C, Del Rio M, Lhermitte B, Olshen AB, Wiedenmann B, Cantley LC, Gray JW, Hanahan D. A colorectal cancer classification system that associates cellular phenotype and responses to therapy. *Nat Med.* 19(5):619-25, 2013 May.

356. Hankin JA, Jones DN, Murphy RC. Covalent binding of leukotriene A4 to DNA and RNA. *Chem Res Toxicol.* 16(4):551-61, 2003 Apr.

357. Funk D, Sorg BL, Lindner SC, Schmeiser HH. 32P-postlabeling analysis of DNA adducts formed by leukotriene A4 (LTA4). *Environ Mol Mutagen.* 51(4):338-43, 2010 May.

358. Speed N, Blair IA. Cyclooxygenase- and lipoxygenase-mediated DNA damage. *Cancer Metastasis Rev.* 30(3-4):437-47, 2011 Dec.

359. Lee JY, Kim WK, Bae KH, Lee SC, Lee EW. Lipid Metabolism and Ferroptosis. *Biology (Basel).* 10(3):184, 2021 Mar 2.

360. V, Syed. TGF-β Signaling in Cancer. *J Cell Biochem.* 117(6):1279-87, 2016 Jun.

361. Haque S, Morris JC. Transforming growth factor-β: A therapeutic target for cancer. *Hum Vaccin Immunother.* 13(8):1741-1750, 2017 Aug 3.

362. Wang L, Lan J, Tang J, Luo N. MCP-1 targeting: Shutting off an engine for tumor development. *Oncol Lett.* 23(1):26, 2022 Jan.

363. Korbecki J, Simińska D, Kojder K, Grochans S, Gutowska I, Chlubek D, Baranowska-Bosiacka I. Fractalkine/CX3CL1 in Neoplastic Processes. *Int J Mol Sci.* 21(10):3723, 2020 May 25.

364. Heldin CH, Lennartsson J, Westermark B. Involvement of platelet-derived growth factor ligands and receptors in tumorigenesis. *J Intern Med.* 283(1):16-44, 2018 Jan.

365. Kamata M, Amano H, Ito Y, Fujita T, Otaka F, Hosono K, Kamata K, Takeuchi Y, Yokomizo T, Shimizu T, Majima M. Role of the high-affinity leukotriene B4 receptor signaling in fibrosis after unilateral ureteral obstruction in mice. *PLoS One.* 14(2):e0202842, 2019 Feb 28.

366. Altraja S, Kadai M, Rekker E, Altraja A. Synthesis of tenascin and laminin beta2 chain in human bronchial epithelial cells is enhanced by cysteinyl leukotrienes via CysLT1 receptor. *Respir Res.* 9(1):44, 2008 May 26.

367. Ochkur SI, Protheroe CA, Li W, Colbert DC, Zellner KR, Shen HH, Luster AD, Irvin CG, Lee JJ, Lee NA. Cys-leukotrienes promote fibrosis in a mouse model of eosinophil-mediated respiratory inflammation. *Am J Respir Cell Mol Biol.* 49(6):1074-84, 2013 Dec.

368. de Araújo Farias V, Carrillo-Gálvez AB, Martín F, Anderson P. TGF-β and mesenchymal stromal cells in regenerative medicine, autoimmunity and cancer. *Cytokine Growth Factor Rev.* 43:25-37, 2018 Oct.

369. Liu Q, Ji S, Xia T, Liu J, Liu Z, Chen X, Zang ZJ. MCP-1 Priming Enhanced the Therapeutic Effects of Human Mesenchymal Stromal Cells on Contact Hypersensitivity Mice by Activating the COX2-PGE2/STAT3 Pathway. *Stem Cells Dev.* 29(16):1073-1083, 2020 Aug.

370. Donnem T, Al-Saad S, Al-Shibli K, Andersen S, Busund LT, Bremnes RM. Prognostic impact of platelet-derived growth factors in non-small cell lung cancer tumor and stromal cells. *J Thorac Oncol.* 3(9):963-70, 2008 Sep.

371. Hou XX, Zhou WJ, Wang XQ, Li DJ. Fractalkine/CX3CR1 is involved in the pathogenesis of endometriosis by regulating endometrial stromal cell proliferation and invasion. *Am J Reprod Immunol.* 76(4):318-25, 2016 Oct.

372. Alphonso A, Alahari SK. Stromal cells and integrins: conforming to the needs of the tumor microenvironment. *Neoplasia.* 11(12):1264-71, 2009 Dec.

373. Masucci MT, Minopoli M, Carriero MV. Tumor Associated Neutrophils. Their Role in Tumorigenesis, Metastasis, Prognosis and Therapy. *Front Oncol.* 9:1146, 2019 Nov 15.

374. Sahai E, Astsaturov I, Cukierman E, DeNardo DG, Egeblad M, Evans RM, Fearon D et al. A framework for advancing our understanding of cancer-associated fibroblasts. *Nat Rev Cancer.* 20(3):174-186, 2020 Mar.

375. Wen Z, Liu H, Li M, Li B, Gao W, Shao Q, Fan B, Zhao F, Wang Q, Xie Q, Yang Y, Yu J, Qu X. Increased metabolites of 5-lipoxygenase from hypoxic ovarian cancer cells promote tumor-associated macrophage infiltration. *Oncogene.* 34(10):1241-52, 2015 Mar 5.

376. W, Mueller-Klieser. Multicellular spheroids. A review on cellular aggregates in cancer research. *J Cancer Res Clin Oncol.* 113(2):101-22, 1987.

377. Kutova OM, Sencha LM, Pospelov AD, Dobrynina OE, Brilkina AA, Cherkasova EI, Balalaeva IV. Comparative Analysis of Cell-Cell Contact Abundance in Ovarian Carcinoma Cells Cultured in Two- and Three-Dimensional In Vitro Models. *Biology (Basel).* 9(12):446, 2020 Dec 4.

378. Nelson CM, Chen CS. Cell-cell signaling by direct contact increases cell proliferation via a PI3K-dependent signal. *FEBS Lett.* 514(2-3):238-42, 2002 Mar 13.

379. Mansoori B, Mohammadi A, Davudian S, Shirjang S, Baradaran B. The Different Mechanisms of Cancer Drug Resistance: A Brief Review. *Adv Pharm Bull.* 7(3):339-348, 2017 Sep.

380. Bakir B, Chiarella AM, Pitarresi JR, Rustgi AK. EMT, MET, Plasticity, and Tumor Metastasis. *Trends Cell Biol.* 30(10):764-776, 2020 Oct.

381. Malgulwar PB, Nambirajan A, Pathak P, Rajeshwari M, Suri V, Sarkar C, Singh M, Sharma MC. Epithelial-to-mesenchymal transition-related transcription factors are up-regulated in ependymomas and correlate with a poor prognosis. *Hum Pathol.* 82:149-157, 2018 Dec.

382. Ramis-Conde I, Chaplain MA, Anderson AR, Drasdo D. Multi-scale modelling of cancer cell intravasation: the role of cadherins in metastasis. *Physical Biology.* 6(1):016008, March 2009.

383. Ganesan R, Mallets E, Gomez-Cambronero J. The transcription factors Slug (SNAI2) and Snail (SNAI1) regulate phospholipase D (PLD) promoter in opposite ways towards cancer cell invasion. *Mol Oncol.* 10(5):663-76, 2016 May.

384. Taraboletti G, Perin L, Bottazzi B, Mantovani A, Giavazzi R, Salmona M. Membrane fluidity affects tumor-cell motility, invasion and lung-colonizing potential. *Int J Cancer.* 44(4):707-13, 1989 Oct 15.

385. Clark SR, Guy CJ, Scurr MJ, Taylor PR, Kift-Morgan AP, Hammond VJ, Thomas CP, Coles B, Roberts GW, Eberl M, Jones SA, Topley N, Kotecha S, O'Donnell VB. Esterified eicosanoids are acutely generated by 5-lipoxygenase in primary human neutrophils and in human and murine infection. *Blood.* 117(6):2033-43, 2011 Feb 10.

386. O'Donnell VB, Aldrovandi M, Murphy RC, Krönke G. Enzymatically oxidized phospholipids assume center stage as essential regulators of innate immunity and cell death. *Sci Signal.* 12(574):eaau2293, 2019 Mar 26.

387. Bell E, Ponthan F, Whitworth C, Westermann F, Thomas H, Redfern CP. Cell survival signalling through PPARδ and arachidonic acid metabolites in neuroblastoma. *PLoS One.* 8(7):e68859, 2013 Jul 9.

388. O'Flaherty JT, Rogers LC, Paumi CM, Hantgan RR, Thomas LR, Clay CE, High K, Chen YQ, Willingham MC, Smitherman PK, Kute TE, Rao A, Cramer SD, Morrow CS. 5-Oxo-ETE analogs and the proliferation of cancer cells. *Biochim Biophys Acta.* 1736(3):228-36, 2005 Oct 1.

389. Powell WS, Rokach J. Biosynthesis, biological effects, and receptors of hydroxyeicosatetraenoic acids (HETEs) and oxoeicosatetraenoic acids (oxo-ETEs) derived from arachidonic acid. *Biochim Biophys Acta.* 1851(4):340-55, 2015 Apr.

Eidesstattliche Erklärung

Hiermit erkläre ich, Hannah Weißer, dass ich die hier vorliegende Dissertation mit dem Titel

„**Influence of the CRISPR/Cas mediated Knockout of 5-Lipoxygenase on Tumour Cells“**

selbstständig verfasst und keine anderen als die angegebenen Quellen und Hilfsmittel verwendet habe.

Teile dieser Arbeit werden im *Peer-Review*-Journal *Cancer Gene Therapy* publiziert. Ein besonderer Dank gilt dem Verlag Nature, da er seinen Autoren die Inklusion von Auszügen oder dem gesamten Inhalt der eigenen Artikel in einer Dissertationsschrift gestattet, insofern diese nicht kommerziell publiziert wird.